THE ROLE OF JIP-1 IN JNK SIGNALLING DURING STRESS AND APOPTOSIS

Thesis submitted for the degree of
Doctor of Philosophy
at the
University of Leicester

by

Mahesh Vaisnav B.Sc. (Hons) (Leicester)
Department of Biochemistry
University of Leicester
January 2002

ProQuest LLC
789 East Eisenhower Parkway
P.O. Box 1346
Ann Arbor, MI 48106-1346

STATEMENT

Unless otherwise acknowledged, the experimental work described in this thesis has been carried out by the author in the Department of Biochemistry at the University of Leicester between October 1998 and December 2001. The work has not been submitted, and is not presently being submitted for any other degree at this or any other university.

Signed: M.N.Vaughan

Date: 9th January 2002

Department of Biochemistry
University of Leicester
University Road
Leicester LE1 7RH
United Kingdom

THE ROLE OF JIP-1 IN JNK SIGNALLING DURING STRESS AND APOPTOSIS

Mahesh Vaisnav

ABSTRACT

The JNK signal transduction pathway responds to cellular stresses and plays a role in embryogenesis, cell survival, proliferation, differentiation and apoptosis. JNK is activated by dual-specificity kinases MKK4 and MKK7, which in turn are activated by a variety of upstream kinases, including the GCKs and the MLK family proteins.

Recently, the JIP group of proteins was shown to organise the JNK pathway components into scaffolds. Transient transfection studies have shown that JIP-1 binds to JNK, MKK7, MLK3 and HPK1 and organises the JNK pathway in the form of a scaffold to selectively mediate JNK activation in response to stressful stimuli. An examination of the interaction of endogenous JIP-1 with JNK, MLK3 and HPK1 *in vivo* demonstrated that JIP-1 interacted with MLK3 and HPK1 in resting N1E-115 cells. In stressed N1E-115 cells, the activation of JNK coincided with the JIP-1-JNK1 interaction while the JIP-1-MLK3 interaction was lost. In the rat brain extracts JIP-1-JNK and MLK3-HPK1 interactions were detected. These data suggest that the JIP-1 scaffold complex is dynamic and the differential interaction of JIP-1 with the JNK pathway kinases may regulate JNK activity *in vivo*. The exchange of the JNK pathway components with the JIP-1 scaffold during stress and the ability of JIP-1 to oligomerise also suggests a possibility of signal amplification.

The presence of putative caspase-3 and –8 cleavage sites in JIP-1 led us to investigate whether JIP-1 was a caspase substrate during apoptosis *in vivo*. The results showed that JIP-1 was cleaved by caspase-3 *in vivo* during both receptor- and chemical-induced apoptosis of HeLa cells. An analysis of caspase-3 cleavage-resistant JIP-1b mutants *in vitro* mapped the caspase-3 cleavage sites as being $DLID^{98}/A$ and $DESD^{405}/S$.

An examination of JIP-1 cleavage and JNK activity in HeLa cells during apoptosis demonstrated that intact JIP-1 was associated with high levels of JNK activity and the cleavage of JIP-1 was coincident with a decrease in JNK activity. Furthermore, during TRAIL-induced apoptosis, the co-immunoprecipitation of JIP-1 and JNK1 was coincident with JNK activation, whereas a decrease in JNK activity correlated with a reduced ability of JIP-1 to interact with JNK1. These results suggest that the interaction of JIP-1 with JNK may be required for JNK activation, and that the cleavage of JIP-1 may attenuate JNK signalling, *in vivo* during apoptosis.

Overall, the results suggest that the interaction of JIP-1 with the JNK pathway components may be necessary for JNK activation *in vivo* during stress and apoptosis.

ACKNOWLEDGEMENTS

I would like to thank Dr. Martin Dickens for his guidance in writing this thesis and encouragement throughout my Ph.D. research, and for putting up with my enthusiasm. I gratefully acknowledge the BBSRC without whose financial support none of this would have been possible.

I am extremely grateful to Drs. Raj Patel, Steve Harding Eilis Byrne and Marion MacFarlane for their friendship, support, and ever willingness to pass on practical and theoretical knowledge; without their help I would not have been able to complete my work in time. I am also thankful to Dr. Jonathan Blank for helping me through some frustrating times during my research.

I would like to express my sincere gratitude to Prof. David Critchley, whose unconditional help and support enabled me to realise my ambition of becoming a researcher. I am sincerely grateful to Dr. Sally Prigent, who helped me through during a very critical time during my research.

Finally, my appreciation goes to members of the department for making my time at Leicester University enjoyable.

CONTENTS

Statement i

Abstract ii

Acknowledgements iii

Contents iv

Abbreviations xi

Table of Figures xv

Table of Tables xvii

CHAPTER 1: Introduction **1**

1.1. Mitogen activated protein kinase (MAPK) pathways 1

1.1.1 Introduction 1

1.1.2 MAPK pathways in mammals 2

1.2. The mammalian JNK pathway 2

1.2.1 Introduction 2

1.2.2 JNK isoforms 3

1.2.3 JNK substrates 3

1.3. Activation of JNK by upstream kinases 5

1.3.1 Activation by MKKs 5

1.3.2 Activation by MKKKs 6

1.3.2.1 MAP ERK kinases (MEKKs) 7

1.3.2.2 Mixed lineage kinases (MLKs) 7

1.3.2.3 Apoptosis signal regulating kinase 1 (ASK1) 8

1.3.3 Activation by germinal centre kinases (GCKs) and small GTPases 9

1.3.4 Regulation of the JNK pathway 10

1.4. Assembly of JNK signalling modules by scaffold proteins 12

1.4.1 Introduction 12

1.4.2 The JIP group of scaffold proteins 12

1.4.2.1 JIP-1 and JIP-2 proteins 13

1.4.2.2 JIP-3 protein 15

1.4.2.3 JIP scaffolds as cargoes in kinesin-dependent axonal

transport in neurons 16
1.4.2.4 Interactions of JIPs with other proteins 16
1.4.3 β-arrestin 2: A scaffold for the ASK1-MKK4-JNK module 17
1.4.4 The role of scaffolds in mediating JNK signalling specificity 18
1.5. Functions of the JNK pathway 20
1.5.1 Regulation of gene expression 20
1.5.2 Oncogenic transformation 20
1.5.3 Immune response 21
1.6. Apoptosis 22
1.6.1 Introduction 22
1.6.2 Caspases: The central effectors of cell death 23
1.6.2.1 Substrate specificity of caspases 23
1.6.3 The death receptor pathway 24
1.6.3.1 Introduction 24
1.6.3.2 Apoptosis signalling by death receptors 25
1.6.3.3 Regulation of the death receptor signalling 25
1.6.4 Apoptosis signalling via the mitochondrial pathway 25
1.6.4.1 Regulation of mitochondrial-initiated caspase activation 26
1.7. The role of JNK in apoptosis 27
1.7.1 Biochemical studies 27
1.7.2 Genetic studies 28
1.7.3 Mechanism of JNK-dependent stress-induced apoptosis 29
1.7.3.1 A model for JNK-dependent stress-induced apoptosis 30
1.7.4 The role of JNK in receptor-mediated apoptosis 32
1.7.5 Suppression of apoptosis by JNK 32
1.8. Aims of the project 33

CHAPTER 2: Materials & Methods **34**
2.1. Materials 34
2.1.1 General laboratory reagents 34
2.1.2 Molecular biology reagents 34

2.1.3 Antibodies 35
2.1.4 Tissue culture 36
2.1.5 Plasmids 36
2.2. Methods 37
2.2.1 Bacterial techniques 37
2.2.1.1 Preparation of competent XL-1 Blue MRF' cells 37
2.2.1.2 Transformation of competent XL-1 Blue MRF' cells 37
2.2.1.3 Preparation of glycerol stocks 37
2.2.1.4 Preparation of bacterial pellets for DNA sequencing 38
2.2.2 Molecular biology methods 38
2.2.2.1 Small- and large-scale preparation of plasmid DNA 38
2.2.2.2 Restriction enzyme digestion of plasmid DNA 38
2.2.2.3 Agarose gel electrophoresis 38
2.2.2.4 Electroelution of DNA from agarose gels 39
2.2.2.5 Construction of pBluescript-JIP-1b 39
2.2.2.6 Construction of caspase-3 cleavage-resistant JIP-1b mutants 40
2.2.3 Biochemical methods 41
2.2.3.1 Preparation of cell extracts 41
2.2.3.2 Determination of protein concentration 42
2.2.3.3 SDS-PAGE 42
2.2.3.4 Coomassie staining of SDS-polyacrylamide gels 42
2.2.3.5 Immunoprecipitation 42
2.2.3.6 Measurement of JNK activity 43
2.2.4 Immunological methods 43
2.2.4.1 Immunoblotting 43
2.2.4.2 Purification of IgG from JIP-1 antisera #608, #609 and #610 44
2.2.4.3 Affinity purification of the JIP-1 antipeptide antibody #609 45
2.2.4.4 Enzyme-linked immunosorbent assay (ELISA) 46
2.2.5 Mammalian cell culture 47
2.2.6 Apoptosis techniques 48
2.2.6.1 Induction of apoptosis and preparation of extracts 48

2.2.6.2 Quantification of apoptosis 48
2.2.6.3 *In vitro* transcription/translation cleavage reactions using purified caspases 49
Appendix **50**

CHAPTER 3: Interactions between JIP-1 scaffold complex components *in vivo* **54**
3.1. Introduction 54
3.2. Results 55
3.2.1 Anti-JIP-1 antibody characterisation 55
3.2.1.1 Characterisation of JIP-1 polyclonal antisera and purified antibodies by ELISA 55
3.2.1.2 Testing anti-JIP-1 antibodies for use in western blotting and immunoprecipitation 57
3.2.2 Western blotting and immunoprecipitation using JNK1, MKK7, MLK3 & HPK1 antibodies 60
3.2.2.1 Detection of JNK1, MKK7, MLK3 and HPK1 by western blotting 60
3.2.2.2 Immunoprecipitation of JNK1, MLK3 and HPK1 61
3.2.3 Interactions between JIP-1 scaffold complex components *in vivo* 62
3.2.3.1 Interactions between JIP-1 scaffold complex components in rat brain 62
3.2.3.2 Interactions between JIP-1 scaffold complex components in N1E-115 cells 63
3.2.3.3 Interaction between JIP-1 and JNK1 in response to various stress stimuli 64
3.3. Discussion 65
3.3.3 Anti-JIP-1 antibody characterisation 65
3.3.1.1 ELISA for anti-JIP-1 polyclonal antibodies 65
3.3.1.2 Western blotting using anti-JIP-1 antibodies 66
3.3.1.3 Immunoprecipitation using anti-JIP-1 antibodies 66
3.3.2 Interactions between JIP-1 scaffold complex components in resting N1E-115 cells 67

3.3.2.1 The interaction between JIP-1 and MLK3 67
3.3.2.2 MLK3 may not be a part of a trimeric JIP-1-MLK3-HPK1 complex 68
3.3.3 Interactions between JIP-1 scaffold complex components in stress-stimulated N1E-115 cells 68
3.3.3.1 The MLK3-HPK1 interaction 70
3.3.3.2 HPK1 may act as a bridge between JIP-1 and MLK3 70
3.3.4 A model for the regulation of JNK activation by protein-protein interactions 71
3.3.5 Concluding remarks 72

CHAPTER 4: JIP-1 is a caspase-3 substrate *in vivo* and *in vitro* **74**
4.1. Introduction 74
4.2. Results 75
4.2.1 JIP-1 cleavage during apoptosis 75
4.2.1.1 Identification of JIP-1 expressing cell lines 75
4.2.1.2 *In vivo* JIP-1 cleavage in selected cell lines during receptor- and chemical-induced apoptosis 75
4.2.1.3 Time course of JIP-1 cleavage during apoptosis in HeLa cells 77
4.2.1.4 Caspase activation during apoptosis in HeLa cells 79
4.2.1.5 DEVD.fmk, a specific caspase-3 inhibitor, inhibits JIP-1 cleavage *in vivo* during apoptosis in HeLa cells 80
4.2.2 JIP-1b is cleaved at $DLID^{98}$/A and $DESD^{405}$/S by caspase-3 *in vitro* 81
4.2.2.1 JIP-1 protein expression *in vitro* 81
4.2.2.2 *In vitro* analysis of JIP-1b cleavage with purified caspase-3 and –8 82
4.2.2.3 Time course of JIP-1b cleavage *in vitro* 84
4.2.2.4 Construction of caspase-3 cleavage-resistant JIP-1b mutants 85
4.2.2.5 *In vitro* analysis of JIP-1b caspase-3 cleavage-resistant mutants 87

4.3. Discussion 88
4.3.1 JIP-1 protein expression in different cell lines 88
4.3.2 JIP-1 cleavage during apoptosis in RinD11, HEK293 and HeLa cells 90
4.3.3 Time course of *in vivo* JIP-1 cleavage in HeLa cells 91
4.3.4 Analysis of JIP-1b cleavage *in vitro* 92
4.3.5 A comparison of JIP-1 cleavage *in vivo* and *in vitro* 93
4.3.6 JIP-1: A novel caspase-3 substrate 93
4.3.7 Functions of JIP-1 during apoptosis 94
4.3.8 JIP-1 cleavage and its implications for JNK signalling during apoptosis 95
4.3.8.1 Conservation of caspase-3 cleavage sites in JIP isoforms 95
4.3.8.2 A functional JIP-1 scaffold may not form due to cleavage of JIP proteins during apoptosis 96

CHAPTER 5: Correlation between JNK activity & JIP-1 cleavage during apoptosis 98
5.1. Introduction 98
5.2. Results
5.2.1 JNK activity during TRAIL- and staurosporine-induced apoptosis 99
5.2.1.1 JNK activity during TRAIL-induced apoptosis 99
5.2.1.2 JNK activity during staurosporine-induced apoptosis 100
5.2.2 A correlation between JIP-1 cleavage and JNK activity in response to other apoptotic stimuli 101
5.2.2.1 JIP-1 cleavage in response to other stimuli 101
5.2.2.2 JNK activation and JIP-1 cleavage in response to other stimuli 103
5.2.3 JIP-1 may mediate sustained JNK activation during apoptosis 106
5.2.3.1 Immunoprecipitation of JIP-1 and JNK1 from HeLa cell extracts 106
5.2.3.2 Co-immunoprecipitation of JIP-1 and JNK1 during TRAIL-induced apoptosis 107

5.3. Discussion 109
5.3.1 JIP-1 cleavage during apoptosis 109
5.3.2 JNK activation during apoptosis is independent of caspase-3 109
5.3.3 JNK activation may be dependent on JIP-1 during apoptosis 110
5.3.4 A possible role for the JIP-1 scaffold in the activation of JNK during apoptosis 111
5.3.5 Role of JNK activity during HeLa cell apoptosis 113
5.3.6 A model for the role of JIP-1 in JNK activation during apoptosis 114

Final discussion **115**
Bibliography **118**

ABBREVIATIONS

General

AP-1	Activating protein-1
Apaf-1	Apoptosis protease activating factor 1
APC	Antigen presenting cell
APP	Amyloid precursor protein
ApoER2	Apolipoprotein E receptor 2
ASK1	Apoptosis signal regulating kinase 1
ATF2	Activating transcription factor 2
Bcl-2	B cell lymphoma 2
CHOP	CREB (cyclic AMP response element binding protein) homologous protein
CRIB	Cdc42/Rac interaction and binding
crmA	Cytokine response modifier A
DD	Death domain
DED	Death effector domain
DISC	Death-inducing signalling complex
DLK	Dual leucine zipper kinase
ERK	Extracellular signal-regulated kinase
ES	Embryonic stem
FADD	Fas-associated death domain
FasL	Fas ligand
FLIP	FADD-like ICE inhibitory protein
GCK	Germinal centre kinase
GEF	Guanine nucleotide exchange factor
GLK	GCK-like kinase
GPCR	G-protein coupled receptor
HPK1	Human progenitor kinase 1
Hsp	Heat shock protein
IAP	Inhibitor of apoptosis protein
IB1	Islet brain 1
ICE	Interleukin-1β-converting enzyme

IL-1	Interleukin 1
JBD	JNK binding domain
JDP2	Jun dimerisation protein 2
JIP	JNK-interacting protein
JNK	c-Jun N-terminal kinase
JSAP1	JNK/SAPK-associated protein 1
KHS	Kinase homologous to Ste20
KLC	Kinesin light chain
KRS1	Kinase responsive to stress 1
LDL	Low density lipoprotein
LOK	Lymphocyte-oriented kinase
LZK	Leucine zipper kinase
MAP2	Microtubule-associated protein 2
MAPK	Mitogen activated protein kinase
MAPKAP-K2	MAPK activating protein kinase 2
MEF	Mouse embryonic fibroblasts
MEKK	MAP/ERK kinase kinase
MKKKK	MAPK kinase kinase kinase
MKKK	MAPK kinase kinase
MKK	MAPK kinase
MLK	Mixed lineage kinase
MP1	MAP/ERK kinase partner 1
MST	Mammalian sterile twenty
MUK	MAPK upstream kinase
NFAT	Nuclear factor of activated T cells
NF-κB	Nuclear factor-κB
NGF	Nerve growth factor
NIK	Nck-interacting kinase
OGD	Oxygen glucose deprivation
p53AIP1	p53-regulated apoptosis-inducing protein 1
PAK3	p21-activated kinase 3
PTB	Phosphotyrosine binding
PTK1	Protein tyrosine kinase 1
REST	Repressor element silencing transcription factor

ROS	Reactive oxygen species
RSK	Ribosomal S6 kinase
SAPK	Stress-activated protein kinase
SH3	Src homology 3
SODD	Silencer of death domain
SOK1	Ste20-like oxidant stress-activated kinase 1
SPRK	SH3 domain-containing proline-rich kinase
STAT3	Signal transducer and activator of transcription 3
SYD	Sunday driver
TAK1	Transforming growth factor β activated kinase 1
TCR	T cell receptor
TGFβ	Transforming growth factor β
TNF	Tumour necrosis factor
TPL2	Tumour progression locus 2
TPR	Tetratricopeptide repeat
TRADD	TNF receptor-associated death domain
TRAF	TNF receptor-associated factor
TRAIL	TNF-related apoptosis-inducing ligand
TRAIL-R	TRAIL receptor
UV	Ultra-violet
ZPK	Zipper-containing kinase

Chemicals/Reagents

ATP	Adenosine 5'-triphosphate
BSA	Bovine serum albumin
DMEM	Dulbecco's modified Eagle medium
DMSO	Dimethylsulphoxide
DTT	Dithiothreitol
ECL	Enhanced chemiluminescence
EDTA	Ethylene diamine tetra acetic acid
ELISA	Enzyme linked immunosorbent assay
FCS	Foetal calf serum
HEK293	Human embryonic kidney 293

HRP	Horseradish peroxidase
H_2O_2	Hydrogen peroxide
LB	Luria-Bertani broth
MMS	Methyl methanosulphate
NHS	N-hydroxy succinimide
PBS	Phosphate buffered saline
PMSF	Phenyl methyl sulfonyl fluoride
SDS	Sodium dodecyl sulphate

Experimental procedures

IP	Immunoprecipitation
PAGE	Polyacrylamide gel electrophoresis
PCR	Polymerase chain reaction
WB	Western blotting

Table of Figures

Fig. 1.1. A generalised scheme of the MAPK signalling module.

Fig. 1.2. Mammalian MAPK pathways.

Fig. 1.3. The domain structure of the JIP family proteins.

Fig. 1.4. Schematic diagram of the postulated JNK modules.

Fig. 1.5. Receptor- and mitochondria-mediated caspase activation pathway during apoptosis.

Fig. 1.6. A model depicting the role of the JNK pathway in the induction of stress-induced apoptosis.

Fig. 3.1. JIP-1 antisera ELISA.

Fig. 3.2. IgG-purified JIP-1 antibody ELISA.

Fig. 3.3. Peptide competition ELISA.

Fig. 3.4. Detection of endogenous JIP-1 by anti-JIP-1 polyclonal antibodies.

Fig. 3.5. Detection of endogenous JIP-1 by the monoclonal anti-JIP-1 antibody.

Fig. 3.6. Immunoprecipitation of transfected JIP-1 by anti-JIP-1 antibodies.

Fig. 3.7. Immunoprecipitation of endogenous JIP-1 by anti-JIP-1 antibodies.

Fig. 3.8. Detection of JNK1, MKK7, MLK3 and HPK1 in N1E-115 and rat brain lysates.

Fig. 3.9. Immunoprecipitation of JNK1, MLK3 and HPK1 from N1E-115 and rat brain lysates.

Fig. 3.10. Interactions among JIP-1 scaffold complex components in rat brain.

Fig. 3.11. Interactions among JIP-1 scaffold complex components in resting N1E-115 cells.

Fig. 3.12. Interactions among JIP-1 scaffold complex components in anisomycin-treated N1E-115 cells.

Fig. 3.13. JNK1 kinase assay and JIP-1, JNK1, MLK3 and HPK1 protein levels in resting and anisomycin-treated N1E-115 cells.

Fig. 3.14. JIP-1-JNK1 interaction in response to various stress stimuli in N1E-115 cells.

Fig. 3.15. A model for the activation of the JNK pathway by protein-protein interactions.

Fig. 4.1. Detection of endogenous JIP-1 in human, mouse and rat cell lines.

Fig. 4.2. Evidence for JIP-1 cleavage during receptor- and chemical-induced apoptosis.

Fig. 4.3. Putative caspase-3 and caspase-8 cleavages sites in JIP-1.
Fig. 4.4. JIP-1 cleavage *in vivo* is mediated by caspases during TRAIL-induced apoptosis in HeLa cells.
Fig. 4.5. JIP-1 cleavage *in vivo* is mediated by caspases during staurosporine-induced apoptosis in HeLa cells.
Fig. 4.6. Caspase activation during TRAIL-induced apoptosis in HeLa cells.
Fig. 4.7. Caspase activation during staurosporine-induced apoptosis in HeLa cells.
Fig. 4.8. DEVD.fmk, a specific caspase-3 inhibitor, inhibits JIP-1 cleavage during TRAIL-induced apoptosis.
Fig. 4.9. DEVD.fmk, a specific caspase-3 inhibitor, inhibits JIP-1 cleavage during staurosporine-induced apoptosis.
Fig. 4.10. Testing pBluescript-JIP-1 and pBluescript-JIP-1b constructs in the *in vitro* transcription/translation reactions.
Fig. 4.11. JIP-1b is a preferential caspase-3 substrate *in vitro*.
Fig. 4.12. Time course of JIP-1b cleavage by caspase-3 and –8 *in vitro*.
Fig. 4.13. Construction of caspase-3 cleavage-resistant JIP-1b mutants by overlapping insertional PCR.
Fig. 4.14. JIP-1b is cleaved at Asp98 and Asp405 by caspase-3 *in vitro*.
Fig. 4.15. Position of caspase-3 cleavage sites in JIP-1, JIP-2 and JIP-3 in relation to the domain positions.
Fig. 5.1. JNK activity during TRAIL-induced apoptosis.
Fig. 5.2. JNK activity during staurosporine-induced apoptosis.
Fig. 5.3. The effect of apoptotic stimuli on % apoptosis in HeLa cells.
Fig. 5.4. Effect of various apoptotic stimuli on JIP-1 cleavage during HeLa cell apoptosis.
Fig. 5.5. JIP-1 cleavage and JNK activity during TNF-α-induced apoptosis.
Fig. 5.6. JIP-1 cleavage and JNK activity during anisomycin-induced apoptosis.
Fig. 5.7. Intact JIP-1 and persistent JNK activity during Fas-induced apoptosis.
Fig. 5.8. Intact JIP-1 and persistent JNK activity during H_2O_2-induced apoptosis.
Fig. 5.9. Immunoprecipitation of JNK1 and JIP-1 from HeLa cell extracts.
Fig. 5.10. The interaction between JIP-1 and JNK1 during TRAIL-induced apoptosis.
Fig. 5.11. A model for the role of JIP-1 in JNK activation during apoptosis in HeLa cells.

Table of Tables

Table 1.1. Homologues of the JNK pathway components in different species.

Table 2.1. Oligonucleotide primers used for JIP-1b mutagenesis.

Table 2.2. Peptides used to generate polyclonal antibodies to JIP-1.

Table 3.1. Available antibodies to JIP-1.

Table 3.2. Summary of the results of JIP-1 antibody characterisation

Table 3.3. Available antibodies to JNK1, MKK7, MLK3 and HPK1.

Table 3.4. Summary of western blotting and immunoprecipitation analysis using JNK1, MLK3 and HPK1 antibodies.

Table 3.5. Antibodies used to study interactions between JIP-1 scaffold components.

Table 4.1. Cell lines tested for the presence of endogenous JIP-1.

Table 5.1. Percentage apoptosis of HeLa cells in response to various apoptotic stimuli.

CHAPTER 1

INTRODUCTION

1. 1. MITOGEN ACTIVATED PROTEIN KINASE (MAPK) PATHWAYS

1.1.1 Introduction

Cells react to environmental changes that are perceived through extracellular signals. Examples of extracellular signals include hormones, growth factors, neurotransmitters and cellular stresses. These signals are conveyed to the interior of the cell through a variety of signal transduction pathways. The activation of these pathways control many cellular functions, including changes in gene expression by activating specific transcription factors in the nucleus. One of the most extensively studied signalling pathways is the MAPK cascade. The MAPK cascade is a major signalling system by which cells respond to growth factors, cytokines and stressful stimuli such as irradiation and high osmolarity. Many steps of this cascade are conserved, and homologues have been discovered in yeast, *Caenorhabditis elegans*, *Drosophila melanogaster*, *Xenopus laevis*, plants and mammalian cells (Widmann *et. al.*, 1999). MAPK play central roles in processes as diverse as differentiation, proliferation, apoptosis, growth control and response to external stress (Davis, 2000). In mammals, the MAPK family includes the extracellular signal regulated kinase 1/2 (ERK1/ERK2), c-Jun amino terminal kinase (JNK), p38 and ERK5.

The basic assembly of MAPK pathways is a three-component module conserved from yeast to humans (Widmann *et. al.*, 1999). The minimal MAPK module is composed of three kinases that establish a sequential activation pathway (Fig. 1.1). The first kinase in this module is a MAPK kinase kinase (MKKK), a serine/threonine kinase activated either by phosphorylation by a MKKK kinase (MKKKK) or by interaction with a small GTP-binding protein of the Ras or Rho family. Activated MKKKs phosphorylate and activate the next kinase in the module, a MAPK kinase (MKK). MKKs are dual-specificity kinases that recognise and phosphorylate a TXY motif in the activation loop of the next kinase in the cascade, a MAPK. MAPK are the final kinases in the three-kinase module and phosphorylate substrates such as transcription factors, other protein kinases, phospholipases and cytoskeletal proteins on serine and threonine residues (Widmann *et. al.*, 1999).

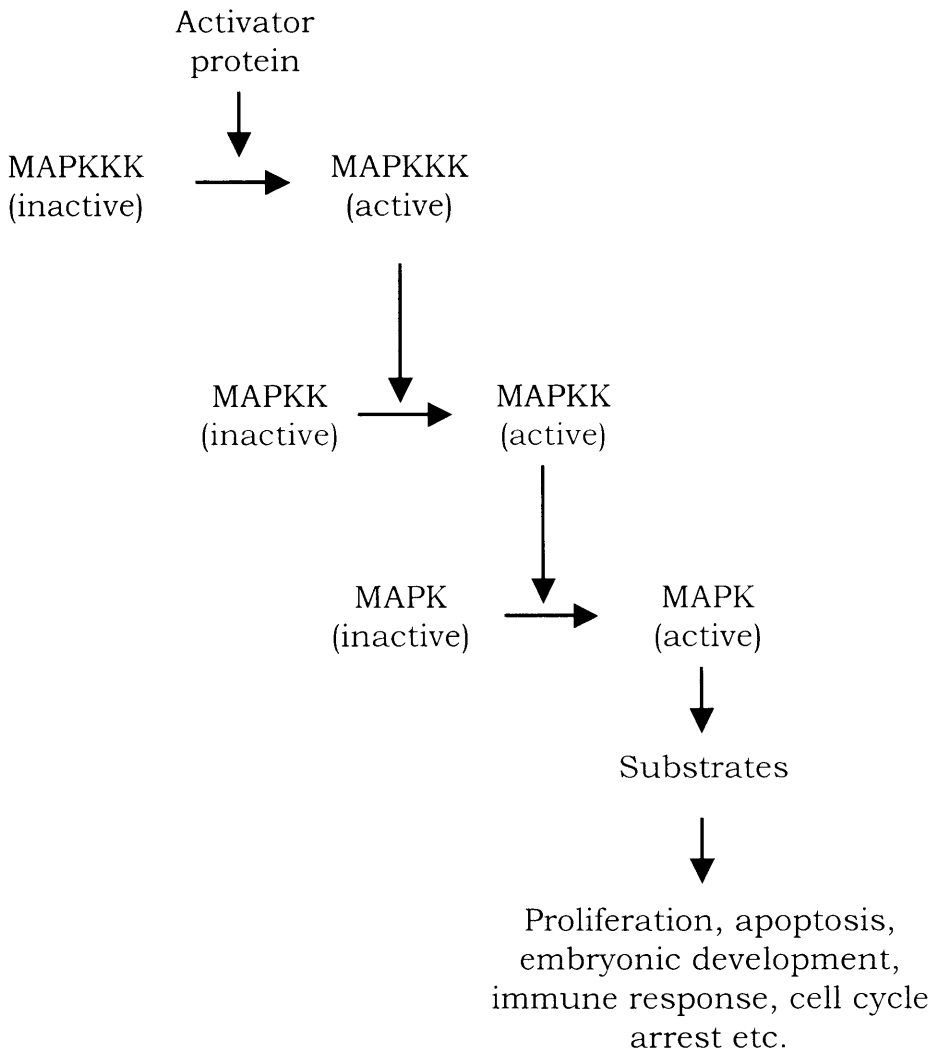

Fig. 1.1. A generalised scheme of the MAPK core signalling module (from Kyriakis & Avruch, 2001).

MAPK is activated by MAPKK, which in turn are activated by MAPKKK. MAPKKK can be activated by activator proteins such as G-proteins. Activated MAPK phosphorylates its substrates, which carry out functions as diverse as proliferation, apoptosis, embryonic development, immune response, cell cycle arrest, etc.

1.1.2 MAPK pathways in mammals

In mammalian cells, fourteen MKKKs, seven MKKs and twelve MAPKs have been identified, which are organised into four MAPK pathways: the extracellular signal-regulated kinase 1/2 (ERK1/2) pathway, the c-Jun N-terminal kinase (JNK) pathway, the p38 pathway and the MKK5/ERK5 pathway (Kyriakis & Avruch, 2001; Fig. 1.2).

Mammalian MAPK pathways can be broadly divided into two groups on the basis of the nature of the activating stimuli: the ERK1/2 pathway and the stress-activated protein kinase (SAPK) pathways. Growth factors, mitogens and hormones activate the ERK1/2 pathway. Inflammatory cytokines (e.g. tumour necrosis factor [TNF]) and cellular stresses (e.g. Ultraviolet [UV] irradiation, protein synthesis inhibitors and redox stresses) activate the SAPK pathways (Fig. 1.2). The SAPK pathway includes three subgroups, namely the JNK pathway, the p38 pathway and the ERK5 pathway. These are regulated by overlapping but not identical sets of extracellular stimuli. The mammalian ERK1/2, p38, ERK5 pathways, and MAPK pathways in other species have been reviewed elsewhere (Herskowitz, 1995; Schaeffer & Weber, 1999; Widmann et. al., 1999; Kyriakis & Avruch, 2001). The present chapter reviews the mammalian JNK pathway, in particular the recent advances in the JNK scaffold proteins and the role of JNK signalling in apoptosis.

1. 2. THE MAMMALIAN JNK PATHWAY

1. 2. 1. Introduction

The JNKs represent a group of enzymes that are activated by the exposure of cells to cytokines and environmental stresses (Ip & Davis, 1998). Apart from mammals, homologues of the components of the JNK pathway have been discovered in *S. cerevisiae*, *D. melanogaster* and *C. elegans* (Table 1.1), thus implying a conserved evolutionary role across various species (Noselli, 1998; Kawasaki *et. al.*, 1999; Widmann *et. al.*, 1999; Koga *et. al.*, 2000; Inoue *et. al.*, 2001).

JNK was originally identified as a 54-kDa protein kinase that was activated by the injection of cycloheximide in rats, which caused the phosphorylation of microtubule-associated protein 2 (MAP2), and was hence initially called p54-MAP2 kinase or p54 (Kyriakis & Avruch, 1990). p54 was later termed c-Jun N-terminal kinase (JNK) when it was demonstrated that p54 was also activated by the stress stimuli that activate c-Jun,

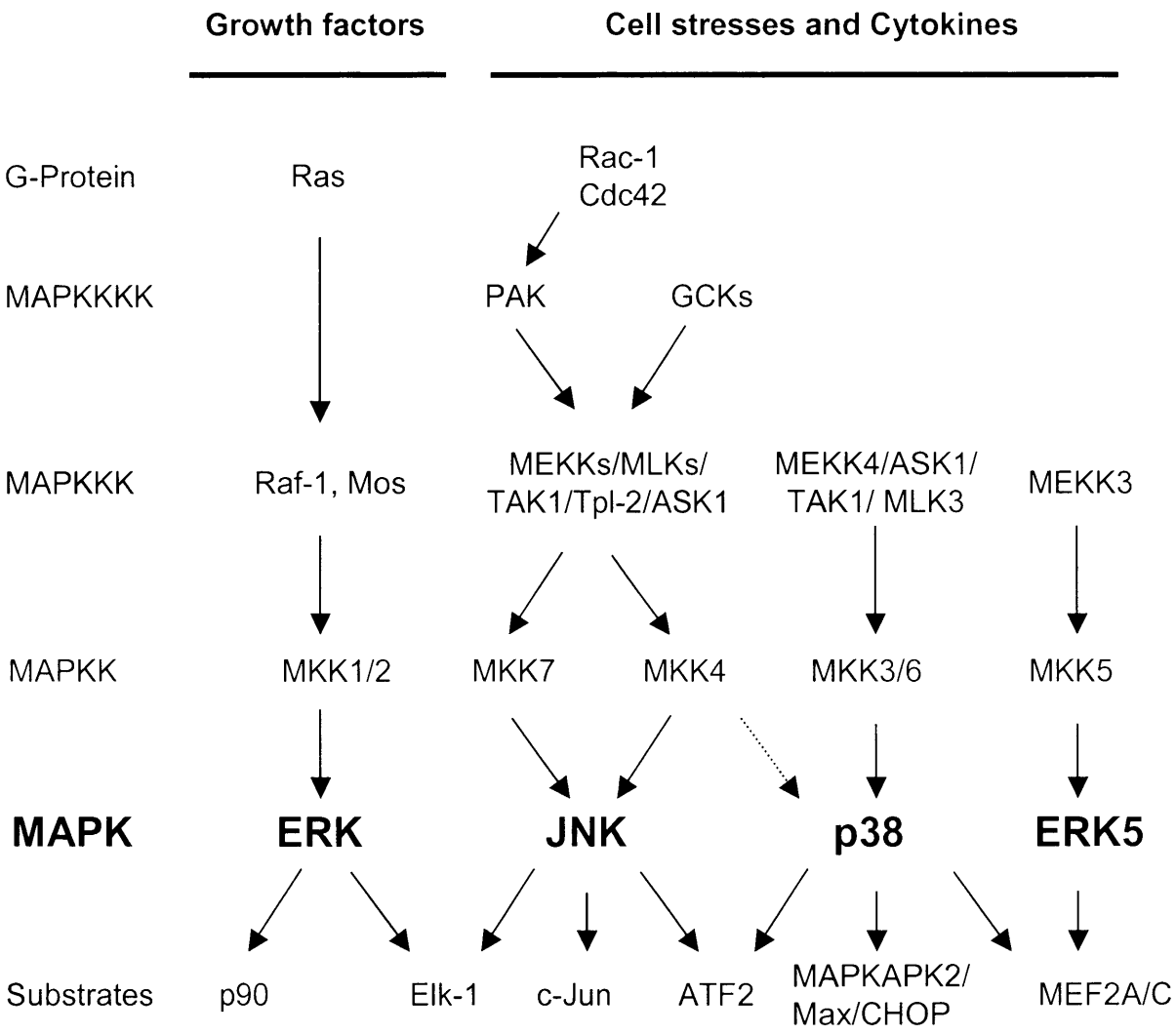

Fig. 1.2. Mammalian MAPK pathways, based on Kyriakis & Avruch (2001).

Four major MAPK signalling pathways have been identified so far. These are the ERK1/ERK2, JNK, p38 and ERK5 pathways. The MAPKs are activated by a specific set of MAPKKs. However, specificity becomes less apparent at levels upstream of MAPKKs. Each MAPK phosphorylates more than one substrate, and, some substrates are phosphorylated by more than one MAPK.

Table 1.1. Homologues of the JNK pathway components in different species

Mammals	*Yeast*	*C. elegans*	*D. melanogaster*
JNK	Hog1	JNK-1	Basket
MKK4	Pbs2	MKK4	D-MKK4
MKK7	Not known	MEK1, JKK1	Hemipterous
JIP-1	Not known	JIP	Not known
JIP-3	Not known	Not known	Sunday Driver
MEKK1	Ste11	Not known	D-MEKK1
HPK1	Ste20	Not known	Not known

and that it phosphorylated c-Jun on Ser^{63} and Ser^{73} in the N-terminus both *in vivo* and *in vitro* (Pulverer *et. al.*, 1991; Hibi *et. al.*, 1993). The kinase domain of JNK shares homology with ERK1 and ERK2, and with yeast MAPKs Hog1, Mpk1, Fus3 and Kss1 (Derijard *et. al.*, 1994).

The study of cloned JNK revealed that it was distinct from the ERKs by two characteristics (Derijard *et. al.*, 1994; Kyriakis *et. al.*, 1994): (a) it was activated maximally by cellular stresses such as heat shock, ionising radiation, inflammatory cytokines etc., but poorly by growth factors, and (b) it phosphorylated c-Jun at the N-terminal sites Ser^{63} and Ser^{73} and not the C-terminal site (Ser^{243}) phosphorylated by ERK2.

1.2.2. JNK isoforms

There are a total of 10 JNK isoforms encoded by three genes *jnk1*, *jnk2* and *jnk3* (Derijard *et. al.*, 1994; Sluss *et. al.*, 1994; Gupta *et. al.*, 1996). The *jnk1* and *jnk2* genes are ubiquitously expressed, whereas *jnk3* is selectively expressed in brain, heart and testis (Gupta *et. al.*, 1996; Davis, 2000). Transcripts derived from all three genes are alternatively spliced to create four JNK1 (α1, α2, β1and β2), four JNK2 (α1, α 2, β1and β2) and two JNK3 isoforms (α and β) (Gupta *et. al.*, 1996). The genes are processed at their 3' end, resulting in the expression of proteins with and without a carboxy-terminal extension to create both 46 kDa (JNK1α, JNK2α) and 55 kDa (JNK1β, JNK2β) isoforms. JNK3 has an extended N-terminus, hence the isoforms JNK3α (48-kDa) and JNK3β (57-kDa) are larger than the corresponding JNK1 and JNK2 proteins.

A second type of alternative splicing is restricted to *jnk1* and *jnk2*; it involves the selection of one of two alternative exons that encodes a part of the kinase domain. The resulting forms of JNK1 and JNK2 differ in their interactions with substrates, e.g. JNK2α isoforms bind c-Jun ~2-fold greater than ATF2, whereas JNK2β isoforms bind ATF2 ~2-fold greater than c-Jun (Gupta *et. al.*, 1996).

1.2.3. JNK substrates

JNK substrates can be divided into two categories: nuclear and cytoplasmic. Nuclear substrates include transcription factors such as c-Jun (Hibi *et. al.*, 1993), Jun D (Kallunki *et. al.*, 1996), activating transcription factor 2 (ATF2) (Gupta *et. al.*, 1995) and Elk-1 (Whitmarsh *et. al.*, 1995). Examples of the cytosolic substrates include B cell

lymphoma (Bcl) proteins Bcl-2 (Mundrell *et. al.*, 1997) and Bcl-xL (Fan *et. al.*, 2000), JNK interacting proteins 1 and 3 (JIP-1 and JIP-3) (Dickens *et. al.*, 1997; Kelkar *et. al.*, 2000), MLK2 (Phelan *et. al.*, 2001) and p53 (Buschmann *et. al.*, 2001). Substrate phosphorylation by JNK has diverse effects. For example, JNK phosphorylates the N-terminus of c-Jun at Ser^{63} and Ser^{73} (Pulverer *et. al.*, 1991; Derijard *et. al.*, 1994; Kyriakis *et. al.*, 1994), ATF2 at Thr^{69} and Ser^{71} (Gupta *et. al.*, 1995) and p53 at Thr^{81} (Buschmann *et. al.*, 2001). Phosphorylation of c-Jun, ATF2 and p53 enhances their transcriptional activity (Gupta *et. al.*, 1995; Buschmann *et. al.*, 2001) and protects them from ubiquitination and proteosome-dependent degradation *in vitro* and *in vivo* (Fuchs *et. al.*, 1997; Fuchs *et. al.*, 1998). In non-stressed cells, association of JNK with c-Jun, JunB, ATF2 and p53 targets these proteins for degradation by ubiquitination (Fuchs *et. al.*, 1997; Fuchs *et. al.*, 1998). Phosphorylation of Bcl-2 by JNK antagonises the anti-apoptotic activity of Bcl-2 (Maundrell *et. al.*, 1997).

Recently, a docking domain called the *CD domain* was found to be present in the substrates and upstream activators of ERK, JNK and p38 (Tanoue *et. al.*, 2000). This domain is located near the C-terminal region outside the catalytic domain and is thought to play a crucial role in promoting specificity, efficiency and accuracy of substrate phosphorylation (Sharrocks, Yang & Galanis, 2000). For example, the δ-domain of c-Jun acts as a docking site for JNK (Derijard *et. al.*, 1994). The binding of JNK to the docking site is thought to result in an increase in the local concentration of the enzyme and, hence, an increase in the efficiency of substrate phosphorylation (Karin, 1995). Even though the viral homologue of c-Jun, v-Jun, has the phosphoacceptor Ser^{63} and Ser^{73} sites, it is not a good JNK substrate because it lacks the docking δ-domain (Derijard *et. al.*, 1994). The specificity of the interaction of JIP-1 and MKK7 with JNK is due to the presence of JNK-specific docking domains in JIP-1 and MKK7 (Sharrocks, Yang & Galanis, 2000).

1.3. ACTIVATION OF JNK BY UPSTREAM KINASES

As the JNK pathway conforms to the three-kinase modular architecture (Fig. 1.1), JNK is activated by MKKs, which in turn are activated by MKKKs.

1.3.1. Activation by MKKs

The activation of JNK requires the dual phosphorylation of Thr^{183} and Tyr^{185} (Derijard *et. al.*, 1994), and this is accomplished by dual specificity kinases MKK4 and MKK7 (Fig. 1.2).

MKK4 (also known as SAPK/ERK kinase 1 [SEK1] and JNK kinase 1 [JNKK1]), was independently cloned by two groups (Sanchez *et. al.*, 1994; Derijard *et. al.*, 1995). Homologues of MKK4 have been discovered in yeast, mammals, *C. elegans* and *D. melanogaster* (Table 1.1) (Derijard *et. al.*, 1995; Noselli, 1998; Widmann *et. al.*, 1999; Villanueva *et. al.*, 2001). The catalytic domain of human MKK4 shares ~40% amino acid sequence identity with the catalytic domains of Pbs2, MKK1 and MKK2 (Derijard *et. al.*, 1995). The most divergent region is the non-catalytic region at the amino terminus, and it is this region that confers specificity in mediating interactions with MEKK1 and JNK (Xia *et. al.*, 1998). MKK4 is phosphorylated by MEKK1 at Ser^{257} and Thr^{261}, and these sites are conserved in other MKKs, suggesting a common mechanism of regulation (Yan *et. al.*, 1994). Endogenous MKK4 localises to both the cytoplasm and the nucleus (Tournier *et. al.*, 1999).

MKK4 is a preferential activator of JNK and a partial activator of p38 *in vivo* and *in vitro* (Sanchez *et. al.*, 1994; Derijard *et. al.*, 1995; Lin *et. al.*, 1995). Genetic analyses of MKK4 function in mice has demonstrated that, homozygous deficiency of MKK4 is embryonically lethal due to defects in JNK signalling and AP-1 transcriptional activity, and that MKK4 is required for liver formation and interleukin-2 production in T lymphocytes (Nishina *et. al.*, 1997;.Yang *et. al.*, 1997; Nishina *et. al.*, 1999). The physiological significance of p38 activation by MKK4 is unclear.

The cloning and the identification of MKK7 (also called JNK kinase 2 [JNKK2]) as a specific JNK activator was independently reported by several groups (Holland *et. al.*, 1997; Lu, Nemato & Lin, 1997; Moriguchi *et. al.*, 1997; Tournier *et. al.*, 1997; Wu *et. al.*, 1997;Yao *et. al.*, 1997; Foltz *et. al.*, 1998). MKK7 is a homologue of *Drosophila hemipterous (hep)* and *C. elegans jkk-1* and *mek-1*, which have been defined by

biochemical and genetic analyses as JNK activators (Table 1.1) (Riesgo-Escovar *et. al.*, 1996; Sluss *et. al.*, 1996; Holland *et. al.*, 1997; Villanueva *et. al.*, 2001).

The specificity of MKK7 as an activator of JNK but not p38 has been established by biochemical and genetic approaches. For example, ectopic expression of MKK7 functionally complemented *Drosophia hep* mutants with much more efficiency than MKK4 (Holland *et. al.*, 1997). Overexpressed and recombinant wild type MKK7 specifically activates JNK in the absence of any stimulus (Foltz *et. al.*, 1997; Holland *et. al.*, 1997; Moriguchi *et.al.*, 1997; Wu *et. al.*, 1997), in contrast to MKK4 which activates both JNK and p38 (Derijard *et. al.*, 1995; Moriguchi *et.al.*, 1997). Analysis of wild-type and *Mkk7*$^{-/-}$ mouse embryonic fibroblasts (MEFs) suggests that MKK7 is essential for cytokine stimulation of JNK activity (Tournier *et. al.*, 2001).

MKK7 is widely expressed in different tissues (Holland *et. al.*, 1997; Tournier *et. al.*, 1997). Endogenous MKK7 is distributed in the cytoplasm as well as the nucleus (Tournier *et. al.*, 1999). Six MKK7 isoforms with different amino and carboxy termini have been identified, which arise as a result of alternative splicing and the utilisation of different promoters (Tournier *et. al.*, 1999). Differential promoter usage yields three isoforms, α, β and γ, each of which are alternatively spliced at the carboxy terminal end to give two further isoforms (termed 1 and 2). Biochemical analysis of these isoforms show that the β and the γ isoforms are more active than the α isoforms under both basal conditions and following activation because of the presence of an amino terminal extension in the β and the γ isoforms that is capable of binding to JNK on its own (Tournier *et. al.*, 1999).

Recent evidence suggests that MKK4 and MKK7 differentially phosphorylate the TPY motif in JNK and that the concerted action of both MKK4 and MKK7 is required for efficient JNK activation (discussed in section 1.3.4).

1.3.2. Activation by MKKKs

MKK4 and/or MKK7 are activated by a large group of MKKKs. These include the MAP ERK kinase kinase group (MEKK1-4), mixed lineage kinase group (MLK1-3, DLK and LZK), apoptosis signal regulating kinase 1 (ASK1), transforming growth factor β activated kinase 1 (TAK1) and tumour progression locus 2 (TPL2) (Davis, 2000; Fig. 1.2). The roles of MEKKs, MLKs and ASK1 in the activation of the JNK pathway are discussed.

1.3.2.1. MAP ERK kinase kinases (MEKKs)

The MEKK proteins, MEKK1, 2, 3 and 4, range from 80-180 kDa in size, with their kinase domains located in the C-terminus (Widmann *et. al.*, 1998). The common feature of the MEKKs is their conserved catalytic domain that is homologous to the Ste11 kinase of *S. cerevisiae* and D-MEKK1 of *Drosophila* (Table 1.1) (Lange-Carter *et. al.*, 1993; Blank *et. al.*, 1996; Gerwins, Blank & Johnson, 1997; Inoue *et. al.*, 2001).

Transient transfection-based studies have shown that MEKK1 activates JNK through MKK4 (Xia *et. al.*, 1998), while MEKK2 and MEKK3 activate JNK through MKK4 and MKK7 (Deacon & Blank, 1997; Deacon & Blank, 1999; Cheng *et. al.*, 2000). An analysis of the wild-type and *Mekk1*$^{-/-}$ embryonic stem (ES) cells suggests that MEKK1 is essential for JNK activation in response to microtubule disruption, cytokines (TNF-α and IL-1) and cold shock (Yujiri *et. al.*, 1998; Xia *et. al.*, 2000; Yujiri *et. al.*, 2000). Also, MEKK1-induced JNK activity seems to contribute to the serum-induced migration of wild type ES cells, as this phenotype is not observed in *Mekk1*$^{-/-}$ ES cells (Xia *et. al.*, 2000). The role of MEKK1 in apoptosis and cell survival is discussed in sections 1.7.1 and 1.7.5.

1.3.2.2. Mixed lineage kinases (MLKs)

The mixed lineage kinases (MLKs) are a family of serine/threonine kinases that consist of two groups: the highly conserved MLK1, MLK2 (also called MKN28 cell-derived serine/threonine kinase [MST]) and MLK3 (also called SH3 domain-containing proline-rich kinase [SPRK] or protein tyrosine kinase 1 [PTK1]), and the less conserved dual leucine zipper kinase (DLK, also known as MAPK upstream kinase [MUK] or zipper-containing kinase [ZPK]) and leucine zipper kinase (LZK) (Kyriakis & Avruch, 2001). With the exception of MLK1, all MLK family members have been shown to function as MKKKs that predominantly activate the JNK pathway.

Structurally, the MLKs share a common configuration, containing an N-terminal kinase domain that is followed by one to two leucine zippers, a Cdc42/Rac interaction and binding (CRIB) domain and a C-terminal proline rich domain with one SH3 domain. Dimerisation via leucine zippers has been shown to be essential for the activation of MLK3, DLK and LZK by autophosphorylation and for the subsequent activation of the JNK pathway (Nihalani, Merrit & Holzman, 2000; Vacratsis & Gallo, 2000; Ikeda *et. al.*, 2001).

MLK3 is expressed in a wide variety of tissues such as brain, thyroid and thymus (Ing *et. al.*, 1994). MLK2 is selectively expressed in brain and skeletal muscles (Dorrow *et. al.*, 1995), while DLK expression is restricted to brain (Holzman, Merritt & Fan, 1994). MLK2, MLK3 and LZK activate JNK via MKK4 and MKK7 (Tibbles *et. al.*, 1996; Hirai *et. al.*, 1998; Whitmarsh *et. al.*, 1998; Ikeda *et. al.*, 2001). However, MLK2 shows preferential association with MKK7 (Hirai *et. al.*, 1998). In contrast, DLK utilises only MKK7 as a substrate (Merritt *et. al.*, 1999; Ikeda *et. al.*, 2001). The activation of JNK by MLK3, DLK and LZK via MKK7 is probably mediated by their interaction with JIPs (Whitmarsh *et. al.*, 1998; Yasuda *et. al.*, 1999; Kelkar *et. al.*, 2000; Ikeda *et. al.*, 2001; discussed later in section 1.5.2.1). It should be noted that MLK3 and DLK can also activate p38 (Fan *et. al.*, 1996; Tibbles *et. al.*, 1996). Recently, MLK3 was also shown to activate the nuclear factor-κB (NF-κB) pathway (Hehner *et. al.*, 2000).

1.3.2.3. Apoptosis signal regulating kinase 1 (ASK1)

Apoptosis signal regulating kinase 1 (ASK1; also called MKKK5) is a MKKK that activates both JNK and p38 (Ichijo *et. al.* 1997). It shares ~42% amino acid identity to the catalytic domain of MEKK1, MEKK2 and MEKK3 (Wang *et. al.*, 1996). It is widely expressed in human tissues and is activated by oxidant stressors such as hydrogen peroxide (H_2O_2) and cytokines such as TNF (Ichijo *et. al.*, 1997; Gotoh & Cooper, 1998). Overexpression of wild-type ASK1 or the constitutively active kinase form of ASK1 induces apoptosis in several cell lines (Ichijo *et. al.*, 1997; Kanamoto *et. al.*, 2000). Experiments with *Ask1*$^{-/-}$ MEF cells have shown that ASK1 is required for apoptosis induced by sustained JNK/p38 activation in response to TNF-α or H_2O_2 (Tobiume *et. al.*, 2001). Furthermore, the ASK1-JNK/p38 pathway also mediates apoptosis induced by genotoxic agents such as cisplatin (Chen, Z. *et. al.*, 1999). ASK1 has been shown to execute its apoptosis-inducing function through both caspase-dependent and caspase-independent pathways (Hatai *et. al.*, 2000; Charette *et. al.*, 2001; Matsuzawa & Ichijo, 2001).

Several proteins have been identified that interact with ASK1. It has been postulated that cell survival is ensured by inhibiting ASK1 activity in resting cells because of its interactions with proteins such as thioredoxin (Saitoh *et. al.*, 1998), 14-3-3 (Zhang, Chen & Fu, 1999) and Akt/PKB (Kim, A. *et. al.*, 2001). The activation of JNK/p38 by ASK1 requires the interaction of ASK1 with a different set of proteins. For

example, ASK1 interacts with TNF-receptor associated factors (TRAFs) 1, 2, 3, 5 and 6, and the TRAF2-ASK1 interaction is essential for TNF-α-induced ASK1 and JNK activation and apoptosis (Nishitoh *et. al.*, 1998; Hoeflich *et. al.*, 1999). The production of ROS by TNF-α results in the dissociation of thioredoxin-ASK1 complexes, dimerisation of ASK1 and the formation of TRAF2-ASK1 complexes, which then mediate JNK activation (Gotoh & Cooper, 1998; Liu *et. al.*, 2000). Fas-induced activation of ASK1 requires the interaction of ASK1 with Daxx (Chang *et. al.*, 1998). Recently, the interaction of ASK1 with the scaffold protein β-arrestin 2 was shown to activate the JNK pathway in response to the stimulation of the G-protein coupled receptors (GPCRs) by agonistic stimuli (MacDonald *et. al.*, 2000).

Of the MKKKs, none have been shown to be a specific JNK activator. MEKK1 can activate both JNK and NF-κB, while MEKK2, MEKK3, MEKK4, MLKs, ASK1, TAK1 and TPL2 can activate both JNK and p38 (reviewed in Karin & Delhase, 1998 and Kyriakis & Avruch, 2001).

1.3.3. Activation by germinal centre kinases (GCKs) and small GTPases

Germinal centre kinases (GCKs) are the mammalian homologues of yeast Ste20p, a MKKKK that activates Ste11, a MKKK involved in the pheromone response pathway (Kyriakis, 1999). GCKs are subdivided into two groups based on overall sequence conservation and function. Group I GCKs have a similar kinase domain and carboxy terminal domain (CTD) structure and are activators of JNK (Burbelo *et. al.*, 1995); e.g. GCK, human progenitor kinase 1 (HPK1), kinase homologous to Ste20 (KHS), GCK-like kinase (GLK) and Nck-interacting kinase (NIK). Group II GCKs are more closely related to the yeast GCK Sps1p and, although they are activated *in vivo* by stress, they do not activate any known MAPK pathways. Examples of group II GCKs include Ste20-like oxidant stress-activated kinase 1 (SOK1), kinase responsive to stress 1 (Krs1), mammalian sterile twenty-like kinases 1 and 2 (MST1 and 2) and lymphocyte-oriented kinase (LOK) (Kyriakis, 1999).

Of the group I GCKs, HPK1 has been shown to activate the JNK pathway by phosphorylating MEKK1 or MLK3 (Hu *et. al.*, 1996; Kiefer *et. al.*, 1996). HPK1 activates JNK through other mechanisms also. For example, activation by TGFβ was demonstrated to activate HPK1-TAK1-MKK4-JNK cascade (Wang *et. al.*, 1997; Zhou

et. al., 1999). HPK1 has also been shown to activate the NF-κB pathway (Hu *et. al.*, 1999). The specificity of HPK1 in activating the JNK pathway may result from its interaction with the scaffold protein JIP-1 (Whitmarsh *et. al.*, 1998; section 1.5.2.1).

JNK activation via HPK1 appears to be modulated by the interaction of HPK1 with adaptor proteins or kinases in Jurkat T cells. For example, it was shown that genotoxic stress induced the interaction of HPK1 with the c-Abl tyrosine kinase, which resulted in HPK1 phosphorylation and the stimulation of HPK1 kinase activity, and the c-Abl-HPK1 interaction was found to be essential for the activation of the JNK pathway (Ito *et. al.*, 2001). The interaction of HPK1 with Crk and CrkL has also been shown to be essential for JNK activation (Ling *et. al.*, 1999). Furthermore, the interaction of HPK1 with Grap2, an adaptor protein that is specifically expressed in lymphoid tissues, has also been shown to be essential for JNK activation in T cells (Ma *et. al.*, 2001).

Group I GCK subfamily members other than HPK1 are thought to activate the JNK pathway independently of their kinase activity in response to TNF-α by interacting with MEKK1 (Dan, Watanabe & Kusumi, 2001).

Among the components proximal to the GCKs and MKKKs, monomeric GTPases of the Ras superfamily are potent activators of the JNK pathway. For example, RhoA activates JNK in certain cell types such as HEK293. Rho guanine nucleotide exchange factors (GEFs) such as FGD1 activate JNK by recruiting Rac and Cdc42. Rac1/Cdc42 activates the JNK pathway through effector kinases such as p21-activated kinases (PAKs), plenty of SH3 domains (POSH), MEKK1, MEKK4, MLK2 and MLK3 (Kyriakis & Avruch, 2001). Recent evidence suggests that PAKs, MEKK1 and MEKK4 interact with both Rac1 and Cdc42; MLK2 and MLK3 are likely effectors for Cdc42, while POSH is a candidate adaptor protein that couples Rac1 to the JNK pathway (Kyriakis & Avruch, 2001).

1.3.4. Regulation of the JNK pathway

Evidence has accumulated that the activation of MKK4 and MKK7, and hence JNK, is regulated by extracellular stimuli, MKKKs and Ste-20 like kinases. Selective activation of MKK7 is observed in response to cytokines TNF-α and IL-1α, while UV-C radiation and anisomycin preferentially activate MKK4 (Moriguchi *et. al.*, 1997; Tournier *et. al.*, 1999; Tournier *et. al.*, 2001). MEKK1 is a potent activator of MKK7 isoforms, while MEKK3 is a potent activator of MKK4 isoforms (Tournier *et. al.*,

1999). Isoform-specific regulation of the activation of MKK4 and MKK7 by the Ste-20-like kinases is also observed: HPK1 preferentially activates MKK7α1 and MKK7α2, while KHS potently activates MKK4β (Tournier *et. al.*, 1999). This suggests that MKK4 and MKK7 may have evolved to sense different types of environmental stresses.

JNK activation is further regulated by differential inputs from MKK4 and MKK7. Recent evidence suggests that the concerted action of both MKK4 and MKK7 is required for the full activation of JNK. MKK4 and MKK7, when present individually at low concentrations, are comparatively poor JNK activators *in vitro*. However, MKK4 and MKK7 synergistically activate JNK ~100 fold when added together (Lawler *et. al.*, 1998). These observations were recently confirmed by *in vivo* analysis. *Mkk4*$^{-/-}$ or *Mkk7*$^{-/-}$ MEFs show ~50% reduction in JNK activation in response to UV or anisomycin compared to their wild-type counterparts, suggesting that MKK4 and MKK7 contribute equally to UV- and anisomycin-induced JNK activation *in vivo* (Tournier *et. al.*, 2001).

MKK4 and MKK7 display marked preferences for the tyrosine and the threonine residue in the TPY motif in the JNK1 isoform. MKK4 preferentially phosphorylates Tyr^{185} but weakly phosphorylates Thr^{183} in JNK1, whereas MKK7 phosphorylates Thr^{183} more strongly than Tyr^{185} *in vitro* (Lawler *et. al.*, 1998), and this is true for all JNK isoforms (Fleming *et. al.*, 2000). Tyr^{185} phosphorylation of JNK1 was lost in *Mkk4*$^{-}$ ES cells in response to a variety of stress stimuli (Wada *et. al.*, 2001). Co-expression of MKK4-JNK1 resulted in Tyr phosphorylation of JNK1, while the co-expression of MKK7-JNK1 resulted in Thr phosphorylation of JNK1, as detected by anti-phospho-Tyr or anti-phospho-Thr antibodies, and the resultant JNK activity was low in either case compared to the JNK activity obtained when MKK4-MKK7-JNK1 were co-expressed (Wada *et. al.*, 2001).

The JNK pathway is additionally regulated by scaffold proteins, as discussed below.

1.4. ASSEMBLY OF JNK SIGNALLING MODULES BY SCAFFOLD PROTEINS

1.4.1. Introduction

In mammalian cells, 20 GCKs, 14 MKKKs, 7 MKKs and 17 MAPKs; of these, some GCKs, MKKKs, MKKs and MAPKs have apparently redundant functions. This is thought to provide the MAPK module the flexibility to respond to a wide range of stimuli (Garrington & Johnson, 1999; Dan, Watanabe & Kusumi, 2001). Some MKKs can activate two MAPKs, and conversely a single MAPK can be activated by more than one MKK, MKKK or MKKKK. For example, MEKK2, MEKK3, MEKK4, MLKs, ASK1, TAK1 and TPL2 can activate both JNK and p38, while JNK can be activated by GCKs, MEKKs, MLKs, PAK, TAK and TPL2 (Kyriakis & Avruch, 2001). This raises the issue of signalling specificity: how do protein kinases with relatively broad specificities achieve fidelity in transducing distinct biological responses, particularly MKKKs that can phosphorylate and activate multiple MKKs?

Evidence suggests that specificity is achieved, in part, through the formation of protein complexes involving the interactions of kinases with a non-enzymatic scaffold protein or interaction between kinases of a single MAPK module (Davis, 2000). Examples of scaffold proteins include JNK interacting proteins (JIPs) and β-arrestin 2 for the JNK pathway, MEK partner 1 (MP1) and kinase suppressor of Ras (KSR) for the ERK pathway in mammals, and Ste5 for the pheromone mating-response pathway in yeast (Whitmarsh & Davis, 1998; Garrington & Johnson, 1999). The presence of scaffold proteins results in the activation of the pathway. For example, KSR-1 binds to both MEK1 and ERK and enhances the kinase activity of Raf-1. This role of KSR-1 is independent from its kinase activity (Garrington & Johnson, 1999).

Examples of kinases mediating JNK signalling specificity in the absence of a scaffold protein include MKK4 and MEKK2. The roles of JIPs, β-arrestin 2, MKK4 and MEKK2 in specificity determination are discussed below.

1.4.2. The JIP group of scaffold proteins

The JIP family of scaffold proteins consist of three members: JIP-1, JIP-2 and JIP-3. All three members have been established as scaffolds for the JNK pathway by

biochemical analysis (Whitmarsh *et. al.*, 1998; Yasuda *et. al.*, 1999; Kelkar *et. al.*, 2000). The role of JIP-1 as the JNK pathway scaffold is additionally supported by genetic analysis (Whitmarsh *et. al.*, 2001). JIP family proteins have been identified in mammals (human, mouse and rat), *D. melanogaster* and *C. elegans*, suggesting an evolutionary conserved role for JIPs (Table 1.1) (Dickens *et. al.*, 1997; Bonny, Nicod & Waeber, 1998; Meyer, Liu & Margolis, 1999; Yasuda *et. al.*, 1999; Bowman *et. al.*, 2000).

1.4.2.1. JIP-1 and JIP-2 proteins

Subcellular localisation of JNK in quiescent and stress stimulated cells provided the first clue that anchor or scaffold protein(s) may be involved in the regulation of the JNK pathway. In quiescent cells, JNK is located in the cytoplasm and the nucleus, but the activation of JNK is associated with the accumulation of JNK in the nucleus (Cavigelli *et. al.*, 1995). It was therefore possible that anchor proteins may be responsible for retaining JNK in the cytoplasm in the absence of any stimulus. JNK-interacting protein 1 (JIP-1) was identified in a two-hybrid screen as a protein that interacted with JNK (Dickens *et. al.*, 1997). JIP-1 was independently identified as a putative transcription factor that bound to the GLUT2 promoter, and was termed as islet brain 1 (IB1) (Bonny, Nicod & Waeber, 1998). Screening a human brain λZAPII cDNA library with a JIP-1 cDNA fragment as a probe led to the discovery of JIP-2 (Yasuda *et. al.*, 1999).

Currently, two isoforms of JIP-1 in mouse (mJIP-1a and –1b) and in rat (rJIP-1b and –1c), and two isoforms of JIP-2 in mouse (mJIP-2a and –2b) and one isoform in rat (rJIP-2a) generated due to alternative splicing are known (Kim *et. al.*, 1999). The founding member of the JIP family of proteins, JIP-1, cloned by Dickens *et. al.* (1997) lacks a 47 amino acid region at its C-terminus and this isoform appears to be present only in mouse. This clone is similar to the JIP-1a isoform cloned by Kim *et. al.* (1999), and is likely to be a rare splice variant. The full-length JIP-1 clone is the JIP-1b isoform, which is similar to IB1 (Bonny, Nicod & Waeber, 1998; Kim *et. al.*, 1999).

Structurally, JIP-1b and JIP-2 contain a JNK binding domain (JBD), a Src homology 3 (SH3) domain and a PTB domain, as shown in Fig. 1.3 (Bonny, Nicod & Waeber, 1998; Yasuda *et. al.*, 1999). JIP-1 is preferentially expressed in brain, kidney, pancreas and testis as well as to a varying degree in other tissues, whereas JIP-2 is almost exclusively expressed in brain (Dickens *et. al.*, 1997; Bonny, Nicod & Waeber,

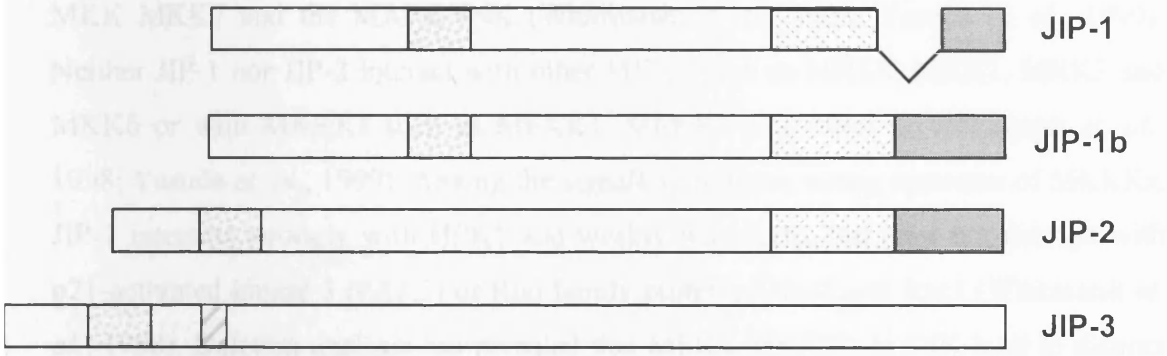

Fig. 1.3. The domain structure of JIP family proteins.

JIP-1b and JIP-2 contain, in the N- to C-terminal direction, a JNK binding domain, an SH3 domain and a PTB domain. JIP-1 contains partial SH3 and PTB domains. JIP-3 contains a JNK binding domain but lacks SH3 and PTB domains. Instead, it contains a leucine zipper domain at the N-terminus.

SH3 = src homology 3; PTB = phosphotyrosine binding domain.

JNK binding domain

Leucine zipper

SH3 domain

PTB domain

1998; Kim *et. al.*, 1999; Yasuda *et. al.*, 1999). The subcellular localisation of endogenous JIP-1 appears to vary depending on the cell type. Endogenous JIP-1 is located in the cytoplasm of Rin5F and βTC3 cells (rat pancreatic cell lines), PC-12 cells (a rat phaeochromocytoma cell line) and N1E-115 cells (a mouse neuroblastoma cell line) (Bonny, Nicod & Waeber, 1998; Meyer, Liu & Margolis, 1999; Yasuda *et. al.*, 1999), while endogenous JIP-1 is located in the nucleus of cerebellar granule cells and βTC3 cells (Bonny, Nicod & Waeber, 1998; Coffey *et. al.*, 2000).

The function of JIP-1 and JIP-2 as scaffold proteins for the JNK pathway was initially proposed on the basis of co-immunoprecipitation/western blot analysis of co-expressed proteins in transfected cells. Thus it has been shown that both JIP-1 and JIP-2 can bind elements at all three levels of the core JNK module: the MKKK MLKs, the MKK MKK7 and the MAPK JNK (Whitmarsh *et. al.*, 1998; Yasuda *et. al.*, 1999). Neither JIP-1 nor JIP-2 interact with other MKKs such as MKK4, MKK1, MKK3 and MKK6 or with MKKKs such as MEKK1, MEKK4 and c-Raf-1 (Whitmarsh *et. al.*, 1998; Yasuda *et. al.*, 1999). Among the signalling proteins acting upstream of MKKKs, JIP-1 interacts strongly with HPK1 and weakly with KHS, but does not interact with p21-activated kinase 3 (PAK3) or Rho family proteins Cdc42 and Rac1 (Whitmarsh *et. al.*, 1998). Deletion analysis has revealed that MLKs, MKK7 and JNK bind to distinct regions of JIP-1/JIP-2, and full-length JIP-1/JIP-2 potentiates JNK activation by MLKs (Whitmarsh *et. al.*, 1998; Yasuda *et. al.*, 1999). Based on these observations, JIP proteins were proposed to act as scaffold proteins for the JNK pathway (Fig. 1.4A). However, recent evidence suggests that JIP-1 does not bind simultaneously to MLK3 and JNK (Nihalani *et. al.*, 2001).

The requirement of JIP-1 as a scaffold for the JNK pathway *in vivo* was confirmed by a recent study. In response to the excitotoxic stress agent kainic acid, *Jip1*$^{-/-}$ hippocampal neurons failed to activate JNK compared to the wild-type hippocampal neurons (Whitmarsh *et. al.*, 2001). Furthermore, in hippocampal neurons stimulated with oxygen and glucose deprivation (OGD), endogenous JIP-1 was re-located from the neurites to the perinuclear region, the site where endogenous activated JNK was present, and JNK activation resulted in increased co-immunoprecipitation of JNK with JIP-1 (Whitmarsh *et. al.*, 2001). Taken together, these results suggest that endogenous JIP-1 is required *in vivo* for the functioning of the JNK pathway in neurons exposed to stress (Whitmarsh *et. al.*, 2001). However, another JIP-1 knockout study showed that *Jip1*$^{-/-}$ mice died embryonically due to increased apoptosis, suggesting that JIP-1 is

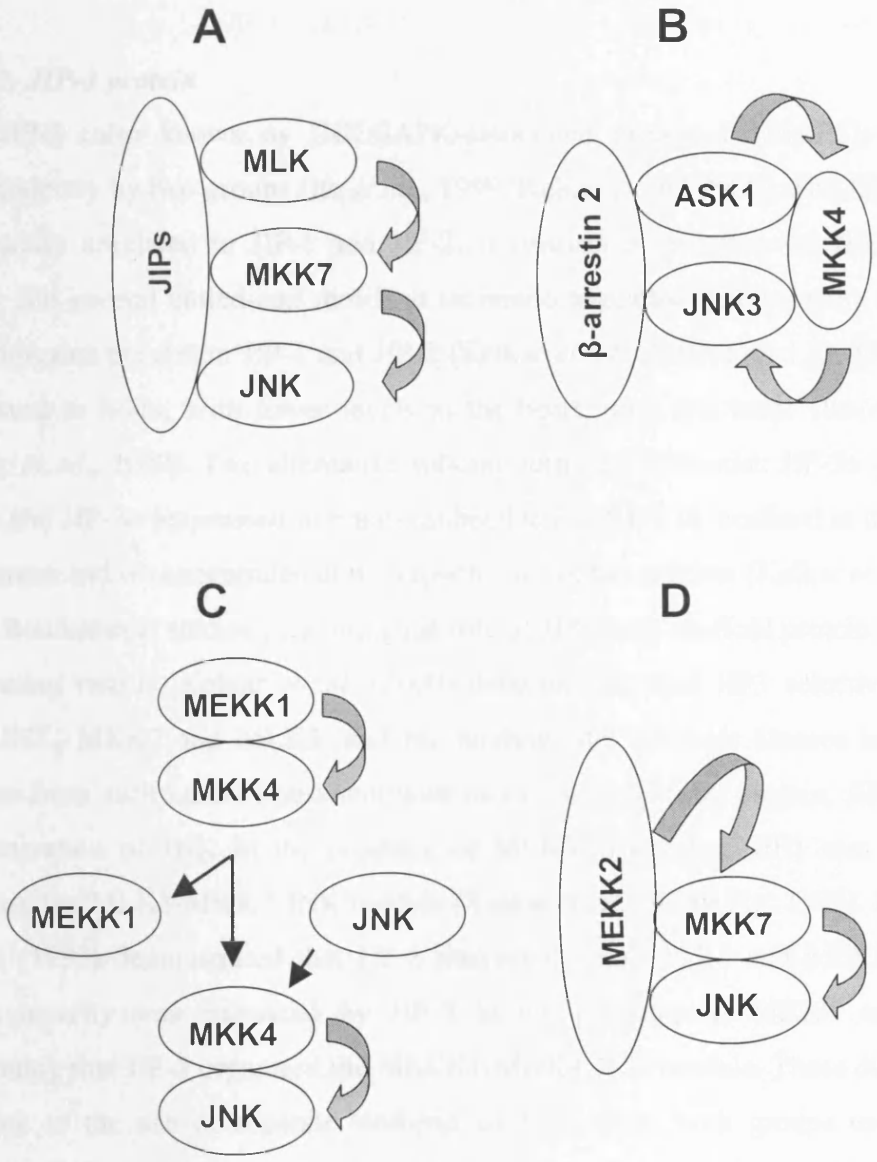

Fig. 1.4. Schematic diagram of postulated JNK modules.

The following modules have been proposed to impart specificity to the JNK signal transduction pathway:

A) The JIP-MLK-MKK7-JNK module;
B) β-arrestin 2-ASK1-MKK4-JNK3 module;
C) The sequential binary MEKK1-MKK4 and MKK4-JNK complexes; and
D) The MEKK2-MKK7-JNK module.
For details please see the text.

required to suppress apoptosis during early embryonic development (Thompson *et. al.*, 2001). The issue of whether JIP-1 plays an anti- or pro-apoptotic during embryogenesis is unresolved at present.

1.4.2.2. JIP-3 protein

JIP-3 (also known as JNK/SAPK-associated protein 1 [JSAP1]) was cloned independently by two groups (Ito *et. al.*, 1999; Kelkar *et. al.*, 2000). The JIP-3 protein is structurally unrelated to JIP-1 and JIP-2; it consists of a conserved JBD, a leucine-zipper and several coiled-coil motifs at its amino terminus, and lacks the SH3 and the PTB domains present in JIP-1 and JIP-2 (Kelkar *et. al.*, 2000; Fig. 1.3). JIP-3 is highly expressed in brain, with lower levels in the heart, lung and testis (Ito *et. al.*, 1999; Kelkar *et. al.*, 2000). Two alternative splicing forms of JIP3 exist: JIP-3a (expressed in heart) and JIP-3b (expressed in brain). Subcellularly, JIP-3 is localised in the cytoplasm of neurons and is concentrated at the growth cone of the neurites (Kelkar *et. al.*, 2000).

Biochemical studies examining the role of JIP-3 as a scaffold protein have yielded conflicting results. Kelkar *et. al.* (2000) demonstrated that JIP3 selectively interacts with JNK, MKK7 and MLK3, and the binding sites of these kinases in JIP-3 were distinct from each other. Consistent with its role as a scaffold protein, JIP-3 increased the activation of JNK in the presence of MLK3. Therefore, JIP3 was proposed to organise the MLK3-MKK7-JNK module (Kelkar *et. al.*, 2000; Fig. 1.4A). However, Ito *et. al.* (1999) demonstrated that JIP-3 interacted with MKK4 and MEKK1, and that JNK3 activity was enhanced by JIP-3 in the presence of MKK4 and MEKK1, suggesting that JIP-3 organised the MEKK1-MKK4-JNK module. These differences are not due to the use of separate isoforms of JIP3, since both groups used the same isoform, JIP3a (Kyriakis & Avruch, 2001). The reason(s) for these differences are not known.

JIP-1, JIP-2 and JIP-3 can self-associate to form homo-oligomers, and JIP-2 can also form hetero-oligomers with JIP-1 and JIP-3 (Yasuda *et. al.*, 1999; Kelkar *et. al.*, 2000). The mechanism of the regulation of the JNK pathway by JIP oligomerisation is not known, but it has been proposed that the JIP oligomer-associated JNK kinase cascade may function *in trans* rather than *in cis* (Davis, 2000). Both JIP-1 and JIP-3 are phosphorylated by JNK, however its functional significance is unclear (Dickens *et. al.*, 1997; Kelkar *et. al.*, 2000).

1.4.2.3. JIPs scaffolds as cargoes in kinesin-dependent axonal transport in neurons

Recent biochemical and genetic analysis suggest that JIP family members are required for the microtubule-dependent axonal transport in neurons (Bowman *et. al.*, 2000; Verhey *et. al.*, 2001). Bowman *et. al.* (2000) identified the *sunday driver* (*syd*) gene in *Drosophila*, in a genetic screen for axonal transport mutant larvae that exhibited the 'tail-flipping' phenotype previously described for the mutants lacking subunits of dyenin and kinesin-I. For clarity, the SYD protein will be referred as JIP-3 in the subsequent sections. Using the yeast two-hybrid procedure with the tetratricopeptide repeat (TPR) motifs of kinesin light chain (KLC) as the bait, Verhey *et. al.* (2001) discovered that JIP-1, JIP-2 and JIP-3 interact directly with kinesin. The interaction between JIPs and KLC *in vivo* has been confirmed by coimmunoprecipitation analysis and immunolocalisation of ectopically expressed JIP-3 and kinesin (Bowman *et. al.*, 2000; Verhey *et. al.*, 2001; Whitmarsh *et. al.*, 2001), and also *in vitro* by GST pull-down assays (Bowman *et. al.*, 2000).

Endogenous JIP-1, DLK and ApoER2 were also detected in the kinesin immunoprecipitates, suggesting that JIP-1, with its associated proteins, is a cargo for kinesin (Verhey *et. al.*, 2001). Endogenous and transfected JIP-1 was demonstrated to be localised to the tip of the neurites (Whitmarsh *et. al.*, 2001; Verhey *et. al.*, 2001), but in contrast, overexpression of a JIP-1 mutant with a deletion of the 11 C-terminal residues that are essential for interaction with kinesin exhibited diffuse localisation throughout the cell, suggesting that the interaction of JIP-1 with kinesin is essential for its proper subcellular localisation (Verhey *et. al.*, 2001). Also, it has been proposed that the cargo is preassembled before being transported by kinesin, because the expression of dominant negative kinesin caused endogenous JIP-1 and DLK to localise throughout the cell (Verhey *et. al.*, 2001).

1.4.2.4. Interactions of JIPs with other proteins

The PTB domain of JIP-1 has been shown to interact with the guanine nucleotide exchange factor (GEF) p190rhoGEF (Meyer, Liu & Margolis, 1999), ApoER2, a low density lipoprotein (LDL) receptor for the extracellular matrix protein Reelin (Stockinger *et. al.*, 2000) and amyloid precursor protein (APP) (Matsuda *et. al.*, 2001). The interaction of JIP-1 with p190rhoGEF has been proposed to localise rhoGEF near its target rhoA to initiate neurite retraction upon the proper signalling cue (Meyer, Liu & Margolis, 1999). The functional significance of the JIP-1-ApoER2 interaction is not

known; however JIP-1 gene disruption studies suggest that JIP-1 is not essential for Reelin/ApoER2 function during brain development (Whitmarsh *et. al.*, 2001). JIP-1 was shown to interact with APP, however the physiological significance of this interaction is unknown (Matsuda *et. al.*, 2001).

1.4.3. β-arrestin 2: A scaffold for the ASK1-MKK4-JNK3 module

G-protein coupled receptors (GPCRs) are a family of cell surface molecules involved in normal cell proliferation and differentiation (Marinissen & Gutkind, 2001). The β-arrestin protein family, which includes two members β-arrestin 1 and β-arrestin 2, have a two-fold function: they are involved in the termination (or desensitisation) of GPCR signalling by uncoupling activated receptors from G proteins, and they can function as adaptors to activate additional signalling pathways emanating from GPCRs (Miller & Lefkowitz, 2001). Recently, β-arrestin 2 was identified as a protein that interacted with JNK3 in a yeast two-hybrid screen. β-arrestin 2 was shown to specifically assemble ASK1, MKK4 and JNK3 (MacDonald *et. al.*, 2000). Furthermore, β-arrestin 2 potentiated JNK activity in the presence of ASK1 following the activation of angiotensin type IA receptor (MacDonald *et. al.*, 2000). These results suggest the existence of a β-arrestin 2-ASK1-MKK4-JNK3 signalling module (Fig. 1.4B). It should be noted that, β-arrestin 2 does not interact with MKK4 but MKK4 is recruited to the complex via its interactions with ASK1 and JNK3; β-arrestin 2 interacts with JNK3 but not with JNK1 or JNK2; and β-arrestin 1 does not interact with JNK3 (MacDonald *et. al.*, 2000).

The scaffolding function of β-arrestin 2 is thought to be important for two reasons. Firstly, the formation of β-arrestin 2-ASK1- MKK4-JNK3 module may prevent inappropriate cross-talk between various MAPK pathways, since both ASK1 and MKK4 can activate JNK as well as p38. Secondly, it may promote phosphorylation of as yet unknown cytosolic targets of JNK3, since β-arrestin 2-mediated JNK3 activation upon the stimulation of AT1A receptor resulted in the co-localisation of activated JNK3 and β-arrestin 2 in cytosolic vesicles (MacDonald *et. al.*, 2000). However, the physiological importance of GPCR-mediated JNK activation is not known at present.

1.4.4. The role of scaffolds in mediating JNK signalling specificity

The study of how a specific biological outcome is generated in response to several putative inputs into the JNK signal transduction pathway, suggests that several mechanisms play a key role in specificity determination; for example, the presence of a specific JNK docking site in c-Jun (see Schaeffer & Weber, 1999 for an extensive review; see also section 1.3.3). The presence of a scaffold protein is one such mechanism. Recent evidence suggests that JNK signalling may be regulated in the context of scaffold proteins by the following mechanisms.

The presence or the absence of a scaffold protein for the JNK pathway in the first instance may give an indication of how the JNK pathway might be regulated. In COS7 cells for example, which lack JIP scaffold proteins (Whitmarsh *et. al.*, 1998; Ito *et. al.*, 1999), the JNK pathway may be regulated by protein complexes organised by proteins other than the scaffold proteins. Two such examples are the sequential-interaction model for organization of the MEKK1- MKK4-JNK MAPK module (Xia *et. al.*, 1998; Fig. 1.4C) and the MEKK2-MKK7-JNK module organised by MEKK2 (Cheng *et. al.*, 2000; Fig. 1.4D). According to the sequential activation model, active (or inactive) MEKK1 binds MKK4. MEKK1 phosphorylates MKK4 upon stress stimulation, and the MEKK1:MKK4 complex dissociates. Active MKK4 then phosphorylates and activates its substrates, JNK and p38. The specificity for JNK signalling by MKK4 may be provided by the presence of proteins such as actin binding protein 280 (ABP-280), which binds MKK4 strongly compared to ERK, p38 or MKK1 (Marti *et. al.*, 1997). Alternatively, in the absence of JIP proteins, specific activation of the JNK pathway may be achieved by the formation of a tripartite MEKK2-MKK7-JNK module (Cheng *et. al.*, 2000). The synergistic interaction of MEKK2, MKK7 and JNK would allow the specific activation of the JNK pathway, since MKK7 is selective activator of JNK.

Recently, repressor element silencing transcription factor (REST) was identified as a transcriptional repressor of JIP-1 expression in certain cell lines (Abderrahmani *et. al.*, 2001). The absence or the level of the expression of JIP proteins may thus be determined, in part, by REST. In a study of cell lines that expressed either none or high levels of JIP-1 transcript, it was shown that the level of REST mRNA inversely correlated with the JIP-1 transcript level; thus in βTC3 cells, high levels of JIP-1 transcript correlated with the absence of REST mRNA expression, and in Jurkat T lymphocytes, absence of JIP-1 mRNA correlated with high levels of REST mRNA

expression (Abderrahmani *et. al.*, 2001). It is postulated that REST may modulate JIP-1 expression and thereby regulate the JNK pathway (Abderrahmani *et. al.*, 2001). However, transcriptional repression by REST alone does not appear to be sufficient to determine the levels of JIP-1 protein expression (see section 5.3, Chapter 5 for discussion). Nevertheless, the regulation of JIP protein expression at transcriptional, translational and post-translational levels may contribute to the regulation of the JNK pathway.

Although all JIP isoforms bind all JNK isoforms, relative binding affinities differ. For example, JIP-1 binds strongly to all JNK isoforms compared to JIP-2 (Yasuda *et. al.*, 1999). Among JNK isoforms, JIP-1 binds strongly to JNK1β1 and JNK1β2 isoforms compared to JNK2 and JNK3 isoforms (Yasuda *et. al.*, 1999), while JIP-3 binds strongly to JNK3α1 and JNK3α2 isoforms compared to JNK1 and JNK 2 isoforms (Kelkar *et. al.*, 2000). Therefore, JIP-1 is more likely to form a scaffold with JNK1β isoforms and JIP-3 is more likely to form scaffold with JNK3α isoforms. This in turn may determine the activation of a specific transcription factor and may thus determine the biological outcome, since JNK isoforms display selectivity in their interactions with their substrate transcription factors. For example, JNK1β1 and JNK3α1 bind to c-Jun with ~2-fold greater affinity than to ATF2 (Gupta *et. al.*, 1996), suggesting that the activation of these JNK isoforms may preferentially activate c-Jun.

In resting cells, the interaction between JNK and scaffold proteins may be avoided by at least two mechanisms: different subcellular localisation of the components associated with the JNK pathway, and interaction of JNK with other proteins. For example, in non-stressed cells, endogenous JNK activity was shown to be inhibited by its association with GSTp in MEFs but upon stress application, the inhibitory effect of GSTp on JNK was relieved (Adler *et. al.*, 1999). In neurons, endogenous JIP-1 and JNK are located in different cellular compartments in the absence of a stress stimulus (Whitmarsh *et. al.*, 2001). In stress-stimulated neurons, JIP-1 and JNK both co-localise to the same subcellular compartment (Whitmarsh *et. al.*, 2001). Thus, in the absence of a stress stimulus, either or a combination of both of these mechanisms, depending on the cell type, may regulate the interaction of JNK with its scaffold proteins and upstream activator kinases and thereby avoid unnecessary JNK activation.

The duration of the activation of JNK also affects the biological outcome. Persistent JNK activity has been demonstrated to induce apoptosis, while transient JNK

activation has been proposed to signal cell survival (discussed in sections 1.7.2 and 1.7.4).

1.5. FUNCTIONS OF THE JNK PATHWAY

1.5.1. Regulation of gene expression

A general function of the JNK pathway is the regulation of gene expression in response to extracellular stimuli. The JNK pathway carries out this function in two ways: by phosphorylating specific transcription factors and post-transcriptional regulation of certain mRNAs. JNKs phosphorylate Jun and ATF2 proteins, stabilise them and enhance their transcriptional activity (see section 1.2.3). The resulting induction of AP-1 activity by Jun/ATF2 homo- and hetero-dimers may contribute to cell proliferation, survival or apoptosis; furthermore, c-Jun can contribute towards oncogenesis or apoptosis (Shaulian & Karin, 2001; Vogt, 2001; see sections 1.5.2 and 1.7.2). JNK post-transcriptionally regulates IL-2 function, because JNK stabilises IL-2 mRNA in activated T cells (Chen *et. al.*, 2000). The target of JNK appears to be an unidentified cytosolic protein that is recruited to the 5' untranslated region of IL-2 mRNA through two other proteins nucleolin and YB-1 (Chen *et. al.*, 2000).

1.5.2. Oncogenic transformation

There is evidence to link the JNK pathway and oncogenic transformation. Transformation by several oncogenes is associated with JNK activation. For example, the *bcr-abl* oncogene causes constitutive activation of JNK in pre-B cells and an increase in AP-1 activity (Raitano *et. al.*, 1995); transformation by the *met* oncogene is associated with the activation of the JNK pathway (Rodriguez, Park & Schlessinger, 1997); cells transformed by the human T cell leukaemia virus activate JNK (Xu *et. al.*, 1996). Ras-induced transformation requires c-Jun (Johnson *et. al.*, 1996), and Ras-induced tumourigenicity is suppressed by mutation of the JNK phosphorylation sites on c-Jun (Behrens *et. al.*, 2000). Skin tumourigenesis is suppressed in *Jnk2*$^{-/-}$ mice in response to tumour promoters, suggesting that JNK2 is required for tumour promotion (Chen, N. *et. al.*, 2001). Also, c-Jun, the transcriptional target of JNK, can induce oncogenic transformation (reviewed by Vogt, 2001). Furthermore, constitutive JNK activation contributes to cell transformation induced by the overexpression of S-

adenosylmethionine decarboxylase, a regulatory enzyme involved in the biosynthesis of higher polyamines (Paasinen-Sohns *et. al.*, 2000).

The mechanism of action of JNK in tumour development is unclear, but a general consequence appears to be the misregulation of unknown target genes (Vogt, 2001) and suppression of JNK-dependent stress-induced apoptosis (Davis, 2000). This implies that the components of the JNK pathway are potential tumour suppressors. Indeed, the *Mkk4* gene has been identified as a candidate tumour suppressor gene (Su *et. al.*, 1998) and as a candidate metastasis suppressor gene (Yoshida *et. al.*, 1999). It also implies that JNK signals cell survival and apoptosis; indeed JNK has been demonstrated to function in either capacity (see section 1.7).

1.5.3. Immune response

The study of the response of the cells of the immune system to inflammatory cytokines has provided evidence for the role of JNK in inflammation. The JNK pathway is required for the induction of E-selectin by TNF-α, a protein required for the infiltration of leukocytes at the sites of tissue injury (Ip & Davis, 1998). Exposure of adherent neutrophils to TNF-α results in the activation of JNK pathway, which has been proposed to contribute to the apoptosis of neutrophils and subsequent resolution of the inflammatory response (Avdi *et. al.*, 2001). Anethole, an agent that blocks inflammation, suppresses TNF-α-induced JNK activation (Chainy *et. al.*, 2000). Activation of the JNK pathway is required for the production of interleukin-6 (IL-6), a multifunctional cytokine that promotes B-cell growth and differentiation and stimulates acute-phase protein synthesis in liver, and IL-8, a chemokine required for leukocyte migration towards the site of inflammation (Krause *et. al.*, 1998; Holtmann *et. al.*, 1999). Taken together, these data suggest that the JNK pathway plays an important role in inflammatory response.

JNK has also been shown to play a role in T cell function. In the immune system, the stimulation of T lymphocytes requires two stimuli: interaction of an antigen with the T cell receptor (TCR), and delivery by the antigen presenting cells (APCs), such as macrophages and dendritic cells, of the antigen to naïve T cells through the TCR. The CD3 subunit of TCR in conjunction with CD28 recruits what is known as the TCR/CD28 costimulatory pathway, the activation of which results in the clonal proliferation and maturation of $CD4^+/CD8^+$ double positive cells to $CD4^+$Th cells and in

the production of cytokines such as IL-2 (Rincon, 2001). JNK has been demonstrated to play a role in T cell function. For example, the TCR CD3/CD28 costimulation strongly activates JNK and AP1, and is required for IL-2 production (Su *et. al.*, 1994). Studies of Jurkat cells suggest that JNK may contribute to IL-2 gene transcription (Matsuda *et. al.*, 1998) and IL-2 mRNA stability (Chen *et. al.*, 1998). JNK1 suppresses the differentiation of Th cells into cytokine producing Th2 cells, since JNK1-deficient mice are refractory to costimulatory JNK activation despite the presence of functional JNK2 (Dong *et. al.*, 1998). JNK2 is required for peripheral T-cell activation. JNK2 knockout mice demonstrated reduced TCR-mediated proliferation and production of IL-2, IL-4 and interferon-γ, the markers of peripheral T-cell activation (Dong *et. al.*, 1998). The role of JNK in the negative selection of thymocytes and $CD4^+$ or $CD8^+$ T cell activation and differentiation has been extensively reviewed by Rincon, Flavell & Davis (2001).

1.6. APOPTOSIS

1.6.1. Introduction

Apoptosis, or programmed cell death, is an intrinsic cell suicide mechanism used by multicellular organisms to eradicate cells in diverse physiological and pathological settings (Jacobson *et. al.*, 1997). The basic apoptotic machinery is conserved from worms to humans. Cells are genetically programmed to die by default and execute apoptosis in the absence of appropriate survival signals from their environment. In addition, cells have internal sensors that can initiate apoptosis if the cell is unable to repair defects such as DNA damage (Ashkenazi & Dixit, 1998). Although apoptosis occurs in diverse cell types, the morphology and the kinetics of the cell death process are in many cases similar (Arends & Wyllie, 1991).

Apoptosis can be triggered by a variety of stimuli including cytokines, hormones, viruses and toxic chemicals, and involves an ordered series of events that lead to morphological changes such as cytoplasmic shrinkage, membrane blebbing, chromatin condensation, disintegration of mitochondria and the formation of membrane-enclosed vesicles (apoptotic bodies) that are removed by phagocytes (Savill & Fadok, 2000). This is in contrast with the necrotic cell death, which is violent and is characterised by cytoplasmic swelling, the rupturing of cellular membranes and the disintegration of subcellular and nuclear components.

1.6.2. Caspases: The central effectors of cell death

The controlled demolition of the cell during apoptosis is executed by a family of cysteine proteases called caspases. These cysteine proteases were first implicated in cell death following the discovery that *C. elegans* death gene, *ced-3*, encoded a protein that was related to the mammalian interleukin-1β-converting enzyme (ICE), and that the overexpression of the *ced-3* gene induced apoptosis in mammalian fibroblasts (Yuan *et. al.*, 1993). To date, fourteen mammalian caspases (termed caspase 1-14) and four Drosophila caspases (termed DCP1, DrICE, DREDD and DRONC) have been cloned (Kidd, 1998).

Based on their sites of action in the apoptotic pathway, mammalian caspases have been divided into initiator (upstream or apical) and effector (downstream) caspases. Initiator caspases (caspases-8 and –9) are activated in response to signals from death receptors or toxic insults, and they in turn activate the effector caspases (caspases-3, -6 and –7) (Muzio *et. al.*, 1996; Slee *et. al.*, 1999). Caspases are synthesised as precursor proenzymes, which are proteolytically processed to their active forms during apoptosis through autoactivation (e.g. caspase-8; Muzio *et. al.*, 1998), as a part of the caspase cascade (e.g. caspase-3 is activated by caspase-8; Stennicke *et. al.*, 1998), by non-caspase proteases such as granzyme B (e.g. caspase-3; Darmon, Nicholson & Bleackley, 1995) or by association with cytosolic factors (e.g. caspase-9 is activated by its association with apoptosis protease activating factor [Apaf-1] and cytochrome c; Zou *et. al.*, 1999).

1.6.2.1. Substrate specificity of caspases

All caspases show a high degree of substrate specificity, with an absolute requirement for cleavage after an aspartic acid residue and a recognition sequence of at least four amino acids N-terminal to the cleavage site. The aspartic acid is said to occupy the P_1 position. The amino acids upstream of the aspartate are said to occupy P_2, P_3 and P_4 positions, while the amino acid that follows the aspartic acid residue is said to be in the P_1' position (Earnshaw, Martins & Kaufmann, 1999).

A combinatorial approach has been used to determine the tetrapeptide substrate specificity (i.e. amino acids that occupy P_1-P_4 positions) of a number of human caspases (Thornberry *et. al.*, 1997). In addition, the selectivity of peptide-based inhibitors against 10 human caspases has been determined (Garcia-Calvo *et. al.*, 1998). Based on these

studies, the human caspases have been classified into three distinct specificity groups: group I (caspases-1, -4, -5 and -13), with a preference for WEHD; group II (caspases-2, -3 and -7), with a preference for DEXD; and group III (caspases-6, -8, -9 and -10), with a preference for (I/V/L)EXD (X = any amino acid). This characteristic specificity is important to the apoptotic process as it allows the cleavage of particular groups of proteins in an ordered manner, rather than indiscriminate proteolysis. Between them, caspases cleave a range of proteins that need to be inactivated for cell death to occur and proteins whose activation is required for the execution of cell death (discussed in detail section 4.1, Chapter 4).

Experiments with transgenic and gene knockout mice have shown that different initiator caspases, together with their specific adaptors and regulators, are required for control and execution of different death stimuli (Strasser, O'Connor & Dixit, 2000). Two major apoptotic pathways have been described so far: one, which involves cell surface 'death receptors', and two, which involves mitochondria. Both pathways culminate in the activation of caspases, which then carry out the execution phase of apoptosis.

1.6.3. The death receptor pathway

1.6.3.1. Introduction

Death receptors (DRs) transmit an apoptosis signal on the binding of a specific 'death ligand' (Ashkenazi & Dixit, 1998). This pathway is also known as the 'extrinsic' death pathway. DRs belong to the tumor necrosis factor (TNF)/nerve growth factor (NGF) receptor superfamily (Baker & Reddy, 1998). Examples include TNF receptor 1 (TNF-R1, also called p55, CD120a), TNF-R2 (p75, CD120b), Fas (CD95, Apo-1), death receptor 3 (DR3), TNF-related apoptosis inducing ligand receptor 1 (TRAIL-R1, DR4) and TRAIL-R2 (DR5). These receptors share a common intracellular protein-protein interaction domain called the death domain (DD), and ligation of these receptors induces apoptosis (Boldin *et. al.*, 1995; Chinnaiyan *et. al.*, 1996; MacFarlane *et. al.*, 1997).

The ligands that activate these receptors are structurally related molecules with homologies to TNF-α (Baker & Reddy, 1998). Fas ligand (FasL) binds to Fas, TNF-α and lymphotoxin α (LTα) bind to TNF-RI, TRAIL binds to TRAIL-R1 and –R2, and Apo3 ligand binds to DR3 (Ashkenazi & Dixit, 1998).

1.6.3.2. Apoptosis signalling by the death receptors

The apoptotic signalling mechanism employed by the widely studied receptors, TNF-R1, Fas, TRAIL-R1 and TRAIL-R2, follows a general theme (Fig. 1.5.). Upon ligand binding, receptor molecules oligomerise (Wallach *et. al.*, 1999). The intracellular DD of the receptor then interacts with the DD of adaptor proteins, resulting in the formation of a structure called the death-inducing signalling complex (DISC). The DD of Fas and TRAIL receptors recruit an adaptor called Fas-associated DD (FADD) protein (Chinnaiyan *et. al.*, 1995; Kuang *et. al.*, 2000), while FADD is recruited to the activated TNF-R1 via an intermediary adaptor called TNF receptor-associated DD (TRADD) protein (Hsu *et. al.*, 1996). In addition to a DD, FADD also possesses an N-terminal death effector domain (DED), through which it binds pro-caspase-8 molecules (Boldin *et. al.*, 1996; Bodmer *et. al.*, 2000). Proc-caspase-8 contains two DEDs at its N-terminal region through which it binds FADD. Pro-caspase-8 is then cleaved at the DISC by autocatalysis, leading to the formation of active caspase-8, which dissociates from the DISC to initiate the caspase cascade and subsequently the execution phase of apoptosis (Medema *et. al.*, 1997).

1.6.3.3. Regulation of the death receptor signalling

There are several mechanisms involved in the regulation of death receptor activity, including the prevention of pro-caspase recruitment and/or activation at the DISC by FADD-like ICE inhibitory proteins (FLIPs); the expression of decoy receptors (DcR) for TRAIL and Fas; the inhibition of the proteolytic activation of procaspase-8 by proteins such as silencer of DD (SODD) and viral cytokine response modifier A (crmA); and the inhibition of the activation/activity of downstream caspases by heat shock protein 70 (Hsp70) and inhibitor of apoptosis proteins (IAPs) (reviewed in Schmitz, Kirchhoff & Krammer, 2000; Fig. 1.5).

1.6.4. Apoptosis signalling via the mitochondrial pathway

The mitochondrial caspase-activating pathway (Fig. 1.5), also known as the 'intrinsic' death pathway, was discovered by the observation that the addition of dATP to cell extracts prepared from normally growing cells initiates an apoptotic program, as measured by caspase-3 activation and DNA fragmentation (Liu *et. al.*, 1996). Biochemical fractionation and reconstitution experiments identified three proteins

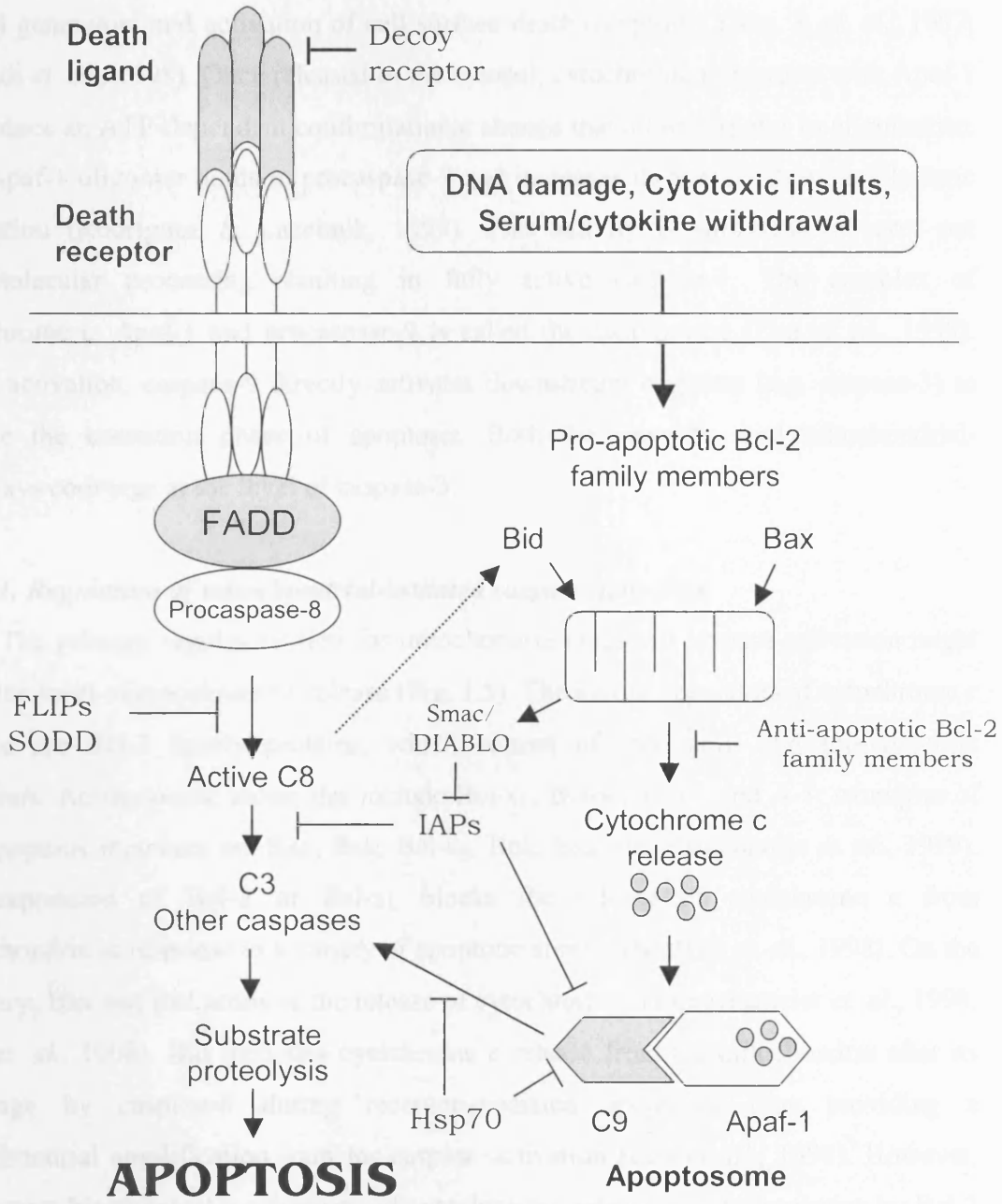

Fig. 1.5. Receptor- and mitochondria-mediated pathways of caspase activation during apoptosis. Please refer to the text for details.

'C' in C3/C8/C9 refers to caspase; FADD = Fas-associated death domain; FLIPs = FADD-like ICE-inhibitory proteins; Hsp70 = heat shock protein 70; IAPs = inhibitor of apoptosis proteins; SODD = silencer of death domain.

necessary and sufficient to activate caspase-3 *in vitro*: cytochrome c, Apaf-1 and procaspase-9 (Li *et. al.*, 1997). It was subsequently shown that cytochrome *c* is indeed released from mitochondria *in vivo* in cells undergoing apoptosis induced by a variety of stimuli, including DNA damaging agents, kinase inhibitors, reactive oxygen species (ROS) generators and activation of cell surface death receptors (Yang, J. *et. al.*, 1997; Scaffidi *et. al.*, 1998). Once released in the cytosol, cytochrome c interacts with Apaf-1 to produce an ATP-dependent conformational change that allows Apaf-1 to oligomerise. The Apaf-1 oligomer binds to procaspase-9 and increases its activity through allosteric regulation (Rodriguez & Lazebnik, 1999). This activity is sufficient to carry out intramolecular processing resulting in fully active caspase-9. The complex of cytochrome c, Apaf-1 and procaspase-9 is called the apoptosome (Zou *et. al.*, 1999). Upon activation, caspase-9 directly activates downstream caspases (e.g. caspase-3) to initiate the execution phase of apoptosis. Both the receptor- and mitochondrial-pathways converge at the level of caspase-3.

1.6.4.1. Regulation of mitochondrial-initiated caspase activation

The primary regulatory step for mitochondria-mediated caspase activation might be at the level of cytochrome *c* release (Fig. 1.5). The known regulators of cytochrome *c* release are Bcl-2 family proteins, which consist of both anti- and pro-apoptotic members. Antiapoptotic molecules include Bcl-x_L, Bcl-w, Mcl-1 and A-1; examples of pro-apoptotic members are Bax, Bak, Bcl-x_S, Bok, Bid, etc. (Budihardjo *et. al.*, 1999). Overexpression of Bcl-2 or Bcl-x_L blocks the release of cytochrome c from mitochondria in response to a variety of apoptotic stimuli (Scaffidi *et. al.*, 1998). On the contrary, Bax and Bid promote the release of cytochrome c (Juergensmeier *et. al.*, 1998; Luo *et. al.*, 1998). Bid mediates cytochrome *c* release from the mitochondria after its cleavage by caspase-8 during receptor-mediated apoptosis, thus providing a mitochondrial amplification loop for caspase activation (Lou *et. al.*, 1998). However, the precise biochemical mechanisms of cytochrome c release and its regulation by Bcl-2 family proteins remain elusive.

In addition to Bcl-2 family proteins, several other proteins regulate mitochondrial-initiated caspase activation. For example, Hsp70 prevents apoptosis by preventing procaspase-9 recruitment and apoptosome formation; IAPs inhibit caspases at several points; and Smac/Diablo, a protein that is also released from mitochondria along with cytochrome c, inactivates IAPs and thus neutralises the inhibition of the activation of

caspase-9 and other downstream caspases (reviewed in Adrian & Martin, 2001; Fig. 1.5).

1.7. THE ROLE OF JNK IN APOPTOSIS

Apoptosis induced by death ligands as well as many forms of cellular stresses cause the activation of JNK (Chen & Tan, 2000). Both biochemical (ectopic expression/inhibition-based) and genetic (knockout) analyses have established a role of the JNK pathway in apoptosis. Although it has never been demonstrated that the activation of JNK alone is sufficient for apoptosis in any system, genetic evidence suggests that the JNK pathway is necessary for stress-induced apoptosis (Shaulian *et. al.*, 2000; Tournier *et. al.*, 2000; Tournier *et. al.*, 2001; Whitmarsh *et. al.*, 2001), and may contribute towards receptor-induced apoptosis (Davis, 2000).

1.7.1. Biochemical studies

Several biochemical studies indicate that the JNK pathway plays a role in apoptosis. The inhibition of the JNK pathway by dominant-negative c-Jun has been shown to protect PC12 cells from NGF withdrawal-induced apoptosis (Xia *et. al.*, 1995) and human monoblastic leukaemia cells from apoptosis induced by various DNA damaging agents (Verheij *et. al.*, 1996). It was shown that, in addition to an enhanced c-Jun expression, phosphorylation of c-Jun by JNK was necessary for the apoptotic response in cerebellar granule and sympathetic neurons (Le-Niculescu *et. al.*, 1999). Overexpression of c-Jun was also shown to induce apoptosis in mouse 3T3 fibroblasts and in sympathetic neurons (Ham *et. al.*, 1995; Bossy-Wetzel, Bakiri & Yaniv, 1997). Expression of the phosphorylation-deficient c-Jun$^{A63/73}$ mutant, or treatment with various JNK inhibitors, blocked apoptosis induced by NGF withdrawal in cultured neuronal cells (Watson *et. al.*, 1998; Li-Niculescu *et. al.*, 1999).

A correlation between JNK activation and apoptosis induction is observed upon the overexpression of upstream JNK activators MEKK1 (Xia *et. al.*, 1995; Bonny *et. al.*, 2000), ASK1 (Ichijo *et. al.*, 1997; Kanamoto *et. al.*, 2000) and mammalian Ste20-like kinase 1 (MST1) (Ura *et. al.*, 2001). During apoptosis, MEKK1, HPK1 and MST1 are cleaved by caspase-3, resulting in the release of their active kinase domain, an event that leads to JNK activation (Cardone *et. al.*, 1997; Chen *et. al.*, 1999; Watabe *et. al.*, 2000). Furthermore, overexpressed MST1 (Graves *et. al.*, 2001; Ura *et. al.*, 2001) and

MLK family members (Mota *et. al.*, 2001; Phelan *et. al.*, 2001; Xu *et. al.*, 2001) have been proposed to induce apoptosis via JNK. The JNK pathway has also been implicated in mediating apoptosis induced by TGFβ (Perlman *et. al.*, 2001).

Biochemical analyses suggest that persistent JNK activity is required for stress-induced apoptosis. Sustained JNK activation induced by γ-irradiation, ultraviolet C (UV-C) and cisplatin correlates with apoptosis (Chen, Meyer & Tan, 1996; Chen *et. al.*, 1996; Sanchez-Perez, Murguia & Perona, 1998). Impaired JNK activation in TR-4 cells, a thermotolerant mouse fibroblast cell line, correlates with resistance to apoptosis in response to heat shock or cisplatin (Zanke *et. al.*, 1996). Jurkat cells transiently overexpressing constitutively active MKK7 leads to the persistent activation of JNK and apoptosis (Chen & Lai, 2001).

1.7.2. Genetic studies

Genetic analyses have shown that the JNK pathway is required for apoptosis induced by certain stress stimuli. *c-jun*$^{-/-}$, *Jnk1*$^{-/-}$*Jnk2*$^{-/-}$ and *Mkk4*$^{-/-}$*Mkk7*$^{-/-}$ MEFs were found to be resistant to UV-C-induced apoptosis (Shaulian *et. al.*, 2000; Tournier *et. al.*, 2000; Tournier *et. al.*, 2001). Furthermore, *c-jun*$^{-/-}$ MEFs are resistant to the apoptotic effects of alkylating agents (Kolbus *et. al.*, 2000), and *Jnk1*$^{-/-}$*Jnk2*$^{-/-}$ MEFs are resistant to anisomycin-induced apoptosis (Tournier *et. al.*, 2000). Deletion of the *Jnk3* gene in mice protected hippocampal neurons from kainate-induced apoptosis (Yang *et. al.*, 1997). Resistance to kainate-induced cytotoxicity was also observed in c-jun$^{A63/73}$ knock-in mice (Behrens, Sibilia & Wagner, 1999) and in *Jip1*$^{-/-}$ mice (Whitmarsh *et. al.*, 2001). However, *Jnk1*$^{-/-}$*Jnk2*$^{+/-}$ mice are not resistant to kainate-induced apoptosis (Sabapathy *et. al.*, 1999). These results suggest that JNK3 may mediate stress-induced apoptotic response in brain, while JNK1/JNK2 may mediate stress-induced apoptosis in other cell types such as fibroblasts. In either case, the pro-apoptotic effects of JNK appear to be mediated by c-Jun.

The requirement of persistent JNK activity for stress-induced has also been demonstrated by genetic analyses. It was shown using compound c-Jun/p53-deficient MEFs that stress-induced persistent c-Jun activity caused p53-dependent apoptosis (Shaulian *et. al.*, 2001; see below). *Ask1*$^{-/-}$ MEFs are deficient in apoptosis induced by persistent JNK activity in response to H_2O_2 (Tobiume *et. al.*, 2001). Taken together,

these data suggest that persistent JNK activation is essential for stress-induced apoptosis.

1.7.3. Mechanisms of JNK-dependent stress-induced apoptosis

The following possible mechanisms of JNK-dependent stress-induced apoptosis can be proposed based on the current progress made in the field (Davis, 2000).

JNK mediates its pro-apoptotic effects in a transcription-dependent manner via c-Jun/AP-1, which directly activates the transcription of genes whose products can trigger apoptosis. One such transcriptional target appears to be the FasL gene. It has been shown that apoptosis induced by anisomycin, etoposide, teniposide, 5-flourouracil, methyl methanosulphate (MMS) or UV irradiation in a variety of cell types activates the JNK pathway that then upregulates FasL expression via AP-1 (Faris *et. al.*, 1998; Kasibhatla *et. al.*, 1998; Harwood *et. al.*, 2000; Kolbus *et. al.*, 2000). NF-κB or p38 may aid in this process (Faris *et. al.*, 1998; Kolbus *et. al.*, 2000). In neuronal cells, growth factor withdrawal- or β-amyloid-induced JNK activation leads to FasL induction and cell death (Le-Niculescu *et. al.*, 1999; Morishima *et. al.*, 2001). *c-Jun*$^{-/-}$ MEFs that are resistant to stress-induced apoptosis are also impaired in FasL expression (Kolbus *et. al.*, 2000). The production of FasL may lead to autocrine or paracrine death signalling via the Fas-FADD-caspase-8 pathway (Faris *et. al.*, 1998; Kasibhatla *et. al.*, 1998). The importance of this mechanism is underpinned by the presence of AP-1 and NF-κB binding sites in the FasL promoter (Kasibhatla *et. al.*, 1998).

However, FasL induction contributes only partly to stress-induced apoptosis, as apoptosis occurs almost normally in mice that are deficient in either Fas or FADD (Yeh *et. al.*, 1998), both of which are essential mediators of FasL action. This suggests that additional targets need to be activated by JNK that would mediate stress-induced apoptosis. One such target is p53. Using homozygous and heterozygous c-Jun/p53 compound mutant MEFs, it was recently shown that UV-induced apoptosis is dependent on c-Jun and p53 (Shaulian *et. al.*, 2000). Activation of p53 leads to growth arrest or apoptosis (Moll & Zaika, 2001). p53 induces or maintains growth arrest through the increased expression of cell cycle regulators such as $p21^{Waf1/Cip1}$. By repressing p53-mediated $p21^{Waf1/Cip1}$ induction, high levels of c-Jun was shown to prevent p53-induced growth arrest and instead channel p53 activity towards the induction of apoptosis, providing genetic evidence that links persistent JNK activity in leading to c-Jun

activation and the induction of apoptosis (Shaulian *et. al.*, 2000). The mechanism by which c-Jun represses p53-mediated gene induction is not fully understood.

The precise mechanism by which p53 induces apoptosis is unclear but seems to involve both transcription-dependent and –independent pathways. In some cells, p53 appears to induce apoptosis through the upregulation of specific pro-apoptotic proteins such as Fas (Muller *et. al.*, 1998), TRAIL-R2 (Wu *et. al.*, 1997), Bax (Miyashita & Reed, 1995) and Apaf-1 (Fortin *et. al.*, 2001; Robles *et. al.*, 2001). A fraction of stress-induced p53 relocalizes to mitochondria during p53-dependent apoptosis, preceding changes in mitochondrial membrane potential and cytochrome *c* release, and direct targeting of p53 to mitochondria induces apoptosis in p53-deficient cells (Marchenko *et. al.*, 2000). A possibility exists that p53 might also induce apoptosis through transcriptionally independent mechanisms. The transcription-independent p53 pathway is believed to act in synergy with the transcription-dependent mode of p53, thus amplifying the apoptotic cascade (Moll & Zaika, 2001).

1.7.3.1. A model for JNK-dependent stress-induced apoptosis

Results from knock-out studies of JNK pathway and apoptotic pathway components show that stress-induced apoptosis is blocked in the absence of c-Jun (Kolbas *et. al.*, 2000; Shaulian *et. al.*, 2000), JNK1/JNK2 (Tournier *et. al.*, 2000), MKK4/MKK7 (Tournier *et. al.*, 2001), JIP-1 (Whitmarsh *et. al.*, 2001), ASK1 (Tobiume *et. al.*, 2001), cytochrome c (Li *et. al.*, 2000), Apaf-1 (Yoshida *et. al.*, 1998), caspase-9 (Hakem *et. al.*, 1998) and caspase-3 (Woo *et. al.*, 1998). The following observations suggest that JNK is likely to act upstream of mitochondria during stress-induced apoptosis. *Jnk1*$^{-/-}$*Jnk2*$^{-/-}$ MEFs were found to be defective in mitochondrial depolarisation and mitochondrial release of cytochrome c (Tournier *et. al.*, 2000), and JNK activation has been reported to induce cytochrome c release (Hatai *et. al.*, 2000). Hsp70 interacts with JNK and is an endogenous inhibitor of JNK (Park *et. al.*, 2001), and Hsp70-mediated suppression of JNK protects cells from stress-induced apoptosis by preventing cytochrome c release (Mosser *et. al.*, 2000). H_2O_2, which induces apoptosis through the mitochondrial pathway, failed to cause apoptosis of *Ask1*$^{-/-}$ MEFs due to a failure in JNK activation (Tobiume *et. al.*, 2001).

Based on these observations, a model of JNK-dependent stress-induced apoptosis, originally proposed by Davis (2000), can be presented (Fig. 1.6). Stress-induced JNK

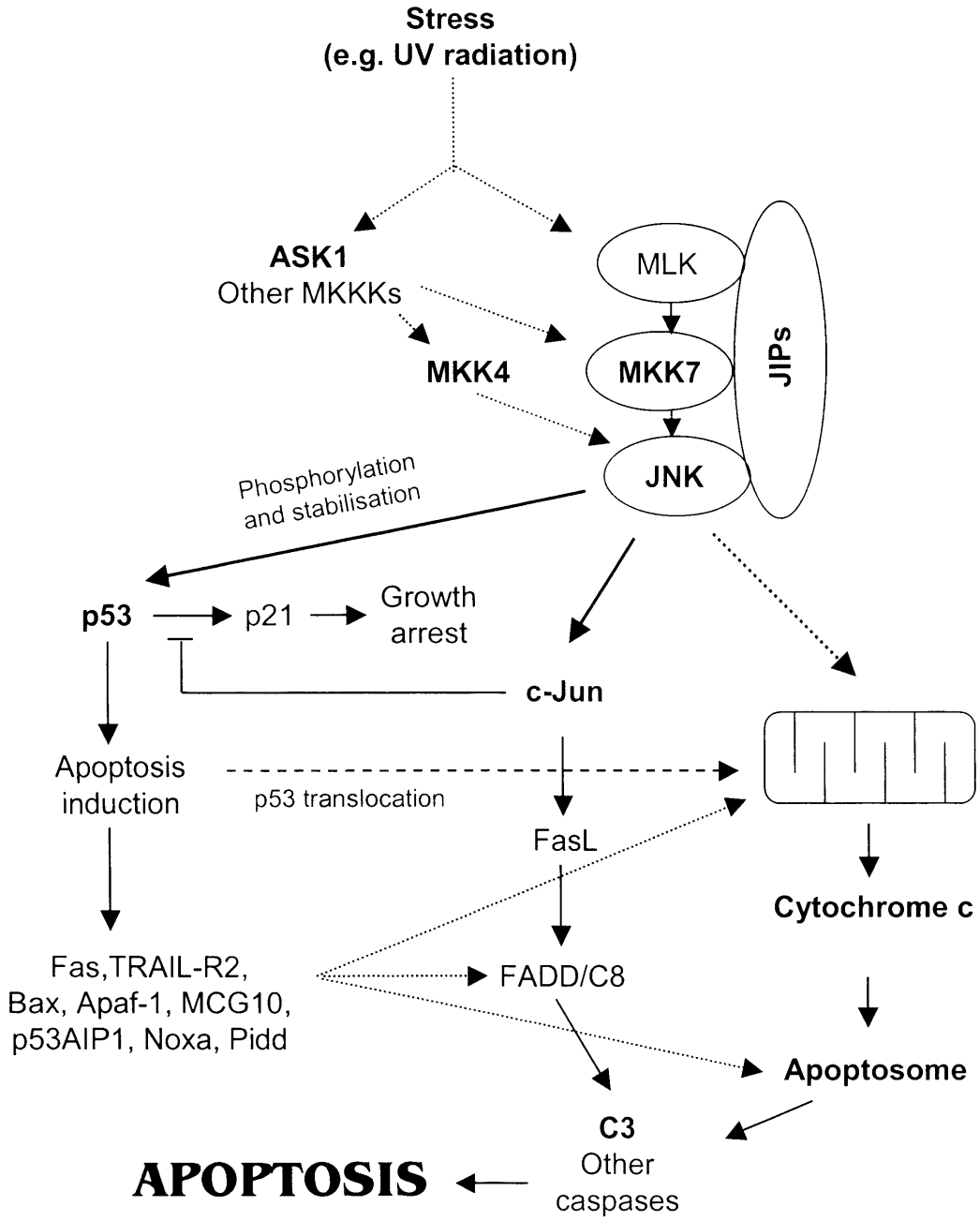

Fig. 1.6. A model depicting the role of the JNK pathway in the induction of stress-induced apoptosis. Components whose function in stress-induced apoptosis has been defined by genetic analysis are shown in bold.

ASK1 = apoptosis signal regulating kinase 1; C3/C8 = caspase 3/8; FADD = Fas-associated death domain; FasL = Fas ligand; JIPs = JNK interacting proteins; JNK = c-Jun amino terminal kinase; MKK4/7 = Mitogen activated protein kinase kinase 4/7; MLK = mixed lineage kinase; TRAIL = TNF receptor associated apoptosis inducing ligand;

activation may induce apoptosis in a transcription-dependent and transcription-independent manner by the following mechanisms.

It may exert is pro-apoptotic effects in a transcription-independent manner by acting directly on mitochondria to release cytochrome c and subsequent activation of caspase-9 and downstream caspases, leading to apoptosis (Davis, 2000). The molecular targets of activated JNK that cause cytochrome c release from mitochondria are currently not known, but proposed targets include pro-apoptotic Bcl-2 family members (Tournier *et. al.*, 2000).

Activated JNK may exert its pro-apoptotic effects in a transcription-dependent manner by phosphorylating c-Jun and p53, which would have following effects. One, c-Jun would upregulate FasL expression, which in turn would amplify the apoptotic potential by engaging Fas/FADD/caspase-8 pathway. Two, JNK-induced p53 phosphorylation would stabilise p53 (Fuchs *et. al.*, 1998), and enhance the transcriptional activity of p53 (Buschmann *et. al.*, 2001). This is supported by the observations that in *Jnk1*$^{-/-}$*Jnk2*$^{-/-}$ and *Mkk4*$^{-/-}$*Mkk7*$^{-/-}$ MEFs, which do not exhibit JNK activity, increased expression of p19^{ARF} (a protein that stabilises p53) was observed (Tournier *et. al.*, 2000; Tournier *et. al.*, 2001). Three, c-Jun would inhibit p53-mediated growth arrest and potentiate p53-mediated apoptosis through transcription-dependent and -independent mechanisms (section 1.7.3). For example, transcriptional upregulation of Fas by p53 would aid FasL-induced apoptosis, while the upregulation of pro-apoptotic Bax and Apaf-1, and the translocation of p53 to mitochondria, would aid mitochondrial apoptosis signalling.

It has been suggested that apoptotic signalling by JNK, which is both transcription-dependent (leading to c-Jun-mediated death ligand induction and suppression of p53-mediated growth arrest) and transcription-independent (leading to cytochrome c release), is not mutually exclusive, and it is likely that these two mechanisms may co-operate to induce cell death (Davis, 2000).

The precise mechanism of JNK activation during stress-induced apoptosis is unclear, but genetic evidence suggests that ASK1, MKK4, MKK7 and JIP-1 scaffolding function are essential (Tobiume *et. al.*, 2001; Tournier *et. al.*, 2001; Whitmarsh *et. al.*, 2001). It has been proposed that during stress-induced apoptosis, ASK1 may activate JNK through MKK7 (Hatai *et. al.*, 2000; Matsuzawa & Ichijo, 2001). However, ASK1 can also interact with MKK4 (MacDonald *et. al.*, 2000), hence it is possible that ASK1 may activate JNK through MKK4. Therefore, JNK activation during stress-induced

apoptosis appears to be mediated at least through JIP-1-MLK-MKK7 and ASK1-MKK7 or ASK1-MKK4 (Fig. 1.6). However, since the synergistic action of MKK4 and MKK7 is required to activate JNK (see section 1.3.4), it is possible that JNK activation during stress-induced apoptosis may be mediated by as yet unidentified MKKKs that activate both MKK4 and MKK7 (Fig. 1.6).

1.7.4. The role of JNK in receptor-mediated apoptosis

The role of JNK in receptor-mediated apoptosis is unclear. *Jnk1*$^{-/-}$*Jnk2*$^{-/-}$ and *Mkk4*$^{-/-}$*Mkk7*$^{-/-}$ MEFs display a normal apoptotic response to Fas ligation (Tournier *et. al.*, 2000; Tournier *et. al.*, 2001). In SHEP neuroblastoma cells, the expression of an inactivatable mutant inhibited Fas-mediated JNK activation and apoptosis, suggesting that JNK is necessary for Fas-mediated killing (Goillot *et. al.*, 1997). However, in Jurkat cells, the expression of dominant negative c-Jun or MKK4 had no effect on Fas-induced apoptosis (Lenczowski *et. al.*, 1997). TNF-α-induced transient JNK activation was demonstrated to be non-essential for TNF-α-induced apoptosis, since JNK activation occurred through a non-cytotoxic TRAF2-dependent pathway (Liu, Z. *et. al.*, 1996; Natoli *et. al.*, 1997; Reinhard *et. al.*, 1997). Similarly, TRAIL induced apoptosis through the FADD-caspase-8 pathway and JNK activation through a FADD-independent, TRAF2-dependent pathway (Hu, Johnson & Shu, 1999), and FADD-independent JNK activation was insufficient to induce apoptosis (Muhlenbeck *et. al.*, 1998). However, a recent study suggests that persistent JNK activity is essential for TNF-α-induced apoptosis (Tobiume *et. al.*, 2001).

1.7.5. Suppression of apoptosis by JNK

Although genetic evidence exists that the JNK pathway is essential for stress-induced apoptosis, the normal physiological function of the JNK pathway, at least during embryogenesis, does not necessarily appear to be the induction of apoptosis. A *Jnk1*$^{-/-}$*Jnk2*$^{-/-}$ double knockout is embryonically lethal; mice harbouring these mutations showed a severe malformation of the brain resulting from failed closure of the neural folds at the hindbrain region due to reduced apoptosis (Sabapathy *et. al.*, 1999). However, these mice exhibited increased apoptosis in the forebrain, suggesting that JNK1 and JNK2 function to induce apoptosis in the hindbrain and suppress apoptosis in the forebrain for brain development (Sabapathy *et. al.*, 1999). *Mkk4*$^{-/-}$ or *c-Jun*$^{-/-}$

embryos exhibit massive liver cell apoptosis, suggesting that MKK4 and c-Jun are required to suppress hepatocyte apoptosis (Ganiatsas *et. al.*, 1998; Eferl *et. al.*, 1999). Disruption of the *Jip1* gene leads to an early embryological death due to increased apoptosis, indicating that JIP-1 is required for cell survival during early embryonic divisions (Thompson *et. al.*, 2001). Taken together, these data suggest that the JNK pathway components are required for regulating regional-specific apoptosis during normal mammalian embryonic development.

Transient JNK activation has been proposed to signal cell survival (Chen & Tan, 2000). For example, integrin-mediated survival signalling is mediated, in part, through the JNK pathway (Almeida *et. al.*, 2000). Furthermore, JNK may signal cell survival in certain cell types or in response to specific stimuli. For example, loss of JNK activation in *Mekk1*$^{-/-}$ ES cells resulted in increased apoptosis in response to taxol (Yujiri *et. al.*, 1999). Inhibition of JNK2 resulted in increased apoptosis in p53-deficient MCF-7, RKO and HCT116 human tumour cell lines (Potapova *et. al.*, 2000). These data thus suggest that JNK may also mediate survival signalling under specific circumstances.

1.8. AIMS OF THE PROJECT

The aims of the project were three-fold:

- ***To study the protein-protein interactions in the JIP-1 scaffold complex in intact cells,*** because the JIP-1 scaffold model is postulated on the basis of transfection studies but the model has not been studied in intact (non-transfected) cells.
- ***To investigate whether JIP-1 is a caspase substrate*** **in vivo** ***and*** **in vitro,** since the JIP1 primary sequence contains four putative caspase-3 and one caspase-8 cleavage sites.
- ***To examine the relationship between JIP-1 cleavage and JNK activity during apoptosis.*** Relatively few proteins are targeted by caspases, and those that are targeted are known to play an important role in normal cellular functions. Cleavage of these proteins by caspases therefore has important functional consequences. Since JIP-1 is a putative scaffold protein for the JNK pathway and JNK plays an important role during apoptosis initiated through the mitochondrial pathway, JIP-1 cleavage may affect JNK signalling during apoptosis.

CHAPTER 2

MATERIALS & METHODS

2.1. MATERIALS

2.1.1. General laboratory reagents

Chemicals were purchased from Fisher Scientific (Loughborough, U. K.) and Sigma (Poole, U. K) unless otherwise stated. Reagents for bacterial culture were obtained from Oxoid (Unipath, Basingstoke, Hampshire, U. K.). Antibiotics were purchased from Melford Laboratories (Suffolk, U. K.). Radiolabelled [γ-^{32}P] ATP was purchased from Amersham Pharmacia Biotech (Little Chalfont, U. K.) and NEN Dupont (Hounslow, U. K.). Bovine serum albumin (BSA) was purchased from First Link U.K. Ltd. (Brookmoor, U. K.).

Petri dishes for the preparation of bacterial agar plates and 96-well plates for enzyme-linked immunosorbent assays (ELISA) were purchased from Bibby Sterilin Ltd. (Staffordshire, U. K.). Nescofilm was purchased from Bendo Chemical Industries Ltd. (Kobe, Japan). X-ray films were purchased from Fuji Photo Film Europe GmbH (Dusseldorf, Germany). Whatman 3MM paper was purchased from Whatman International Ltd. (Maidstone, Kent, U. K.). For filter sterilisation, 0.2μ filters were purchased from Pall Gelman Laboratory (Portsmouth, Hampshire, U. K.).

2.1.2. Molecular biology reagents

For plasmid DNA preparation on small and large scales, miniprep and maxiprep kits were purchased from QIAGEN (Crawley, U. K.). For DNA gel electrophoresis, DNAse- and RNAse-free agarose was purchased from BioWhittaker Molecular Applications (Rockland, U. S. A.). DNA markers (size range 0.5-12 kb) and a solution of ethidium bromide (10mg/ml) were purchased from Life Technologies (Paisley, Scotland). All restriction enzymes were purchased from Roeche Molecular Biochemicals (Lewes, U. K.), except *Bst*EII, which was purchased from New England Biolabs (Hitchin, U. K.). For polymerase chain reaction (PCR), deoxyribonucleotide triphosphate (dNTP) mix was purchased from Life Technologies (Paisley, Scotland) and Vent DNA polymerase was purchased from New England Biolabs (Hitchin, U. K.). For DNA ligations, Lightning® DNA Ligation kit was purchased from Bioline (London, U. K.).

For sodium dodecyl suphate polyacrylamide protein gel electrophoresis (SDS-PAGE), 30% (w/v) acrylamide:0.8% (w/v) bis-acrylamide stock solution was purchased from National Diagnostics (Atlanta, Georgia, U. S. A.). Pre-stained protein markers

(size range 4-250 kDa) were purchased from Biorad (Hemel Hempstead, Hertfordshire, U. K.). Dalton Mark VII-L unstained protein markers (size range 14-70 kDa) were purchased from Sigma (Poole, U. K.). For *in vitro* protein translation reactions, TNT® T7-coupled *in vitro* transcription/translation kit was purchased from Promega (Southampton, U. K.). ^{35}S-labelled methionine was a kind gift from Dr. Andrew Fry (Department of Biochemistry, University of Leicester, Leicester, U. K.). For the affinity purification of the JIP-1 anti-peptide antibody #609, N-hydroxy succinimide (NHS)-activated Sepharose® 4 fast flow was purchased from Amersham Pharmacia Biotech (Little Chalfont, U. K.). For immunoprecipitation reactions, Protein A sepharose was purchased from Sigma (Poole, U. K.). For immunoblots analysis, Immobilon-P® membranes were purchased from Millipore (Bedford, Massachusetts, U. S. A.) and enhanced chemiluminescence™ (ECL™) kit was purchased from Amersham Pharmacia Biotech (Little Chalfont, U. K.). For ELISA assays, foetal calf serum (FCS) was purchased from Life Technologies (Paisley, Scotland).

Mouse and rat brain tissues were kindly provided by Drs. Jenny Luckett and Steve Harding (Department of Biochemistry, University of Leicester, Leicester).

2.1.3. Antibodies

Anti-JNK1 (cat. no. 554286) and anti-PARP (cat. no. 65196E) monoclonal antibodies were purchased from Pharmingen (Heidelberg, Germany). Anti-α-tubulin and anti-Flag monoclonal antibodies were purchased from Sigma. Anti-JIP-1 (cat. no. sc-7145 and sc-7147), anti-JNK1 (cat. no. sc-571), anti-MKK7 (cat. no. sc-7103), anti-MLK3 (cat. no. sc-536), and anti-HPK1 (cat. no. sc-6231) polyclonal antibodies were purchased from Santacruz Biotechnology Inc (Santcruz, California, U. S. A.).

Anti-JIP-1 monoclonal antibody #7 was a kind gift from Dr. Roger Davis (University of Massachusetts Medical School, Worcester, Massachusetts, USA) and Dr. Alan J. Whitmarsh (School of Biological Sciences, University of Manchester, Manchester). Monoclonal p38 antibody was a kind gift from Dr. Raj Patel (Department of Biochemistry, University of Leicester, Leicester). Caspase-3, -7, -8 and –9 polyclonal antibodies and agonistic Fas antibody were kind gifts from Dr. Marion MacFarlane (Medical Research Council [MRC] Toxicology Unit, University of Leicester, Leicester). HPK1 antibodies #2, #5 and #6 were kind gifts from Dr. Friedmann Kiefer (Max-Planck Institute for Physiological and Clinical Research, Bad Nauheim,

Germany). Anti-JIP-1 antisera #608, #609, #610 and #9A and anti-JNK1 antiserum #355 were raised in rabbits by Dr. Martin Dickens.

Anti-rabbit and anti-mouse horseradish peroxidase (HRP) conjugates were purchased from Sigma (Poole, U. K.).

2.1.4. Tissue Culture

Dulbecco's modified eagle medium (DMEM), RPMI 1640, L-Glutamine, penicillin, streptomycin and heat-inactivated foetal bovine serum (FBS) and horse serum were purchased from Life Technologies (Paisley, Scotland). Caspase-3 inhibitor DEVD.fmk was purchased from Alexis Biochemicals (Nottingham, U. K.). Tfx-50^{TM} transfection reagent was purchased from Promega (Southampton, U. K.). Tissue culture plastic ware was purchased from Nalge (Europe) Ltd. (Hereford, U. K.).

N1E-115 cells were purchased from American Type Culture Collection (Manassas, Virginia, U.S.A.). GC-1 cells were kind gift from Dr. Ian Eperon (Department of Biochemistry, University of Leicester, Leicester). HeLa and HEK293 cells were kind gifts from Dr. Raj Patel (Department of Biochemistry, University of Leicester, Leicester). For apoptosis assays, zVAD.fmk, TRAIL, TNF-α and MG132 were kind gifts from Dr. Marion MacFarlane (MRC Toxicology Unit, University of Leicester, Leicester, U. K.). Poly-L-lysine-coated coverslips were a kind gift from Dr. Raj Patel (Department of Biochemistry, University of Leicester, Leicester).

2.1.5. Plasmids

The plasmids used were: pCMV5-Flag-JIP-1; pBK-JIP-1b (a kind gift from Dr. Gerard Waeber, Division of Medical Genetics and the Department of Internal Medicine, CHUV University Hospital, 1011 Lausanne, Switzerland); pcDNA3-HA-JNK1; pCMV5-Flag-MKK7; pcDNA3-HA-MLK3 (a kind gift from Dr. Jonathan Blank, Department of Cell Physiology & Pharmacology, University of Leicester, Leicester); pMT2-HA-HPK1 (a kind gift from Dr. F. Keifer, Germany) and pBluescript SK+ (purchased from Stratagene, Cambridge, U. K.).

2.2. METHODS

The reagents used in various techniques were prepared as described in the Appendix.

2.2.1. Bacterial techniques

2.2.1.1. Preparation of competent XL-1 Blue MRF' cells

The *E. coli* strain XL-1 Blue MRF' strain was used in bacterial manipulations. XL-1 Blue MRF' cells were streaked from the glycerol stock onto Luria Bertani (LB) agar plate. The plate was incubated overnight at 37°C. A single colony from the LB agar plate was inoculated into 5ml of LB medium and incubated overnight with shaking at 37°C. The entire overnight culture was inoculated into 250ml of LB and incubated at 37°C until the absorbance at 600 nm (A_{600}) reached 0.4-0.6. Cells were then transferred into four pre-chilled 50ml Falcon tubes and were left on ice for 15 minutes. Cells were collected by centrifugation at 3000 rpm for 10 minutes at 4°C in a Sorvall RC-5B Superspeed Centrifuge (DuPont Instruments). The pellet was resuspended in 50ml ice-cold sterile buffered $CaCl_2$ solution and centrifuged as before. The pellet was resuspended again in 50ml of ice-cold buffered $CaCl_2$ solution, and the mixture was left on ice for 30 minutes. Cells were collected by centrifugation as before. The pellet was resuspended in 10ml of ice-cold buffered $CaCl_2$ solution, the cells were snap frozen in an ethanol/dry ice bath in 200µl aliquots and stored at –70°C.

2.2.1.2. Transformation of competent XL-1 Blue MRF' cells

Plasmid DNA (100ng) or ligation products (10µl) were added to 100µl of competent XL-1 Blue MRF' cells and mixed by gentle pipetting. The cells were incubated on ice for 45 minutes. The cells were then heat shocked for 2 minutes at 42°C, followed by incubation for 2 minutes on ice. The cells were transferred to 1ml of LB medium and incubated for 1 hour at 37°C with gentle shaking. The medium was spread-plated on to a pre-warmed LB agar containing an appropriate antibiotic. The plates were incubated overnight at 37°C.

2.2.1.3. Preparation of glycerol stocks

Following the transformation of competent cells, a single bacterial colony was inoculated into 10ml of LB medium containing an appropriate antibiotic and incubated

overnight with shaking. Glycerol stocks were then prepared by mixing 0.5 ml of bacterial culture and 0.5 ml of sterile 50% glycerol, and were stored at –70°C.

2.2.1.4. Preparation of bacterial pellets for DNA sequencing

Bacterial cultures were grown overnight in 10ml of LB medium supplemented with an appropriate antibiotic at 37°C. The culture (5ml) was centrifuged at 3000rpm for 10 minutes at room temperature. The supernatant was discarded and the bacterial pellet was sent to the Protein & Nucleic Acid Chemistry Laboratory (PNACL) (Centre for Mechanisms of Human Toxicity, University of Leicester, Leicester, U. K) for DNA sequencing on a Perkin Elmer Applied Biosystems 377 automated sequencer (Perkin Elmer, Foster City, California, U. S. A).

2.2.2. Molecular biology methods

2.2.2.1. Small- and large-scale preparation of plasmid DNA

Plasmid DNA was prepared on a small or on a large scale by alkaline lysis using an appropriate QIAGEN plasmid purification kit as per the manufacturer's instructions. The purified plasmid, bound to the QIAGEN anion-exchange resin, was eluted in an appropriate volume of sterile deionised water, and the concentration of plasmid DNA was determined by measuring absorbance at 260nm. Diagnostic restriction enzyme digests were performed on purified plasmid DNA to ensure the identity of the construct.

2.2.2.2. Restriction enzyme digestion of plasmid DNA

Plasmid DNA (2μg) was digested with restriction enzyme(s) in a total volume of 40μl under the conditions recommended by the suppliers. Reactions were incubated at an appropriate temperature for 1-2 hours and were terminated by the addition of 1x agarose gel loading buffer.

2.2.2.3. Agarose gel electrophoresis

PCR products, restriction enzyme-digested plasmid DNA or undigested plasmid DNA were fractionated according to their molecular weight by electrophoresis through 0.8% or 1.4% agarose gels. Agarose was melted in 1x TAE buffer and cooled. A solution of ethidium bromide (Life Technologies) was added to a final concentration of 0.4μg/ml to the melted agarose, and the agarose was cast into a gel. The gel was

submerged in 1x TAE buffer in a horizontal electrophoresis tank (Hybaid, Ashford, Middlesex, U. K.). Samples were mixed with 1x agarose gel loading buffer and separated by electrophoresis for 1 hour at 80V, and the DNA was visualised on a low intensity Syngene UV transilluminator (Sony Corporation, Tokyo, Japan).

2.2.2.4. Electroelution of DNA from agarose gels

The desired DNA fragment was excised from the gel with the help of a sterile scalpel while viewing under low intensity UV light. The excised gel piece was placed in a dialysis bag filled with 450µl of sterile deionised water. The bag was sealed at both ends using plastic clips and was placed in an electrophoresis tank filled with 0.2x TAE buffer. The DNA was electroeluted at 80V for 1 hour. The liquid from the dialysis bag was recovered, and the DNA in the eluate was ethanol precipitated with 2 volumes of absolute ethanol and 0.1 volumes of 3M sodium acetate (pH 4.6) for 10 minutes on ice. The DNA pellet was recovered by centrifugation at 14000 rpm for 15 minutes at 4°C in an Eppendorf 5417R centrifuge (Eppendorf, Cambridge, U. K.). The DNA pellet was rinsed with ice-cold 70% ethanol, air-dried and resuspended in 25µl of sterile deionised water.

2.2.2.5. Construction of pBluescript-JIP-1b

The construction of pBluescript-JIP-1b for *in vitro* transcription/translation reactions was carried out in two steps. First, the 5' end of JIP-1b contained in the pBK-JIP-1b construct was cloned into pBluescript SK+. For this, 2µg of each of pBK-JIP-1b and pBluescript SK+ were digested with *Eco*RI and *Hind*III. The digested products were separated by electrophoresis on a 0.8% agarose gel for 1 hour at 80V. The *Eco*RI-*Hind*III JIP-1b and the *Eco*RI-*Hind*III pBluescript SK+ fragments were electroeluted as described (section 2.2.2.4) and were ligated using the Lightning® DNA Ligation kit (Bioline) as per the manufacturer's instructions.

In the second step, the 3'end of JIP-1b was cloned into pBluescript-JIP-1b (*Eco*RI-*Hind*III) by ligating the *Kpn*I fragment of pBK-JIP-1b into the *Kpn*I site of pBluescript-JIP-1b (*Eco*RI-*Hind*III) as described above. The pBluescript-JIP-1b construct, containing the full-length JIP-1b, was then transformed into competent XL-1 Blue MRF' cells (section 2.2.1.2) and verified by DNA sequencing using T7 and T3

primers at the PNACL facility as described (section 2.2.1.4). Glycerol stocks of pBluescript-JIP-1b were then prepared as described in section 2.2.1.3.

2.2.2.6. Construction of caspase-3 cleavage-resistant JIP-1b mutants

1. Synthesis and purification of oligonucleotides

The oligonucleotide primers used for JIP-1b mutagenesis are listed in Table 2.1. Oligonucleotide primers were synthesised at the PNACL facility on an Applied Biosystems model 394 machine at a 0.2μM scale. Oligonucleotides were purified by ethanol precipitation as described in section 2.2.2.4. The pellet was resuspended in 200μl of sterile deionised water, and the concentration of the oligonucleotide was determined by measuring the absorbance at 260nm.

2. PCR conditions

The PCR conditions used for PCR mutagenesis (section 2.3.6.3) were as follows. The PCR reaction mixture consisted of 50ng of pBluescript-JIP-1b or 2μl of PCR products as a template, 1.5mM $MgSO_4$, 0.2 mM dNTP mix (Life Technologies), 2μM forward primer, 2μM reverse primer, 5 units of Vent DNA polymerase (New England Biolabs) and sterile deionised water to a final volume of 50μl. For PCR using the T7-D105AR and T7-FBsmR primer pairs, 2% (v/v) dimethyl sulphoxide (DMSO) was also included in the reaction mixture.

The cycling parameters employed were: initial denaturation for 4 minutes at 95°C, followed by 20 cycles of 95°C (60 seconds)-X°C (60 seconds)-72°C (90 seconds), and final extension for 10 minutes at 72°C (X°C denotes the annealing temperature). Reactions were performed in a Perkin Elmer Applied Biosystems GeneAmp® PCR System 9700 (Perkin Elmer, Foster City, California, U. S. A.).

3. PCR mutagenesis

Caspase-3 cleavage-resistant JIP-1b mutants D98A and D405A were constructed using insertional overlapping polymerase chain reaction (PCR) mutagenesis (Ho *et. al.*, 1989). The PCR conditions employed for PCR mutagenesis were as described in the previous section. PCR mutagenesis was performed in two steps, as explained in detail for the JIP-1b D98A mutant (see also section 4.2.2.4 and Fig. 4.13).

To construct the D98A mutant, the first step involved two separate PCR reactions that were carried out on the wild-type full-length pBluescript-JIP-1b template using

Table 2.1. Oligonucleotide primers used for JIP-1b mutagenesis

Primer	*Sequence*
T7	5'- AATACGACTCACTATAGGG-3'
D105AR	5'-GTCACTTGCCGCAGCGATCAGGTCC-3'
D105AF	5'-GGACCTGATCGCTGCGGCAAGTGAC-3'
D412AR	5'-GTGGCAGAGGCGCTTTCGTC-3'
D412AF	5'-GACGAAAGCGCCTCTGCCAC-3'
FBsmR	5'-TGCGGGAAAAGGTTGAGCGTGG-3'
FBglF	5'-CGAATCCACTATCAGGCAGATG-3'
FBstR	5'-TTGTGATAAGGAACCTGGACAG-3'

oligonucleotide pairs T7-D105AR (annealing temperature 60°C) and D105AF-FBsmR (annealing temperature 55°C). The resulting products were fractionated through a 1.4% agarose gel, electroeluted and ethanol-precipitated as described (sections 2.2.2.3 and 2.2.2.4), and were used as templates in the second step for the amplification by PCR using the T7-FBsmR oligonucleotide pair (annealing temperature 55°C). The 0.7 kb product (from the second step PCR) was digested with *Eco*RI and *Nar*I, and cloned into *Eco*RI/*Nar*I digested pBluescript-JIP-1b using the Lighting™ DNA Ligation kit (Bioline). The cloned product was transformed into competent XL-1 Blue MRF' cells, and the presence of the desired mutation was confirmed by DNA sequencing using T7 and FBsmR primers at the PNACL facility as described (section 2.2.1.4).

The D405A mutant was constructed similarly, using primer pairs FBglF-D412AR and D412AF-FBstR at an annealing temperature of 55°C for the first step, and the primer pair FBglF-FBstR at an annealing temperature of 50°C for the second step. The 0.95 kb product (from the second step) was digested with *Bgl*II and *Bst*EII, and cloned into *Bgl*II/*Bst*EII digested pBluescript-JIP-1b. The cloned product was transformed into XL-1 Blue MRF' cells and verified by DNA sequencing using FBglF and FBstR primers at the PNACL facility as described (section 2.2.1.4).

A cleavage-resistant double mutant, JIP-1b D98A/D405A, was generated by excising the *Bgl*II-*Bst*EII fragment from pBluescript-JIP1b (D405A) and cloning it into pBluescript-JIP-1b (D98A Δ*Bgl*II-*Bst*EII). Glycerol stocks of the single and the double mutants were prepared as described (section 2.2.1.3).

2.2.3. Biochemical methods

2.2.3.1. Preparation of cell extracts

For the preparation of cultured mammalian cell extracts, the medium was aspirated using a vacuum pump and the adherent cells were washed twice with ice-cold phosphate buffered saline (PBS). Cells were lysed on ice by scraping into 200µl of ice-cold triton lysis buffer using a "rubber policeman". The extracts were clarified by centrifugation at 14000 rpm for 20 minutes at 4°C. The supernatant was snap-frozen and stored at –80°C.

Mouse and rat brain extracts were prepared by pulverising 50-100 mg of the tissue under liquid nitrogen using a pestle and a mortar. The tissue powder was extracted in 500µl of ice-cold triton lysis buffer, clarified and stored as above.

2.2.3.2. Determination of protein concentration

The protein concentration of clarified cell extracts was measured according to the method of Bradford (Bradford, 1976). The sample (5µl) was diluted 20-fold with 95µl of sterile deionised water. The stock concentration of BSA (1mg/ml) was diluted with sterile deionised in a final volume of 100µl such that the final concentration of BSA in the samples was between 0-30µg. The Bradford reagent was added to a final volume of 1ml. The mixture was incubated for 30 minutes at room temperature, after which the absorbance was measured at 595nm using Unicam SP 1750 Ultraviolet Spectrophotometer. The protein concentration of the sample was deduced from the standard BSA calibration curve.

2.2.3.3. SDS-PAGE

Protein extracts were denatured by the addition of 6x SDS Laemelli buffer to a final concentration of 1x. The samples were heated for 3 minutes at 100°C, and were loaded on a 7% or a 10% SDS-PAGE minigel (Biorad). Proteins were separated by electrophoresis for 90 minutes at 100V as described by Laemmeli (1970), alongside appropriate protein markers, in 1x running buffer. Pre-stained protein markers (Biorad) were used for immunoblots analysis, and Dalton Mark VII-L (Sigma) protein markers were used if the gel was to be stained/destained.

2.2.3.4. Coomassie staining of SDS-polyacrylamide gels

Gels were stained in a solution containing Coomassie Brilliant Blue R-250 for 15 minutes at room temperature. The gel was destained in a destaining solution for 3 hours at room temperature. The gels were then dried for 2 hours under vacuum on a gel dryer (Flowgen) at 80°C.

2.2.3.5. Immunoprecipitation

Equal amounts of lysates in a total volume of 500µl of ice-cold triton lysis buffer were pre-cleared with 10mg of protein A sepharose (Sigma) for 1 hour at 4°C. The cleared lysate was then incubated with fresh 10mg of protein A sepharose and appropriate antisera/purified antibody (see Figure legends). The volume was made up to 500µl with ice-cold triton lysis buffer, and the mixture was tumbled for 3 hours at 4°C. The immunoprecipitates were washed thrice with 1ml of ice-cold triton lysis buffer. The proteins in the immunoprecipitates were denatured by the addition of 2x SDS Laemelli

buffer and heated for 3 minutes at 100°C. The samples were then subjected to 7% or 10% SDS-PAGE, followed by immunoblot analysis.

2.2.3.6. Measuring JNK activity

Cell extracts from cultured mammalian cells (section 2.2.6.1) were used for assaying JNK activity by kinase assay. Equal amounts (400μg) of cell extracts were incubated with 10mg of protein A sepharose and 5μl of the rabbit polyclonal JNK1 antiserum #355, and the total volume was made up to 500μl with ice-cold triton lysis buffer. The mixture was then tumbled for 3 hours at 4°C. The immunoprecipitates were washed twice with 1ml of ice-cold triton lysis buffer and once with 1ml of ice-cold kinase assay buffer. The protein A sepharose beads were resuspended in a total volume of 50μl of kinase assay buffer containing 50μM [γ-^{32}P] ATP (2200 cpm/pmol) and 5μg of purified GST-c-Jun substrate (kindly provided by Dr. Steve Harding, Department of Biochemistry, University of Leicester, Leicester). The mixture was incubated for 30 minutes at 30°C. The reaction was terminated by the addition of 10μl of 6x SDS Laemelli buffer, and the samples were heated for 3 minutes at 100°C.

The samples were then subjected to 10% SDS-PAGE, the gel was stained with Coomassie Brilliant Blue R-250, destained and dried as described (sections 2.2.3.3 and 2.2.3.4). The dried gel was exposed to a PhosphorImager screen for 72h at room temperature and was visualised using an ImageQuant™ software (Molecular Dynamics). The results were quantified using the ImageQuant™ software, and were converted to fold-over-the-basal values. The experiments were repeated four times, and the data obtained were expressed graphically as mean ± standard error of the mean (S. E. M.). Where indicated, a two-tailed paired t-test for means was carried out using a t-test calculator (available free at GraphPad.com).

2.2.4. Immunological methods

2.2.4.1. Immunoblotting

Equal amounts of proteins were separated by SDS-PAGE (section 2.2.3.3) and transferred to Immobilon-P™ (Millipore) using a semi-dry transfer apparatus (Biorad) for 40 minutes at 10V using transfer buffer. The transfer of the proteins was judged on the basis of the presence of pre-stained markers on Immobilon-P™.

For immunoblotting, the membranes were blocked overnight in a solution tris-buffered saline (TBS) containing 0.2% (v/v) Polyoxyethylene sorbitan monlaurate (Tween-20) and 3% (w/v) BSA (First Link U. K. Ltd.) at 4°C. The membranes were incubated with an appropriate primary antibody for 2 hours at room temperature, followed by 6 x 10 minutes washes with TBS/0.1% (v/v) Tween-20. The membranes were then incubated with anti-rabbit or anti-mouse HRP-conjugated secondary antibody (Sigma) diluted to 1:20,000 in a solution of TBS/0.1% (v/v) Tween-20 at room temperature for 40 minutes, followed by 6 x 10 minutes washes with TBS/0.1% (v /v) Tween-20. The membranes were then placed in a 1:1 mix of ECL™ reagents (Amersham Pharmacia Biotech) for 1 minute at room temperature, wrapped in Saran wrap (Dow Chemical Company) and exposed to X-ray film (Fuji Photo Film Europe GmbH).

For reprobing the immunoblots, antibodies were stripped from the membranes by incubating the membranes for 1 hour at 60°C with gentle shaking in the stripping buffer.

2.2.4.2. Purification of IgG from JIP-1 antisera #608, #609 & #610

1. JIP-1 antisera production

Polyclonal antisera to JIP-1, termed #608, #609 and #610, were raised in rabbits against three peptides (MD1, MD2 and MD3 respectively) coupled to keyhole limpet haemocyanin (KLH) using maleimidobenzoic acid N-hydroxysuccinimide ester by Dr. Dickens as per the protocol of Liu *et. al.* (1979). The peptides were synthesised at the PNACL facility. The sequences of these peptides are shown in Table 2.2. MD1 and MD2 peptide sequence correspond to the N- and C-termini of JIP-1 respectively, while MD3 peptide sequence corresponds to the 47aa insertion at the C-terminus that is absent in the JIP-1a clone but is present in the full-length protein JIP-1b (Ito *et. al.*, 1999).

2. Purification of IgG from JIP-1 antisera

IgG was purified from JIP-1 antisera #608, #609 and #610 according to the method of McKinney & Parkinson (1987). JIP-1 antiserum #608, #609 or #610 (5ml) was added to 20ml of 60mM sodium acetate (pH 4.0) and the pH of the mixture was adjusted to 4.5 with a solution of 5M NaOH. Caprylic acid (25µl per ml of the antiserum/sodium acetate mixture) was added dropwise, with constant stirring, for 30 minutes at room temperature. The mixture was then centrifuged at 10,000g for 30 minutes at room temperature, and the supernatant was filtered through a nylon mesh.

Table 2.2. Peptides used to generate polyclonal antibodies to JIP-1

Name	*Sequence*	*Comments*
MD1	NFRLTHDISLE	Residues 32-42 of JIP-1a
MD2	EYTCPTEDIYLE	Residues 649-660 of JIP-1a
MD3	IDQFRVKFLGS	Residues 564-574 of JIP-1b

The filtered supernatant was mixed with 5ml of PBS, and the pH was adjusted to 7.4 with a solution of 5M NaOH. The temperature of the solution was decreased to 4°C by incubating it for 20 minutes on ice. Solid ammonium sulphate (0.277g per ml of the solution) was added to the solution, which was kept on ice, with constant stirring for 30 minutes. The solution was centrifuged at 5000rpm for 15 minutes at 4°C and the supernatant discarded. The pellet was resuspended in 2.3ml of PBS, and the protein concentration was measured using the Bradford assay. The solution was then stored at –20°C in 200µl aliquots. The concentration of the purified #608 and #610 antibodies was 570µg/ml, and that of the #609 antibody was 950µg/ml.

2.2.4.3. Affinity purification of the JIP-1 antipeptide antibody #609

The JIP-1 antibody #609 was purified from the antiserum using the immunising peptide MD2 coupled to an affinity column.

1. Coupling the peptide MD2 to NHS-activated sepharose

A 2ml of the settled volume of NHS-activated Sepharose® 4 Fast Flow (Amersham Pharmacia Biotech) was placed in a 15ml Falcon tube, and washed three times with 13ml of ice-cold 1mM HCl by centrifugation at 2000rpm for 1 minute at 4°C. 4ml of the MD2 peptide solution (in 100mM sodium acetate, pH 4.8), containing a total of 40µmoles of the MD2 peptide, was added to the sepharose and incubated overnight with tumbling at 4°C. After overnight incubation, the mixture was centrifuged at 2000rpm for 1 minute at 4°C, and both the gel and the supernatant were retained. The supernatant was stored at –20°C. The unreacted groups in the gel were blocked by incubation in 7ml of 100mM Tris-HCl (pH 8.8) for 2 hours at 4°C. The sepharose beads were recovered by centrifugation at 2000rpm for 30 seconds at 4°C and the supernatant was discarded. The sepharose was washed three times with 5ml of ice-cold 100mM sodium acetate (pH 3.5), resuspended in 5ml of ice-cold 20% (v/v) ethanol and stored at 4°C until required.

To determine the coupling efficiency of the peptide to the sepharose, absorbance at 215nm of the peptide solution before and after coupling was measured. The results suggested that ~33% (~7µmoles/ml) of the peptide had bound to the column.

2. Affinity purification of the #609 antibody

The affinity purification of the #609 antibody was carried out at room temperature.

The sepharose in 20% (v/v) ethanol was spun at 2000rpm for 30 seconds at 4°C, and the supernatant was discarded. A 2ml settled volume of the sepharose was transferred to a column, and was washed three times with 7ml of PBS. The column was loaded with 5ml of JIP-1 antiserum #609, and the antiserum/sepharose mixture was recirculated for 2 hours at a flow rate of 0.5ml/minute using a peristaltic pump. The flow-through obtained after 2 hours was collected and stored at -20°C. The sepharose was washed with 100ml of PBS to remove the unbound proteins. To monitor the complete removal of the unbound proteins, 50µl of the flow-through during the washing procedure was assayed at regular intervals with the Bradford assay. Washing was continued until no proteins were detected in the flow-through, as determined by the Bradford assay.

The purified JIP-1 antibody #609 was eluted with 0.1M glycine/0.15M NaCl buffer, and 20 x 0.5ml fractions were collected in eppendorfs containing 20µl of ice-cold 1M Tris. Each fraction was assayed by the Bradford assay. Fractions containing the highest amount of proteins were pooled together, and the protein concentration of pooled fractions was again measured using the Bradford assay (100µg/ml). The purified JIP-1 antibody was then aliquoted and stored at -20°C.

2.2.4.4. Enzyme-linked immunosorbent assay (ELISA)

The antigens (BSA-MD1, BSA-MD2 and BSA-MD3) and the control antigen BSA were dissolved in 0.05M Na_2CO_3 to a final concentration of 20µg/ml. The antigen (50µl) or BSA (50µl) was added to the wells in a 96-well plate (Bibby Sterilin Ltd.). The plate was sealed with Nescofilm (Bendo Chemical Industries Ltd.) and incubated overnight at 4°C. Unbound antigen was removed by flooding each well three times with PBS/0.05% (v/v) Tween-20. Non-specific protein binding sites in the wells were blocked by incubation with 30% non-fat dried milk in PBS for 1 hour at 37°C. The blocking agent was removed, and the wells were flooded three times with PBS/0.05% (v/v) Tween-20.

The antiserum/purified antibody to be tested was diluted as desired in PBS/0.05% (v/v) Tween-20 solution, and 50µl of this solution was added to each well. The plate

was sealed with Nescofilm and incubated for 1 hour at 4°C. Excess antibody was removed by three washes with PBS/0.05% (v/v) Tween-20. A 50µl solution of anti-rabbit HRP conjugate, diluted to 1:2000 in PBS/0.05% (v/v) Tween-20/10% FCS, was added to each well. The plate was sealed with Nescofilm and was incubated for 1 hour at 4°C. Wells were then washed three times with PBS/0.05% (v/v) Tween-20 and twice with distilled water. The chromogenic substrate (50µl) was added to the wells. The plate was incubated in the dark for 15 minutes at room temperature. The reaction was terminated by the addition of 50µl of 4M sulphuric acid. The absorbance in each well was read at 490nm using a microplate EL 340 reader (Bio-Tek instruments).

For peptide competition assays, peptides MD1, MD2 and MD3 were dissolved in 100mM Hepes (pH 7.4) to a final concentration of 10mM. The ELISA procedure was essentially the same as described above, except that the peptides (0-640µM) were added immediately after the antiserum had been added.

2.2.5. Mammalian cell culture

HeLa (human cervical carcinoma), HEK 293 (human embryonic kidney), GC1 (mouse testes) and N1E 115 (mouse neuroblastoma) cell lines were routinely maintained in DMEM (high glucose; Life Technologies) supplemented with 10% (v/v) FBS, 2mM L-Glutamine, 100 units/ml of each of penicillin and streptomycin. Min6 cells were maintained under similar conditions except that DMEM was supplemented with 15% (v/v) FBS. PC12 cells (rat phaeochromocytoma) were maintained similarly except that the DMEM was supplemented with 5% (v/v) FBS and 5% (v/v) horse serum. Rat pancreatic β cells RinD11 and Rin5F were maintained in RPMI 1640 (with L-Glutamine) supplemented with 10% (v/v) FBS, 2mM L-Glutamine, 100 units/ml of each of penicillin and streptomycin. All cells were grown in an atmosphere of 5% CO_2 at 37°C.

For routine maintenance, the adherent cells were grown to confluence in 80 cm^2 flasks and trypsinised with 2ml of trypsin-versene solution. Cells were subcultured every 3-4 days at a ratio of 1:10.

Transfection of DNA into HEK293 cells was carried out using Tfx-50™ transfection reagent (Promega) according to the manufacturer's instructions. Approximately 16 hours after transfection, cell extracts were prepared as described (section 2.2.3.1).

2.2.6. Apoptosis techniques

2.2.6.1. Induction of apoptosis and preparation of extracts

HeLa cells were plated on 10cm petri dishes and grown to ~75% confluency. The apoptotic stimuli used to induce apoptosis were added to the serum-containing culture medium, except for the agonistic Fas antibody, which was added to serum-free culture medium. Apoptosis induction by TNF-α was carried out in combination with cycloheximide (CHX) (Lin *et. al.*, 1999), and by agonistic Fas antibody was carried out in combination with 30μM PD98059 (Holmstrom *et. al.*, 1999). The concentrations of the apoptotic stimuli used are stated in Figure legends. Where indicated, cells were pre-treated for 1 hour with zVAD.fmk (added to a final concentration of 50μM) or DEVD.fmk (added to a final concentration of 10-50μM as described in Figure legends) before exposure to the apoptotic stimulus. After the desired incubation period with the apoptotic stimulus, detached cells were collected by centrifugation at 1000 rpm for 3 minutes at 4°C. Both attached and detached cells were washed once with 2ml of ice-cold PBS and lysed in 200μl of ice-cold triton lysis buffer. The extracts were clarified as described (section 2.2.3.1), and were stored at –70°C until required. The protein concentration of the extract was measured using the Bradford assay.

2.2.6.2. Quantification of apoptosis

To quantify the number of apoptotic cells, DNA fragmentation assay using Hoechst 33258 staining was used since DNA fragmentation is indicative of active caspase 3 (Liu *et. al.*, 1997). HeLa cells were plated on to sterile 22 x 22 mm coverslips placed in 3cm dishes. After 24 hours, cells were treated with an appropriate apoptotic stimulus, as described in Figure legends. The medium containing the detached cells was transferred to a separate set of poly-L-lysine-coated coverslips placed in 3cm dishes, and the detached cells were fixed with 1ml of ice-cold methanol for 30 minutes at –20°C. Adherent and detached cells fixed to coverslips were washed three times with calcium- and magnesium-free PBS, and were blocked with 1ml of PBS/1% BSA for 1 hour at room temperature. Coverslips were then washed five times with calcium- and magnesium-free PBS, and incubated with Hoechst 33258 (1μM) for 5 minutes at room temperature. Finally, coverslips were washed three times with calcium- and magnesium-free PBS, and were mounted and fixed on glass slides. Apoptotic cells were quantified on the basis of the presence of nuclear DNA fragmentation, and non-

apoptotic cells were quantified on the basis of the absence of nuclear DNA fragmentation, by visualisation under a fluorescence microscope. The percentage of apoptotic cells was deduced from the total number of cells. The experiment was performed in duplicate or triplicate, and the data was presented graphically as the mean of duplicate/triplicate experiments.

2.2.6.3. In vitro transcription/translation cleavage reactions using purified caspases

[^{35}S]Met-labelled proteins were produced *in vitro* with a coupled transcription/translation system (TNT® T7 kit, Promega). The reaction mixture included 2μg of circular template DNA (pBluescript containing the wild type or mutant JIP-1b), 1x TNT® reaction buffer, 1 unit of T7 RNA polymerase, 1mM amino acid mixture (minus methionine), [^{35}S] methionine (1000 Ci/mmol at 10mCi/ml), 1 unit RNasin® ribonuclease inhibitor, and sterile deionised water to a final volume of 50μl. The sample was incubated for 90 minutes at 30°C.

For *in vitro* cleavage reactions, 10μl of the lysate containing [^{35}S]Met-labelled protein product was incubated with the required amount of purified caspase-3 or -8 (see the Figure legends), and the final volume was made up to 25μl with Hepes buffer. The reaction was incubated at 30°C as indicated in Figure legends.

In vitro cleavage reactions were terminated by the addition of 1x SDS Laemelli buffer, heated for 3 minutes at 100°C and separated by 10% SDS-PAGE. The gel was stained with Coomassie Brilliant blue, destained, dried and exposed to a PhosphorImager screen for 72 hours and visualised using ImageQuant™ software (Molecular Dynamics).

APPENDIX

All the media/reagents/buffers were prepared in deionised water unless otherwise stated.

Agarose gel loading buffer

15% Ficoll, 0.2% bromophenol blue, 0.2% xylene cyanol FF in sterile deionised water.

Antibody stripping buffer

62.5mM Tris (pH 6.7), 2% (w/v) SDS and 0.8% (v/v) β-mercaptoethanol.

Bradford reagent

100mg of Coomassie Brilliant Blue G-250 was dissolved in 50ml of 95% (v/v) ethanol, to which 100ml of 85% (w/v) phosphoric acid was added. The solution was diluted to 1 litre with deionised water, filtered through Whatmann 3MM paper and stored at 4°C.

Buffered $CaCl_2$ solution

60mM $CaCl_2$, 10mM piperazine-N,N'-bis[2-ethanesulfonic acid] (PIPES; pH 7.0) and 15% glycerol. The solution was autoclaved and stored at 4°C.

Chromogenic substrate for ELISA assays

To prepare the chromogenic substrate, firstly the citrate-phosphate buffer (pH 5.4) containing 250mM disodium hydrogen phosphate and 100mM citric acid was prepared. The pH was adjusted to 5.4 with a solution of 10M HCl. 12.25ml of citrate phosphate buffer (pH 5.4) was mixed with 1.25µl 30% H_2O_2 and 5mg ortho-phenylenediamine, and this mixture was used as a substrate in ELISA assays.

Coomassie staining solution

0.1% (w/v) Coomassie Brilliant blue R-250, 10% (v/v) acetic acid and 40% (v/v) ethanol.

Destaining solution

10% (v/v) acetic acid and 25% (v/v) methanol.

Hepes buffer for *in vitro* caspase cleavage reactions

10mM Hepes (pH 7.5), 2mM EDTA, 0.1% CHAPS, 10μg/ml antipain, 10μg/ml pepstatin, 10μg/ml leupeptin, 2mM PMSF and 5mM DTT.

Kinase assay buffer

25mM Hepes (pH 7.4), 25mM β-glycero phosphate, 25mM magnesium chloride, 0.5mM sodium orthovanadate, 0.5mM EDTA and 0.5mM DTT.

Luria Bertani (LB) agar

4g bacto-tryptone, 2g bacto-yeast extract, 4g NaCl and 6g agar were dissolved in a final volume of 400ml of deionised water. The mixture was autoclaved and allowed to cool at room temperature. Where required, antibiotics were added to the autoclaved agar solution before preparing the agar plates.

LB medium

4g bacto-tryptone, 2g bacto-yeast extract and 4g NaCl were dissolved in a final volume of 400ml of deionised water. The mixture was autoclaved and stored at 4°C.

Phosphate-buffered saline (PBS)

5mM sodium dihydrogen phosphate, 5mM disodium hydrogen phosphate and 0.14M NaCl.

SDS Laemmeli buffer (6x)

7% (v/v) of 0.5M Tris (pH 6.8), 3% glycerol, 0.6M DTT and 0.35M SDS. 1.2mg Bromophenol blue was added per 10ml of the solution.

SDS-PAGE running buffer (10x)

1.92M glycine, 247.7mM Tris and 34.7mM SDS.

SDS-PAGE separating and stacking gels

A 10ml solution of a 7% separating gel consisted of 5.3ml of deionised water, 2.5ml of 1.5M Tris (pH 8.8), 2.3ml of 30% acrylamide:0.8% bis-acrylamide, 8µl of N,N,N`,N-tetramethyl ethylenediamine (TEMED) and 100µl of 10% ammonium persulphate (APS).

A 10ml solution of a 10% separating gel consisted of 4ml of deionised water, 2.5ml of 1.5M Tris (pH 8.8), 3.3ml of 30% acrylamide:0.8% bis-acrylamide, 4µl TEMED and 100µl of 10% APS.

A 10ml solution of the stacking gel consisted of 6.8ml of deionised water, 1.25ml of 0.5M Tris (pH 6.8), 1.7ml of 30% acrylamide:0.8% bis-acrylamide, 10µl TEMED and 100µl of 10% APS.

Stock solutions of antibiotics

Stock solutions of 50mg/ml ampicillin, 15mg/ml tetracycline and 75mg/ml kanamycin were prepared using sterile deionised water. The solutions were filter-sterilised using 0.2µ filter (Pall Gelman Laboratory). The stock solutions of ampicillin and tetracycline were stored at –20°C, and the stock solution of kanamycin was stored at room temperature. The working concentrations of the antibiotics were: ampicillin - 50µg/ml, tetracycline - 15µg/ml and kanamycin - 75µg/ml.

Stock solutions of apoptosis inducers

Stock solutions of 1mM staurosporine and 50mg/ml anisomycin were prepared in dimethyl sulphoxide (DMSO) and were stored at –70°C. Stock solutions of 150mM sodium arsenite, 1M glucose and 1M H202 were prepared in deionised water, filter-sterilised using a 0.2µ filter (Pall Gelman Laboratory) and stored at 4°C.

TAE buffer (50x)

2M Tris, 0.1M ethylene diamine tetra acetic acid (EDTA) and 5.7% (v/v) acetic acid.

Transfer buffer

0.19M glycine, 24.8mM Tris and 3.5mM SDS.

Triton lysis buffer

20mM Tris (pH 7.4), 137mM NaCl, 25mM β-glycero phosphate, 2mM sodium pyrophosphate, 2mM EDTA, 1mM sodium orthovanadate, 2mM benzamidine, 0.5mM dithiothreitol (DTT), 5μg/ml pepstatin, 5μg/ml antipain, 5μg/ml leupeptin, 1% Triton X-100, 10% glycerol and 1mM phenyl methyl sulphonyl fluoride (PMSF).

Tris-buffered saline (TBS)

10mM Tris base, 1mM EDTA and 0.15M NaCl.

Trypsin-versene

0.25% (w/v) solution of trypsin was added to 0.5mM EDTA in PBS, and the resulting solution was filter-sterilised. The solution was stored at 4°C.

CHAPTER 3

INTERACTIONS BETWEEN JIP-1 SCAFFOLD COMPLEX COMPONENTS *IN VIVO*

3.1. INTRODUCTION

The ERK, JNK and p38 pathways altogether consist of seven MKKs and fourteen MKKKs. These protein kinases, particularly MKKKs, have broad specificity. For example, ASK1 or TAK1 can activate both p38 and JNK (Ichijo *et. al.*, 1997; Wang *et. al.*, 1997; Hanafusa *et. al.*, 1999). Of the MKKs, MKK4 can activate both p38 and JNK (Sanchez *et. al.*, 1994). Moreover, one extracellular signal can activate several MKKKs that lead to the activation of more than one MAPK pathway (Garrington & Johnson, 1999). Therefore, the question arises of how specific responses are generated in a system that appears redundant at the level of MKKs, MKKKs and further upstream messengers.

Recent research has led to the understanding that protein-protein interactions are critical in maintaining signalling specificity (Pawson & Nash, 2000). The discovery of scaffold proteins that function to segregate the MAPK signalling cascades by assembling the cascades within large protein complexes represents an important step in understanding signalling specificity (Davis, 2000). For the JNK pathway, a family of proteins, known as the JNK-interacting proteins 1, 2 and 3 (JIP-1, -2 and -3), have been proposed on the basis of transient transfection studies to act as scaffolds by binding specifically to JNK, MKK7 and MLKs (section 1.4).

A critical test for the JIP scaffold model is whether the proposed interactions between kinases of the JNK pathway and JIPs occur in intact, non-transfected cells. This question was addressed using an immunoprecipitation/western blotting approach. If the interaction between JIP-1 and the JNK pathway components exists in intact cells, then, in theory, immunoprecipitation of one endogenous protein should precipitate its interacting partner(s), each of which should then be detectable by western blotting. JIP-1, JNK1, MKK7, MLK3 and HPK1 are all expressed at moderate or high levels in brain (Derijard *et. al.*, 1994; Ing *et. al.*, 1994; Kiefer *et. al.*, 1996; Dickens *et. al.*, 1997; Foltz *et. al.*, 1998), hence the likelihood of these proteins interacting would be higher in brain. Therefore to test the above hypothesis, rat brain and N1E-115 mouse neuroblastoma cell lysates were used for biochemical analysis. For this purpose, rabbit polyclonal antibodies #608, #609 and #610 were raised against JIP-1. Then, available antibodies to JIP-1, JNK1, MKK7, MLK3 and HPK1 were tested for their ability to detect the endogenous protein by western blotting and to precipitate the endogenous protein by immunoprecipitation. Finally, the components of the JIP-1 scaffold were

immunoprecipitated and the presence of the interacting partner(s) in the resulting precipitates was detected by western blotting.

3.2. RESULTS

3.2.1. Anti-JIP-1 antibody characterisation

Polyclonal antisera to JIP-1, termed #608, #609 and #610, raised against the immunising peptides KLH-MD1, KLH-MD2 and KLH-MD3 respectively were available (see section 2.2.4.2, Materials & Methods). The peptides were also available as bovine serum albumin (BSA) conjugates for use as antigen in enzyme-linked immunosorbent assay (ELISA). BSA conjugates were designated BSA-MD1, BSA-MD2 and BSA-MD3.

IgGs were purified from antisera #608, #609 and #610 by caprylic acid/ammonium sulphate precipitation as described in Materials & Methods in section 2.2.4.2. #609 antiserum was also purified by affinity chromatography using the immobilised MD2 peptide (section 2.2.4.3, Materials & Methods).

JIP-1 polyclonal antisera were first characterised by ELISA to test for their reactivity with the immunising peptide. Available JIP-1 polyclonal and monoclonal antibodies were next characterised by western blotting and immunoprecipitation with an aim to identify antibodies that could detect and immunoprecipitate endogenous JIP-1 from rat brain lysate and N1E-115 mouse neuroblastoma cells.

3.2.1.1. Characterisation of JIP-1 polyclonal antisera and purified antibodies by ELISA

Antigen-coated ELISA was employed to test the reactivity of JIP-1 antisera to the immunising peptides by two methods (section 2.2.4.4, Materials & Methods). In the first method, JIP-1 antisera or purified antibodies were diluted against a fixed amount of antigen. In the second method, an increasing amount of the free peptide in solution was allowed to compete with a fixed concentration of the bound antigen.

1. JIP-1 antisera ELISA

Serial dilutions of the JIP-1 antisera ranging from 1:1000 to 1:512000 were tested for their reactivity against a fixed amount (1μg) of BSA-MD1, BSA-MD2 or BSA-MD3. The data was plotted as $\log_{10}$(serum dilution) against absorbance at 490nm. For

#609 and #610, antisera from three bleeds were compared to the control serum. For #608, only one bleed was available for analysis since the rabbit had to be sacrificed due to infection.

The results show that, for all three JIP-1 antisera, an increase in serum dilution led to a decrease in the absorbance at 490nm (A_{490}), irrespective of the bleed tested (Fig 3.1). With #609 and #610, the A_{490} values were higher with successive bleeds. The results suggested that for #609 and #610, the antibody titre in the second bleed was higher than in the first, and higher in the final bleed than in the second.

The A_{490} values obtained with pre-immune serum or with BSA as the control antigen were basal values, suggesting that JIP-1 antisera did not cross-react with BSA, and that the pre-immune serum did not cross-react with BSA-MD1, -MD2 and –MD3.

2. JIP-1 purified antibody ELISA

IgG-purified #608, #609 and #610 antibodies were titrated against a fixed antigen amount to determine their reactivity against BSA-MD1, -MD2 or -MD3. The antibody concentration used was in the range of 0.03μg/ml to 16μg/ml. The results were plotted as $\log_{10}$ (antibody concentration) against absorbance at 490nm. The results showed that higher antibody concentration yielded higher A_{490} values, and lower antibody concentrations yielded lower A_{490} values (Fig 3.2). The use of the control antigen BSA and a control antibody did not give A_{490} values above basal levels (Fig. 3.2), suggesting that the antibodies in the samples tested did not cross-react with BSA, and that the control antibody did not cross-react with antigens BSA-MD1, -MD2 and –MD3.

3. Peptide competition assay

To study the effectiveness of the immunising peptides in blocking the binding of the antibody to its cognate antigen, increasing concentrations (0.04μM to 640μM) of the immunising peptide or the control peptide were used in an ELISA assay against a fixed amount (1μg) of BSA-MD1, -MD2 or –MD3 or the control antigen BSA in the presence of a fixed dilution (1:2000) of #608, #609 or #610. Thus, for example, peptide MD2 or control peptide MD3 was used against the specific antigen BSA-MD2 or the control antigen BSA in the presence of antiserum #609. The results obtained were plotted as $\log_{10}$(peptide concentration) against A_{490} value.

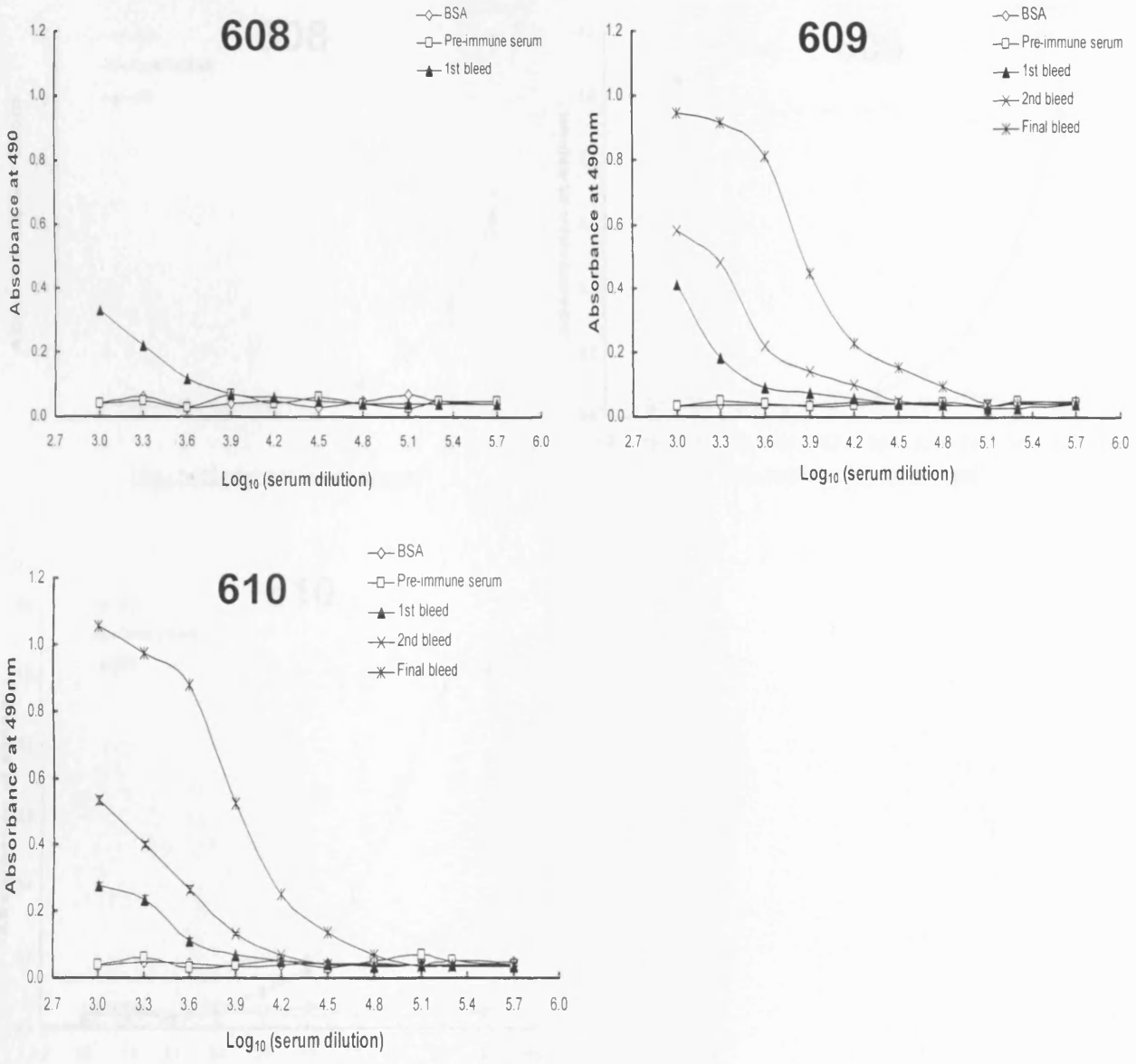

Fig. 3.1. JIP-1 antisera ELISA.

Antiserum #608 from the first bleed and antisera #609 and #610 from three bleeds were diluted against a fixed amount (1μg) of BSA-MD1, BSA-MD2 or BSA-MD3, and the absorbance was measured at 490nm as described in Materials & Methods (section 2.2.4.4). Preimmune sera and unconjugated BSA were used as controls. The results shown are mean of three independent experiments. The standard error of the mean for a given absorbance value was less than ± 0.025, and is hence not shown.

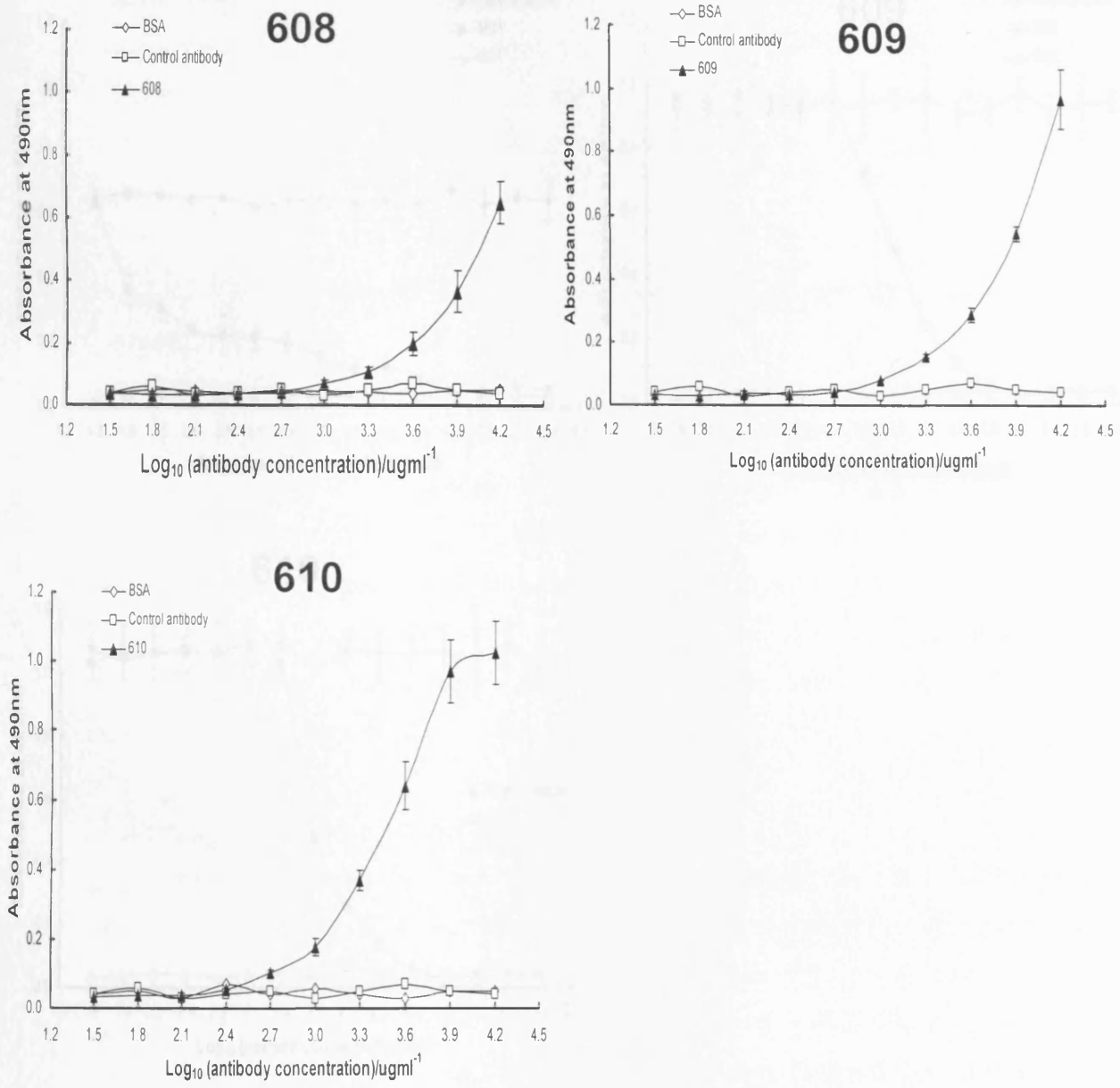

Fig. 3.2. IgG-purified JIP-1 antibody ELISA.

Different concentrations of IgG-purified JIP-1 antibodies #608, #609 or #610, or the control antibody were titrated against 1μg of BSA-MD1, BSA-MD2, BSA-MD3 or unconjugated BSA. The antigen-antibody complexes were detected and quantified as described in Fig. 3.1. The results shown are mean of three independent experiments.

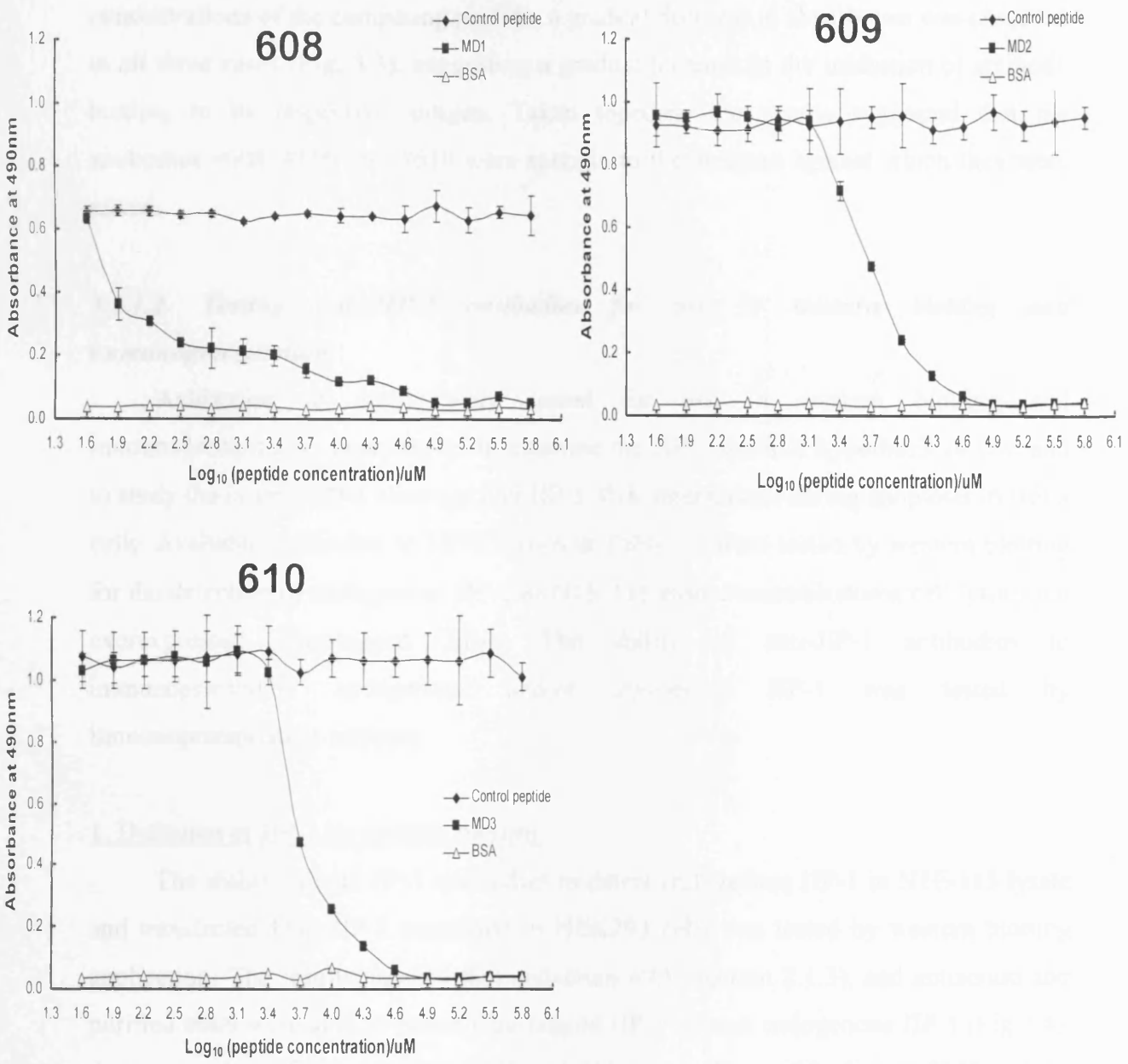

Fig. 3.3. Peptide competition ELISA.

Increasing concentrations of free peptides MD1, MD2 or MD3 were titrated against a fixed amount (1μg) of immobilised BSA conjugates. The effect of free peptides on the antibody binding to the antigen was tested in the presence of a fixed dilution (1:2000) of JIP-1 antisera and quantified as described in Fig. 3.1. For control, the assay was carried out in the presence of increasing concentrations of a control peptide (see text for explanation), or the antisera were used against an amount (1μg) of control antigen BSA. The results shown are the mean of three independent experiments.

The results in Fig. 3.3 show that, in the presence of the control peptide, the signal obtained at A_{490} did not decay (Fig. 3.3). In the presence of the increasing concentrations of the competing peptide, a gradual decrease in absorbance was observed in all three cases (Fig. 3.3), suggesting a gradual increase in the inhibition of antibody binding to its respective antigen. Taken together, the results suggested that the antibodies #608, #609 and #610 were specific to the antigens against which they were raised.

3.2.1.2. Testing anti-JIP-1 antibodies for use in western blotting and immunoprecipitation

Antibodies to JIP-1 were tested for use in western blotting and immunoprecipitation experiments to examine the JIP-1 scaffold hypothesis *in vivo* and to study the *in vivo* JIP-1 cleavage and JIP-1-JNK interactions during apoptosis in HeLa cells. Available antibodies to JIP-1 shown in Table 3.1 were tested by western blotting for the detection of endogenous JIP-1 in N1E-115 mouse neuroblastoma cell lysate and overexpressed Flag-tagged JIP-1. The ability of anti-JIP-1 antibodies to immunoprecipitate endogenous and/or transfected JIP-1 was tested by immunoprecipitation analysis.

1. Detection of JIP-1 by western blotting

The ability of anti-JIP-1 antibodies to detect endogenous JIP-1 in N1E-115 lysate and transfected Flag-JIP-1 expressed in HEK293 cells was tested by western blotting application. The results showed that antiserum #9A (section 2.1.3), and antiserum and purified #609 were able to detect Flag-tagged JIP-1 but not endogenous JIP-1 (Fig 3.4). Antisera and purified antibodies #608 and #610, as well as antibodies sc-7145 and sc-7147 did not detect endogenous or transfected JIP-1 (data not shown).

The monoclonal JIP-1 antibody #7 detected endogenous JIP-1 at ~120kDa in both rat brain and N1E-115 lysates (Fig. 3.5). The same blot was reprobed with affinity-purified #609 antibody, which recognised transfected Flag-JIP-1 but not the endogenous form (Fig. 3.5).

Table 3.1. Available antibodies to JIP-1

Antibody	*Type*
Antisera #608, #609 and #610	Rabbit polyclonal
IgG-purified #608, #609 and #610	Rabbit polyclonal
Affinity-purified #609	Rabbit polyclonal
Antiserum #9A	Rabbit polyclonal
sc-7145*	Goat polyclonal
sc-7147*	Goat polyclonal
#7*	Mouse monoclonal

* - See section 2.1.3, Materials & Methods.

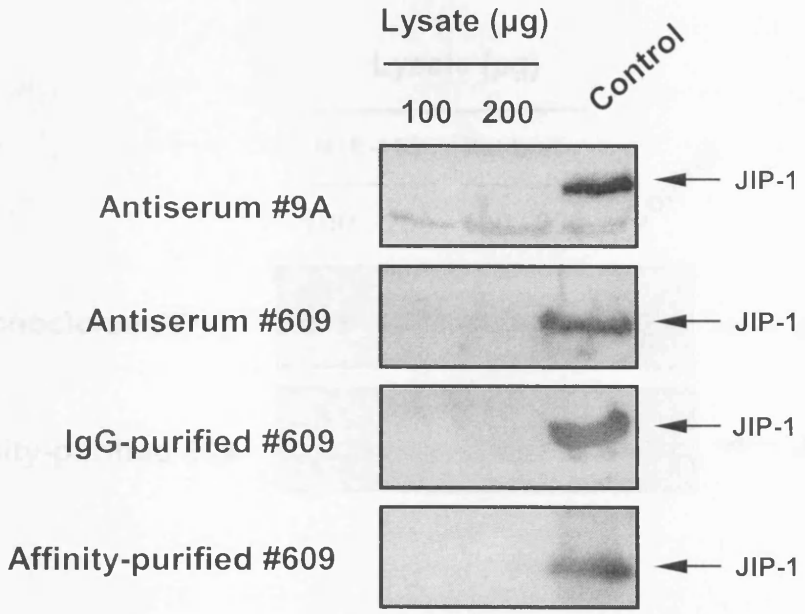

Fig. 3.4. Detection of endogenous JIP-1 by anti-JIP-1 polyclonal antibodies.

Indicated amounts of lysate from N1E-115 cells were separated by electrophoresis on 7% SDS-PAGE gels. Proteins were transferred to Immobilon-P® membranes and immunoblotted for JIP-1 using antiserum #9A (1:2000), antiserum #609 (1:2000), IgG-purified #609 (2µg/ml) or affinity-purified #609 (0.1µg/ml) anti-JIP-1 antibodies. Lysate (50µg) from HEK293 cells transfected with pCMV5-Flag-JIP-1 using Tfx-50 transfection reagent (Promega) (section 2.2.5, Materials & Methods) was used as a control.

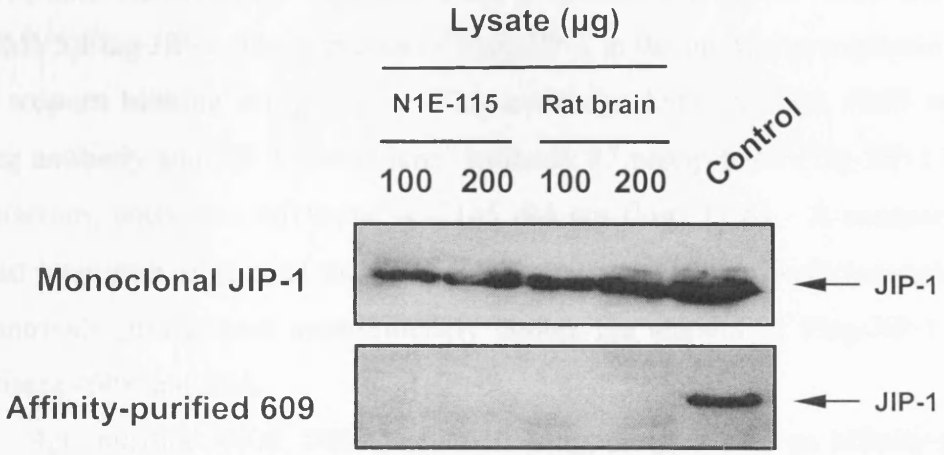

Fig. 3.5. Detection of endogenous JIP-1 by the monoclonal anti-JIP-1 antibody.

Different amounts of N1E-115 cell and rat brain lysates were separated by electrophoresis on a 7% SDS-PAGE gel and immunoblotted for JIP-1 with monoclonal anti-JIP-1 antibody (at 1:5000) or affinity-purified #609 antibody (0.1µg/ml) as indicated. Lysate (50µg) from HEK293 cells transfected with pCMV5-Flag-JIP-1 using Tfx-50 transfection reagent (Promega) (section 2.2.5, Materials & Methods) was used as a control.

2. Immunoprecipitation of transfected Flag-JIP-1

Anti-JIP-1 antibodies were next tested in their ability to precipitate endogenous JIP-1 present in rat brain and N1E-115 cell lysates and Flag-JIP-1 overexpressed in HEK293 cells.

JIP-1 antisera (#608, #609, #610 and #9A), commercially available JIP-1 antibody sc-7145 (Santacruz Biotechnology Inc.), anti-Flag antibody (Sigma) and monoclonal JIP-1 antibody #7 were tested in an immunoprecipitation assay for their ability to precipitate transfected Flag-JIP-1 from a lysate of HEK293 cells transfected with pCMV5-Flag-JIP-1. The presence of Flag-JIP-1 in the immunoprecipitates was detected by western blotting using the anti-Flag antibody. Antisera #608, #609 and #9A, anti-Flag antibody and JIP-1 monoclonal antibody #7 precipitated Flag-JIP-1 while control antiserum, antiserum #610 and sc-7145 did not (Fig. 3.6A). A comparison of JIP-1 band intensities suggested that antiserum #609/anti-Flag antibody/monoclonal anti-JIP-1 antibody precipitated approximately double the amount of Flag-JIP-1 compared to antisera #608 and #9A.

IgG-purified #608, #609 and #610 antibodies, as well as affinity-purified #609 antibody, were also tested in immunoprecipitation reactions to precipitate transfected Flag-JIP-1. IgG-purified #608 and #609 antibodies as well as affinity-purified #609 antibody immunoprecipitated Flag-JIP-1, whereas IgG-purified #610 did not (Fig. 3.6B). The amount of transfected Flag-JIP-1 precipitated by IgG-purified #609 was approximately double than that precipitated by IgG-purified #608 or affinity-purified #609 (Fig. 3.6B), as judged by band intensities.

Taken together, these results suggested that, to precipitate transfected Flag-JIP-1, antiserum #609 was more efficient compared to antisera #608 and #9A, and IgG-purified #609 was more efficient than IgG-purified #608 and affinity-purified #609.

3. Immunoprecipitation of endogenous JIP-1

JIP-1 antisera #608, #609, #610 and #9A, as well as sc-7145 and monoclonal JIP-1 antibodies were tested in their ability to immunoprecipitate endogenous JIP-1 from equal amounts of rat brain and N1E-115 cell lysates. The presence of JIP-1 in the immunoprecipitates was detected by western blotting with the monoclonal JIP-1 antibody. The results showed that, from N1E-115 cell lysates, antisera #609 and #9A, and monoclonal anti-JIP-1 antibody #7 successfully immunoprecipitated endogenous JIP-1 but control antiserum, antiserum #608, antiserum #610 and sc-7145 antibody did

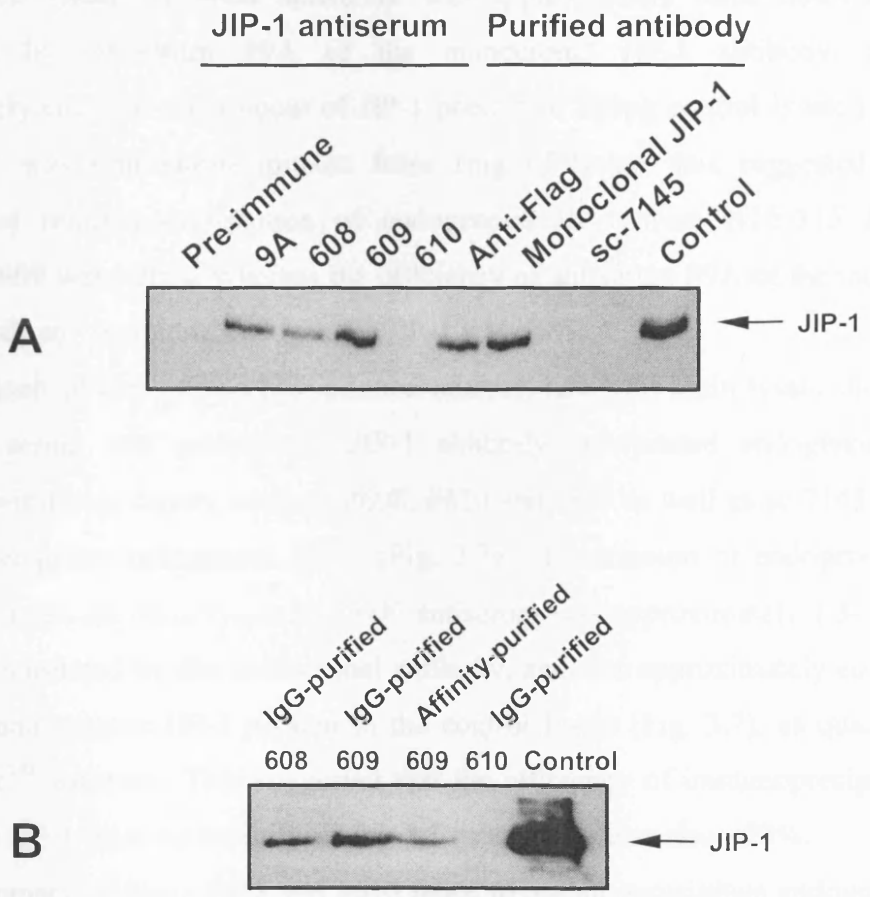

Fig. 3.6. Immunoprecipitation of transfected JIP-1 by anti-JIP-1 antibodies.

HEK293 cells, transfected with pCMV5-Flag-JIP-1, were lysed and 250μg of this lysate was immunoprecipitated with 5μl of the indicated antiserum, 3μl of the monoclonal anti-JIP-1 antibody, 1μg of anti-Flag (Sigma) or 1μg of sc-7145 (Santacruz Biotechnology Inc.) antibodies **(A)** or with 1μg of the indicated purified anti-JIP-1 antibodies **(B)**. Lysate (50μg) from HEK293 cells transfected with pCMV5-Flag-JIP-1 was used as a control. The immunoprecipitates were subjected to 7% SDS-PAGE and immunoblotted for JIP-1 using anti-Flag antibody (5μg/ml).

not (Fig. 3.7). IgG-purified and affinity-purified JIP-1 antibodies did not precipitate endogenous JIP-1 from either rat brain or N1E-115 cell lysates (data not shown).

Based on band intensities, the amount of endogenous JIP-1 precipitated from N1E-115 cell lysate by #609 antiserum was approximately three times than that precipitated by antiserum #9A or the monoclonal JIP-1 antibody, and was approximately equal to the amount of JIP-1 present in 200μg control lysate (Fig. 3.7). Since JIP-1 was immunoprecipitated from 1mg of lysate, this suggested that the efficiency of immunoprecipitation of endogenous JIP-1 from N1E-115 lysate by antiserum #609 was ~20%, whereas the efficiency of antiserum #9A or the monoclonal JIP-1 antibody to precipitate endogenous JIP-1 was ~6%.

The result of the immunoprecipitation analysis using rat brain lysate showed that only #609 serum and monoclonal JIP-1 antibody precipitated endogenous JIP-1, whereas pre-immune serum, antisera #608, #610 and #9A as well as sc-7145 antibody failed to precipitate endogenous JIP-1 (Fig. 3.7). The amount of endogenous JIP-1 precipitated from rat brain lysate by #609 antiserum was approximately 1.5-fold more than that precipitated by the monoclonal antibody, and was approximately equal to the amount of endogenous JIP-1 present in the control lysate (Fig. 3.7), as quantified by ImageQuant™ software. This suggested that the efficiency of immunoprecipitation of endogenous JIP-1 from rat brain lysate by antiserum #609 was also ~20%.

In summary, antisera #608 and #610 failed to immunoprecipitate endogenous JIP-1 and antiserum #9A precipitated JIP-1 from N1E-115 cells only. Although antiserum #609 and monoclonal JIP-1 antibody precipitated JIP-1 from both rat brain and N1E-115 cells, antiserum #609 was more efficient than the monoclonal JIP-1 antibody.

Overall, the results of Western blotting and immunoprecipitation using different JIP-1 antibodies suggested that antiserum #609 was efficient at immunoprecipitating transfected JIP-1 as well as endogenous JIP-1 from both N1E-115 and rat brain lysates, while monoclonal JIP-1 antibody was the only antibody that detected endogenous JIP-1 by western blotting. These results are summarised in Table 3.2.

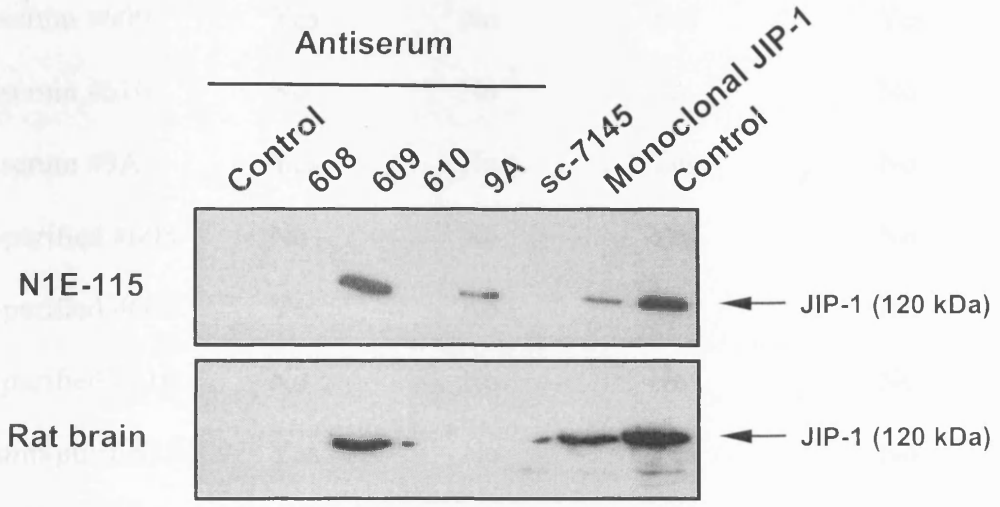

Fig. 3.7. Immunoprecipitation of endogenous JIP-1 by anti-JIP-1 antibodies.

1mg of N1E-115 or rat brain lysate was immunoprecipitated with 5µl of the indicated JIP-1 antisera, 5µl p38 (control) antiserum, 3µl of monoclonal antibody or 1µg of sc-7145 antibody (Santacruz Biotechnology Inc.). The immunoprecipitates were subjected to 7% SDS-PAGE and immunoblotted for JIP-1 using monoclonal JIP-1 antibody (1:5000). 100µg lysate from N1E-115 or rat brain was used as a control.

Table 3.2. Summary of the results of JIP-1 antibody characterisation

Antibody	*Western blotting*		*Immunoprecipitation*	
	Transfected JIP-1	Endogenous JIP-1	Transfected JIP-1	Endogenous JIP-1
Antiserum #608	No	No	Yes	No
Antiserum #609	Yes	No	Yes	Yes
Antiserum #610	No	No	No	No
Antiserum #9A	Yes	No	Yes	No
IgG-purified #608	No	No	Yes	No
IgG-purified #609	Yes	No	Yes	No
IgG-purified #610	No	No	No	No
Column-purified #609	Yes	No	Yes	No
sc-7145	No	No	No	No
Monoclonal	Yes	Yes	Yes	Yes

3.2.2. Western blotting and immunoprecipitation using JNK1, MKK7, MLK3 and HPK1 antibodies

The components that make up the JIP-1 scaffold complex are JIP-1, JNK1, MKK7, MLKs and HPK1 (Whitmarsh *et. al.*, 1998). JIP-1 antibodies were characterised by western blotting and immunoprecipitation (section 3.2.1). As a prelude to test the presence of the endogenous JIP-1 scaffold complex in the rat brain and N1E-115 neuroblastoma cells, all the available antibodies to other members of the JIP-1 scaffold were tested for their ability to detect the endogenous protein by western blotting and for their ability to immunoprecipitate the endogenous protein.

The list of the antibodies tested for JNK1, MKK7, MLK3 and HPK1 is shown in Table 3.3.

3.2.2.1. Detection of JNK1, MKK7, MLK3 and HPK1 by western blotting

For western blotting analysis, 100μg and 200μg of the rat brain and N1E-115 lysate were used to test the presence of endogenous JNK1, MKK7, MLK3 or HPK1. As a positive control, lysates from HEK293 cells transfected with pCDNA3-HA-JNK1, pCMV5-Flag-MKK7, pcDNA3-HA-MLK3 or pMT2-HA-HPK1 were used.

The results of the western blotting analysis showed that endogenous JNK1 was detected by the monoclonal anti-JNK1 antibody #554286 (Pharmingen) (Fig. 3.8A), endogenous MLK3 was detected by MLK3 antibody sc-536 (Fig. 3.8A) and endogenous HPK1 was detected by HPK1 antiserum #2 (Fig. 3.8A). The monoclonal anti-JNK1 antibody (Pharmingen) detected the 46-kDa JNK1 protein irrespective of the amount of lysate used, which co-migrated with the transfected control (Fig. 3.8A). However, both MLK3 and HPK1 antibodies barely detected the appropriate endogenous protein with 100μg N1E-115 lysate, but with 200μg N1E-115 and 100μg/200μg rat brain lysates, appropriate proteins were detected by these antibodies. Apart from the monoclonal anti-JNK1 antibody #554286 (Pharmingen) and HPK1 antiserum #2, the rest of the JNK1 and HPK1 antibodies listed in Table 3.4 did not detect the appropriate endogenous proteins from either rat brain or N1E-115 cell lysates as well as transfected controls (data not shown).

The anti-MKK7 antibodies did not detect endogenous MKK7 or transfected Flag-MKK7 (Fig. 3.8B). However, re-probing the blots with anti-Flag antibody detected a single band at ~45kDa, suggesting that the transfected MKK7 protein was expressed in

Table 3.3. Available antibodies to JNK1, MKK7, HPK1 and MLK3

Protein	*Available antibodies*	*Characteristic*
JNK1	sc-571*	Rabbit polyclonal
	Antierum #355	Rabbit polyclonal
	#554286*	Mouse monoclonal
MKK7	sc-7103*	Goat polyclonal
	Antisera #830 and #831	Rabbit polyclonal
MLK3	sc-536*	Rabbit polyclonal
HPK1	sc-6231*	Goat polyclonal
	Antisera #2, #5 and #6*	Rabbit polyclonal

* - See section 2.1.3, Materials & Methods.

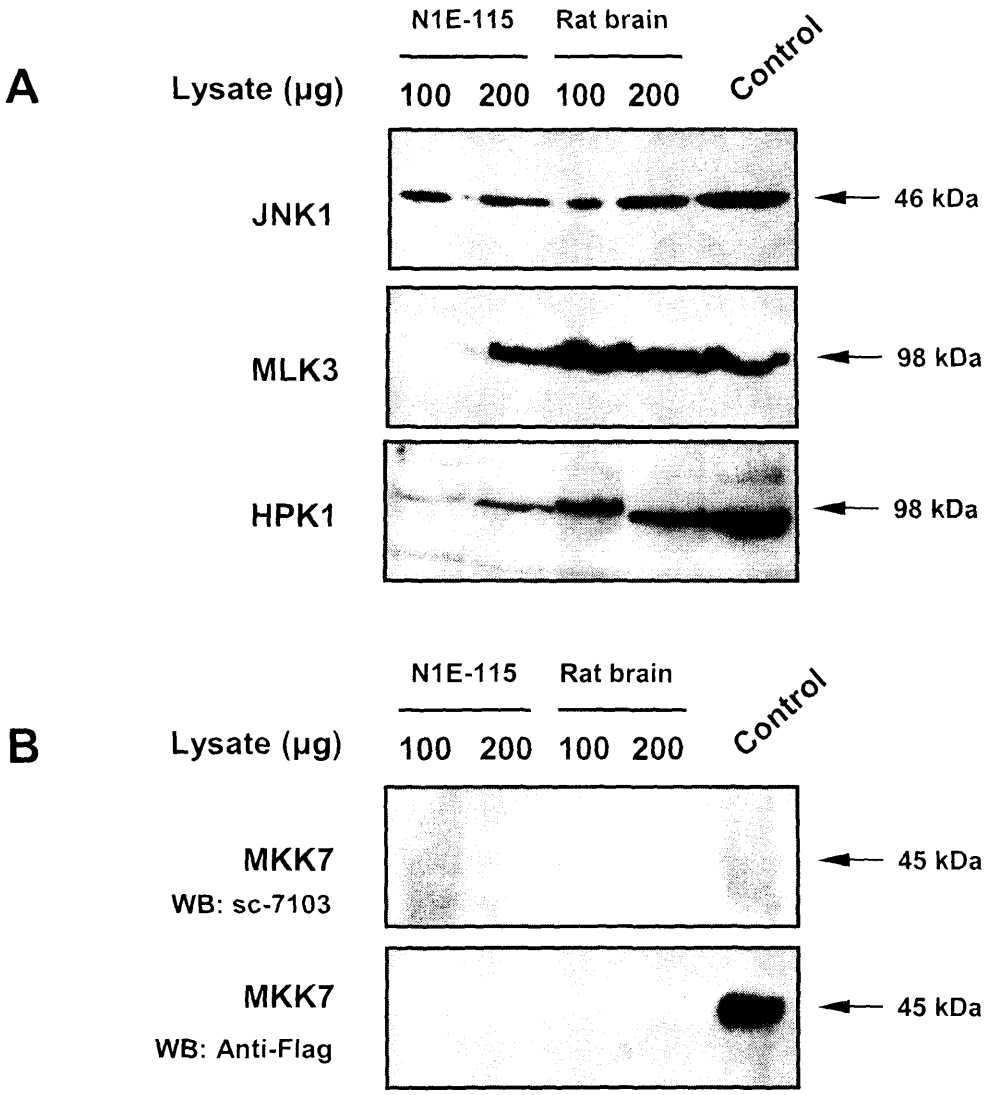

Fig. 3.8. Detection of endogenous JNK1, MLK3, HPK1 and MKK7 in N1E-115 and rat brain lysates.

N1E-115 and rat brain lysates were separate by electrophoresis on 10% (for JNK1 and MKK7) or 7% (for MLK3 and HPK1) SDS-PAGE and immunoblotted with the monoclonal anti-JNK1 antibody #554286 (Pharmingen; at 1:1000), MLK3 antibody sc-536 (Santacruz Biotechnology Inc; at 2µg/ml) or HPK1 antiserum #2 (1:2000) **(A)** or with anti-MKK7 antibody sc-7103 (1µg/ml) or anti-Flag antibody (5µg/ml) **(B)**. Lysate (50µg) from HEK293 cells transfected with pcDNA3-HA-JNK1, pcDNA3-HA-MLK3, pMT2-HA-HPK1 or pCMV5-Flag-MKK7 using Tfx-50 transfection reagent (Promega) was used as controls.

HEK293 cells (Fig. 3.8B), and hence the failure of MKK7 antibodies to detect transfected Flag-MKK7 was not due to the inefficiency of the transfection procedure used.

3.2.2.2. Immunoprecipitation of JNK1, MLK3 and HPK1

Antibodies to JNK1, MLK3 and HPK1 (Table 3.4) were next tested in their ability to immunoprecipitate the appropriate endogenous protein from rat brain and N1E-115 neuroblastoma cell lysates. The presence of the endogenous protein in the immunoprecipitates was detected by western blotting with the antibody identified to detect the endogenous protein by western blotting (see Fig. 3.8A).

From the JNK antibodies tested, only the JNK antiserum #355 successfully immunoprecipitated JNK from the rat brain and N1E-115 lysates, but the monoclonal (Pharmingen) and the polyclonal sc-571 (Santacruz Biotechnology Inc.) antibodies failed to do so (Fig. 3.9). Judging from the intensity of the bands, the amount of JNK precipitated by antiserum #355 from rat brain was approximately double than that from N1E-115 lysate. The control antibody did not precipitate JNK from either the rat brain or N1E-115 lysate.

Endogenous MLK3 was immunoprecipitated from rat brain and N1E-115 cells by the MLK3 antibody sc-536 but not by the control antibody (Fig. 3.9). The amount of MLK3 precipitated from the rat brain was approximately double than that precipitated from N1E-115 lysate.

Anti-HPK1 antisera #2 and #6 precipitated endogenous HPK1 from the N1E-115 cell lysate, while only antiserum #6 immunoprecipitated endogenous HPK1 from rat brain (Fig. 3.9). Approximately equal amounts of HPK1 were precipitated by antiserum #6 from both the rat brain and N1E-115 lysates, whereas the amount of HPK1 precipitated from N1E-115 lysate by antiserum #2 was approximately four-fold more than that precipitated by antiserum #6. The control antibody did not precipitate HPK1 from either rat brain or N1E-115 cell lysates.

The results of Western blotting/immunoprecipitation analysis of JNK1, MLK3 and HPK1 antibodies are summarised in Table 3.4. Antibodies selected for the work on JIP-1 scaffold complex are listed in Table 3.5.

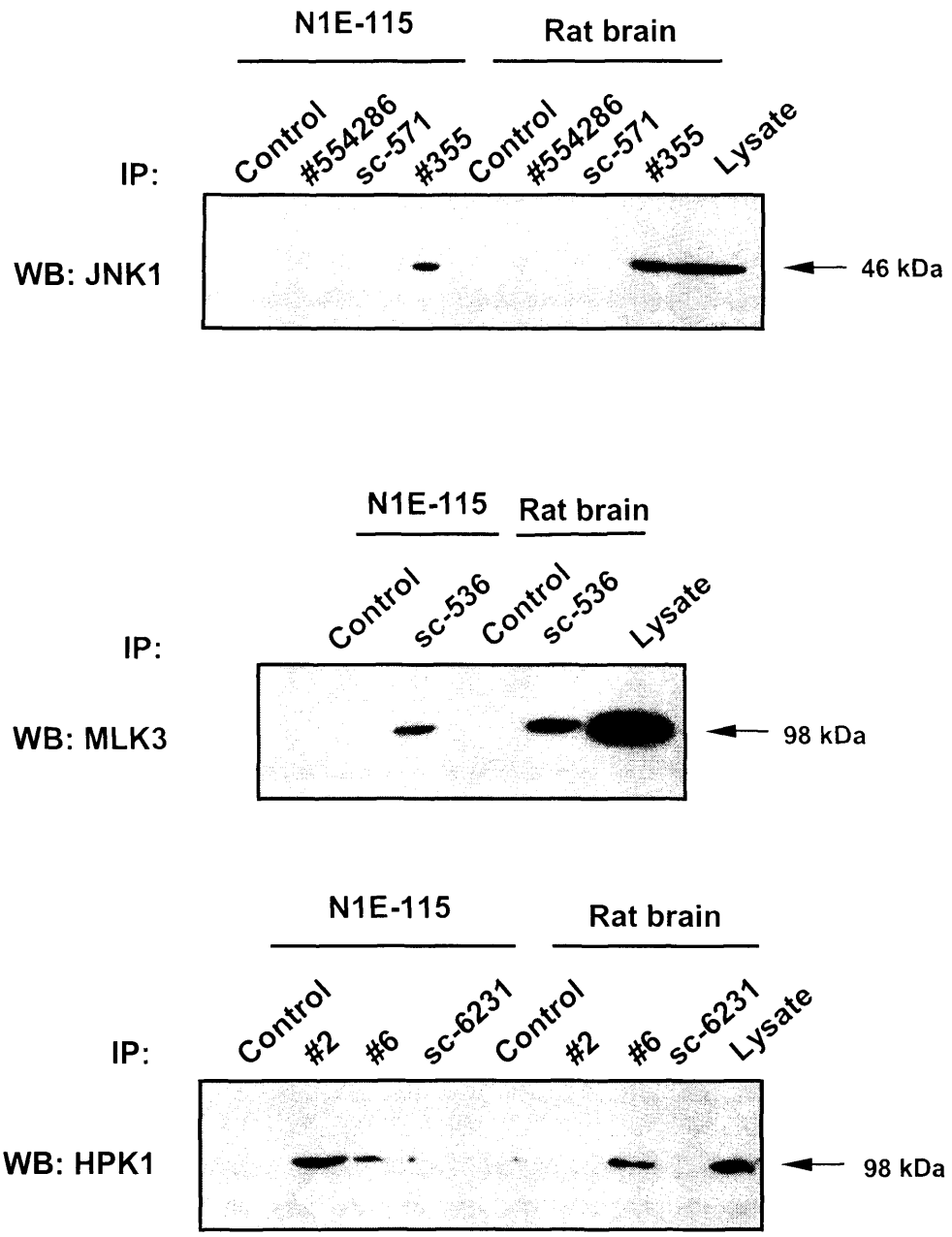

Fig. 3.9. Immunoprecipitation of JNK1, MLK3 and HPK1 from N1E-115 and rat brain lysates.

JNK1, MLK3 and HPK1 were immunoprecipitated from 1mg of N1E-115 or rat brain lysate using 5µl of antibodies listed in Table 3.4 as described in Materials & Methods (section 2.2.3.5). The immunoprecipitates were blotted for the presence of the appropriate protein using JNK1, MLK3 and HPK1 antibodies as described in Fig. 3.8. Lysates (50µg) from HEK293 cells transfected with pcDNA3-HA-JNK1, pcDNA3-HA-MLK3 or pMT2-HA-HPK1 were used as controls.

Table 3.4. Summary of western blotting and immunoprecipitation analysis using JNK1, MLK3 and HPK1 antibodies

Protein	*Antibody*	*Western blotting*	*Immunoprecipitation*	
			N1E-115 cells	Rat brain
JNK1	sc-571	No	No	No
	Antiserum #355	No	Yes	Yes
	#554286	Yes	No	No
MLK3	sc-536	Yes	Yes	Yes
HPK1	sc-6231*	No	No	No
	Antiserum #2	Yes	Yes	No
	Antiserum #6	No	Yes	Yes

Table 3.5. Antibodies used to study interactions between JIP-1 scaffold proteins

Component	*Immunoprecipitation*	*Western blotting*
JIP-1	Antiserum #609	Monoclonal JIP-1
JNK1	Antiserum #355	Monoclonal JNK1
MLK3	sc-536	sc-536
HPK1	Antiserum #2 (N1E-115 cells)	Antiserum #2
	Antiserum #6 (rat brain)	

3.2.3. Interactions between JIP-1 scaffold components *in vivo*

JIP-1 is proposed to form a scaffold complex by binding to JNK, MKK7, MLK3 and HPK1 (Whitmarsh *et. al.*, 1998). However, the JIP-1 scaffold complex model is based on transient transfection studies (Whitmarsh *et. al.*, 1998). To investigate the presence of the JIP-1 scaffold complex in intact (non-transfected) cells, interactions between JIP-1 scaffold complex components were examined in rat brain and N1E-115 neuroblastoma cells.

The results described in sections 3.2 and 3.3 show the best antibodies for use in western blotting and immunoprecipitation for a given endogenous JIP-1 scaffold complex protein, except for MKK7 because antibodies to MKK7 did not detect endogenous MKK7 in either rat brain or N1E-115 cells (Fig. 3.8B). These antibodies were used to investigate the interactions between the endogenous JIP-1, JNK1, MLK3 and HPK1 in rat brain and N1E-115 cells by immunoprecipitation and western blotting analysis. Antibodies for a given scaffold protein used for this purpose are shown in Table 3.5.

The strategy used was as follows. Each scaffold protein was immunoprecipitated from rat brain/N1E-115 lysate with an appropriate antibody. For N1E-115 cells, the interactions were tested in the presence or the absence of a stress stimulus to detect changes in interactions upon JNK stimulation. Precipitates from equivalent amounts of the lysates were loaded on 7% or 10% SDS PAGE gels along with untreated lysate as a control. Each gel was then immunoblotted for the presence of a specific scaffold component.

3.2.3.1. Interactions between JIP-1 scaffold complex components in rat brain

The results of the study of protein-protein interactions among JIP-1 scaffold components in rat brain showed that, both JIP-1 and JNK1 were detected in JIP-1 and JNK1 immunoprecipitates, but not in MLK3 and HPK1 immunoprecipitates (Fig. 3.10). A similar reciprocal precipitation was observed between MLK3 and HPK1: MLK3 and HPK1 were detected in MLK3 and HPK1 immunoprecipitates but not in JIP-1 and JNK1 immunoprecipitates (Fig. 3.10). The control antibody precipitated p38 but did not precipitate JIP-1, JNK1, MLK3 or HPK1.

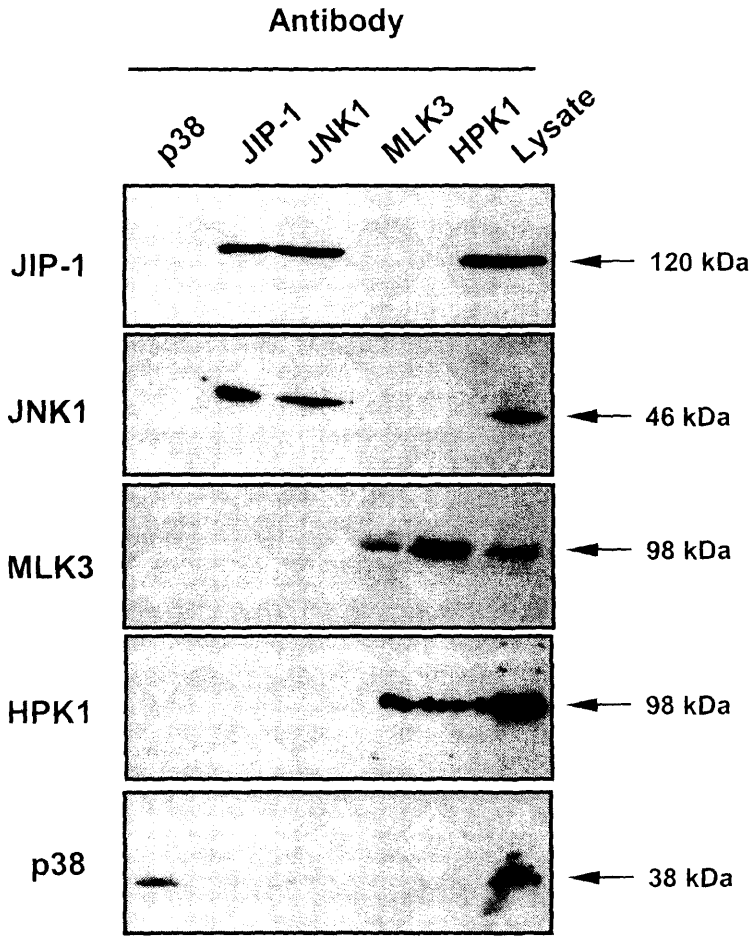

Fig. 3.10. Interactions among JIP-1 scaffold complex components in rat brain.

JIP-1, JNK1, MLK3 and HPK1 were immunoprecipitated from 1mg of rat brain lysate (as described in section 2.2.3.5, Materials & Methods) with 5µl of antibodies listed in Table 3.5. p38 was immunoprecipitated using 5µl of anti-p38 antiserum. The immunoprecipitates were subjected to 7% (for JIP-1, MLK3 and HPK1) or 10% (for JNK1 and p38) SDS-PAGE along with 100µg of lysate as a control and immunoblotted for JIP-1 with monoclonal antibody #7 at 1:5000; JNK1 with JNK1 monoclonal antibody (Pharmingen) at 1:1000; MLK3 with MLK3 antibody sc-536 at 2µg/ml; HPK1 with #2 antiserum at 1:2000; and p38 with p38 monoclonal antibody at 1:1000. Results shown are representative of three independent experiments.

3.2.3.2. Interactions between JIP-1 scaffold complex components in N1E-115 cells

The results of Whitmarsh *et. al.* (1998) suggested that JNK, MLK, MKK7 and HPK1 interacted with JIP-1 to form a scaffold complex in the absence of a stress stimulus. However, since the activation of JNK by a stress stimulus has been shown to result in the translocation of active JNK in the nucleus (Cavigelli *et. al.*, 1995), it is likely that the activation of JNK pathway may be associated with functional changes in the interactions between the JIP-1 scaffold components. Therefore, interactions between JIP-1, JNK1, MLK3 and HPK1 in N1E-115 cells were tested in the presence or the absence of a stressful stimulus anisomycin. JNK activation was determined in parallel by an *in vitro* kinase assay.

In untreated N1E-115 cells, JIP-1 was detected in the immunoprecipitates of JIP-1 and MLK3 but not in JNK1 and HPK1 immunoprecipitates (Fig.3.11). JNK1 was detected in the immunoprecipitates of JNK1 but not in the immunoprecipitates of JIP-1, MLK3 and HPK1 (Fig. 3.11). MLK3 was present in JIP-1, MLK3 and HPK1 immunoprecipitates but not in JNK1 immunoprecipitates. HPK1 was detected in the immunoprecipitates of MLK3 and HPK1 antibodies (Fig. 3.11). p38 was present in the immunoprecipitates of p38 but not in the immunoprecipitates of any of the tested JIP-1 scaffold proteins. Overall, the results suggested an interaction between JIP-1-MLK3 and MLK3-HPK1 in resting N1E-115 cells.

Interactions between JIP-1, JNK1, MLK3 and HPK1 were next determined in N1E-115 cells treated with anisomycin, a classical activator of JNK. The presence of active JNK in anisomycin-treated cells was demonstrated by an *in vitro* immune complex kinase assay using purified c-Jun as a substrate (Fig. 3.13A). Immunoprecipitation analysis showed that JIP-1 was detected in the immunoprecipitates of JNK1 and HPK1 but not in the immunoprecipitates of MLK3 in anisomycin-treated N1E-115 cells (Fig. 3.12). JNK1 was detected in the immunoprecipitates of JIP-1 and JNK1, but not in the immunoprecipitates of MLK3 and HPK1. MLK3 and HPK1 were detected in the immunoprecipitates of both MLK3 and HPK1 but not in the immunoprecipitates of JIP-1 and JNK1 (Fig. 3.12).

The results of JNK1 kinase assay performed in parallel showed that JNK1 was activated in the anisomycin-treated cells compared to the untreated cells (Fig. 3.13A). Furthermore, the levels of JNK1 protein remained unchanged in control and stressed cells (Fig. 3.13B), suggesting that anisomycin treatment activated existing JNK1, and thus the increase in JNK1 activity was not due to *de novo* synthesis of JNK1.

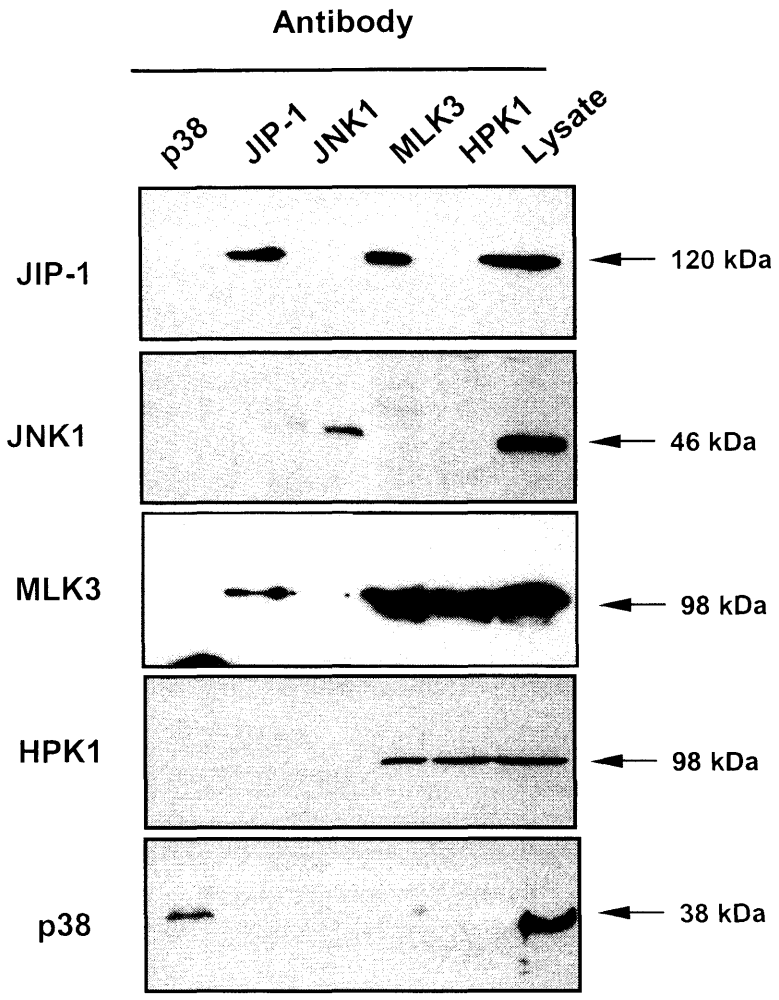

Fig. 3.11. Interactions among JIP-1 scaffold complex components in resting N1E-115 cells.

JIP-1, JNK1, MLK3, HPK1 and p38 were immunoprecipitated from 1mg of N1E-115 cell lysate and immunoblotted as described in Fig. 3.10, except that HPK1 was immunoprecipitated using 5µl antiserum #2. Results shown are representative of three independent experiments.

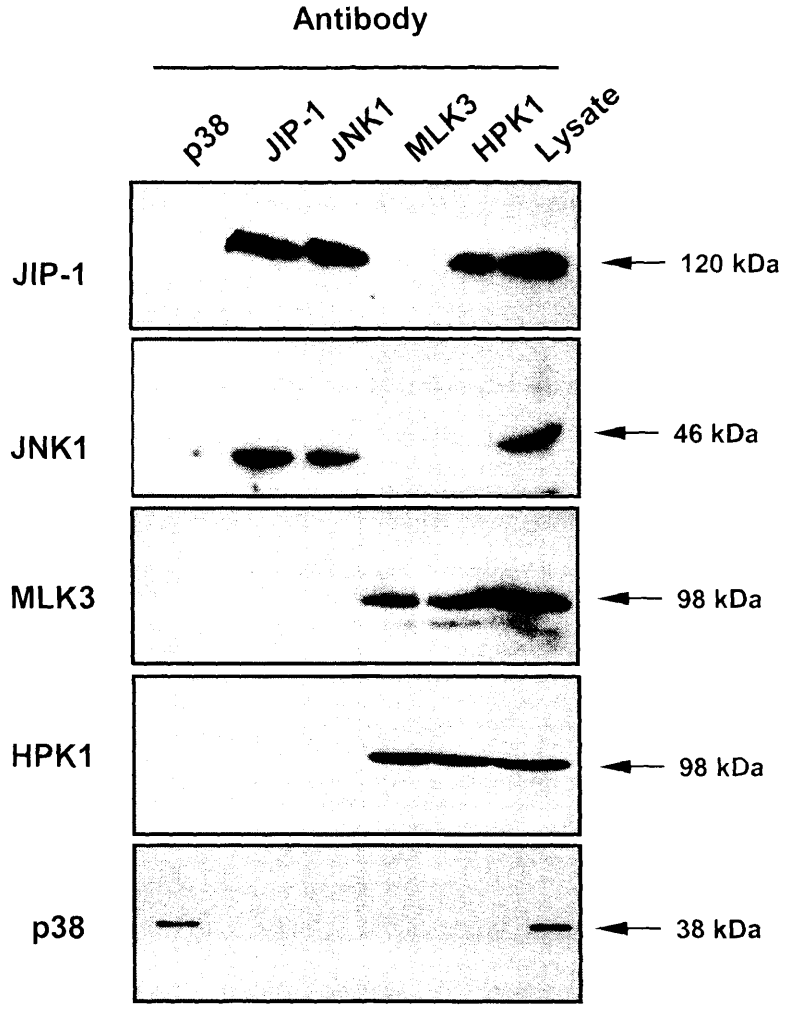

Fig. 3.12. Interactions among JIP-1 scaffold complex components in anisomycin-treated N1E-115 cells.

JIP-1, JNK1, MLK3, HPK1 and p38 were immunoprecipitated from 1mg of N1E-115 cells treated with anisomycin (10μM) for 30 minutes, and immunoblotted as described in Fig. 3.12, except that HPK1 was immunoprecipitated using 5μl antiserum #2. Results shown are representative of three independent experiments.

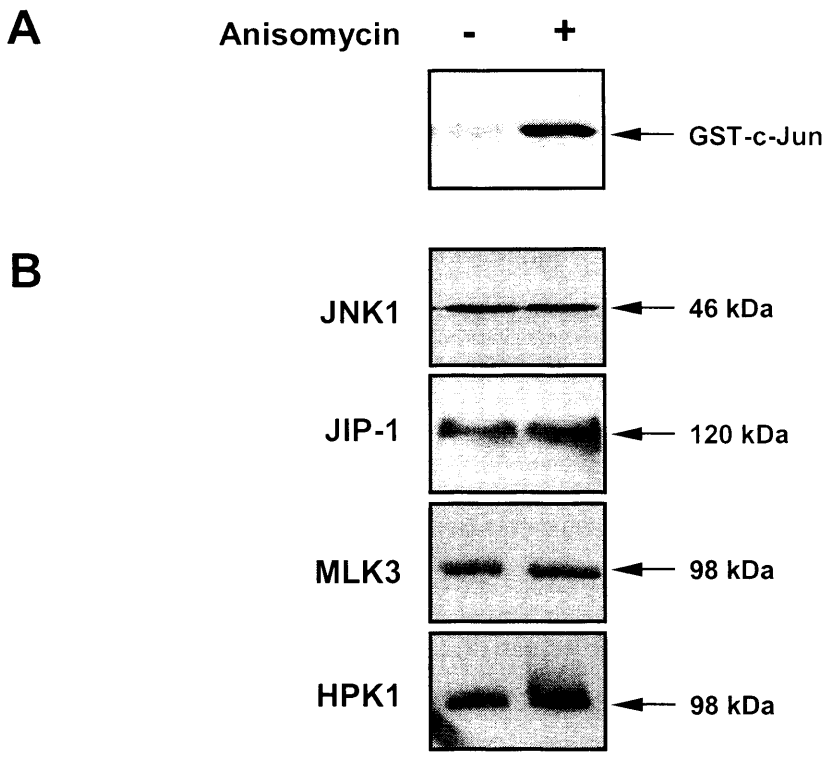

Fig. 3.13. JNK1 kinase assay and JNK1, JIP-1, MLK3 and HPK1 protein levels in resting and anisomycin stimulated N1E-115 cells.

(A) JNK1 was immunoprecipitated from 400μg of lysate from resting N1E-115 cells or from N1E-115 cells treated with anisomycin (10μM) for 30 minutes with 5μl JNK1 antiserum #355 as described in Materials & Methods (section 2.2.3.6). JNK activity was measured using an immune complex kinase assay with GST-c-Jun as a substrate and quantified by PhosphorImager analysis as described in Materials & Methods (section 2.2.3.6).
(B) Equal amounts of lysate (100μg) from resting and anisomycin-treated N1E-115 cells were immunoblotted for JNK1, JIP-1, MLK3 and HPK1 as described in Fig. 3.10.

Furthermore, levels of JIP-1, MLK3 and HPK1 also remained unaltered in the presence or the absence of anisomycin (Fig. 3.13B), suggesting that the differences in the interaction between JIP-1, JNK1, MLK3 and HPK1 in control and stressed N1E-115 cells were not due to the synthesis of new proteins following stress but due to the changes in the affinity or localisation of existing proteins. Taken together, these results suggested an interaction between JIP-1-JNK1, JIP-1-HPK1 and MLK3-HPK1 complexes in stress-stimulated N1E-115 cells.

In resting N1E-115 cells an interaction between JIP-1 and JNK1 and between JIP-1 and HPK1 was not observed (Fig. 3.11), whereas in stress-stimulated N1E-115 cells the JIP-1-JNK1 and JIP-1-HPK1 interaction was detected (Fig. 3.12). In addition, the interaction between JIP-1 and MLK3 observed in resting cells (Fig. 3.11) was lost in stress stimulated N1E-115 cells (Fig. 3.12). This suggested that the JIP-1 scaffold complex in N1E-115 cells is dynamic in which an exchange of components is taking place.

3.2.3.4. Interaction between JIP-1 and JNK1 in response to various stress stimuli

The results presented in section 3.2.3 suggested that JIP-1 and JNK1 interacted only in anisomycin-treated N1E-115 cells but not in unstimulated cells. To test whether this was true for other stressful stimuli that activate JNK, the interaction between JIP-1 and JNK1 was studied in the presence of sorbitol, 12-O-tetradecanoylphorbol-13-acetate (TPA), sodium arsenite, and in serum starved N1E-115 cells. Anisomycin was used as a positive control. JNK activation was determined as before by an *in vitro* kinase assay. JIP-1 was immunoprecipitated from control and treated cells, and JIP-1 immunoprecipitates were blotted for the presence of JNK1. Similarly, JNK was immunoprecipitated from control and stimuli-treated cells, and JNK1 immunoprecipitates were blotted for the presence of JIP-1.

The results showed that, JNK1 was activated in response to different stress stimuli (Fig. 3.14A). JIP-1 was detected in JNK1 immunoprecipitates prepared from different stress stimuli-treated cells, but not in control cells (Fig. 3.14B). Similarly, JNK1 was detected in JIP-1 immunoprecipitates from stimuli-treated cells, but not from control cells (Fig. 3.14B). These results showed that the stress-induced JIP-1-JNK1 interaction was not confined to a specific stress stimulus but may be a general response to stress in N1E-115 cells.

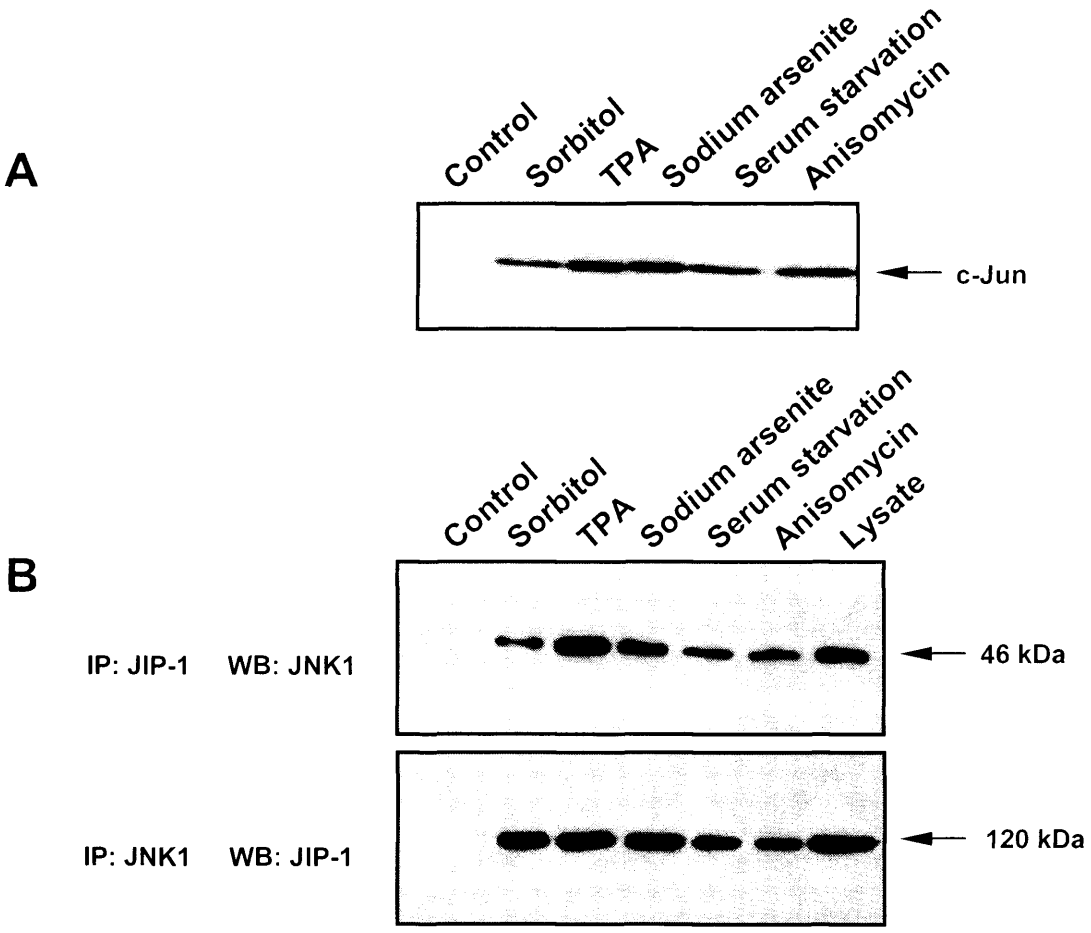

Fig. 3.14. JIP-1-JNK1 interaction in response to various stress stimuli in N1E-115 cells.

N1E-115 neuroblastoma cells were either left untreated or treated with sorbitol (300mM) for 30 minutes, TPA (100nM) for 1h, sodium arsenite (15mM) for 1h, anisomycin (10μM) for 30 minutes, or serum starved for 4h. **(A)** JNK1 was immunoprecipitated from equal amounts of lysate (400μg) from untreated and treated N1E-115 cells and subjected to JNK1 kinase assay as described in Fig. 3.13. **(B)** JIP-1 and JNK1 were immunoprecipitated from equal amounts of lysate (1mg) from untreated or treated N1E-115 cells as described in Fig. 3.10 JIP-1 immunoprecipitates were blotted for JNK1 with JNK1 monoclonal antibody (Pharmingen) at 1:1000, and JNK1 immunoprecipitates were blotted for the presence of JIP-1 with anti-JIP-1 monoclonal antibody at 1:5000.

3.3. DISCUSSION

The JNK signalling pathway is organised by modules held together by the JIP group of scaffold proteins. The JIP-1/JIP-2/JIP-3 scaffold complex model is based on overexpression studies that have demonstrated that JIP proteins interact selectively and independently with HPK1, MLKs (DLK, MLK2 and MLK3), MKK7 and JNK (Whitmarsh *et. al.*, 1998; Yasuda *et. al.*, 1999; Kelkar *et. al.*, 2000). Experiments that show the binding of endogenous JIP to all four kinases in a single cell line has not been reported. Since the JIP scaffold model has not been investigated in intact (non-transfected) cells, it is possible that the proposed model based on overexpression studies may not reflect the situation existing with endogenous components of the scaffold. Therefore an investigation of the JIP-1 scaffold complex was undertaken to determine the interactions between endogenous scaffold components *in vivo*. As a preliminary step in this investigation, antibodies to JIP-1, JNK1, MLK3 and HPK1 were characterised to identify the best antibodies for western blotting and immunoprecipitation of a given component (sections 3.2.1 and 3.2.2). Based on the results of this analysis, interactions between JIP-1 scaffold complex components in rat brain and N1-115 neuroblastoma cells was investigated.

3.3.1. Anti-JIP-1 antibody characterisation

3.3.1.1. ELISA for anti-JIP-1 polyclonal antibodies

ELISAs are widely used to test the reactivity of whole antisera and purified antibodies with the peptide (Kemeny, 1997). JIP-1 antisera #608, #609 and #610 were tested for their reactivity to the antigens BSA-MD1, -MD2 and -MD3. Antiserum and antibody dilution ELISA showed that the antibody titre of #609 and #610 antisera was higher in the second bleed than in the first bleed, and higher in the final bleed than in the second bleed (Figs. 3.1 and 3.2). The higher antibody titre in antisera #609 and #610 compared to antiserum #608 was also reflected in peptide competition assay (Fig. 3.3). The peptide competition assay also showed that the #608, #609 and #610 antibodies were specific to the immunising peptides against which they were raised since the reactivity of the anti-JIP-1 antisera with the appropriate antigen was inhibited in the presence of the immunising peptide but not in the presence of the control peptide (Fig. 3.3).

3.3.1.2. Western blotting using anti-JIP-1 antibodies

Western blotting analysis with the available JIP-1 antibodies (Table 3.2) showed that only the monoclonal anti-JIP-1 antibody detected endogenous JIP-1 present in neuronal lysates (Fig. 3.5). ELISA analysis had shown that antiserum #609 had high JIP-1 antibody titre (section 3.2.1.1). Anti-JIP-1 antiserum #609 detected transfected Flag-JIP-1 (Fig. 3.4) but failed to detect endogenous JIP-1 (Fig. 3.5). This suggested that the #609 antibody titre was not high enough to permit the detection of endogenous JIP-1. Anti-JIP-1 antiserum #610 did not detect transfected Flag-JIP-1 or endogenous JIP-1 (data not shown). The failure of #610 to detect transfected Flag-JIP-1 is consistent with the fact that the JIP-1 construct used for transfection was the mouse clone JIP-1a, which lacked the 47 amino acid insertion at the C-terminus (Dickens *et. al.*, 1997; Bonny, Nicod & Waeber, 1998), and #610 antibody was raised against the peptide MD3 that contained a part of this 47 amino acid insertion sequence (Table 3.1). Therefore, the recognition motif for the #610 antibody was absent in transfected JIP-1. Antiserum #610 had high JIP-1 antibody titre, as determined by ELISA analysis (section 3.2.1.1), but failed to detect endogenous JIP-1 (data not shown). This suggests that the antibody titre was not high enough for endogenous JIP-1 detection. #608 failed to detect endogenous or transfected JIP-1 (data not shown), and this was consistent with low antibody titre as determined by ELISA (section 3.2.1.1).

3.3.1.3. Immunoprecipitation using anti-JIP-1 antibodies

Immunoprecipitation analysis of available anti-JIP-1 antibodies (Table 3.2) showed that antiserum #609 precipitated endogenous JIP-1 from N1E-115 or rat brain lysates more efficiently than other anti-JIP-1 antibodies (Fig. 3.7). This is consistent with the high JIP-1 antibody titre in #609 as determined by ELISA (section 3.2.1.1). The failure of antiserum and purified #610 to precipitate Flag-JIP-1 was expected, since transfected Flag-JIP-1 that was used for the study lacked the 47 amino acid region at the C-terminus, and #610 was raised against a part of this extra sequence (see also section 3.3.1.2).

3.3.2. Interactions between JIP-1 scaffold components in resting N1E-115 cells

3.3.2.1. The interaction between JIP-1 and MLK3

In untreated N1E-115 cells, interactions between endogenous JIP-1 and MLK3 and between HPK1 and MLK3 were detected (Fig. 3.11). The JIP-1-MLK3 interaction in non-stressed cells is in agreement with a similar result obtained very recently by Nihalani *et. al.* (2001) using an overexpression approach. They showed that active MLK3/DLK proteins are homodimers, while in their monomeric form they are inactive (Nihalani, Merritt & Holzman, 2000; Nihalani *et. al.*, 2001). JIP-1 associates with MLK3/DLK in their monomeric, inactive form (Nihalani *et. al.*, 2001). This suggests that MLK3 detected in JIP-1 immunoprecipitates (Fig. 3.11) is likely to be monomeric and thus inactive. Endogenous MLK3-HPK1 interaction in non-stressed cells is a new finding, and implicates a role of HPK1 in regulating MLK3 activity.

An earlier study, using purified recombinant proteins, had shown that the affinity of JNK for JIP-1 was ~100-fold more than that for its substrates c-Jun and ATF2 (Dickens *et. al.*, 1997). Our results suggest that, in unstimulated cells, endogenous JIP-1 preferentially interacts with MLK3 rather than JNK (Fig. 3.11). However, it is possible that in unstimulated cells, endogenous JIP-1 and JNK may interact to such a small extent so as to be undetectable by co-immunoprecipitation and western blotting.

JIP-1 interacts with the N-terminal of DLK (Nihalani, Merritt & Holzman, 2000) and LZK (Ikeda *et. al.*, 2001). Since JIP-1 can homo-oligomerise via its C-terminal domain (Yasuda *et. al.*, 1999), and the interaction of JIP-1 with MLK proteins is also mediated by its C-terminal domain (Whitmarsh *et. al.*, 1998; Yasuda *et. al.*, 1999), this suggests two possibilities. Firstly, if the binding site of JIP-1 and MLK proteins on the C-terminus of JIP-1 spans a similar region, the interaction of JIP-1 with MLK proteins may prevent JIP-1 oligomerisation due to the competition for binding. On the other hand, if the binding sites of JIP-1 and MLK proteins are distinct within the C-terminus of JIP-1, JIP-1 oligomerisation may aid the localisation of MLK-JIP-1 complexes in to a specific location. An indirect approach to validate either possibility would be to study the ability of JIP-1 to oligomerise in the presence of one or more MLK family proteins.

What could be the possible reasons for tethering MLK3 to JIP-1? Apart from the possibility of localising JIP-1-MLK3 complexes to a specific location in the cell, there are two further likely explanations. One, it may increase JNK signalling specificity.

MLK3 has been reported to activate JNK, p38 and NF-κB pathways (Tibbles *et. al.*, 1996; Hehner *et. al.*, 2000). Therefore tethering MLK3 to JIP-1 would ensure the activation of the JNK pathway by keeping MLK3 molecules in the vicinity of the JIP-1 upon stress stimulation. Second, by binding to inactive MLK3 molecules, JIP-1 may prevent unnecessary MLK3 as well as JNK activation.

3.3.2.2. MLK3 may not be a part of a trimeric JIP-1-MLK3-HPK1 complex

The presence of MLK3 in JIP-1 and HPK1 immunoprecipitates in non-stimulated N1E-115 cells (Fig. 3.11) suggests that these three proteins may be a part of a single complex (JIP-1-MLK3-HPK1) or two separate complexes (JIP-1-MLK3 and MLK3-HPK1). The following arguments suggest that the presence of two separate complexes is likely. MLK3 and HPK1 bind to a similar region of JIP-1, amino acids 471-660 (Whitmarsh *et. al.*, 1998), suggesting that the presence of both kinases to a single JIP-1 molecule may not be possible due to steric hindrance or competition for binding. MLK3 binds to HPK1 (Kiefer *et. al.*, 1996) and JIP-1 (Nihalani *et. al.*, 2001) via its N-terminus. This also suggests that MLK3 may not be able to bind both JIP-1 and HPK1 simultaneously. Also, the interaction between JIP-1 and HPK1 was not detected in non-stimulated N1E-115 cells (Fig. 3.11). Clarification of these issues would require further experimentation to determine the precise binding sites of JIP-1 on MLK3, and that of MLK3 on JIP-1 and HPK1 by mutational analysis, and to demonstrate whether overexpressed MLK3, JIP-1 and HPK1 fail to interact to form a trimeric complex in the absence of a stress stimulus.

It is possible that MLK3 detected in JIP-1 and HPK1 immunoprecipitates may reflect separate subcellular localisation of JIP-1, MLK3 and HPK1. MLK3 may be compartmentalised in N1E-115 cells such that one fraction of MLK3 molecules associates with JIP-1, and another fraction associates with HPK1. However, the subcellular localisation of MLK3 and HPK1 in N1E-115 cells is currently unknown and warrants further investigation.

3.3.3. Interactions between JIP-1 scaffold components in stress-stimulated N1E-115 cells

In anisomycin-treated N1E-115 cells, interactions between endogenous JIP-1-JNK1, JIP-1-HPK1 and MLK3-HPK1 were evident (Fig. 3.12). In the absence of a

stress stimulus, JIP-1-MLK3 and MLK3-HPK1 interactions were detected (Fig. 3.11). This suggests that the JIP-1 scaffold complex in N1E-115 cells is dynamic in which an exchange of components is taking place upon stress stimulation.

The formation of the JIP-1-JNK1 complex and the loss of the interaction between JIP-1 and MLK3 in stress-stimulated N1E-115 cells (Fig. 3.12) is in agreement with several recent observations. Co-immunoprecipitation analysis in transfected cells has shown that the activation of the JNK pathway by UV-C radiation leads to an increased formation of JNK-JIP complex (Kelkar *et. al.*, 2000). In stress-stimulated cells, the JIP-1-MLK3 complex dissociates (Nihalani *et. al.*, 2001). MLK3 dimerisation and activation by phosphorylation, induced by okadaic acid, only occurs after its release from JIP-1, and this results in decreased affinity of JIP-1 for MLK3 (Nihalani *et. al.*, 2001).

The difference in the interactions between JIP-1, JNK1, MLK3 and HPK1 in resting and stress-stimulated N1E-115 cells can be investigated further by examining co-localisation by immunoflourescence microscopy. For example, co-localisation of JIP-1 and MLK3 to the same subcellular compartment in resting cells would support the observed interaction between JIP-1 and MLK3 in resting N1E-115 cells. The localisation of JIP-1 and MLK3 to different subcellular compartments in stressed N1E-115 cells would support the absence of the JIP-1-MLK3 interaction observed in stressed N1E-115 cells.

In rat brain, interactions between JIP-1 and JNK1 and between MLK3 and HPK1 were observed (Fig. 3.10). These results are similar to the results obtained with anisomycin-treated N1E-115 cells (Fig. 3.12). This suggests that the rat brain may have been stressed while being excised from rat. Alternatively, it is possible that JIP-1 and JNK1, and MLK3 and HPK1 may interact in resting rat brain. In support of this possibility, the interaction between endogenous JIP-1 and JNK has been detected by co-immunoprecipitation analysis in mouse brain (Kelkar *et. al.*, 2000).

3.3.3.1. The MLK3-HPK1 interaction

Endogenous JIP-1-HPK1 and HPK1-MLK3 interactions were detected in stress-stimulated N1E-115 cells (Fig. 3.12). The interaction between MLK3 and HPK1 was also detected in the absence of a stress stimulus (Fig. 3.11). The endogenous MLK3-HPK1 interaction is consistent with observations that HPK1 interacts with MLK3 in yeast two-hybrid screen as well as in transfected cells challenged with stressful stimuli (Kiefer *et. al.*, 1996). MLK3 has also been reported to be activated by dimerisation-induced autophosphorylation and HPK1 phosphorylation (Kiefer *et. al.*, 1996; Leung & Lassam, 2001), and dimeric MLK3 does not bind to JIP-1 (Nihalani *et. al.*, 2001). Therefore, in stress-stimulated N1E-115 cells, loss of the JIP-1-MLK3 interaction may be required for MLK3 dimerisation, and an interaction between HPK1 and MLK3 (Fig. 3.12) may be required for the activation of MLK3 by HPK1 phosphorylation.

3.3.3.2. HPK1 may act as a bridge between JIP-1 and MLK3

The interaction of JIP-1 with MLK3 in stressed N1E-115 cells was not detected (Fig. 3.12), This is in agreement with a recent report that demonstrated that stress stimulation lead to a decreased affinity between JIP-1 and MLK3 and consequent loss of JIP-1-MLK3 interaction (Nihalani *et. al.*, 2001). This suggests that active MLK3 may not directly interact with JIP-1, and thus may not be a part of the JIP-1 scaffold *in vivo* in stimulated N1E-115 cells. However, the interaction of JIP-1 with HPK1 and of MLK3 with HPK1 was detected in stress-stimulated N1E-115 cells (Fig. 3.12). This suggests that HPK1 may act as bridge between JIP-1 and MLK3 and thus may play a vital role in activating JNK. MLK3 is an essential part of the JIP-1 scaffold complex as it phosphorylates the downstream kinase MKK7 (Whitmarsh *et. al.*, 1998). HPK1, by interacting with JIP-1 and MLK3, may keep active MLK3 in the vicinity of MKK7 and JNK bound to JIP-1, and may thus facilitate MKK7 phosphorylation by MLK3, and phosphorylation of JNK1 by MKK7. Although the interaction of MKK7 with JIP-1 scaffold components could not be determined in the present study, this model assumes, based on previous findings (Whitmarsh *et. al.*, 1998; Yasuda *et. al.*, 1999), that MKK7 is bound to JIP-1 in stress-stimulated N1E-115 cells.

The model of HPK1 as a bridge between JIP-1 and MLK3 is consistent with the results discussed above, namely the absence of JIP-1-MLK3 interaction, reduced affinity of JIP-1 for MLK3 and JIP-1-JNK interaction in stressed cells. Furthermore, it is also consistent the scaffold function of JIP-1, which was recently shown by a *Jip-1*

gene knockout study to be critical in mediating JNK activation in stress-stimulated neurons (Whitmarsh *et. al.*, 2001). The proposed role of HPK1 as a bridge between JIP-1 and MLK3 also satisfies the arguments presented in section 3.3.2.1, which suggested that MLK3 and HPK1 could not bind to a similar region of JIP-1 and that MLK3 could not bind both JIP-1 and HPK1 simultaneously.

HPK1 was detected in JIP-1 immunoprecipitates (Fig. 3.12). If HPK1 indeed acts as a bridge between JIP-1 and MLK3, then, in theory, MLK3 should also have been detected in JIP-1 immunoprecipitates and vice versa, but this was not the case (Fig. 3.12). However, it is possible that MLK3 may be present in JIP-1 immunoprecipitates and vice versa, but the amount present may be small and hence not detectable by western blotting. Alternatively, JIP-1-MLK3-HPK1 complex bridged by HPK1 may not exist and instead two separate complexes, JIP-1-HPK1 and HPK1-MLK3, may exist. An argument in favour of this hypothesis is the absence of a JIP-1-MLK3 interaction in stressed N1E-115 cells (Fig. 3.12). In this case, for JNK signalling to occur via the JIP-1 scaffold, mechanism(s) that ensure the presence of MLK3 in the vicinity of JIP-1 might be required. One such mechanism may be the localisation of JIP-1 scaffold components to the same subcellular compartment.

3.3.4. A model for the regulation of JNK activation by protein-protein interactions

On the basis of the above discussions, and other reported observations, the following general model of the regulation of JNK activation by protein-protein interactions may be presented (Fig. 3.15):

In resting cells, JNK may be kept in an inactive state by its interactions with other proteins such as GSTp (Adler *et. al.*, 1999), and/or by a different subcellular localisation from other JIP-1 scaffold components (Whitmarsh *et. al.*, 2001) (section 1.4.4, Chapter 1). MLK3 activity in resting cells may be suppressed by its interactions with JIP-1 (this study; Nihalani *et. al.*, 2001).

Upon stress stimulation, an increase in the JIP-1-JNK interaction, concomitant with a decreased affinity of JIP-1 for MLK, may take place. The formation of stress-induced JIP-1-JNK complex would require increased local concentrations of JNK and the loss of JNK-GSTp interaction. The loss of JNK-GSTp interaction has been shown to occur due to GSTp oligomerisation because of increased ROS formation following

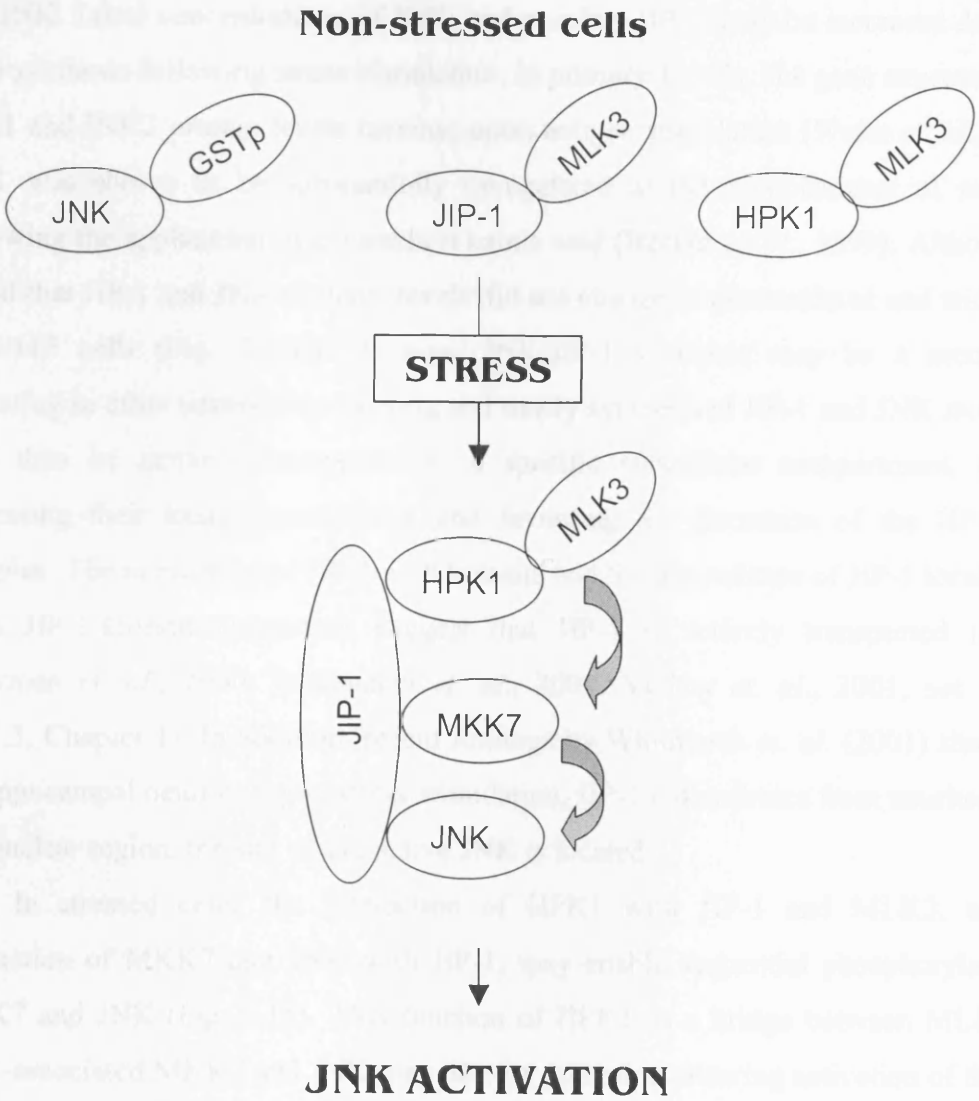

Fig. 3.15. A model for the activation of the JNK pathway by protein-protein interactions.
For details please see the text.

stress (Adler *et. al.*, 1999). Redistribution of JIP-1 and JNK to the same subcellular compartment would bring both proteins in close proximity with each other, thereby increasing the local concentration of JNK and enhancing the interaction between JIP-1 and JNK. Local concentrations of JNK, and possibly JIP-1, may be increased due to *de novo* synthesis following stress stimulation. In primary T cells, *Jnk* gene expression and JNK1 and JNK2 protein levels increase upon antigen stimulation (Weiss *et. al.*, 2000). JIP-1 was shown to be substantially upregulated in the hippocampus of rat brain following the application of excitotoxin kainic acid (Becker *et. al.*, 1999). Although we found that JIP-1 and JNK proteins levels did not change in unstimulated and stimulated N1E-115 cells (Fig. 3.13B), *de novo* JNK/JIP-1 synthesis may be a mechanism operating in other tissues. Pre-existing and newly synthesised JIP-1 and JNK molecules may then be actively transported to a specific subcellular compartment, thereby increasing their local concentration and favouring the formation of the JIP-1-JNK complex. The interaction of JIP-1 with kinesin, and the dependence of JIP-1 localisation on a JIP-1-kinesin interaction suggest that JIP-1 is actively transported in cells (Bowman *et. al.*, 2000; Whitmarsh *et. al.*, 2001; Verhey *et. al.*, 2001; see section 1.4.2.3, Chapter 1). In addition, recent findings by Whitmarsh *et. al.* (2001) show that, in hippocampal neurons, upon stress stimulation, JIP-1 redistributes from neurites to the perinuclear region, the site where active JNK is located.

In stressed cells, the interaction of HPK1 with JIP-1 and MLK3, and the interaction of MKK7 and JNK with JIP-1, may enable sequential phosphorylation of MKK7 and JNK (Fig. 3.15). This function of HPK1 as a bridge between MLK3 and JIP-1-associated MKK7 and JNK may be very critical in ensuring activation of the JNK pathway via the JIP-1 scaffold. Because the JIP-1 scaffold complex is dynamic (section 3.3.3), it is possible that MLK3 bound to one JIP-1 molecule via HPK1 may phosphorylate MKK7 bound to another JIP-1 molecule. JIP-1 oligomerisation may be involved in such cross-phosphorylation of the JNK pathway components.

3.3.5. Concluding remarks

Based on overexpression studies, JIP-1 was proposed to have a scaffolding function that facilitated the activation of the JNK pathway because it could selectively interact with MLK, MKK7 and JNK, and enhance JNK activation in the presence of MLK (Whitmarsh *et. al.*, 1998). However, even mild protein overexpression may allow

the unbound proteins to engage in non-physiological interactions (Dumont, Pecasse & Maenhaut, 2001). In the present work, we attempted to study the interaction of endogenous JIP-1 with endogenous JNK, MLK and HPK1. Our results show the evidence of the interaction between endogenous JIP-1 and JNK in intact cells upon stress application, JIP-1-MLK3 and MLK3-HPK1 interactions in the absence of a stress stimulus and MLK3-HPK1 interaction upon stress stimulation. Furthermore, the results show that the JIP-1 scaffold complex is dynamic in which an exchange of components may take place. Such an exchange of components may result in signal amplification. This contradicts the simple JIP-1 scaffold model in which the kinases bound to JIP-1 sequentially phosphorylate the downstream kinase to activate the JNK pathway with no signal amplification (Whitmarsh *et. al.*, 1998).

The results presented in this chapter need to be verified by other approaches such as subcellular localisation and sizing of complexes.

CHAPTER 4

JIP-1 IS A CASPASE-3 SUBSTRATE *IN VIVO* AND *IN VITRO*

4.1. INTRODUCTION

Central to the understanding of the molecular mechanism of apoptosis is the identification of caspase targets and the elucidation of the consequences of their proteolytic cleavage. So far more than 60 proteins have been found to be caspase substrates (Stroh and Schulze-Osthoff, 1998). These include cytoskeletal and structural proteins, e.g. focal adhesion kinase (FAK) (Levkau *et. al.*, 1998); cell cycle proteins, e.g. retinoblastoma (Janicke *et. al.*, 1996); proteins involved in replication, transcription and translation, e.g. DNA replication factor C140 (Rheaume *et. al.*, 1997); and DNA cleavage and repair proteins, e.g. poly-ADP ribose polymerase (PARP) and DNA fragmentation factor-45 (DFF-45) (Lazebnik *et. al.*, 1994; Tang & Kidd, 1998). Cleavage of these key proteins, which are involved in processes that maintain cellular integrity, aids apoptosis.

Cell death is determined by an integration of conflicting signals. The tripping of the balance towards survival or death depends on whether survival or apoptotic pathways dominate. Initially, it was thought that cell death was made possible by the cleavage of key proteins involved in cell cycle and DNA repair. Now the list of caspase substrates also includes signalling proteins involved in maintaining normal cell morphology and cell survival. Kinases that maintain cell morphology, such as FAK and p21-activated kinase 2 (PAK2), are cleaved during apoptosis to facilitate the development of morphological changes associated with apoptosis (Utz & Anderson, 2000). A study of proteins involved in the ERK, JNK and p38 MAPK pathways showed that caspases cleave signalling proteins involved in the ERK and Akt/PKB pathways that regulate cell growth and survival, suggesting that switching off survival pathways is necessary to facilitate cell death (Widmann, Gibson & Johnson, 1998). Of the proteins involved in the JNK pathway, only MEKK1 has been shown to be cleaved during apoptosis, while MKK4 and JNK1 are not (Cardone *et. al.*, 1997; Widmann, Gibson & Johnson, 1998). Cleavage of MEKK1 during apoptosis results in the release of the active kinase domain of MEKK1, which causes the activation of the JNK pathway and promotes apoptosis (Cardone *et. al.*, 1997). JNK is activated by a variety of stimuli in several cell types and is thought to contribute to apoptosis (section 1.7).

Within the primary sequence of JIP-1, the presence of four putative caspase-3 cleavage sites that conform to the DXXD motif (DLID^{98}/A, DYSD^{402}/E, DESD^{405}/S and DEPD^{450}/V) and one caspase-8 cleavage site that conforms to the (L/V)EXD motif

(LEVD^{510}/D) (see appendix B) suggested that JIP-1 might be cleaved by caspases during apoptosis. Since its initial discovery as an inhibitor of the JNK pathway, studies on JIP-1 have led to the understanding that it may act as a scaffold for the JNK pathway by binding to MLK, MKK7 and JNK, thereby facilitating sequential activation of kinases (Whitmarsh *et. al.*, 1998). JIP-1 knockout experiments suggest that it is essential for the activation of JNK pathway in response to stress and chemical apoptotic stimuli (Whitmarsh *et. al.*, 2001). Since the JNK pathway has been shown to play a role in both receptor- and chemical-induced apoptosis, and JIP-1 is essential for JNK activation, we wished to test the hypothesis that JIP-1 was a caspase-3 substrate *in vivo* and *in vitro*. For this, selected cell lines were examined for endogenous JIP-1 expression and for their susceptibility to apoptosis. The effect of receptor- and chemical-induced apoptosis on JIP-1 cleavage *in vivo* was examined in HeLa cells. This was followed by an *in vitro* analysis of JIP-1 cleavage using purified caspases.

4.2. RESULTS

4.2.1. JIP-1 cleavage during apoptosis

4.2.1.1. Identification of JIP-1 expressing cell lines

To identify cell lines that expressed endogenous JIP-1, representative samples of the human, mouse and rat cell lines (Table 4.1) derived from some tissues known to express JIP-1 were tested for the presence of endogenous JIP-1 by Western blotting using the monoclonal anti-JIP-1 antibody.

Endogenous JIP-1 was detected to varying degrees in all cell lines tested (Fig. 4.1A and B). JIP-1 was detected at relatively low levels in HuVEC, GC-1 and PC-12 cells, at moderate levels in U2OS, HeLa and NIH-3T3 cells, and at high levels in HEK293, N1E-115, Min6 and RinD11 cells (Fig. 4.1 A & B).

4.2.1.2. In vivo JIP-1 cleavage in selected cell lines during receptor- and chemical-induced apoptosis

Distinct caspase cascades are activated during receptor-mediated and chemical-induced apoptosis (Sun *et. al.*, 1999). Therefore, to study JIP-1 cleavage *in vivo*, a JIP-1 expressing cell line that would respond to both receptor- and chemical-induced apoptosis was sought using stimuli that activate the receptor- and chemical-induced apoptotic pathways.

Table 4.1. Cell lines tested for the presence of endogenous JIP-1

Name	*Cell line*
HeLa	Human cervical carcinoma
U2OS	Human osteosarcoma
HEK293	Human embryonic kidney
HuVEC	Human umbilical vein endothelial
N1E-115	Mouse neuroblastoma
GC-1	Mouse testis
NIH-3T3	Mouse fibroblast
RinD11	Rat pancreatic β cell
Min6	Rat pancreatic β cell
PC12	Rat phaechromocytoma

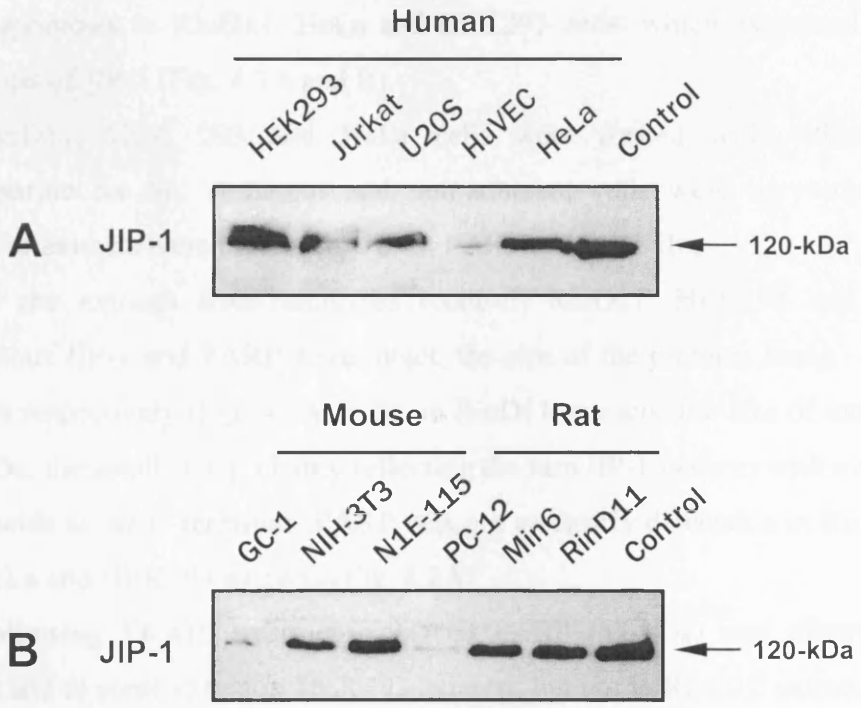

Fig. 4.1. Detection of endogenous JIP-1 in human, mouse and rat cell lines.

Extracts from the indicated cell line were prepared as described in Materials & Methods (section 2.2.3.1). Equal amounts of extract (200μg of the total protein) from the indicated cell line were separated by electrophoresis on a 7% SDS-PAGE gel. Proteins were transferred to Immobilon-P® membranes as described (section 2.2.4.1, Materials & Methods) and immunoblotted for JIP-1 using monoclonal anti-JIP-1 antibody at a dilution of 1:1000. Extract (10μg) from HEK293 cells transfected with 4μg of pCMV5-Flag-JIP-1 using Tfx-50 transfection reagent (Promega) was used as a control.

TRAIL ligand induces apoptosis through a receptor-mediated mechanism (MacFarlane *et. al.*, 1997; Pan *et. al.*, 1997), and staurosporine induces apoptosis through the mitochondrial pathway (Sun *et. al.*, 1999). TRAIL and staurosporine have been shown to induce apoptosis in many cell lines, including HT-29, SW620, HCT-15, HeLa, MOLT-4 and COLO-25 (Falcieri *et. al.*, 1993; Qiao *et. al.*, 1996; Gliniak & Le, 1999; Stoneley *et. al.*, 2000). Therefore, TRAIL and staurosporine were chosen to induce apoptosis in RinD11, HeLa and HEK293 cells, which expressed moderate or high levels of JIP-1 (Fig. 4.1A and B).

RinD11, HEK 293 and HeLa cells were treated with either TRAIL or staurosporine for 8h. Adherent and non-adherent cells were harvested, and equal amount of extracts were blotted for JIP-1, PARP and α-tubulin.

In the extracts from untreated (control) RinD11, HEK293 and HeLa cells, endogenous JIP-1 and PARP were intact, the size of the proteins being ~120-kDa and 116-kDa respectively (Fig. 4.2A & B). In RinD11 extracts, the size of intact JIP-1 was ~117-kDa, the small size probably reflecting the rare JIP-1 isoform with a deletion of 47 amino acids at the C-terminus. PARP was not as clearly detectable in RinD11 extracts as in HeLa and HEK293 extracts (Fig. 4.2A).

Following TRAIL treatment, cleaved PARP (85-kDa) was observed in HeLa extracts and to some extent in HEK293 extracts, but not in RinD11 extracts (Fig. 4.2A). In response to staurosporine, PARP cleavage was observed in HeLa and RinD11 extracts, but not in HEK293 extracts (Fig. 4.2A). In RinD11 extracts, the cleaved PARP fragment was not clearly detectable (Fig. 4.2A). Since the 116-kDa intact PARP is cleaved by caspase-3 to an 85-kDa fragment during apoptosis (Tewari *et. al.*, 1995), this suggested that TRAIL treatment induced apoptosis in HeLa and HEK293 cells but not in RinD11 cells, and staurosporine induced apoptosis in HeLa and RinD11 cells but not in HEK293 cells.

Following TRAIL treatment, JIP-1 cleavage was detected in HeLa extracts, but not in RinD11 and HEK293 extracts (Fig. 4.2B). JIP-1 cleavage was detected in both HeLa and RinD11 extracts, but not in HEK293 extracts, following staurosporine treatment (Fig. 4.2B). In HeLa and RinD11 extracts, the size of the cleaved JIP-1 fragment was 100-kDa. JIP-1 cleavage in HeLa cells in response to TRAIL and staurosporine, and in RinD11 cells in response to staurosporine, correlated with PARP cleavage (Fig. 4.2A & B).

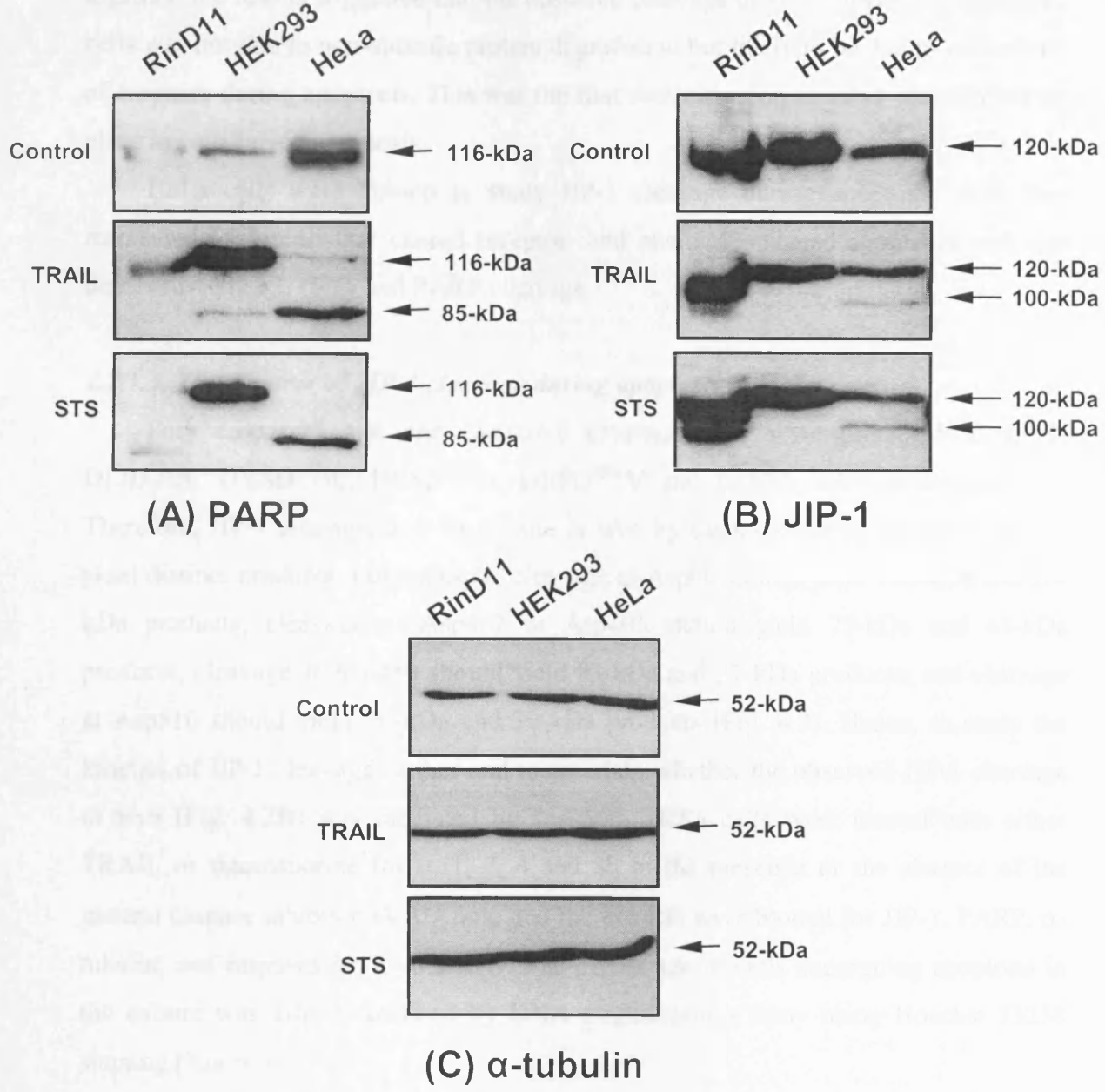

Fig. 4.2. Evidence for JIP-1 cleavage during receptor- and chemical-induced apoptosis.

RinD11, HEK293 or HeLa cells were treated with TRAIL (1μg/ml), staurosporine (1μM) or left untreated (control) for 8h. Extracts were prepared from adherent and detached cells as described in Materials & Methods (section 2.2.6.1). Equal amount of extracts (200μg of the total protein) were electrophoresed on a 7% SDS-PAGE gel and immunoblotted for JIP-1 using monoclonal anti-PARP (1μg/ml; Pharmingen; panel **A**) anti-JIP-1 (1:1000; panel **B**), and anti-α-tubulin (1:500; Sigma; panel **C**) antibodies.

In the extracts of control, TRAIL-treated and staurosporine-treated RinD11, HEK293 and HeLa cells, the levels of α-tubulin were constant (Fig. 4.2C). Taken together, the results suggested that the observed cleavage of JIP-1 in HeLa and RinD11 cells was not due to non-specific protein degradation but likely to be due to the activity of caspases during apoptosis. This was the first demonstration of JIP-1 cleavage taking place *in vivo* during apoptosis.

HeLa cells were chosen to study JIP-1 cleavage during apoptosis since they responded to stimuli that caused receptor- and chemical-induced apoptosis, and also demonstrated both JIP-1 and PARP cleavage.

4.2.1.3. Time course of JIP-1 cleavage during apoptosis in HeLa cells

Four caspase-3 and one caspase-8 cleavage sites were predicted in JIP-1: $DLID^{98}/A$, $DYSD^{402}/E$, $DESD^{405}/S$, $DEPD^{450}/V$ and $LEVD^{516}/D$ (see section 4.1). Therefore, JIP-1 cleavage at a single site *in vivo* by caspases during apoptosis should yield distinct products. For example, cleavage at Asp98 should yield 100-kDa and 20-kDa products; cleavage at Asp402 or Asp405 should yield 75-kDa and 45-kDa products; cleavage at Asp450 should yield 83-kDa and 37-kDa products; and cleavage at Asp516 should yield 90-kDa and 30-kDa products (Fig. 4.3). Hence, to study the kinetics of JIP-1 cleavage further and to ascertain whether the observed JIP-1 cleavage *in vivo* (Fig. 4.2B) was mediated by caspases, HeLa cells were treated with either TRAIL or staurosporine for 0, 1, 2, 4 and 8h in the presence or the absence of the general caspase inhibitor zVAD.fmk, and the extracts were blotted for JIP-1, PARP, α-tubulin, and caspases-3, -7, -8 and -9. The percentage of cells undergoing apoptosis in the culture was also determined by DNA fragmentation assay using Hoechst 33258 staining (Xia *et. al.*, 1995).

A quantitative analysis of the apoptotic response to TRAIL or staurosporine showed that, increasing the stimulus incubation time led to an increase in the percentage of cells undergoing apoptosis (Figs. 4.4 and 4.5, panel A). After 8h, the percentage of apoptotic cells in response to either stimulus was approximately 100%. However, the kinetics of apoptosis in response to TRAIL or staurosporine differed. For example, in response to TRAIL, ~50% cells were apoptotic at 4h, while staurosporine treatment for 2h caused ~50% apoptosis (Figs. 4.4 and 4.5, panel A).

In the extracts from untreated (control) HeLa cells, both JIP-1 and PARP were present as 120-kDa and 116-kDa proteins respectively (Figs. 4.4 and 4.5, panel B).

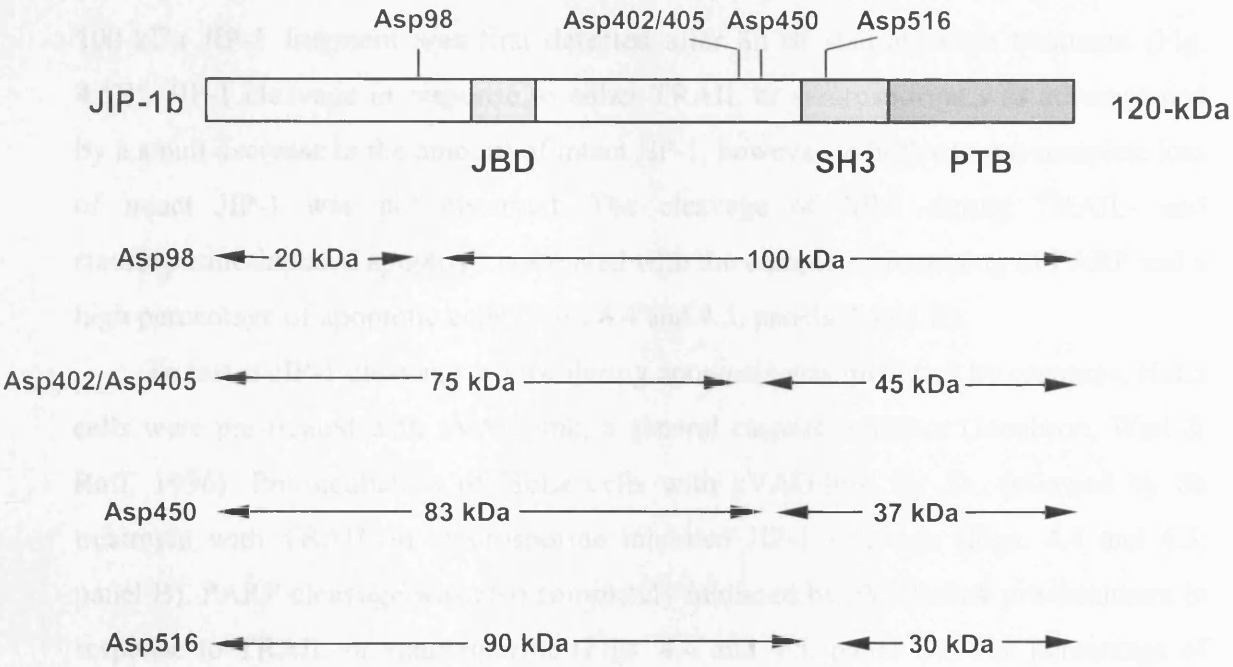

Fig. 4.3. Putative caspase-3 and caspase-8 cleavage sites in JIP-1.

A schematic diagram showing the position of the predicted caspase-3 and –8 cleavage sites in JIP-1 in relation to the domain structure, and the predicted sizes of cleavage products resulting from cleavage at these sites. JBD = JNK binding domain; SH3 = Src homology 3 domain; PTB = phosphotyrosine binding domain.

PARP was cleaved to an 85-kDa fragment at 2h in response to TRAIL, and at 1h in response to staurosporine treatment. A complete processing of the intact PARP into the 85-kDa product was first observed after 4h of TRAIL and after 8h of staurosporine treatment (Figs. 4.4 and 4.5, panel B).

JIP-1 was still present as an intact 120-kDa protein after 2h in response to TRAIL or staurosporine (Figs. 4.4 and 4.5, panel B). During TRAIL-induced apoptosis, a 100-kDa JIP-1 cleavage product was first observed after 4h (Fig. 4.4B), whereas JIP-1 cleavage was not clearly evident after 4h of staurosporine treatment (Fig. 4.5B). The 100-kDa JIP-1 fragment was first detected after 8h of staurosporine treatment (Fig. 4.5B). JIP-1 cleavage in response to either TRAIL or staurosporine was accompanied by a small decrease in the amount of intact JIP-1, however in both cases a complete loss of intact JIP-1 was not observed. The cleavage of JIP-1 during TRAIL- and staurosporine-induced apoptosis correlated with the complete processing of PARP and a high percentage of apoptotic cells (Figs. 4.4 and 4.5, panels A and B).

To test if JIP-1 cleavage *in vivo* during apoptosis was mediated by caspases, HeLa cells were pre-treated with zVAD.fmk, a general caspase inhibitor (Jacobson, Weil & Raff, 1996). Pre-incubation of HeLa cells with zVAD.fmk for 1h, followed by 8h treatment with TRAIL or staurosporine inhibited JIP-1 cleavage (Figs. 4.4 and 4.5, panel B). PARP cleavage was also completely inhibited by zVAD.fmk pre-treatment in response to TRAIL or staurosporine (Figs. 4.4 and 4.5, panel B). The percentage of apoptotic cells in the presence of zVAD.fmk in response to either stimulus was less than 5% (Figs. 4.4 and 4.5, panel A), suggesting that zVAD.fmk also inhibited apoptosis. PARP cleavage (Tewari *et. al.*, 1995) and DNA fragmentation (Tang & Kidd, 1998) are a part of the execution phase of apoptosis, which is mediated by caspases (Nicholson, 1999). Taken together, these results suggested that the inhibition of JIP-1 cleavage in the presence of zVAD.fmk in response to TRAIL or staurosporine was due to the inhibition of caspases, and therefore the observed JIP-1 cleavage during apoptosis (Figs. 4.4 and 4.5, panel B) was mediated by caspases.

Constant levels of α-tubulin in response to TRAIL or staurosporine in the presence or absence of zVAD.fmk (Figs. 4.4 and 4.5, panel B) demonstrated equal protein loading and excluded the possibility that JIP-1 cleavage might have been due to non-specific protein degradation during apoptosis.

Based on the scheme presented in Fig. 4.3, these results suggested that JIP-1 might be cleaved by caspases *in vivo* at the Asp98 site, since only the 100-kDa JIP-1 cleavage

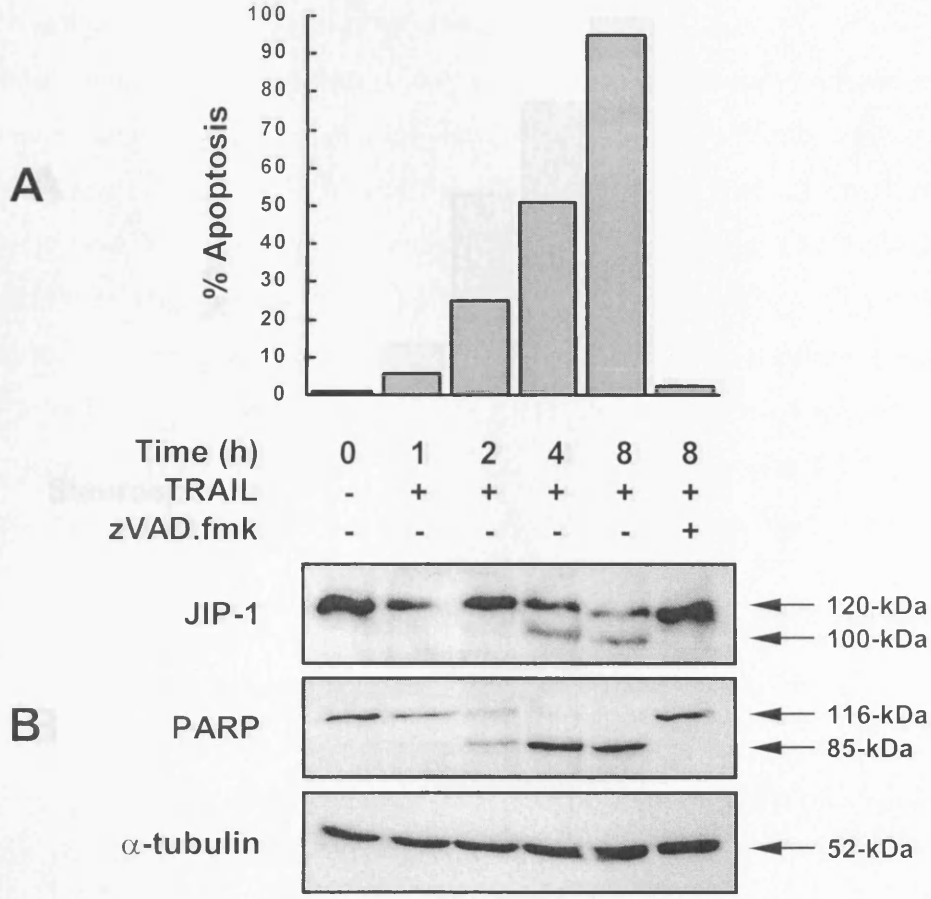

Fig. 4.4. JIP-1 cleavage* in vivo *is mediated by caspases during TRAIL-induced apoptosis in HeLa cells.

HeLa cells were either left untreated or treated with TRAIL (1μg/ml) in the presence or the absence of 50μM zVAD.fmk for the times indicated. **(A)** Cells undergoing apoptosis were quantified by DNA fragmentation assay using Hoechst 33258 staining (section 2.2.6.2, Materils & Methods). The results shown are means of experiments performed in triplicate. **(B)** Extracts were prepared and subjected to electrophoresis as described in Fig. 4.2. Equal amounts of extract (200μg of the total protein) were immunoblotted for PARP as described in Fig. 4.2. Antibodies were stripped from the immunoblot as described in Materials & Methods (section 2.2.4.1) and reprobed for JIP-1and α-tubulin as described in Fig. 4.2.

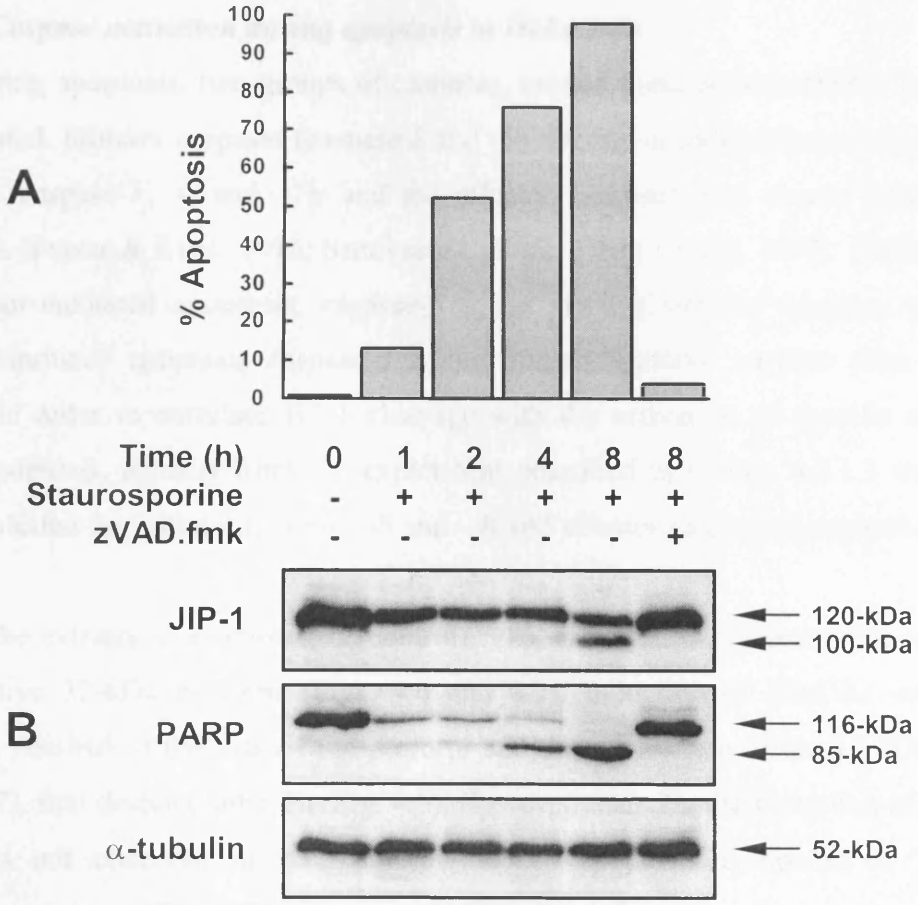

Fig. 4.5. JIP1-1 cleavage* in vivo *is mediated by caspases during staurosporine-induced apoptosis in HeLa cells.

HeLa cells were either left untreated or treated with staurosporine (1μM) in the presence or the absence of 50μM zVAD.fmk for the times indicated. **(A)** Cells undergoing apoptosis were quantified as described in Fig. 4.4A. The results shown are means of experiments performed in triplicate. **(B)** Extracts were prepared, subjected to electrophoresis and immunoblotted for JIP-1, PARP and α-tubulin as described in Fig. 4.4B.

fragment was observed during TRAIL- and staurosporine-induced apoptosis (Figs. 4.4 and 4.5, panel B).

4.2.1.4. Caspase activation during apoptosis in HeLa cells

During apoptosis, two groups of caspases, termed initiator and effector caspases, are activated. Initiator caspases (caspase-8 and –9) directly or indirectly activate effector caspases (caspase-3, -6 and –7), and the effector caspases then cleave intracellular substrates (Fraser & Evan, 1996; Srinivasula, *et. al.*, 1996; Cohen, 1997). Furthermore, in receptor-mediated apoptosis, caspase-8 is the primary initiator caspase, while in chemical-induced apoptosis caspase-9 is the primary initiator caspase (Sun *et. al.*, 1999). In order to correlate JIP-1 cleavage with the activation of specific caspases during apoptosis, extracts from the experiment described in section 4.2.1.3 were also immunoblotted for initiator (caspases-8 and –9) and effector caspases (caspases-3 and –7).

In the extracts from untreated (control) cells, caspase-3 was detected as an intact and inactive 32-kDa proform (Figs. 4.6 and 4.7). Induction of TRAIL- -mediated apoptosis resulted in the loss of the proform and the appearance of the 17-kDa active form (p17), first detected after 2h (Fig. 4.6). However, after 2h, the formation of the p17 form was not observed in staurosporine-induced apoptosis compared to TRAIL-mediated apoptosis (Fig. 4.7). Staurosporine treatment for 4h resulted in the efficient processing of caspase-3 and an increased formation of the p17 fragment.

Caspase-7 was detected in control cell extracts primarily as the inactive 36-kDa protein (Figs. 4.6 and 4.7). Induction of apoptosis by TRAIL or staurosporine resulted in a time-dependent processing of caspase-7 accompanied by the formation of two major products, a 32-kDa and a 19-kDa fragment (p19, active form). The appearance of the p19 fragment of caspase-7 was first observed 2h after treatment with either stimulus. However, as was the case with caspase-3, efficient processing of caspase-7 was observed after 2h of TRAIL but only after 4h of staurosporine treatment.

In the control cell extracts, caspase-8 was detected primarily as two isoforms of ~55-kDa (Figs. 4.6 and 4.7), corresponding to caspase-8a and –8b (Scaffidi *et. al.*, 1997). The p18 fragment (active form) was first observed 2h after TRAIL treatment and 4h after staurosporine treatment.

The control cell extracts contained the 46-kDa proform of caspase-9 (Figs. 4.6 and 4.7), which upon the induction of apoptosis was processed in a time-dependent manner

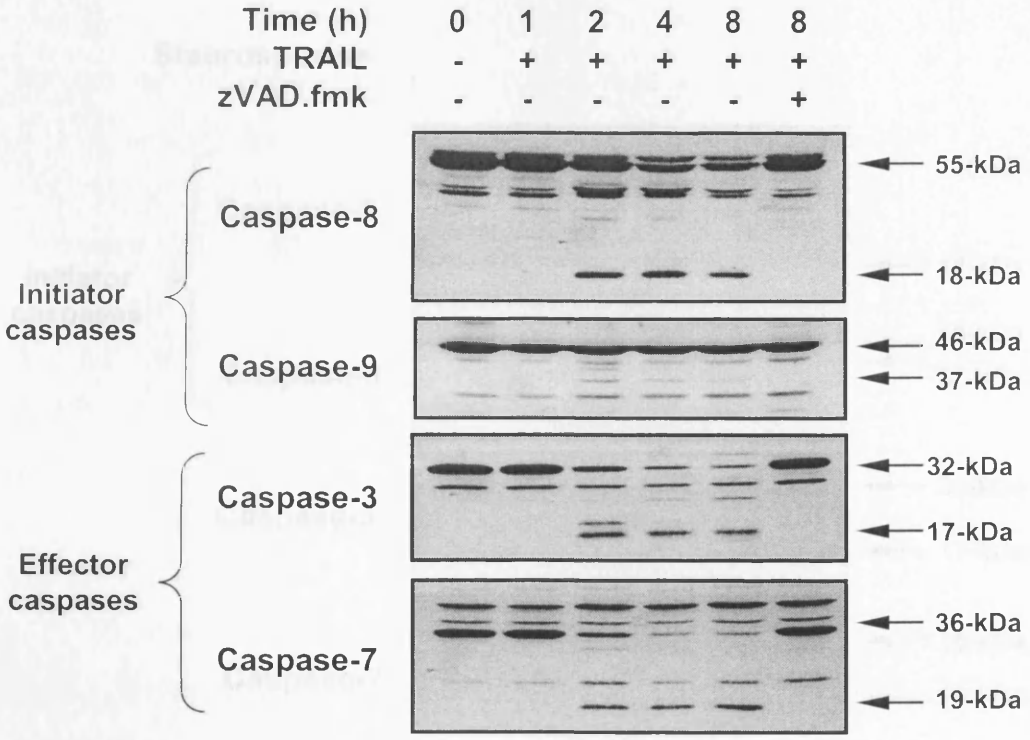

Fig. 4.6. Caspase activation during TRAIL-induced apoptosis in HeLa cells.

HeLa cells were treated with TRAIL/zVAD.fmk as described in Fig. 4.4. Equal amounts of extract (100μg) from the experiment described in Fig. 4.4B were electrophoresed on 10% (for caspase-8 and -9) and 13% (for caspase-3 and -7) SDS-PAGE gels and immunoblotted with caspase-3 (1:10,000), caspase-7 (1:2000), caspase-8 (1:2000) and caspase-9 (1:2000) antibodies. Caspase blotting was kindly performed by Dr. Marion MacFarlane (MRC Toxicology Unit, University of Leicester, Leicester).

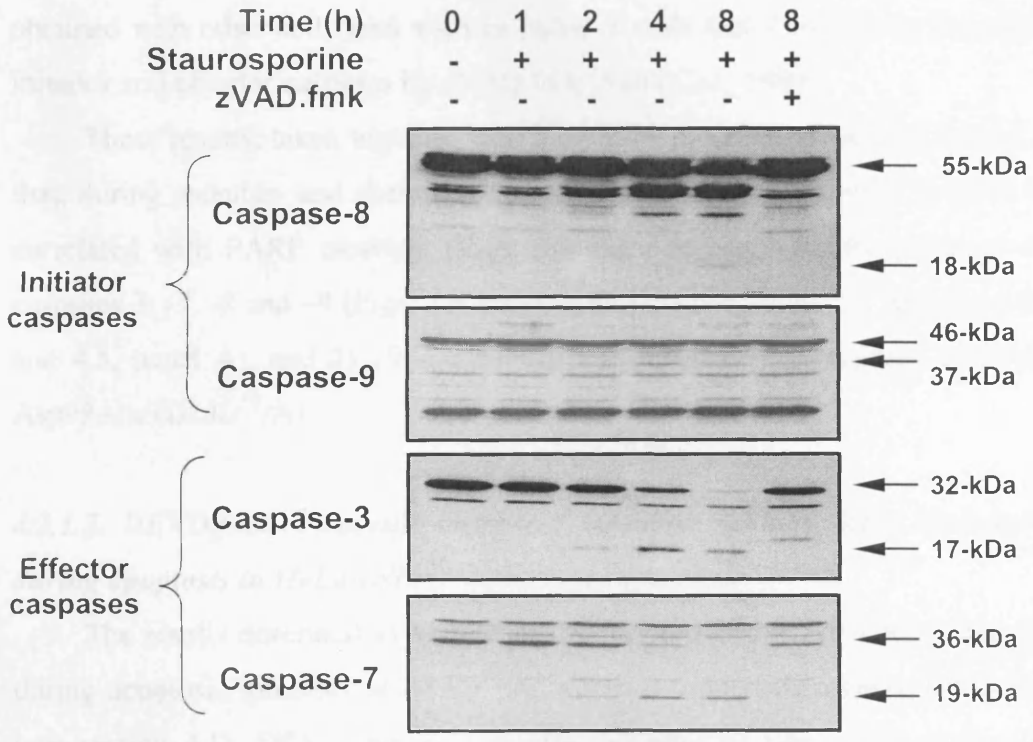

Fig. 4.7. Caspase activation* in vivo *during staurosporine-induced apoptosis in HeLa cells.

HeLa cells were treated with staurosporine/zVAD.fmk as described in Fig. 4.5. Equal amounts of extract (100μg) from the experiment described in Fig. 4.5B were immunoblotted for caspases-3, -7, -8 and –9 as described in Fig. 4.6. Caspase blotting was kindly performed by Dr. Marion MacFarlane (MRC Toxicology Unit, University of Leicester, Leicester).

to yield the active form, a 37-kDa fragment (p37). The first detectable p37 was evident after 2h TRAIL and staurosporine treatments.

Processing of caspases-3, -7, -8 and -9 to their corresponding active forms in response to TRAIL or staurosporine treatment for 8h was inhibited in cells pre-treated with zVAD.fmk (Figs. 4.6 and 4.7). This result was consistent with the role of zVAD.fmk as a general caspase inhibitor. It was also in agreement with the results obtained with other cell types such as Jurkat T cells that demonstrate the inhibition of initiator and effector caspases by zVAD.fmk (Sun *et. al.*, 1999).

These results, taken together with the results described in section 4.2.1.3, showed that, during receptor- and chemical-induced apoptosis of HeLa cells, 1) JIP-1 cleavage correlated with PARP cleavage (Figs. 4.4 and 4.5, panel B), the presence of active caspases-3, -7, -8 and –9 (Figs. 4.6 and 4.7) and the progression of apoptosis (Figs. 4.4 and 4.5, panel A), and 2) JIP-1 cleavage was mediated by caspases, possibly at the Asp98 site ($DLID^{98}/A$).

4.2.1.5. DEVD.fmk, a specific caspase-3 inhibitor, inhibits JIP-1 cleavage in vivo during apoptosis in HeLa cells

The results described in section 4.2.1.3 suggested that JIP-1 was cleaved *in vivo* during apoptosis, possibly at $DLID^{98}/A$, which is a putative caspase-3 processing site (see section 4.1). DEVD.fmk is a specific inhibitor of caspase-3 activity (Casciola-Rosen *et. al.*, 1996; Gamen *et. al.*, 1996; Hasegawa *et. al.*, 1996; Tomita *et. al.*, 1996). Therefore, to investigate the possibility that JIP-1 might be a caspase-3 substrate *in vivo*, HeLa cells were pre-treated with increasing concentrations of DEVD.fmk, followed by an exposure to TRAIL or staurosporine for 8h, and the resulting extracts were immunoblotted for JIP-1 and PARP. The percentage of cells undergoing apoptosis in culture was also determined as before (section 4.2.1.3). If JIP-1 is a caspase-3 substrate, then DEVD.fmk should inhibit JIP-1 cleavage during apoptosis.

A quantitative analysis of apoptosis in the presence of DEVD.fmk showed that, increasing the concentration of DEVD.fmk led to a progressive decrease in the percentage of cells undergoing apoptosis in response to TRAIL or staurosporine (Figs. 4.8 and 4.9, panel A). At 40μM DEVD.fmk, the inhibitory effect on apoptosis was almost identical to that obtained with 50μM zVAD.fmk, suggesting that caspase-3 activity was significantly inhibited at 40μM DEVD.fmk.

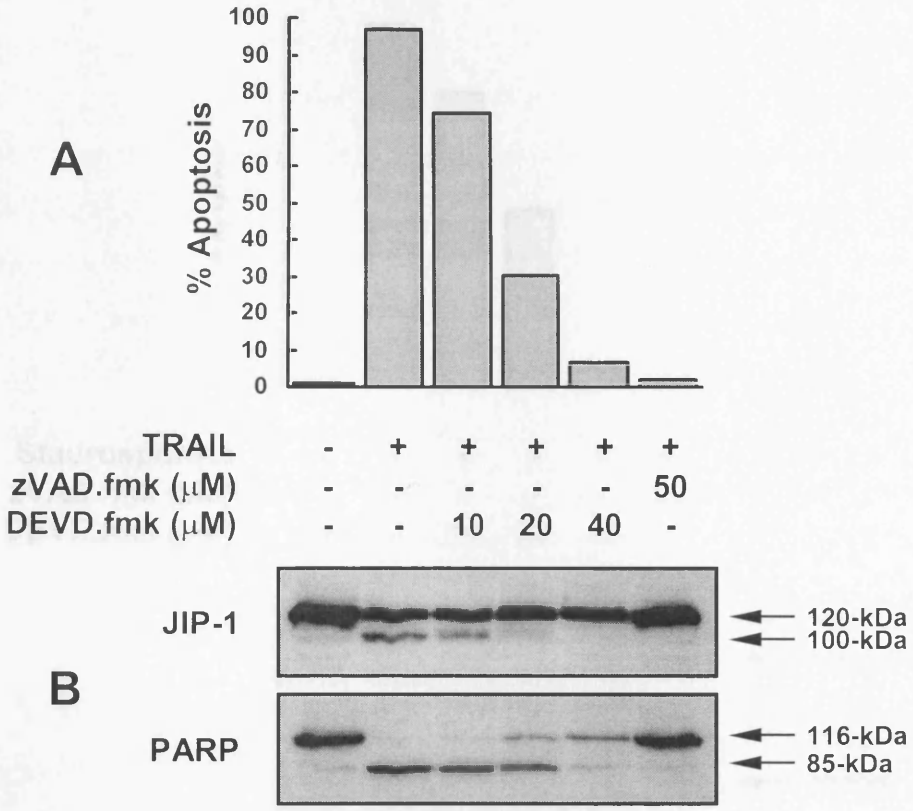

Fig. 4.8. DEVD.fmk, a specific caspase-3 inhibitor, inhibits JIP-1 cleavage during TRAIL-induced apoptosis.

HeLa cells were either left untreated or treated with TRAIL (1μg/ml) for 8h in the presence or the absence of the indicated concentration(s) of zVAD.fmk or DEVD.fmk. **(A)** Cells undergoing apoptosis were quantified as described in Fig. 4.4A. The results shown are means of experiments performed in triplicate. **(B)** Extracts were prepared and immunoblotted for JIP-1 and PARP as described in Fig. 4.2.

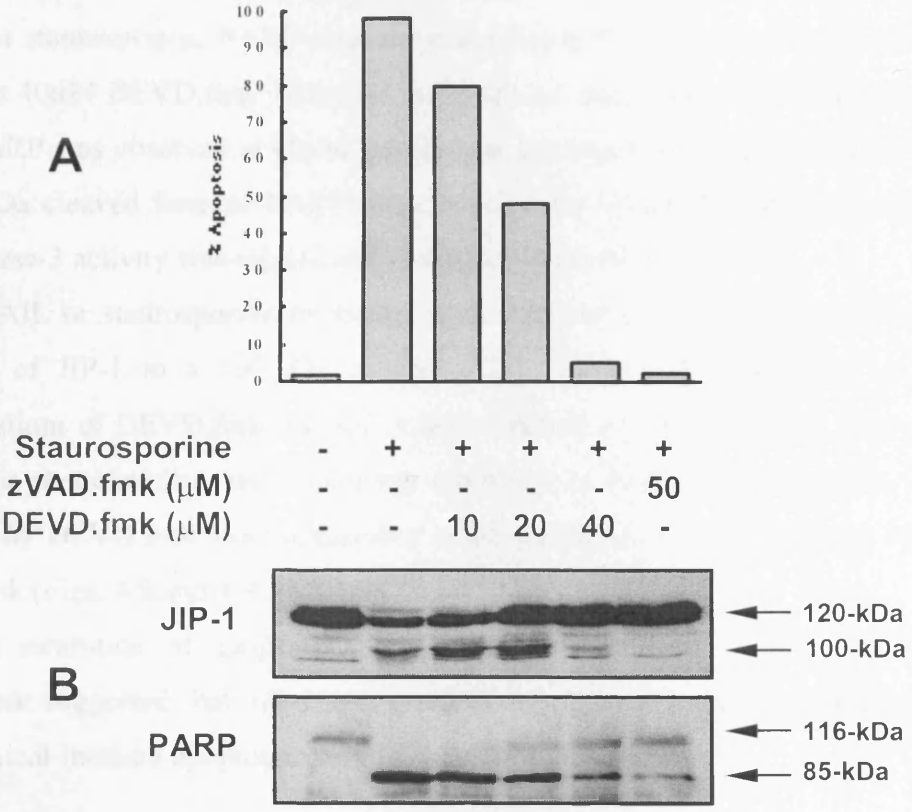

Fig. 4.9. DEVD.fmk, a specific caspase-3 inhibitor, inhibits JIP-1 cleavage during staurosporine-induced apoptosis.

HeLa cells were either left untreated or treated with staurosporine (1μM) for 8h in the presence or the absence of the indicated concentration(s) of zVAD.fmk or DEVD.fmk. **(A)** Cells undergoing apoptosis were quantified as described in Fig. 4.4A. The results shown are means of experiments performed in triplicate. **(B)** Extracts were prepared and immunoblotted for JIP-1 and PARP as described in Fig. 4.2.

In the extracts from untreated (control) cells, JIP-1 and PARP were present as 120-kDa and 116-kDa proteins respectively (Figs. 4.8 and 4.9, panel B). In the absence of DEVD.fmk, PARP was cleaved to an 85-kDa fragment in response to TRAIL or staurosporine. The inhibition of PARP cleavage in the presence of increasing concentrations of DEVD.fmk was observed (Figs. 4.8 and 4.9, panel B). In response to TRAIL or staurosporine, PARP cleavage was completely blocked at 50μM zVAD.fmk but not at 40μM DEVD.fmk. However, a significant inhibition of the processing of the intact PARP was observed at 40μM DEVD.fmk, as judged by a decrease in the level of the 85-kDa cleaved form of PARP (Figs. 4.8 and 4.9, panel B). This again suggested that caspase-3 activity was significantly inhibited at 40μM DEVD.fmk.

TRAIL or staurosporine treatment in the absence of DEVD.fmk resulted in the cleavage of JIP-1 to a 100-kDa product (Figs. 4.8 and 4.9, panel B). Increasing concentrations of DEVD.fmk resulted in the inhibition of JIP-1 cleavage in response to TRAIL or staurosporine, with complete inhibition at 40μM. The inhibition of JIP-1 cleavage by DEVD.fmk was comparable to the inhibition of JIP-1 cleavage caused by zVAD.fmk (Figs. 4.8 and 4.9, panel B).

The inhibition of apoptosis, JIP-1 cleavage and PARP cleavage *in vivo* by DEVD.fmk suggested that JIP-1 was possibly cleaved by caspase-3 during receptor- and chemical-induced apoptosis, very likely at $DLID^{98}/A$.

4.2.2. JIP-1b is cleaved at $DLID^{98}/A$ and $DESD^{405}/S$ by caspase-3 *in vitro*

4.2.2.1. JIP-1 protein expression in vitro

The study of JIP-1 cleavage *in vivo* during apoptosis in HeLa cells suggested that JIP-1 was very likely to be cleaved by caspase-3, most probably at $DLID^{98}/A$ (sections 4.2.1.3 and 4.2.1.5). To confirm this observation, JIP-1 cleavage analysis using purified caspases was carried out *in vitro*. For this, firstly the available JIP-1 constructs pBluescript-JIP-1 and pBluescript-JIP-1b were used as templates to test for protein expression using the TNT® T7 coupled *in vitro* transcription/translation system (Promega). pBluescript-JIP-1b was constructed as described in Materials & Methods (section 2.2.2.5). Luciferase T7 DNA was used as a functional control in the *in vitro* transcription/translation reactions.

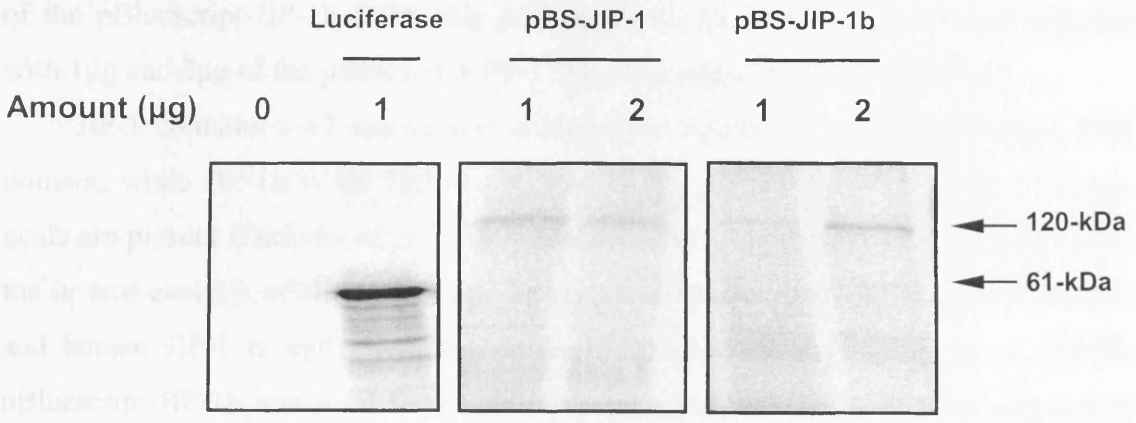

Fig. 4.10. Testing pBluescript-JIP-1 and pBluescript-JIP-1b constructs in the* in vitro *transcription/translation reactions.

Different amounts of the indicated template DNA was translated *in vitro* using Promega's TNT® coupled transcription/translation system as described in Materials & Methods (section 2.2.6.3). The reaction products were separated on 10% SDS-PAGE and visualised by PhosphorImager analysis after 72 hours for JIP-1 expression. pBS = pBluescript.

The results showed that the luciferase T7 DNA yielded a 61-kDa protein product as expected (Fig. 4.10). No protein products were observed in the absence of a DNA template (Fig. 4.10). Similar levels of a 112-kDa protein product was obtained with 1μg and 2μg of the pBluescript-JIP-1 DNA (Fig. 4.10), suggesting that the amount of template used had no effect on transcription/translation efficiency. However, detectable levels of the 120-kDa protein product was obtained only with 2μg of the pBluescript-JIP-1b DNA, whereas with 1μg of the pBluescript-JIP-1b DNA the level of the 120-kDa product obtained was very low (Fig. 4.10). The level of the product obtained with 2μg of the pBluescript-JIP-1b DNA was comparable to the level of the product obtained with 1μg and 2μg of the pBluescript-JIP-1 DNA, as judged by band intensities.

JIP-1 contains a 47 amino acid deletion that results in a partial SH3 and PTB domain, while JIP-1b is the full-length form of the protein in which these 47 amino acids are present (Dickens *et. al.*, 1997; Waeber *et. al.*, 1998; Kim *et. al.*, 1999). Since the *in vivo* analysis of JIP-1 cleavage during apoptosis was done in human HeLa cells, and human JIP-1 is more homologous to JIP-1b than JIP-1 (Mosser *et. al.*, 1999), pBluescript-JIP-1b was used for *in vitro* expression studies using purified caspases to correlate the sizes of the cleaved JIP-1b fragment(s) obtained *in vitro* with the size of the cleaved JIP-1 (100-kDa) *in vivo* (Figs. 4.4 and 4.5, panel B). The amount of the pBluescript-JIP-1b DNA used for *in vitro* transcription/translation studies was 2μg, since 2μg gave detectable levels of the JIP-1b protein (Fig. 4.10).

4.2.2.2. In vitro analysis of JIP-1b cleavage with purified caspases-3 and -8

JIP-1b cleavage by purified caspases-3 or -8 was next tested *in vitro*. The physiological concentrations of caspases-3 and -8 are in the nM range (Stennicke *et. al.*, 1998). Therefore the concentrations of purified enzymes used were in the range of 0-25nM. JIP-1b cleavage using purified caspase-8 was done to test for the possibility of the LEVD^{516}/D site being a caspase-8 cleavage site *in vitro*. The ability of purified caspases-3 and –8 to cleave JIP-1b *in vitro* was tested under identical conditions.

In the absence of purified caspase-3 or -8, JIP-1b was present as a 120-kDa fragment and no cleavage products were observed (Fig. 4.11A and B). However, the control lane did show the presence of two other bands, approximately of sizes 80-kDa and 48-kDa, in the absence of caspase treatment (these bands are marked by * in Fig. 4.11A and B). These may have arisen due to the use of alternative internal translation

initiation sites at amino acid positions 310 and 469, respectively, in the JIP-1b sequence.

Incubation of the *in vitro* translated JIP-1b with 2.5nM caspase-3 led to the formation of 100-kDa and 45-kDa products (Fig. 4.11A). The 100-kDa product observed *in vitro* correlated with the 100-kDa product detected *in vivo* in JIP-1 immunoblots (Figs. 4.4 and 4.5, panel B). However, the 45-kDa product observed *in vitro* was not detected in JIP-1 immunoblots (see Figs. 4.4 and 4.5, panel B). The formation of 100-kDa and 45-kDa products *in vitro* suggested that JIP-1b was cleaved at Asp98 and Asp402/Asp405 sites by caspase-3, according to the scheme presented in Fig. 4.3. Increasing concentrations of purified caspase-3 resulted in a gradual loss of the 120-kDa and 100-kDa fragments and an increase in the formation of the 55-kDa and 45-kDa products *in vitro* (Fig. 4.11A). At high concentrations of caspase-3 (10nM and 25nM), an additional product of 37-kDa was observed (Fig. 4.11A). This suggested that at high concentrations, caspase-3 cleaved JIP-1b at Asp450, according to the scheme presented in Fig. 4.3. At 25nM caspase-3 concentration, the 120-kDa intact protein and 100-kDa cleavage product were not visible, indicating that they had been subjected to further cleavage by caspase-3.

Caspase-8 at 2.5nM concentration had not effect on JIP-1b, as no cleavage products were observed *in vitro* (Fig. 4.11B). At 25nM, caspase-8 cleaved JIP-1b to yield 100-kDa and 45-kDa cleavage products (Fig. 4.11B). However, 100-kDa and 45-kDa JIP-1b cleavage products were obtained with 2.5nM caspase-3 (Fig. 4.11A), suggesting that JIP-1b was 10-fold more sensitive to cleavage by caspase-3 than caspase-8 *in vitro* under identical conditions. The formation of the 55-kDa JIP-1b cleavage product was not observed with the concentrations of caspase-8 used in the assay (Fig. 4.11B). A complete loss of the intact JIP-1b protein was not observed with 25nM caspase-8 (Fig. 4.11B). This contrasted with a complete loss of the intact protein observed with 10nM caspase-3 (Fig. 4.11A), again demonstrating the sensitivity of JIP-1b to cleavage *in vitro* by caspase-3 compared to caspase-8. The formation of cleavage products of the same size by caspases-3 and –8 was a surprising result, considering that there was only one putative caspase-8 cleavage site (Asp516) in JIP-1b, and cleavage at this site could not account for the size of the cleavage products obtained (Figs. 4.3 and 4.11B). This suggested that, at high concentrations, caspase-8 possibly cleaved JIP-1b at sites preferred by caspase-3.

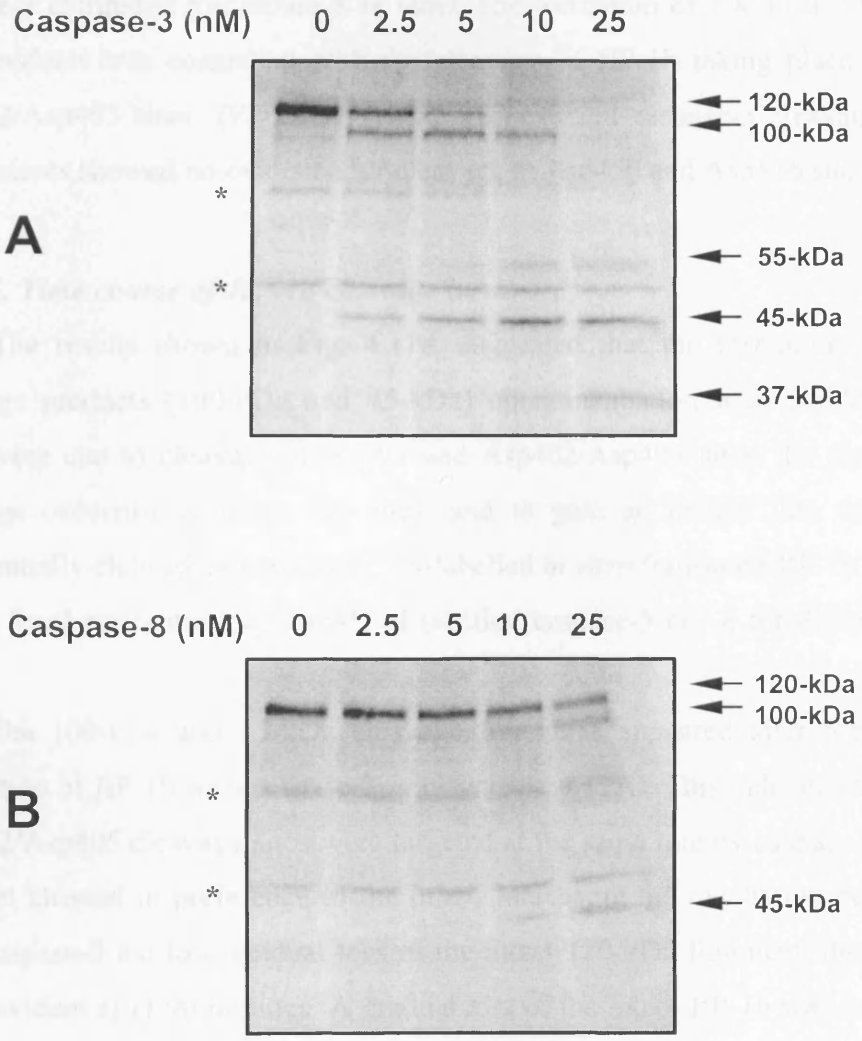

***Fig. 4.11. JIP-1b is a preferential caspase-3 substrate* in vitro.**

pBluescript-JIP-1b (2μg) was translated *in vitro* as described in Materials & Methods (section 2.2.6.3). Equal volumes of the lysate containing ^{35}S-labelled *in vitro* translated JIP-1b were either left untreated or were incubated with the indicated concentrations of purified caspase-3 **(A)** or –8 **(B)** for 1h. The reaction products were separated by 10% SDS-PAGE and visualised by Phosphor Imager analysis after a 72 hour exposure.

In vitro analysis of cleavage of the JIP-1 isoform by caspases-3 and -8 gave almost identical results (data not shown), suggesting that there were no caspase-3 cleavage sites in the extra 47 amino acid sequence present in JIP-1b.

Overall, the results obtained suggested that JIP-1b was preferentially cleaved by caspase-3 compared to caspase-8 *in vitro*. The formation of 100-kDa, 55-kDa and 45-kDa products was consistent with the cleavage of JIP-1b taking place at Asp98 and Asp402/Asp405 sites (Fig. 4.3), which are preferred caspase-3 cleavage sites. These experiments showed no evidence for cleavage at Asp450 and Asp516 sites.

4.2.2.3. Time course of JIP-1b cleavage in vitro

The results shown in Fig. 4.11A suggested that the formation of two JIP-1b cleavage products (100-kDa and 45-kDa) upon incubation with 2.5nM caspase-3 *in vitro* were due to cleavage at Asp98 and Asp402/Asp405 sites. To study the rate of cleavage occurring at these two sites, and to gain an insight into the JIP-1b sites preferentially cleaved by caspase-3, ^{35}S-labelled *in vitro* translated JIP-1b was incubated with a fixed concentration (10nM) of purified caspase-3 or –8 for different lengths of time.

The 100-kDa and 45-kDa cleavage fragments appeared after 5 minutes of the incubation of JIP-1b with caspase-3 *in vitro* (Fig. 4.12A). This indicated that Asp98 and Asp402/Asp405 cleavage sites were targeted at the same rate by caspase-3, and one site was not cleaved in preference to the other. Increasing the incubation period of JIP-1b with caspase-3 led to a gradual loss of the intact 120-kDa fragment, the complete loss being evident after 90 minutes. A gradual loss of the intact JIP-1b was accompanied by the increasing formation of the 100-kDa, 55-kDa and 45-kDa products. The 100-kDa product was maximally formed after 15 minutes (Fig. 4.12A), after which a time-dependent decrease in the intensity of the 100-kDa band was observed, suggesting that it was subject to further processing by caspase-3. The 55-kDa fragment was first detectable after 30 minutes and was then present throughout the time course of the assay.

The results of JIP-1b cleavage time course with 10nM caspase-8 showed that the cleavage kinetics of JIP-1b were very slow compared to the cleavage kinetics observed with caspase-3. The 100 kDa and 45 kDa products were first visible after 60 minutes of

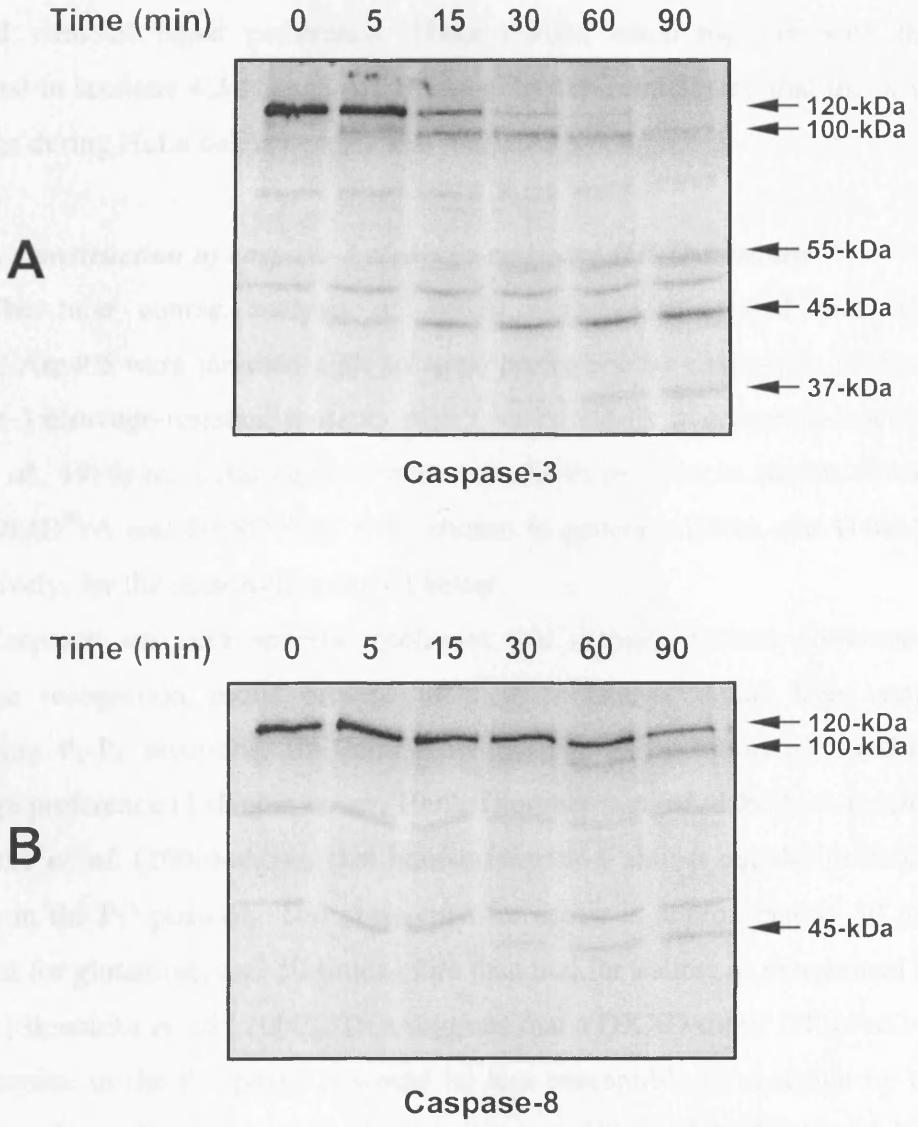

***Fig. 4.12. Time course of JIP-1b cleavage by caspases-3 and -8* in vitro.**

pBluescript-JIP-1b (2μg) was translated *in vitro* as described in Materials & Methods (section 2.2.6.3). Equal volumes of the lysate containing ^{35}S-labelled *in vitro* translated JIP-1b were either left untreated or were incubated with a fixed concentration (10nM) of caspase-3 **(A)** or -8 **(B)** for the times indicated. The reaction products were separated by 10% SDS-PAGE and visualised by Phosphor Imager analysis after a 72 hour exposure.

the incubation of JIP-1b with caspase-8 (Fig. 4.12B), as opposed to 5 minutes with an equal concentration of caspase-3 (Fig. 4.12A).

Thus, the results of the time course analysis further confirmed that JIP-1b was a preferential caspase-3 substrate *in vitro*, and Asp98 and Asp402/Asp405 sites were targeted with an equal preference. These results, taken together with the results presented in sections 4.2.1.3 and 4.2.1.5 supported the conclusion that the *in vivo* JIP-1 cleavage during HeLa cell apoptosis was mediated by caspase-3.

4.2.2.4. Construction of caspase-3 cleavage-resistant JIP-1b mutants

The time course analysis of JIP-1b cleavage suggested that Asp98 and Asp402/Asp405 were targeted with an equal preference by caspase-3. To confirm this, caspase-3 cleavage-resistant mutants were constructed by overlapping insertional PCR (Ho *et. al.*, 1989) by mutating the aspartate in the P_1 position to alanine. Two cleavage sites, $DLID^{98}$/A and $DESD^{405}$/S, were chosen to generate D98A and D405A mutants respectively, for the reasons mentioned below.

Caspases are very specific proteases that display distinct preferences in the cleavage recognition motif present in their substrates. Apart from amino acids occupying P_1-P_4 positions, the amino acid in the P_1' position also influences the cleavage preference (Talanian *et. al.*, 1997; Thornberry *et. al.*, 1997). A recent study by Stennicke *et. al.* (2000) shows that human caspase-3 almost equally prefers serine or alanine in the P_1' position. The preference for serine is approximately 30 times more than that for glutamine, and 50 times more than that for valine, as determined by kinetic studies (Stennicke *et. al.*, 2000). This suggests that a DXXD motif followed by a valine or glutamine in the P_1' position would be less susceptible to cleavage by caspase-3. Based on this information, two cleavage sites in JIP-1b, $DLID^{98}$/A and $DESD^{405}$/S, would be preferred by caspase-3 since they contain alanine or serine in the P_1' position. However, the other two possible cleavage sites, $DYSD^{402}$/E and $DEPD^{450}$/V, would not be preferable caspase-3 cleavage sites since they contain glutamine and valine respectively in the P_1' position. Therefore, $DLID^{98}$/A and $DESD^{405}$/S were considered the most likely caspase-3 cleavage sites. To confirm this, we generated JIP-1b D98A and D405A mutants.

1. The PCR strategy for mutant construction

The PCR strategy for the mutant construction included two sets of PCRs, as shown schematically in Fig. 4.13A.

Two unique restriction enzyme sites were identified in JIP-1b, one present upstream (restriction enzyme site 1) and the other present downstream (restriction enzyme site 2) of the aspartate ('x') to be mutated (Fig. 4.13A). These sites were *Eco*RI (site 1) and *Nar*I (site 2) for the D98A mutation, and *Bgl*II (site 1) and *Bst*EII (site 2) for the D405A mutation. Primers b and c in Fig. 4.13A are the forward and the reverse primers respectively containing the nucleotide change for the mutant construction. These were D105AF (primer b) and D105AR (primer c) for the D98A mutation, and D412AF (primer b) and D412AR (primer c) for the D405A mutation. Primer a is the forward primer upstream of the restriction enzyme site 1 and Primer d is the reverse primer downstream of the restriction enzyme site 2 (Fig. 4.13A). In the case of the D98A mutation, primer a was T7 and the primer d was FBsmR. For the D405A mutation, primer a was FBglF, and primer d was FBstR.

The first set of PCR involved the use of two separate sets of primer pairs, a/c and b/d (Fig. 4.13A). The amplified products from these two sets of PCRs were used as templates for the final PCR using the primer pair a/d to amplify the fragment that would contain the desired mutation as well as the two unique restriction enzyme sites. The final PCR products were then doubly digested with the two enzymes and cloned into pBluescript-JIP-1b digested with the same enzymes.

2. JIP-1b D98A and D405A mutant construction

JIP-1b mutants D98A and D405A were constructed as explained in Materials & Methods (section 2.2.2.6).

For the D98A mutation, in the first set of PCR, the T7/D105AR primer pair yielded a specific product of the expected size, 515 bp, at an annealing temperature of 60°C in the presence of 2% DMSO (Fig. 4.13B). The primer pair D105AF/FBsmR yielded a specific product of the expected size, 213 bp, in the absence of DMSO at an annealing temperature of 55°C (Fig. 4.13B). For the second set of PCR, the amplified DNA products (515 bp and 213 bp) were used as templates for the amplification of a 709 bp fragment by the primer pair T7/FBsmR in the presence of 2% DMSO. As shown in Fig. 4.13C, at the annealing temperatures of 55°C and 60°C a specific band corresponding to the control 709 bp fragment was observed, but at temperatures above

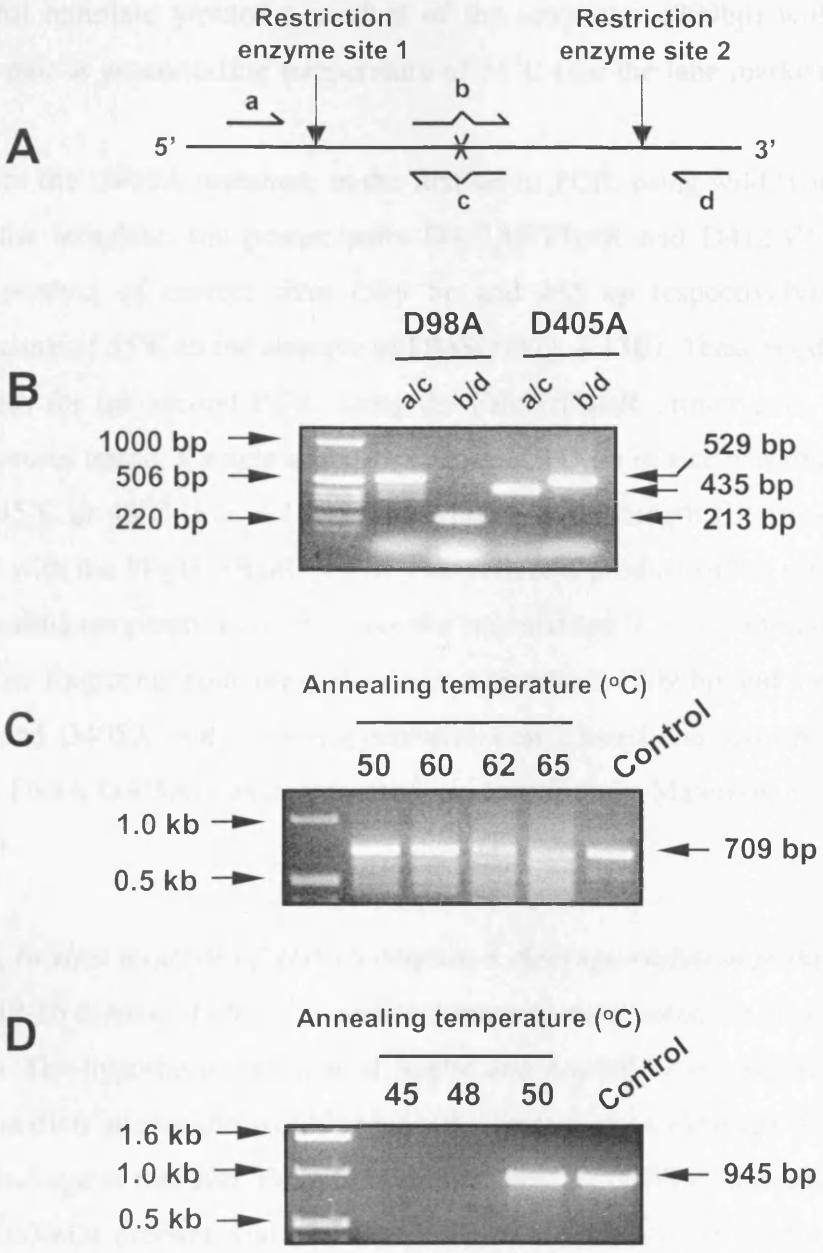

Fig. 4.13. Construction of caspase-3 cleavage-resistant JIP-1b mutants by overlapping insertional PCR.

(A) An outline of the PCR approach used for constructing the mutants. a, b, c and d denote primers. **(B)** First set of PCR for the construction of D98A and D405A mutants. a = T7 or FBglF; b = D105AF or D412AF; c = D105AR or D412AR; d = FBsmR or FBstR. **(C)** Second set of PCR for the construction of D98A using T7/FBsmR primers, and **(D)** second set of PCR for D405A mutant construction using FBglF/FBstR primers. See text for details.

60°C the specificity was lost. PCR using the wild type, full-length JIP-1b DNA used as a control template yielded a product of the same size (709bp) with the T7/FBsmR primer pair at an annealing temperature of 55°C (see the lane marked 'control' in Fig. 4.13C).

For the D405A mutation, in the first set of PCR, using wild type, full-length JIP-1b as the template, the primer pairs D412AF/FBstR and D412AR/FBglF yielded a single product of correct sizes (529 bp and 435 bp respectively) at an annealing temperature of 55°C in the absence of DMSO (Fig. 4.13B). These products were used as templates for the second PCR, using the FBglF/FBstR primer pair. Of the annealing temperatures tested, a single specific product of 945 bp in size was obtained at 50°C but not at 45°C or 48°C (Fig. 4.13D). The wild type, full-length JIP-1b template used as a control with the FBglF/FBstR primer pair yielded a product of the same size (945bp) at an annealing temperature of 50°C (see the lane marked 'control' in Fig. 4.13D).

The fragments containing the desired mutations (709 bp and 945 bp products for D98A and D405A mutations respectively) were cloned and sequenced, and a double mutant D98A/D405A was constructed, as described in Materials & Methods (section 2.2.2.6).

4.2.2.5. In vitro analysis of JIP-1b caspase-3 cleavage-resistant mutants

JIP-1b caspase-3 cleavage-resistant mutants were tested for cleavage by caspase-3 *in vitro*. The hypothesis was that, if Asp98 and Asp405 were caspase-3 cleavage sites, then mutation at one site would inhibit the formation of cleavage product(s) resulting from cleavage at that site. For example, mutation at Asp98 would inhibit the formation of the 100-kDa product, and mutation at Asp405 would inhibit the formation of the 45-kDa product. Also, if Asp98 and Asp405 were targeted with an equal preference by caspase-3, then that mutation at one site should not affect the formation of the products resulting from cleavage at the second site. For example, the formation of the 45-kDa product should be unaffected in the D98A mutant, and the formation of the 100-kDa product should be unaffected in the D405A mutant.

^{35}S-labelled *in vitro* translated JIP-1b (wild type), JIP-1b (D98A), JIP-1b (D405A) or JIP-1b (D98A/D405A) were incubated in the presence or the absence of 10nM purified caspase-3 for 1h, the reaction products were separated on a 10% SDS-PAGE gel and visualised by PhosphorImager analysis.

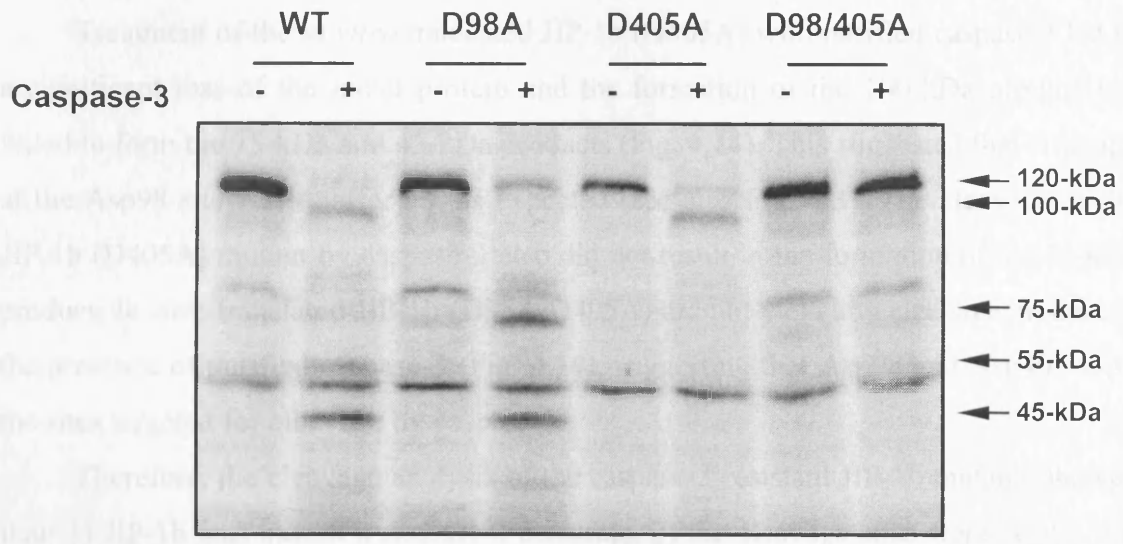

***Fig. 4.14. JIP-1b is cleaved at Asp98 and Asp405 by caspase-3* in vitro.**

Equal amounts (2μg) of pBluescript-JIP-1b (WT), pBluescript-JIP-1b (D98A), pBluescript-JIP-1b (D405A) and pBluescript-JIP-1b (D98A/D405A) were translated *in vitro* as described in Materials & Methods (section 2.2.6.3). Equal volumes of the lysate containing ^{35}S-labelled products were either left untreated or were incubated with 10nM of caspase-3 for 1h. The reaction products were separated by 10% SDS-PAGE and visualised by Phosphor Imager analysis after a 72 hour exposure. The results shown are representative of three independent experiments. WT = wild type.

The results showed that, in the absence of purified caspase-3, JIP-1b (wild type), JIP-1b (D98A), JIP-1b (D405A) and JIP-1b (D98A/D405A) were present as 120-kDa fragments (Fig. 4.14). In the presence of purified caspase-3, *in vitro* translated JIP-1b (wild type) yielded three major products of sizes 100-kDa, 55-kDa and 45-kDa, with a considerable loss of the intact protein (Fig. 4.14). Incubation of the *in vitro* translated JIP-1b (D98A) with purified caspase-3 resulted in the formation of 75-kDa and 45-kDa products but did not yield 100-kDa and 55-kDa products. This suggested that 75-kDa and 45-kDa products were formed due to cleavage at the Asp405 site as expected (see also Fig. 4.3).

Treatment of the *in vitro* translated JIP-1b (D405A) with purified caspase-3 led to a significant loss of the intact protein and the formation of the 100-kDa product but failed to form the 75-kDa and 45-kDa products (Fig. 4.14). This suggested that cleavage at the Asp98 site was unaffected, as expected (see also Fig. 4.3). The cleavage of the JIP-1b (D405A) mutant by caspase-3 also did not result in the formation of the 55-kDa product. *In vitro* translated JIP-1b (D98A/D405A) did not yield any cleavage product in the presence of purified caspase-3 (Fig. 4.14), suggesting that Asp98 and Asp405 were the sites targeted for cleavage by caspase-3.

Therefore, the cleavage analysis of the caspase-3-resistant JIP-1b mutants showed that: 1) JIP-1b was indeed a caspase-3 substrate, 2) the cleavage sites were Asp98 and Asp405, and 3) these sites were equally preferred by caspase-3. These results also discounted the possibility of Asp402 and Asp450 as other putative caspase-3 cleavage sites.

4.3. DISCUSSION

4.3.1. JIP-1 protein expression in different cell lines

In order to identify cell lines expressing endogenous JIP-1, an examination of JIP-1 protein expression using the monoclonal anti-JIP-1 antibody revealed that JIP-1 was expressed in all the cell lines investigated (Fig. 4.1). A very recent report shows that JIP-1 mRNA transcripts are not present in HeLa, NIH-3T3 and Jurkat cells, while JIP-1 mRNA transcripts are abundant in βTC3, INS1 and PC-12 cells (Abderrahmani *et. al.*, 2001). The reason for this cell-specific JIP-1 transcript levels was the expression of a transcription factor called REST (Abderrahmani *et. al.*, 2001). Abderrahmani *et. al.* (2001) showed that JIP-1 expression in neuronal/pancreatic cells and non-neuronal/non-

pancreatic cells was inversely dependent on REST expression. Thus, REST transcripts are absent in βTC3, INS1 and PC-12 cells and therefore JIP-1 expression is high, whereas REST transcripts are present in HeLa, NIH-3T3 and Jurkat cells and therefore JIP-1 expression is low in these cells. This is in contrast with our result, where we clearly detected JIP-1 protein at moderate levels in HeLa and NIH-3T3 cells and at low levels in Jurkat and PC-12 cells (Fig. 4.1A and B).

This apparent disparity between JIP-1 protein expression and the absence/abundance of JIP-1 transcripts in HeLa, Jurkat, PC12 and NIH-3T3 cells can be explained by following reasons. There is growing evidence that mRNA levels are a poor indicator of the levels of the corresponding protein. For example, an examination of mRNA and protein abundance for glutathione-S-transferase in 57 human cell lines showed that, compared to the mRNA level, the protein level varied up to 40-fold and vice versa (Tew *et. al.*, 1996). Furthermore, the correlation between mRNA and protein levels for glutathione-S-transferase was even weaker in tumour cell lines (Tew *et. al.*, 1996). Studies in yeast have also yielded similar results (Gygi *et. al.*, 1999). The amount of protein that accumulates from a particular transcript is influenced not only by the amount of mRNA present in the cytoplasm but also by the rate of translation of the mRNA and stability of the protein product (Kozak, 1999). Thus, it is possible that mRNA levels for a given protein may be low but these mRNA may be subject to a higher rate of translation, thereby yielding moderate or increased levels of the corresponding protein. On the other hand, mRNA may be abundant for a particular protein but the protein may not be translated efficiently, or that the half-life of the protein may be very low. These studies have led to the conclusion that absence or abundance of mRNA transcripts is not an indication of protein expression.

Our JIP-1 protein expression data are further supported by the following findings. JIP-1 mRNA is expressed ubiquitously in several non-neuronal and non-pancreatic tissues (Yasuda *et. al.*, 1999). REST transcripts have been detected in testis and kidney tissues (Palm *et. al.*, 1998). However, JIP-1 transcripts are also detected in these tissues (Dickens *et. al.*, 1997; Bonny *et. al.*, 1998; Mosser *et. al.*, 1999; Thompson *et. al.*, 2001), and consistent with this, we detected JIP-1 protein in GC-1 (mouse testis) and HEK293 (human embryonic kidney) cells (Fig. 4.1). JIP-1 protein expression is induced in differentiated PC-12 cells but is not detectable in undifferentiated PC-12 cells (Meyer, Liu & Margolis, 1999). We had used extracts from undifferentiated PC-12 cells, in which a very faint JIP-1 band was detected (Fig. 4.1B).

Taken together, above discussion suggests that REST expression alone may not be a determinant of JIP-1 protein expression in a given cell line.

4.3.2. JIP-1 cleavage during apoptosis in RinD11, HEK293 and HeLa cells

To identify a cell line suitable for the study of JIP-1 cleavage during receptor- and chemical-induced apoptosis *in vivo*, RinD11, HEK293 and HeLa cells were treated with TRAIL or staurosporine. PARP cleavage was used as a marker of apoptosis, as PARP is a caspase-3 substrate and PARP cleavage is a hallmark of cells undergoing apoptosis (Tewari *et. al.*, 1995). In response to TRAIL, partial PARP cleavage was observed in HEK293 cells while PARP was completely cleaved to an 85-kDa product in HeLa cells (Fig. 4.2A), suggesting that HEK293 cells were relatively insensitive to TRAIL-induced apoptosis compared to HeLa cells. A very recent report explains the differential sensitivity of HEK293 and HeLa cells to TRAIL-induced apoptosis.

Harper *et. al.* (2001) found that a DISC containing small amounts of the adaptor protein FADD and some processed caspase-8 was formed in HEK293 upon TRAIL treatment, however the recruitment of FADD and caspase-8 to the DISC was less efficient in HEK293 cells compared to HeLa cells. c-FLIP$_L$ (cellular FLICE-inhibitory protein, a procaspse-8 homologue) is an anti-apoptotic molecule that is capable of protecting cells from death receptor-induced apoptosis, because it interacts with FADD and caspase-8 and prevents further recruitment of procaspase-8 to the DISC (Irmler *et. al.*, 1997; Scaffidi *et. al.*, 1999). The ratio of c-FLIP$_L$ to caspase-8 in the TRAIL DISC was much higher in HEK293 cells than in HeLa cells, thus resulting in a greater inhibition of TRAIL-induced apoptosis in HEK293 cells than in HeLa cells (Harper *et. al.*, 2001). Furthermore, TRAIL treatment led to the activation of nuclear factor κ B (NF-κB), an anti-apoptotic signalling molecule, in HEK293 cells but not in HeLa cells, which may, in part, contribute towards the insensitivity of HEK293 cells to TRAIL-induced apoptosis (Harper *et. al.*, 2001).

PARP cleavage was not observed in HEK293 cells in response to staurosporine (Fig. 4.2B), suggesting that HEK293 cells were also relatively insensitive to 8h staurosporine treatment. PARP cleavage was observed in RinD11 cells in response to staurosporine but not in response to TRAIL (Fig. 4.2B). The presence of TRAIL

receptors on RinD11 cells have not been reported to date, and this could be a possible reason for the insensitivity of RinD11 cells to TRAIL-induced apoptosis.

4.3.3. Time course of *in vivo* JIP-1 cleavage in HeLa cells

The cleavage of JIP-1 during TRAIL- or staurosporine-mediated apoptosis in HeLa cells (Figs. 4.4 and 4.5, panel B) suggested that JIP-1 cleavage might be a common consequence of both receptor- and chemical-induced apoptosis. The results showed a difference in the timing of JIP-1 cleavage following receptor- and chemical-induced apoptosis. In response to TRAIL, JIP-1 cleavage was observed after 4h (Fig. 4.4B), while JIP-1 was cleaved after 8h following staurosporine treatment (Fig. 4.5B). These time points correlated with the activation of initiator (caspases-8 and –9) and effector caspases (caspases-3 and –7) (Figs. 4.6 and 4.7), complete processing of intact PARP into an 85-kDa cleaved product (Figs. 4.4 and 4.5, panel B) and a high percentage of apoptotic cells (Figs. 4.4 and 4.5, panel A).

The complete blockage of TRAIL- and staurosporine-induced JIP-1 cleavage, and the inhibition of DNA fragmentation and PARP cleavage by 40μM DEVD.fmk (Figs. 4.8 and 4.9, panel B) suggested that caspase-3 was responsible for the apoptotic cleavage of JIP-1 *in vivo*. The fragmentation of genomic DNA during apoptosis is caused primarily by DNA fragmentation factor 45 (DFF-45), alternatively known as caspase-activated DNAse (CAD). DFF-45 is a part of a heterodimeric protein DFF that consists of 40-kDa and 45-kDa subunits (Liu *et. al.*, 1997). During apoptosis, caspase-3 cleaves this heterodimeric protein and releases the 45-kDa subunit that has the enzymatic activity required for DNA fragmentation (Liu *et. al.*, 1997). The activity of DFF-45/CAD is normally inhibited by a protein called ICAD (inhibitor of CAD); however during apoptosis caspase-3 also cleaves ICAD and removes its inhibitory effect on DFF-45/CAD (Sakahira, Enari & Nagata, 1998). Both DNA fragmentation and PARP cleavage are a result of caspase-3 activity (Tewari *et. al.* 1995; Liu *et. al.*, 1997; Tang & Kidd, 1998), and therefore the inhibition of DNA fragmentation and PARP cleavage by DEVD.fmk were indicative of the inhibition of caspase-3 activity.

A complete inhibition of PARP cleavage in the presence of 40μM DEVD.fmk was not observed (Figs. 4.8 and 4.9, panel B). A recent report suggests that caspase-7 can in part substitute for caspase-3 activity (Slee, Adrian & Martin, 2001). Therefore, the

partial cleavage of PARP observed in the presence of 40μM DEVD.fmk may have been due to caspase-7 activity.

4.3.4. Analysis of JIP-1b cleavage *in vitro*

A comparison of *in vitro* JIP-1b cleavage by caspase-3 and caspase-8 showed that caspase-3 cleaved JIP-1b efficiently at low concentrations, while caspase-8 cleaved JIP-1b inefficiently even at high concentrations (Fig. 4.11A and B). Incubation of JIP-1b with higher concentrations of caspase-8 yielded similar-sized products as that obtained with caspase-3 (Fig. 4.11A and B), suggesting that caspase-8 targeted the same cleavage sites as those preferred by caspase-3. Considering that the tetrapeptide sequence preferred by caspase-8 is (L/V)EXD and not DXXD (Thornberry *et. al.*, 1997), and that caspase-8 cleavage sites conforming to (L/V)EXD do not occur in the JIP-1 primary sequence at positions near the caspase-3 cleavage sites, this was a surprising finding. However, recent kinetic studies on the substrate specificities of different human caspases reveal that caspase-8 can tolerate an aspartic acid in the P_4 position, although it would cleave the substrate four-fold more efficiently if leucine was present in the P_4 position compared to aspartic acid (Stennicke *et. al.*, 2000). Furthermore, caspase-8 can tolerate serine or alanine in the P_1' position compared to the preferred choice of glycine (Stennicke *et. al.*, 2000). $LEVD^{516}/D$, thought to be a putative caspase-8 cleavage site in JIP-1b, thus would not have been targeted by caspase-8 *in vitro*, since the aspartic acid in the P_1' position is not tolerated by caspase-8 (Stennicke *et. al.*, 2000). Also, if $LEVD^{516}/D$ had been a caspase-8 target, a 90-kDa product resulting from this cleavage event (see the scheme in Fig. 4.3) would have appeared at low caspase-8 concentrations, which was not the case. *In vitro* analysis of the cleavage of JIP-1b caspase-3 cleavage-resistant mutants by caspase-8 might confirm whether caspase-8 targets caspase-3 cleavage sites.

The 55-kDa cleavage product was observed with JIP-1b (wild type), but not with the JIP-1b (D98A) mutant, upon the incubation with caspase-3 *in vitro* (Fig. 4.14). The 75-kDa cleavage product was not observed with JIP-1b (wild type), but was observed with the JIP-1b (D98A) mutant, upon the incubation with caspase-3 *in vitro* (Fig. 4.14). Taken together, these results suggested that caspase-3 cleaved the 75-kDa product at the Asp98 site to yield the 55-kDa product (see also Fig. 4.3).

4.3.5. A comparison of JIP-1 cleavage *in vivo* and *in vitro*

The 100-kDa JIP-1b cleavage product observed *in vitro* with caspase-3 (Figs. 4.11 and 4.12, panel A) correlated to the 100-kDa cleavage product observed in JIP-1 immunoblots using the monoclonal anti-JIP-1 antibody (Figs. 4.4 and 4.5, panel B). The 55-kDa and 45-kDa JIP-1b cleavage products observed *in vitro* were not detected *in vivo* in JIP-1 immunoblots. The JIP-1 epitope against which the monoclonal anti-JIP-1 antibody is raised is not published. Hence, a possible reason for these observations could be that the monoclonal anti-JIP-1 antibody may not cross-react with the 55-kDa and 45-kDa products. Therefore, a possible epitope site might be the region spanning the D405S cleavage site, since cleavage at this site would disrupt the epitope recognition by the antibody, resulting in a failure to detect the 45-kDa and 55-kDa JIP-1 cleavage fragments *in vivo*. Alternatively, it is possible that the monoclonal anti-JIP-1 antibody may cross react with the 45-kDa and 55-kDa products *in vivo*, but the level of these products may not be high enough to be detected by Western blotting.

A further comparison of JIP-1 cleavage *in vivo* and *in vitro* showed that, a complete loss of intact JIP-1b was observed *in vitro* with 10nM caspase-3 (Figs. 4.11 and 4.12, panel A), while *in vivo* the loss of intact JIP-1 was not observed (Figs. 4.4 and 4.5, panel B). Intact JIP-1 was not lost *in vivo* in HeLa cells treated with TRAIL or staurosporine for up to 12 hours (data not shown). There are several possible explanations to account for these observations. JIP-1 may be a poor caspase-3 substrate *in vivo* compared to *in vitro*. The *in vivo* concentration of active caspase-3 may not reach a concentration level of 10nM, in which case some full-length, uncleaved JIP-1 would persist. A pool of JIP-1 molecules *in vivo* may be compartmentalised such that they might be inaccessible to caspase-3 during apoptosis. JIP-1 may be in complex with other proteins *in vivo* due to which it may be inaccessible to caspase-3. Candidate proteins include JNK, MLK3, MKK7 and HPK1, kinases with which JIP-1 is known to interact (Whitmarsh *et. al.*, 1998).

4.3.6. JIP-1: A novel casapse-3 substrate

JIP-1 cleavage by caspase during apoptosis is interesting in two ways. The presence of two caspase-3 cleavage sites in a single substrate is rare, since almost all the substrates identified for caspase-3 to date contain only one cleavage site. One exception is DFF-45, which is cleaved by caspase-3 at two sites (Liu *et. al.*, 1997). A survey of the

published caspase-3 cleavage sites present in various substrates, especially amino acids in P_1', P_2 and P_3 positions (Talanian *et. al.*, 1997; Thornberry *et. al.*, 1997; Stennicke *et. al.*, 2000), leads to the conclusion that one of the cleavage site in JIP-1, $DLID^{405}/A$, is the first case in which amino acids in the P_1' (A), P_2 (I) and P_3 (L) positions have been identified. JIP-1 is therefore a novel caspase-3 substrate.

4.3.7. Functions of JIP-1 during apoptosis

Experimental evidence is accumulating showing that JIPs may have a pro-apoptotic and anti-apoptotic role during apoptosis. Overexpression of JIP-1 inhibits NGF withdrawal-induced JNK activation and apoptosis of PC-12 cells (Dickens *et. al.*, 1997). In neurogliomal cells N18TG, JIP-2a overexpression suppresses JNK activation and apoptosis induced by etoposide (Kim *et. al.*, 1999). Overexpression of JIP-1 prevents IL-1β-induced cell death of pancreatic cell line βTC3 as well as JNK activation, whereas decreasing the levels of endogenous JIP-1 using an antisense approach is associated with an increased apoptotic rate (Bonny *et. al.*, 2000). Overexpression of the JBD of JIP-1 also prevents JNK activation, c-Jun phosphorylation and apoptosis in sympathetic neurons (Eilers *et. al.*, 2001; Harding *et. al.*, 2001). Protection from apoptosis by overexpression of anti-apoptotic proteins such as Bcl-2 has been well characterised (e.g. Yin & Schmike, 1996; Bonnotte *et. al.*, 1998). *Jip-1*$^{-/-}$ null mice embryos die early, suggesting that JIP-1 is essential for survival (Thompson *et. al.*, 2001). Again, this is consistent with the phenotype observed with the disruption of other well-established anti-apoptotic proteins; e.g. targeted disruption of the p65 subunit of NFκB results in the death of embryos around day 14.5 due to massive apoptosis of hepatocytes (Beg & Baltimore, 1996). Middle cerebral artery occlusion *in vivo* in rat results in the activation of JNK after 8h, followed by the induction of the expression of JIP-1 after 24h, which, the authors suggest, may be a possible attempt by the cells to avoid cell death (Hayashi *et. al.*, 2000). JIP-1 and JIP-3 are induced by nerve growth factor (NGF) in PC12 cells (Meyer, Liu & Margolis, 1999; Kelkar *et. al.*, 2000), and JIP-1 is induced by an activated form of Akt, a protein involved in cell survival (Levresse *et. al.*, 2000), suggesting that one of the mechanisms employed by pathways that regulate cell survival is the up-regulation of JIP proteins. Since proteins that signal cell survival, such as Raf-1, Akt, Cbl and Ras are cleaved during apoptosis

(Widmann, Gibson & Johnson, 1998), the cleavage of JIP-1 (this study) suggests that it may have a survival function during apoptosis.

A recent study on *Jip-1*$^{-/-}$ knock-out mice shows that JIP-1 deficiency protects hippocampal neurons from kainate-induced apoptosis (Whitmarsh *et. al.*, 2001), a phenotype which is also observed in JNK3-deficient mice (Yang *et. al.*, 1997b) or c-Jun phosphorylation-deficient mice (Behrens, Sibilia & Wagner, 1999) in response to kainate. Furthermore, JIP-1-deficient mice showed reduced JNK activation and were also resistant to the apoptotic effects of oxygen-glucose deprivation (Whitmarsh *et. al.*, 2001). These data indicate that JIP-1 is essential for stress-induced JNK activation and apoptosis.

The above observations lead to the conclusion that JIP-1 may play different roles during apoptosis, depending on the cell type. This is further supported by differences in JIP-1 subcellular localisation in different cells. JIP-1 has been reported to be located in the cytoplasm of Chinese hamster ovary cells (Dickens *et. al.*, 1997), COS7 cells (Whitmarsh *et. al.*, 1998), Rin5F cells (Yasuda et. al., 1999) N1E-115 cells (Meyer *et. al.*, 1999) and primary cortical neurons (Whitmarsh *et. al.*, 2001), while JIP-1 was shown to be a nuclear protein in cerebellar granule cells (Coffey *et. al.*, 2000) and βTC3 cells (Bonny et. al., 1998). During stress-induced apoptosis, endogenous JIP-1 was shown to be pro-apoptotic in cortical neurons (Whitmarsh *et. al.*, 2001), while in βTC3 cells endogenous JIP-1 was shown to have a protective function (Bonny *et. al.*, 2000). Thus, it seems that nuclear JIP-1 may have an anti-apoptotic function while cytoplasmic JIP-1 may have a pro-apoptotic role. Since JIP-1 is required for JNK signalling (Whitmarsh *et. al.*, 1998; Yasuda *et. al.*, 1999; Kelkar *et. al.*, 2000; Whitmarsh *et. al.*, 2001), the pro- or the anti-apoptotic role of JIP-1 may depend on the pro- or the anti-apoptotic role of JNK during apoptosis.

4.3.8. JIP-1 cleavage and its implications for JNK signalling during apoptosis

4.3.8.1. Conservation of caspase-3 cleavage sites in JIP isoforms

Caspase-3 cleavage sites DLID^{98}/A and DESD^{405}/S are conserved in human, mouse and rat JIP-1 isoforms, and in mouse and rat JIP-2 isoforms. JIP-3 has been shown to be cleaved at DVQD^{344}/I by caspase-3 during apoptosis (Kelkar *et. al.*, 2000). Human JIP-2 contains several putative caspase-3 cleavage sites that conform to the

consensus DXXD: $DSED^{258}/A$, $DAED^{484}/S$ and $DSPD^{569}/L$. Therefore it is likely that human JIP-2 may also be a caspase-3 substrate. Thus, caspase-3-mediated cleavage of JIP proteins during apoptosis may be evolutionary conserved.

4.3.8.2. A functional JIP scaffold may not form due to the cleavage of JIP proteins during apoptosis

JIP-1, JIP-2 and JIP-3 are proposed to act as scaffold proteins for the JNK pathway by binding to MKK7, MLK3 and JNK (Whitmarsh *et. al.*, 1998; Yasuda *et. al.*, 1999; Kelkar *et. al.*, 2000). In JIP-1 and JIP-2, JNK binds to the JBD, while MKK7 and MLK proteins bind to a region downstream of the JBD that covers the SH3 and PTB domains (Whitmarsh *et. al.*, 1998; Yasuda *et. al.*, 1999). An examination of the position of the caspase-3 cleavage sites in JIP-1 and JIP-2 suggests that, during apoptosis, caspase-3-mediated cleavage of JIP-1, and possibly JIP-2, would result in the separation of JBD from the SH3 and PTB domains (Fig. 4.15), and therefore the formation of a functional JIP-1 or JIP-2 scaffold containing JNK, MKK7 and MLK may not be possible. The caspase-3 cleavage site in JIP-3 lies downstream of the JBD of JIP-3 (Kelkar *et. al.*, 2000; Fig. 4.15). MKK7 binds to JIP-3 in a region downstream of the JBD, and MLK3 binds to the N-terminus of JIP-3 in a region that lies upstream and downstream of the JBD (Kelkar *et. al.*, 2000). Therefore, JIP-3 cleavage by caspase-3 during apoptosis would separate the JBD from the MKK7-binding region, and may result in a failure of the formation of a functional JIP-3 scaffold containing JNK, MKK7 and MLK3. Thus, a consequence of caspase-3-mediated cleavage of JIP proteins may be that a functional JIP scaffold might not be able to assemble, which could result in a failure to activate JNK.

Taken together, this suggests that caspase-3 mediated cleavage of JIP-1 and JIP-3, and possibly JIP-2, during apoptosis may be a general outcome that may serve to attenuate JNK signalling.

JNK, JIP-1 and MKK4/MKK7 knockout experiments support the idea that JNK signalling is required for stress-induced apoptosis (Tournier *et. al.*, 2000; Tournier *et. al.*, 2001; Whitmarsh *et. al.*, 2001), and ASK1 and RelA knockout experiments suggest that persistent JNK activity is essential for TNF-α-induced apoptosis (De Smaele *et. al.*, 2001; Tang *et. al.*, 2001; Tobiume *et. al.*, 2001). However, JNK activation during apoptosis has been proposed to act as a survival signal under certain circumstances (see section 1.7.5, Chapter 1). Whether JNK promotes cell death, or plays a role in survival

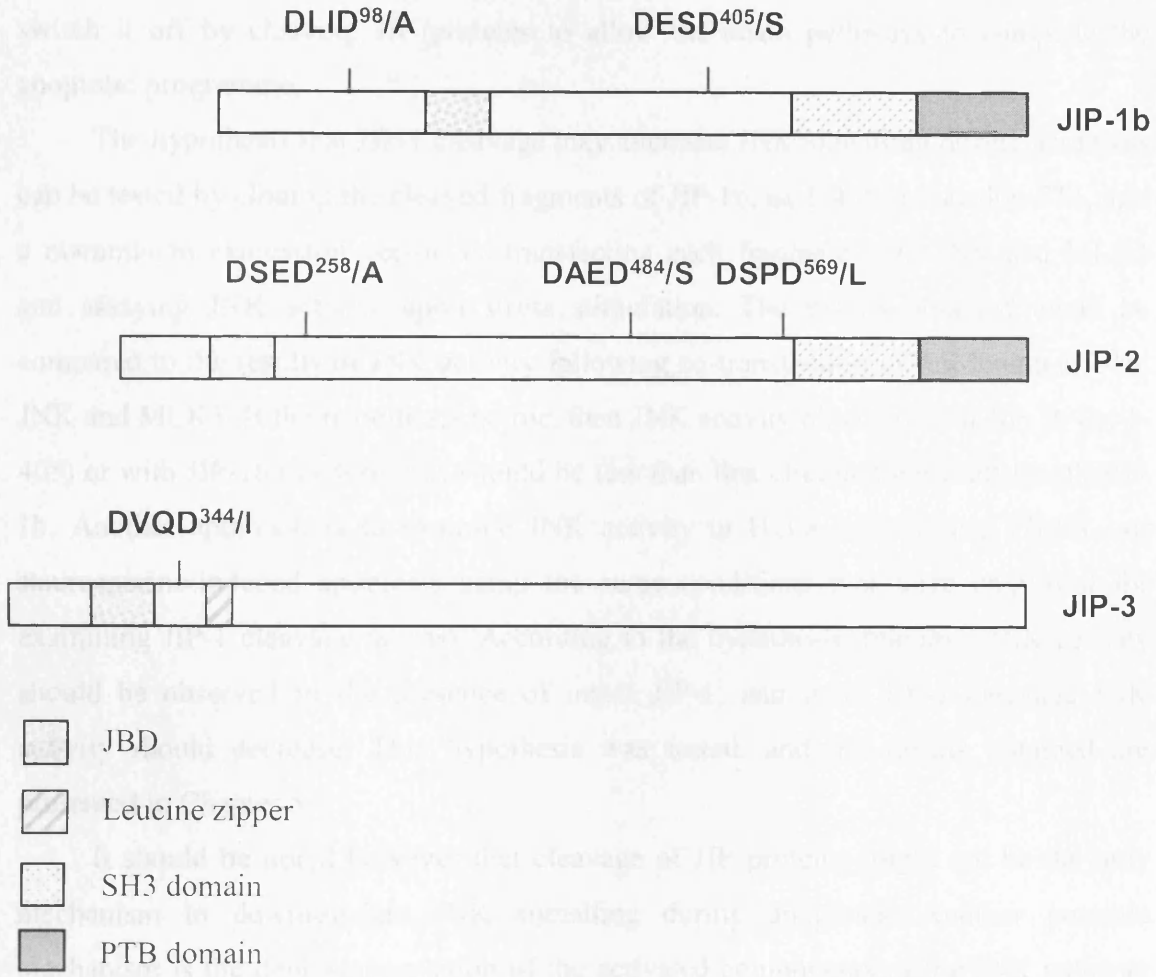

Fig. 4.15. Position of caspase-3 cleavage sites in JIP-1, JIP-2 and JIP-3 in relation to the domain positions.

JBD = JNK binding domain; SH3 = Src homology 3; PTB = phosphotyrosine binding.

signalling during apoptosis, JIP cleavage during apoptosis may attenuate JNK signalling. This would be a logical recourse for the cell irrespective of the role of JNK signalling during apoptosis. If JNK signalling contributes towards apoptosis, the activity of the pathway would not be required once it has played its role in promoting apoptosis and therefore JIP cleavage may serve to switch off the JNK pathway. If the activation of the JNK pathway acts as a survival signal during apoptosis, it would be appropriate to switch it off by cleaving JIP proteins to allow the death pathways to complete the apoptotic programme.

The hypothesis that JIP-1 cleavage may attenuate JNK signalling during apoptosis can be tested by cloning the cleaved fragments of JIP-1b, aa 1-405 and aa 406-714, into a mammalian expression vector, co-transfecting each fragment with JNK and MLK3 and assaying JNK activity upon stress stimulation. The results obtained could be compared to the results of JNK activity following co-transfection of full-length JIP-1b, JNK and MLK3. If the hypothesis is true, then JNK activity obtained with JIP-1b (aa 1-405) or with JIP-1b (aa 406-714) should be less than that obtained with full-length JIP-1b. Another approach is to examine JNK activity in HeLa cells during TRAIL- or staurosporine-induced apoptosis using the same conditions that were employed for examining JIP-1 cleavage *in vivo*. According to the hypothesis, maximal JNK activity should be observed in the presence of intact JIP-1, and upon JIP-1 cleavage JNK activity should decrease. This hypothesis was tested, and the results obtained are presented in Chapter 5.

It should be noted however that cleavage of JIP proteins might not be the only mechanism to downregulate JNK signalling during apoptosis. Another possible mechanism is the dephosphorylation of the activated components of the JNK pathway by phosphatases. If phosphatases do play a role in switching off JNK activity, cleavage of JIP proteins may ensure that the JNK pathway is not re-activated during apoptosis.

CHAPTER 5

CORRELATION BETWEEN JNK ACTIVITY AND JIP-1 CLEAVAGE DURING APOPTOSIS

5.1. INTRODUCTION

Apoptotic signalling is initiated through receptor- and mitochondrial cytochrome c-mediated pathways (sections 1.6.3 and 1.6.4). Analysis of JNK activity during apoptosis in different cell types suggests that it contributes to both types of death pathways (section 1.7).

Examples of ligands other than TRAIL that cause apoptosis through the receptor-mediated pathway are Fas and TNF-α. JNK activation has been detected in cells undergoing TNF-α-induced apoptosis. For example, sustained JNK activity correlates with TNF-α-induced apoptosis of rat mesangial cells (Guo *et. al.*, 1998). Gene disruption studies have shown that persistent JNK activity is required for TNF-α-induced receptor-mediated apoptosis. *Ask1*$^{-/-}$ MEFs were shown to be resistant to apoptosis induced by TNF-α because of a failure to activate JNK (Tobiume *et. al.*, 2001). A comparison of TNF-α-induced apoptosis in wild type and *RelA*$^{-/-}$ MEFs showed that JNK activity was required for apoptosis signalling by TNF-α (De Smaele *et. al.*, 2001; Tang *et. al.*, 2001).

JNK activation also correlates with Fas-induced apoptosis, for example in SHEP neuroblastoma and Jurkat T cells (Goillot *et. al.*, 1997; Lenczowski *et. al.*, 1997). However, the role of JNK in Fas-mediated apoptosis is not clear. For example, Fas-mediated JNK activation and apoptosis is inhibited by the expression of a non-activatable JNK mutant, suggesting that JNK is necessary for Fas-mediated killing (Goillot *et. al.*, 1997). However, the apoptotic response of both the wild type and the *Jnk1*$^{-/-}$*Jnk2*$^{-/-}$ MEFs in response to the activation of the Fas death signalling pathway was normal, suggesting that JNK is not required for Fas-mediated apoptosis (Tournier *et. al.*, 2000). Although JNK may not be required for Fas-mediated death receptor signalling, there is evidence to suggest that JNK upregulates FasL expression and thus contributes to Fas-mediated apoptosis (Kasibhatla *et. al.*, 1998; Kolbus *et. al.*, 2000). This has been proposed to result in the slow killing of some cells by Fas (Davis, 2000).

JIP-1 is a caspase-3 substrate that is cleaved during receptor- and chemical-induced apoptosis in HeLa cells (Chapter 4). JIP-1 has been suggested as a putative scaffold protein that organises the MLK-MKK7-JNK module (Whitmarsh *et. al.*, 1998). JIP-1 cleavage may therefore result in the disassembly of the module and consequently cause a decrease in JNK signalling during apoptosis. To address this possibility, a correlation between JIP-1 cleavage and JNK activity during apoptosis induced by death

ligands (TRAIL, TNF-α and Fas) and chemicals (staurosporine, anisomycin and H_2O_2) in HeLa cells was examined. To further correlate the relationship between JIP-1 cleavage and JNK activity, the interaction of JIP-1 with JNK during TRAIL-induced apoptosis was also examined.

5.2. RESULTS

5.2.1. JNK activity during TRAIL- and staurosporine-induced apoptosis

To test the hypothesis that JIP-1 cleavage would result in a decrease in JNK activity during receptor- and chemical-induced apoptosis, extracts from HeLa cells treated with TRAIL or staurosporine for 0, 1, 2, 4 and 8h (the same time course as used for investigating JIP-1 cleavage) were prepared and analysed for JNK activity. The JNK activity data was compared with the time course of JIP-1 cleavage. Since DEVD.fmk was shown to inhibit JIP-1 cleavage (Figs. 4.8 and 4.9, Chapter 4), JNK activity in HeLa cells pre-treated with DEVD.fmk followed by TRAIL or staurosporine treatment was also examined. Control cells were treated with DEVD.fmk only or left untreated. The levels of JNK1 protein were determined by Western blotting.

5.2.1.1. JNK activity during TRAIL-induced apoptosis

In untreated (control) cells, JNK activity remained at the basal level (Fig. 5.1A). In cells treated with TRAIL only, maximal JNK activity (4.2 ± 0.8 fold) was detected at 2h compared to the basal activity (Fig. 5.1A). The activity dropped to 3.5 ± 0.7 fold at 4h. JNK activity was lower at 8h (1.6 ± 0.2) compared to the activity at 4h. These results indicated a correlative relationship between JIP-1 cleavage and JNK activity. JNK activity was maximal at 2h following TRAIL treatment, and at this time point JIP-1 cleavage was not observed (Fig. 4.4B). JNK activity decreased at 4h following TRAIL treatment, and this correlated with JIP-1 cleavage. The correlation between JIP-1 cleavage and low JNK activity was maintained at 8h following TRAIL treatment (Figs. 5.1A and 4.4B).

DEVD.fmk in the absence of TRAIL treatment did not have any effect on JNK activity (Fig. 5.1A). A comparison of JNK activity in TRAIL-treated HeLa cells pre-incubated with DEVD.fmk with the activity data obtained with TRAIL-only treatment showed that, the activity remained high in DEVD.fmk pre-treated cells compared to

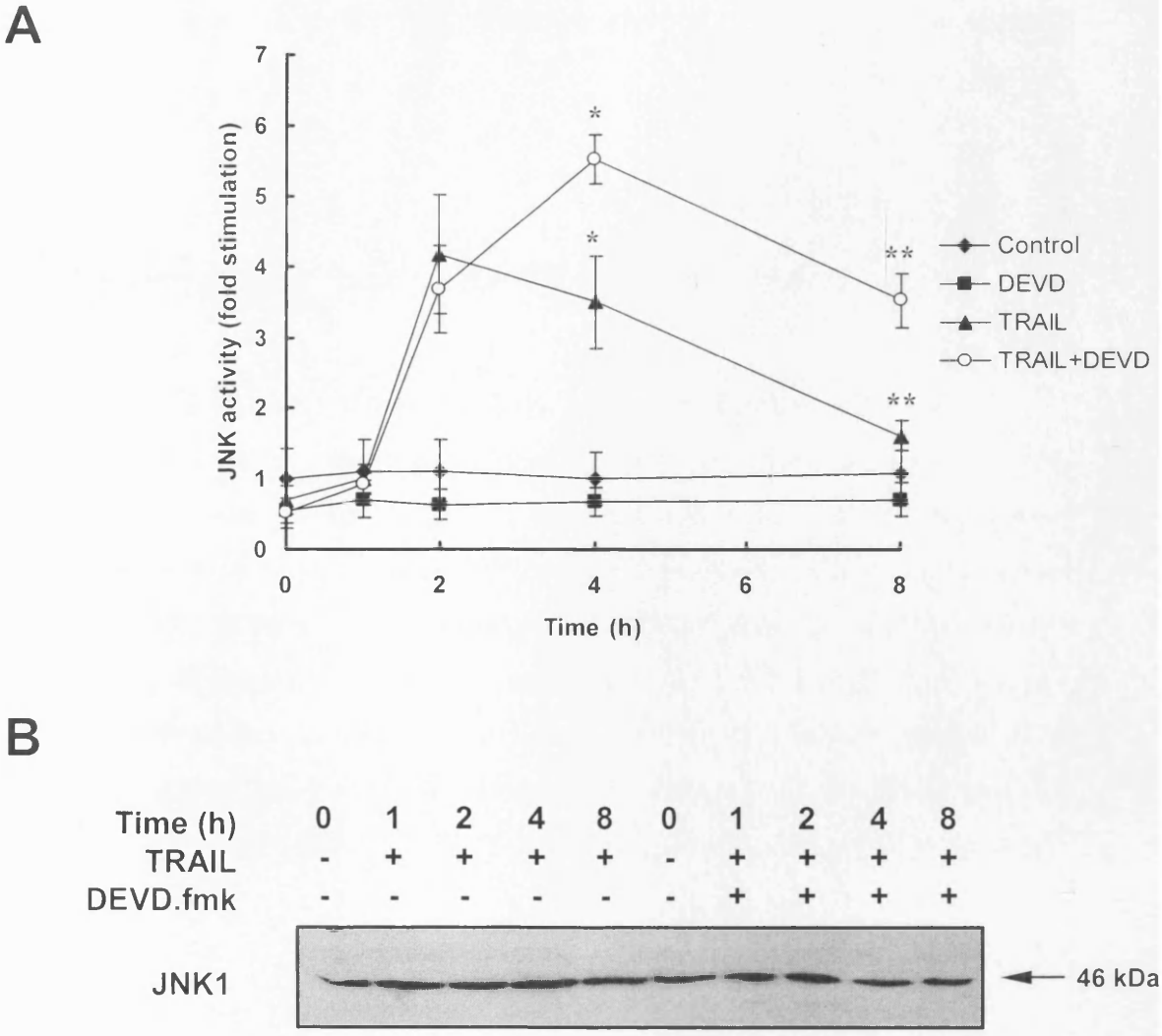

Fig. 5.1. JNK activity during TRAIL- induced apoptosis.

(A) Cells were treated with TRAIL (1μg/ml) in the presence or absence of DEVD.fm (40μM), left untreated or treated with DEVD.fmk only for the times indicated. JNK w immunoprecipitated and its activity was measured using an immune complex kinase assa with GST-c-Jun as a substrate and quantified by PhosphorImager analysis as described Materials & Methods (section 2.2.3.6). The results shown are mean ± S.E.M. of fo independent experiments. Data points marked by asterisks indicate $p<0.05$. **(B)** Extrac (200μg) from the experiment in A were immunoblotted for JNK1 using monoclonal JNK antibody (Pharmingen) at 1:1000 dilution.

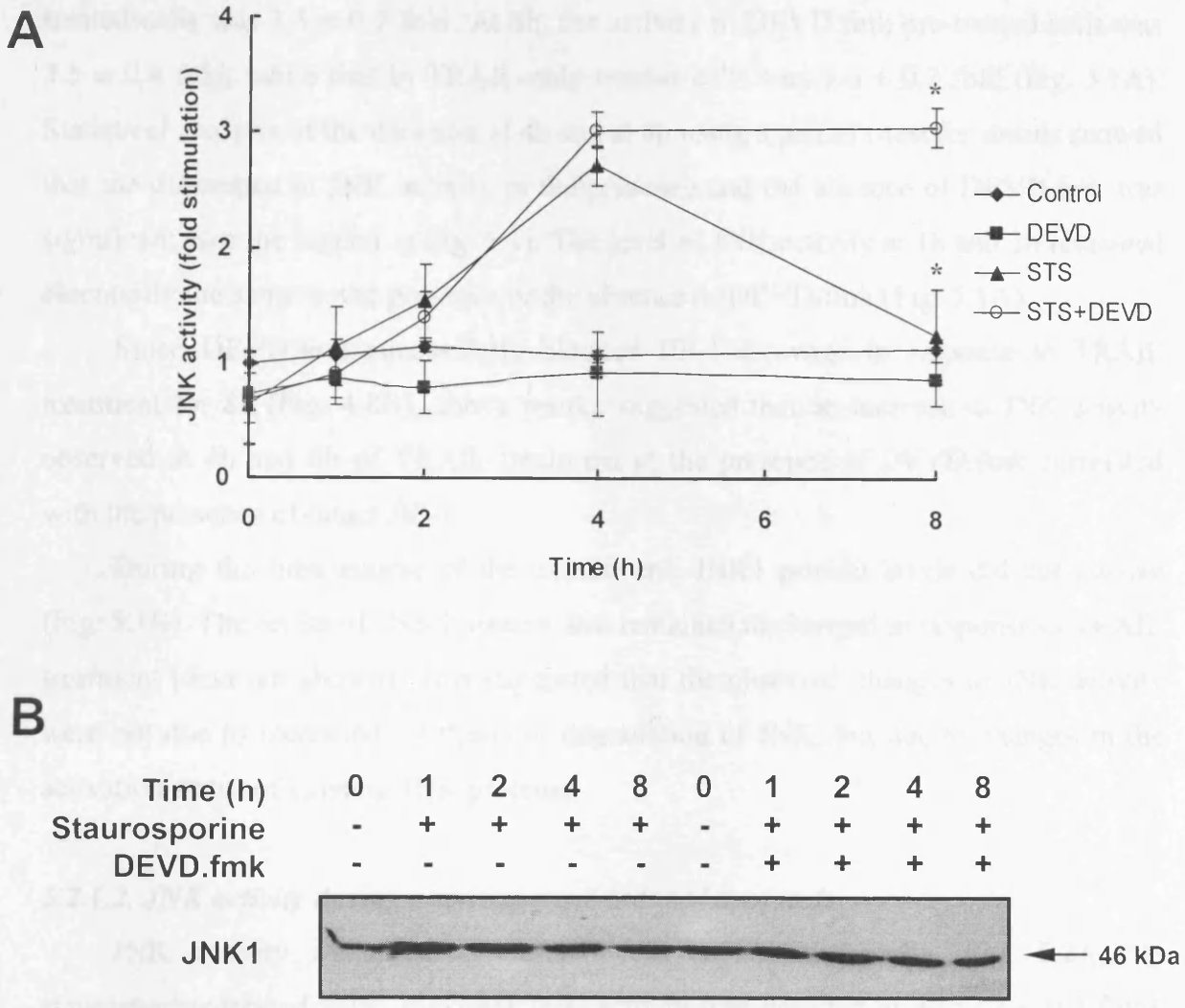

Fig. 5.2. JNK activity during staurosporine-induced apoptosis.

(A) HeLa cells were treated with staurosporine (1μM) in the presence or absence of DEVD.fmk (40μM), left untreated or treated with DEVD.fmk only for the times indicated. JNK activity was assayed from equivalent amounts of lysates as described in Fig. 5.1. The results shown are mean ± S.E.M. of four independent experiments. Data points marked by asterisks indicate $p<0.05$. **(B)** Extracts (200μg) from the experiment in A were immunoblotted for JNK1 as described in Fig. 5.1.

TRAIL-only treated cells at 4h and 8h (Fig. 5.1A). At 4h, JNK activity in HeLa cells pre-treated with DEVD.fmk was 5.5 ± 0.3 fold, whereas the activity in TRAIL-only treated cells was 3.5 ± 0.7 fold. At 8h, the activity in DEVD.fmk pre-treated cells was 3.5 ± 0.4 fold, while that in TRAIL-only treated cells was 1.6 ± 0.2 fold (Fig. 5.1A). Statistical analysis of the data sets at 4h and at 8h using a paired t-test for means showed that the difference in JNK activity in the presence and the absence of DEVD.fmk was significant (see the legend in Fig. 5.1). The level of JNK activity at 1h and 2h remained essentially the same in the presence or the absence of DEVD.fmk (Fig. 5.1A).

Since DEVD.fmk successfully blocked JIP-1 cleavage in response to TRAIL treatment for 8h (Fig. 4.8B), above results suggested that an increase in JNK activity observed at 4h and 8h of TRAIL treatment in the presence of DEVD.fmk correlated with the presence of intact JIP-1.

During the time course of the experiment, JNK1 protein levels did not change (Fig. 5.1B). The levels of JNK2 protein also remained unchanged in response to TRAIL treatment (data not shown). This suggested that the observed changes in JNK activity were not due to increased synthesis or degradation of JNK, but due to changes in the activation status of existing JNK proteins.

5.2.1.2. JNK activity during staurosporine-induced apoptosis

JNK activity remained at basal levels in untreated cells (Fig. 5.2A). In staurosporine-treated cells, maximal JNK activity was detected at 4h (2.7 ± 0.2 fold). JNK activity observed at 8h was 1.2 ± 0.4 fold. A similar correlation between JNK1 activity and JIP-1 cleavage, which was observed during TRAIL-induced apoptosis, was also apparent during staurosporine-induced apoptosis. JNK activity in staurosporine-treated HeLa cells was maximal at 4h (Fig. 5.2A), and JIP-1 was intact at this time point (Fig. 4.5B). The activity decreased at 8h, and JIP-1 was cleaved at this time point (Figs. 5.2A and 4.5B).

In cells treated with DEVD.fmk only, JNK activity did not increase above basal levels (Fig. 5.2A), suggesting that DEVD.fmk on its own did not have any effect on JNK activity. In HeLa cells treated with staurosporine in the presence of DEVD.fmk, maximal JNK activity was observed at 4h (3.0 ± 0.2 fold) and 8h (3.1 ± 0.2 fold) (Fig. 5.2A). Statistical analysis using a paired t-test for means showed that the difference in JNK activity at 8h in the presence or the absence of DEVD.fmk was significant (see the legend in Fig. 5.2). This again suggested a correlative relationship between JIP-1

cleavage and JNK activity. Pre-treatment of DEVD.fmk inhibited JIP-1 cleavage at 8h following staurosporine treatment (Fig. 4.9B), and this correlated with a significant increase in JNK activity (Fig. 5.2A). JIP-1 was intact at 4h following staurosporine treatment (Fig. 4.5B), and the presence of DEVD.fmk did not alter JNK activity significantly at this time point (Fig. 5.2A).

JNK1 protein levels remained unaltered in staurosporine-treated cells in the presence or the absence of DEVD.fmk (Fig. 5.2B). JNK2 protein levels also did not change in response to staurosporine treatment (data not shown). This suggested that the observed changes in JNK activity were not due to *de novo* synthesis or degradation of JNK but due to the changes in the activation status of existing JNK proteins.

The above results showed that, during TRAIL- and staurosporine-induced apoptosis in the presence or the absence of DEVD.fmk, maximal JNK activity correlated with the presence of intact JIP-1 and a decrease in JNK activity correlated with JIP-1 cleavage. In addition, the presence of DEVD.fmk significantly increased TRAIL- or staurosporine-induced JNK activity, which was coincident with the inhibition of JIP-1 cleavage.

5.2.2. A correlation between JIP-1 cleavage and JNK activity in response to other apoptotic stimuli

Genetic and biochemical evidence suggests that persistent JNK activity is required for receptor- and stress-induced apoptosis (see section 5.1). During TRAIL- and staurosporine-induced apoptosis of HeLa cells, we observed differential activation of the initiator and effector caspases and differential effects on JIP-1 cleavage (sections 4.2.1.3 and 4.2.1.4, Chapter 4), and a correlation between the status of JIP-1 (intact or cleaved) and JNK activity (section 5.2.1). Therefore the correlation between the status of JIP-1 (intact or cleaved) and JNK activity during apoptosis induced by other stimuli was examined to ascertain whether it is a general phenomenon or specific to TRAIL and staurosporine.

5.2.2.1. JIP-1 cleavage in response to other stimuli

HeLa cells were treated with stimuli that could induce apoptosis via the receptor- or the mitochondrial cytochrome c-mediated pathway in HeLa cells, and their effect on JIP-1 cleavage was tested.

To induce apoptosis through the receptor-mediated pathway, HeLa cells were treated with TNF-α and agonistic Fas antibody, since HeLa cells express TNF-R1 (Engelmann *et. al.*, 1990; Thoma *et. al.*, 1990; Hsu *et. al.*, 1996) and the Fas receptor (Yang *et. al.*, 1997). TNF-α was used in combination with cycloheximide (CHX), since CHX inhibits the activation of the anti-apoptotic NF-κB pathway (Miura, Friedlander & Yuan, 1995; Lin *et. al.*, 1999; Wajant *et. al.*, 2000). The agonistic Fas antibody was used in combination with serum starvation and the MKK1 inhibitor PD98059, as serum starvation/PD98059 treatment inhibits the ERK pathway (Holmstrom *et. al.*, 2000). To induce apoptosis through the receptor-mediated pathway, HeLa cells were treated with MG132, anisomycin, sodium arsenite, ethanol, H_2O_2 and glucose. These stimuli were chosen because they induce apoptosis as well as JNK activation (Gabai *et. al.*, 1997; Meriin *et. al.*, 1998; Wang *et. al.*, 1998; Ho *et. al.*, 2000; Hossain *et. al.*, 2000; Namgung & Xia, 2000).).

HeLa cells were treated with varying concentrations of the above stimuli, and apoptotic cells were quantified by DNA fragmentation assay using Hoechst 33258 staining. The concentration of each stimulus that yielded ~50% apoptosis was determined. The results obtained are shown in Fig. 5.3. The concentration of the apoptotic stimulus that yielded ~50% apoptosis is denoted by an asterisk (*) in Fig. 5.3, and is shown in Table 5.1.

At 50% apoptosis, JIP-1 cleavage was observed during TRAIL-induced apoptosis of HeLa cells (Fig. 4.4A and B), but not during staurosporine-induced apoptosis (Fig. 4.5A and B). Therefore to determine the effect of 50% apoptosis on JIP-1 cleavage, HeLa cells were treated with stimuli using the conditions mentioned in Table 5.1, and the extracts were blotted for JIP-1, PARP and α-tubulin.

1. JIP-1 cleavage during receptor-mediated apoptosis

During receptor-mediated apoptosis, JIP-1 cleavage was detected in response to a combination of TNF-α/CHX treatment, but not in response to agonistic Fas antibody/PD98059 treatment (Fig. 5.4A). JIP-1 cleavage was not detected in cells treated with CHX, TNF-α, Fas, PD98059, or in control cells.

A study of PARP cleavage showed that, intact PARP was completely processed to 85-kDa cleavage product in response to TNF-α/CHX and Fas//PD98059 (Fig. 5.4A), suggesting that caspase-3 was active. PARP cleavage was not observed in cells treated

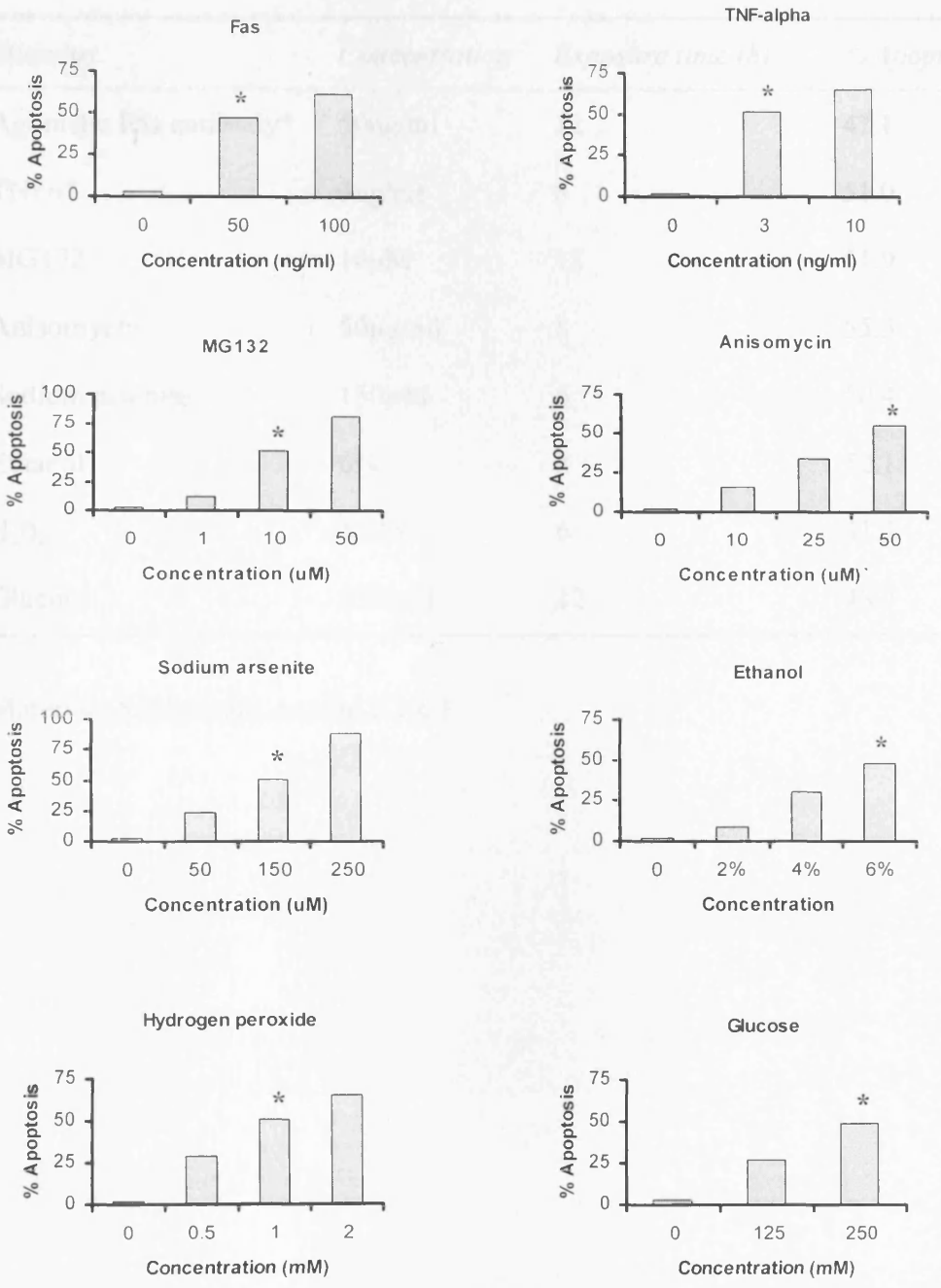

Fig. 5.3. The effect apoptotic stimuli on % apoptosis in HeLa cells.

HeLa cells were treated with the indicated concentrations of sodium arsenite or H_2O_2 for 6h; anisomycin, ethanol or TNF-α (in combination with 10μg/ml CHX) for 8h; MG132, glucose or agonistic Fas antibody (in combination with serum starvation and 30μM PD98059) for 12h. Apoptotic cells were quantified by DNA fragmentation assay using Hoechst 33258 staining. The concentration of a given stimulus that yielded ~50% apoptosis is marked with an asterisk. The data shown are a mean of duplicate experiments.

Table 5.1. Percentage apoptosis of HeLa cells in response to different stimuli

Stimulus	*Concentration*	*Exposure time (h)*	*% Apoptosis*
Agonistic Fas antibody*	50ng/ml	12	47.1
TNFα*	3ng/ml	8	51.0
MG132	10μM	12	51.9
Anisomycin	50μg/ml	8	55.3
Sodium arsenite	150μM	6	50.4
Ethanol	6%	8	52.1
H_2O_2	1mM	6	51.2
Glucose	250mM	12	48.7

* see Materials & Methods, section 2.2.6.1.

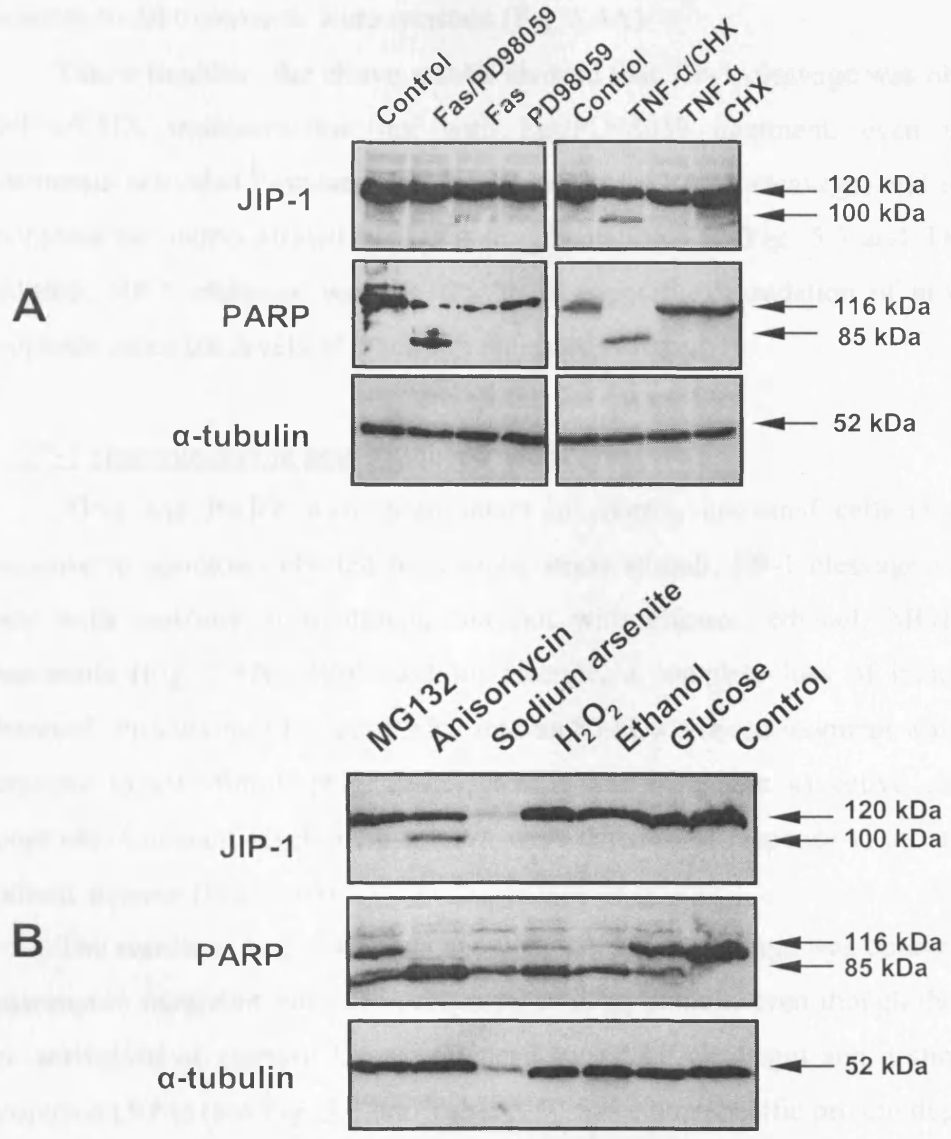

Fig. 5.4. Effect of various apoptotic stimuli on JIP-1 cleavage during HeLa cell apoptosis.

(A) HeLa cells were either left untreated or treated with serum starvation/PD98059 (30μM), serum starvation/Fas(50ng/ml) or Fas(50ng/ml)/PD98059(30μM)/serum starvation for 12h; or with CHX (10μg/ml), TNF-α (3ng/ml), or CHX(10μg/ml)/TNF-α(3ng/ml) for 8h. Equivalent amounts of extracts (200μg) were immunoblotted for JIP-1, PARP and α-tubulin as described in Fig. 4.3. **(B)** HeLa cells were left untreated or treated with sodium arsenite (150μM) and H_2O_2 (1mM) for 6h; anisomycin (25μg/ml) and ethanol (4%) for 8h; and MG132 (10μM) and glucose (250mM) for 12h. Equivalent amount of extracts (200μg) were immunoblotted for JIP-1, PARP and α-tubulin as described in Fig. 4.3.

with CHX, TNF-α, Fas, PD98059, and in control cells. The levels of α-tubulin in response to all treatments were constant (Fig. 5.4A).

Taken together, the above results showed that JIP-1 cleavage was observed with TNF-α/CHX treatment but not with Fas/PD98059 treatment, even though both treatments activated caspase-3 (as demonstrated by PARP cleavage) and induced 50% apoptosis (as demonstrated by DNA fragmentation; see Fig. 5.3 and Table 5.1). In addition, JIP-1 cleavage was not due to non-specific degradation of proteins during apoptosis since the levels of α-tubulin remained constant.

2. JIP-1 cleavage during stress-induced apoptosis

JIP-1 and PARP were both intact in control, untreated cells (Fig. 5.4B). In response to apoptosis elicited by various stress stimuli, JIP-1 cleavage was observed only with anisomycin treatment, but not with glucose, ethanol, MG132 or H_2O_2 treatments (Fig. 5.4B). With sodium arsenite, a complete loss of intact JIP-1 was observed. Processing of intact PARP into an 85-kDa cleaved fragment was observed in response to all stimuli (Fig. 5.4B), which was indicative of active caspase-3 and apoptosis. Constant levels of α-tubulin were detected in response to all stimuli except sodium arsenite (Fig. 5.4B).

The results in Fig. 5.4B thus showed that, JIP-1 cleavage was observed only with anisomycin treatment but not in response to other stimuli, even though they all caused the activation of caspase-3 (as evidenced by PARP cleavage) and a similar level of apoptosis (50%) (see Fig. 5.3 and Table 5.1). Since non-specific protein degradation is a feature of necrosis (Fiers *et. al.*, 1999), the loss of JIP-1 and α-tubulin observed with sodium arsenite treatment might have been due to necrosis.

Thus, apoptotic stimuli that cause ~50% apoptosis can be grouped into two categories: one, in which JIP-1 cleavage is observed (TNF-α and anisomycin), and two, in which JIP-1 is not cleaved (Fas, H_2O_2, ethanol and MG132). To correlate JIP-1 cleavage and JNK activation during apoptosis, we examined a time course of JIP-1 cleavage and JNK activation during apoptosis induced by TNF-α, anisomycin, Fas and H_2O_2.

5.2.2.2. JNK activation and JIP-1 cleavage in response to other stimuli

Based on the results obtained with TRAIL and staurosporine (section 5.2.1), it was postulated that the presence of intact JIP-1 would correlate with maximal JNK

activation, and JIP-1 cleavage would correlate with a decrease in JNK activity during apoptosis induced by TNF-α, Fas, H_2O_2 and anisomycin. In addition, JIP-1 cleavage would be blocked in the presence of DEVD.fmk, and this would enhance JNK activation. To confirm this, JIP-1 cleavage and JNK activation in the presence and the absence of DEVD.fmk during TNF-α-, Fas-, H_2O_2- and anisomycin-induced apoptosis were examined. PARP cleavage and DNA fragmentation analysis, the hallmarks of apoptosis, were assessed at each time point during apoptosis induced by each stimulus. Also, the levels of JNK1 were examined by western blotting.

1. Time course of JIP-1 cleavage

TNF-α, Fas, anisomycin and H_2O_2 treatments of HeLa cells led to an increase in the percentage of cells undergoing apoptosis, and intact PARP (116-kDa) was progressively cleaved into an 85-kDa fragment (Figs. 5.5-5.8, panels A and B). Furthermore, DEVD.fmk inhibited both DNA fragmentation and PARP cleavage, and the levels of α-tubulin remained the same during the time course of the assay in all cases. Taken together, these results suggested that each of the four stimuli tested elicited an apoptotic response in HeLa cells.

During TNF-α- and anisomycin-induced apoptosis, a 100-kDa JIP-1 cleavage fragment was observed at 8h and 12h, the formation of which was inhibited in the presence of DEVD.fmk (Figs. 5.5B and 5.6B.). JIP-1 cleavage was not observed in response to Fas- and H_2O_2-induced apoptosis (Figs. 5.7B and 5.8B).

2. JNK activity during TNF-α- and anisomycin-induced apoptosis

A time course analysis of JNK activity during TNF-α-induced apoptosis showed that, compared to the basal level, JNK activity was 8.8 ± 2.1 fold at 2h and reached a maximum of 15.0 ± 0.0 fold at 4h. This correlated with the presence of intact JIP-1 at these time points (Fig. 5.5B). JNK activity decreased to 12.0 ± 1.3 fold at 8h, and at 12h it declined to 8.7 ± 0.6 fold. Thus JNK activity exhibited a gradual decrease at 8h and 12h, and this correlated with the appearance of the 100-kDa JIP-1 cleavage fragment at these time points (Fig. 5.5B). However, TNF-α-induced JNK activity in cells pre-treated with DEVD.fmk was 22 ± 3.0 fold (Fig. 5.5C), which coincided with the inhibition of JIP-1 cleavage (Fig. 5.5B). The levels of JNK1 protein remained unaltered throughout the time course of the assay (Fig. 5.5B). The JNK2 protein levels also did not change upon TNF-α treatment (data not shown).

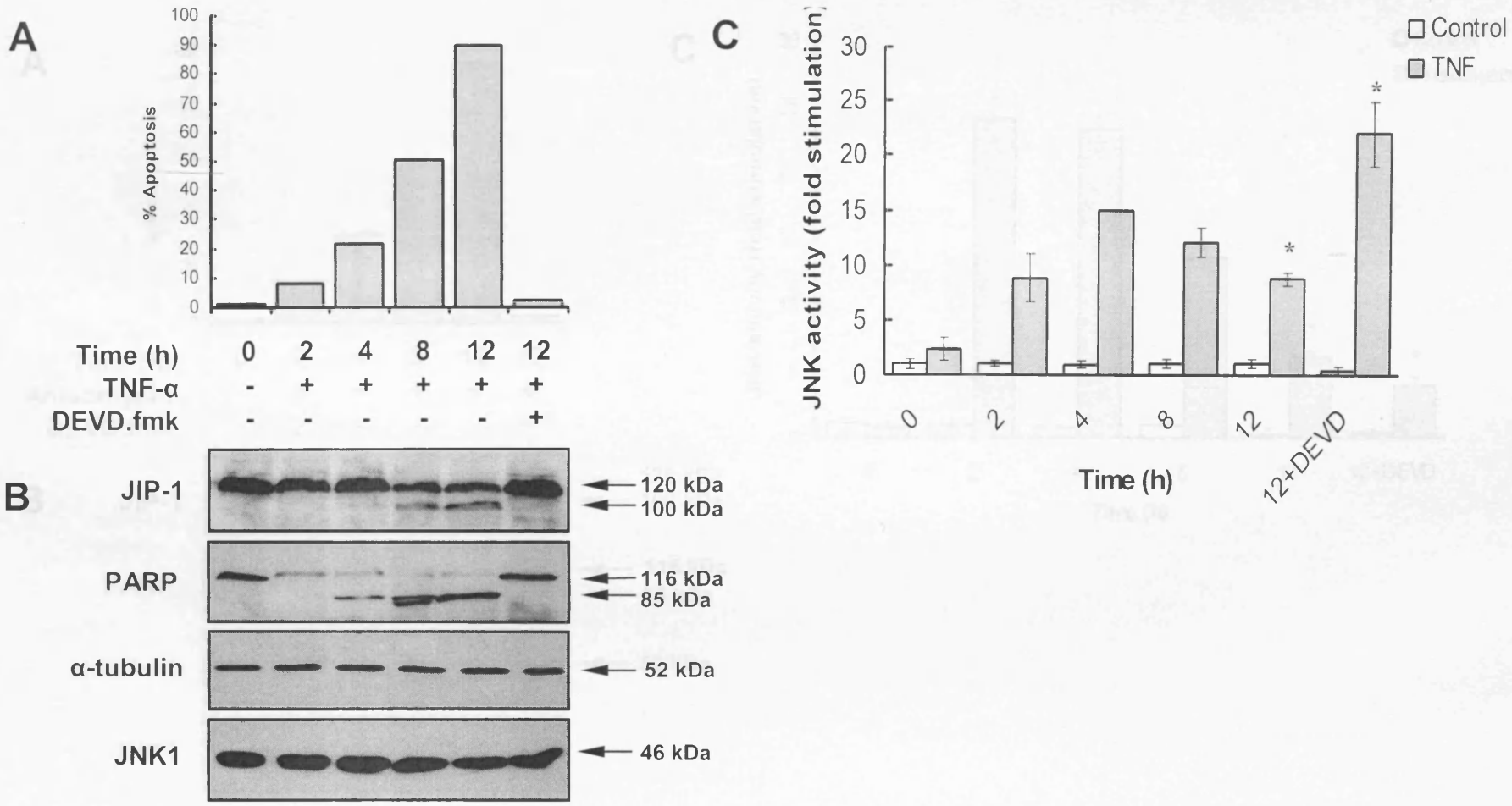

Fig. 5.5. JIP-1 cleavage and JNK activity during TNF-α-induced apoptosis.

HeLa cells were treated with TNF-α (3ng/ml) in combination with CHX (10μg/ml) in the presence or the absence of DEVD.fmk (40μM) for the times indicated. **(A)** Cells undergoing apoptosis were quantified by DNA fragmentation assay using Hoechst 33258 staining. The results shown are mean of triplicate experiments. **(B)** Equivalent amounts of extracts (200μg) were immunoblotted for JIP-1, PARP, α-tubulin and JNK1 as described previously (Figs. 4.3 and 5.1). **(C)** JNK was assayed from equivalent amounts of extracts from each time point as described in Fig. 5.1. The results shown are mean ± S.E.M. of four independent experiments. Data points marked by asterisks indicate $p<0.05$.

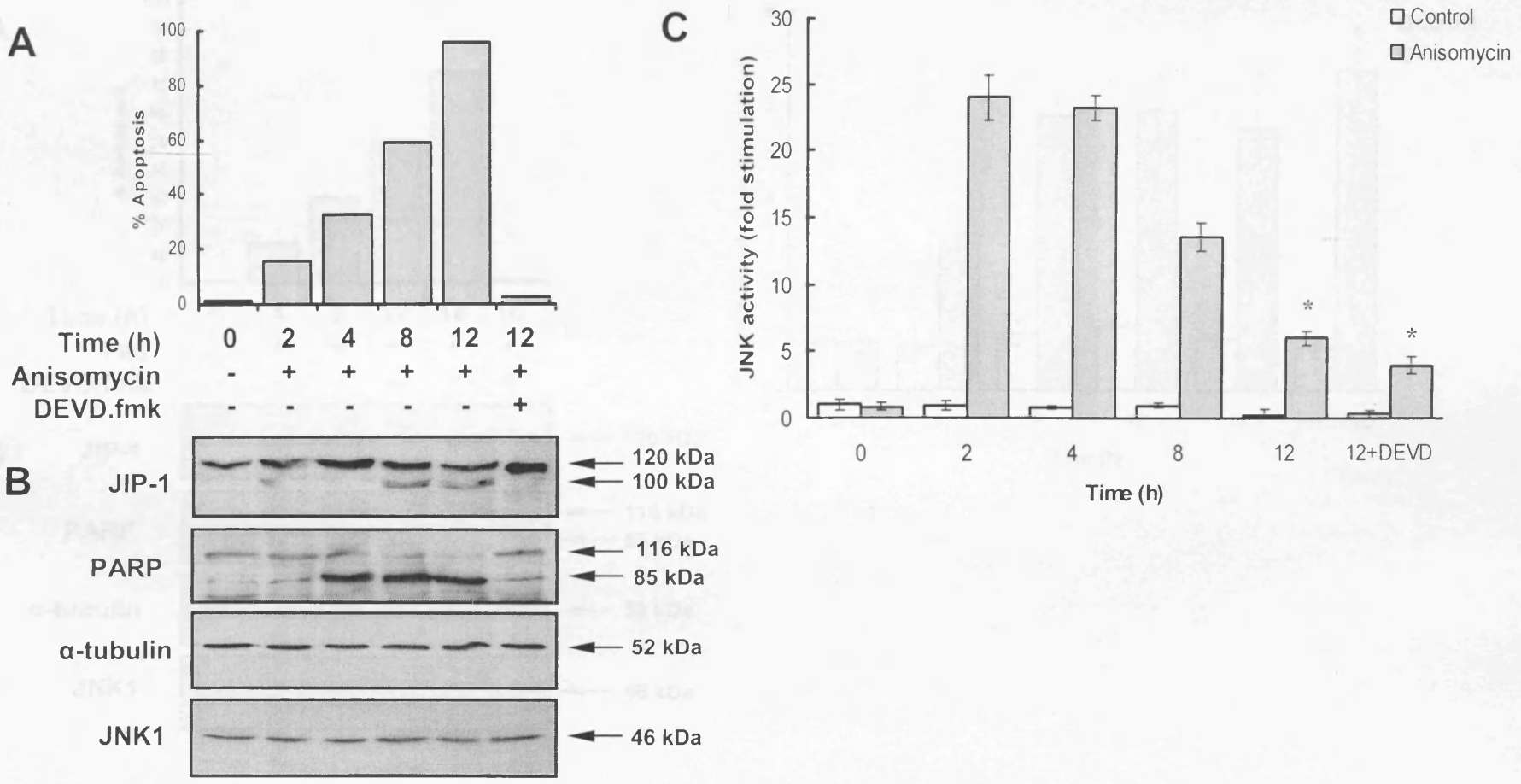

Fig. 5.6. JIP-1 cleavage and JNK activity during anisomycin-induced apoptosis.

HeLa cells were treated with anisomycin (50μg/ml) in the presence or the absence of DEVD.fmk (40μM) for the times indicated. **(A)** Cells undergoing apoptosis were quantified by DNA fragmentation assay using Hoechst 33258 staining. The results shown are mean of triplicate experiments. **(B)** Equivalent amounts of extracts (200μg) were immunoblotted for JIP-1, PARP, α-tubulin and JNK1 as described previously (Figs. 4.3 and 5.1). **(C)** JNK was assayed from equivalent amounts of lysates from each time point as described in Fig. 5.1. The results shown are mean ± S.E.M. of four independent experiments. Data points marked by asterisks indicate $p>0.05$.

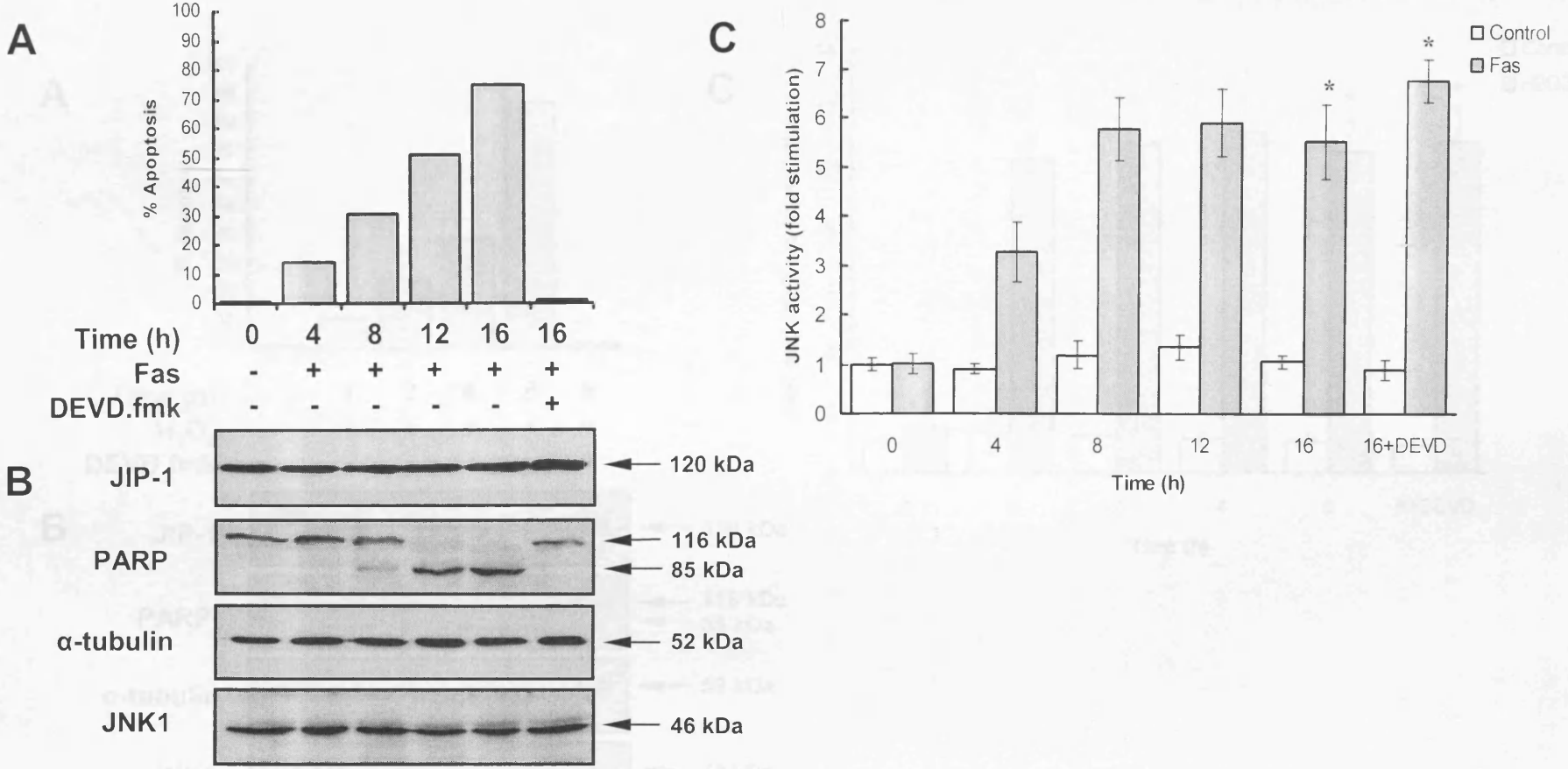

Fig. 5.7. Intact JIP-1 and persistent JNK activity during Fas-induced apoptosis.

Serum-starved HeLa cells were treated with Fas (50ng/ml)/ PD98059 (30μM) in the presence or the absence of DEVD.fmk (40μM) for the times indicated. **(A)** Cells undergoing apoptosis were quantified by DNA fragmentation assay using Hoechst 33258 staining. The results shown are mean of triplicate experiments. **(B)** Equivalent amounts of extracts (200μg) were immunoblotted for JIP-1, PARP, α-tubulin and JNK1 as described previously (Figs. 4.3 and 5.1). **(C)** JNK was assayed from equivalent amounts of lysates from each time point as described in Fig. 5.1. The results shown are mean ± S.E.M. of four independent experiments. Data points marked by asterisks indicate $p>0.05$.

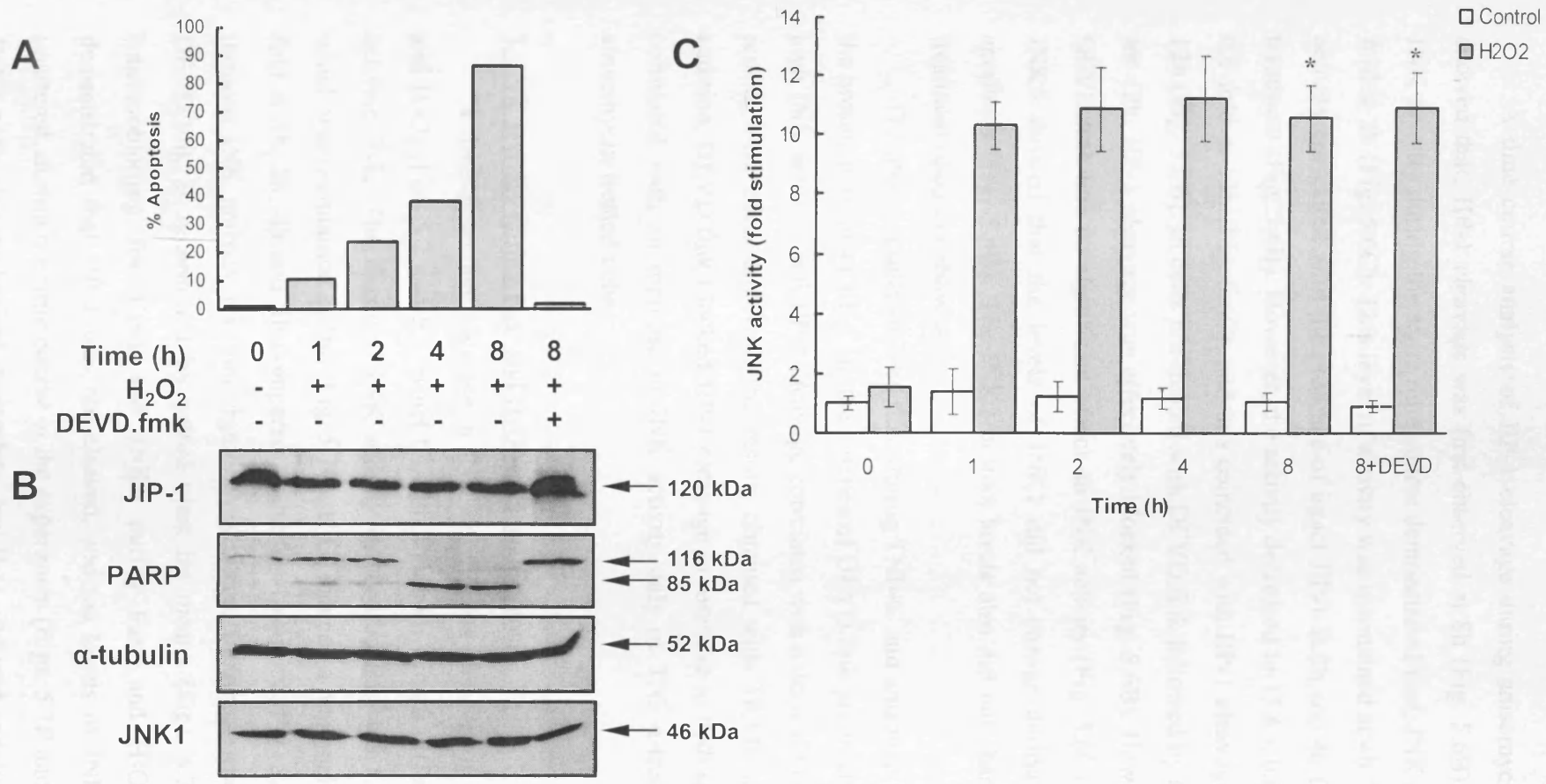

Fig. 5.8. Intact JIP-1 and persistent JNK activity during H_2O_2-induced apoptosis.

HeLa cells were treated with H_2O_2 (1mM) in the presence or the absence of DEVD.fmk (40μM) for the times indicated. **(A)** Cells undergoing apoptosis were quantified by DNA fragmentation assay using Hoechst 33258 staining. The results shown are mean of triplicate experiments. **(B)** Equivalent amounts of extracts (200μg) were immunoblotted for JIP-1, PARP, α-tubulin and JNK1 as described previously (Figs. 4.3 and 5.1). **(C)** JNK was assayed from equivalent amounts of lysates from each time point as described in Fig. 5.1. The results shown are mean ± S.E.M. of four independent experiments. Data points marked by asterisks indicate $p>0.05$.

A time course analysis of JIP-1 cleavage during anisomycin-induced apoptosis showed that, JIP-1 cleavage was first observed at 8h (Fig. 5.6B). Parallel analysis of JNK activity during the same time course demonstrated that, JNK activity was 24 ± 0.9 fold at 2h (Fig. 5.6C). This level of activity was maintained at 4h. This increase in JNK activity correlated with the presence of intact JIP-1 at 2h and 4h following anisomycin treatment (Fig. 5.6B). However, the activity decreased to 13.6 ± 0.6 fold at 8h and 6.0 ± 0.6 fold at 12h (Fig. 5.6C), and this coincided with JIP-1 cleavage observed at 8h and 12h (Fig. 5.6B). In cells pre-treated with DEVD.fmk followed by anisomycin treatment for 12h, JIP-1 cleavage was effectively blocked (Fig. 5.6B). However, the presence of DEVD.fmk had no significant effect on JNK activity (Fig. 5.6C). Immunoblotting for JNK1 showed that the levels of JNK1 did not change during anisomycin-induced apoptosis (Fig. 5.6B). The JNK2 protein levels also did not change upon anisomycin treatment (data not shown).

The above results showed that, during TNF-α- and anisomycin-induced apoptosis, the presence of intact JIP-1 (in the absence of DEVD.fmk pre-treatment) correlated with high JNK activity, and JIP-1 cleavage correlated with a decrease in JNK activity. These results were consistent with the results obtained with TRAIL and staurosporine. In addition, DEVD.fmk blocked JIP-1 cleavage in response to both stimuli. However, this correlated with an increase in JNK activity only in TNF-α-treated cells but not in anisomycin-treated cells.

3. JNK activity during Fas- and H_2O_2-induced apoptosis

A time-dependent increase in JNK activity was observed in response to both Fas and H_2O_2 (Figs 5.7 and 5.8, panel C), although both stimuli differed in their ability to activate JNK. The maximal JNK activity induced by Fas was 5.9 ± 0.7 fold at 12h, which was maintained at 16h (Fig. 5.7C). H_2O_2 induced a maximal JNK activity of ~11 fold at 1h, 2h, 4h and 8h compared to the basal activity (Fig. 5.8C). Fas- and H_2O_2-induced JNK activity was not significantly altered in the presence or the absence of DEVD.fmk as determined by paired t-test for means (Figs. 5.7 and 5.8, panel C). Immunoblotting for JIP-1 and JNK1 during Fas- and H_2O_2-induced apoptosis demonstrated that JIP-1 was not cleaved, and the levels of JNK1 protein remained unaltered, during the time course of the experiment (Figs. 5.7B and 5.8B). The levels of JNK2 were also unchanged during Fas- and H_2O_2-induced apoptosis (data not shown).

Taken together, these data strongly supported the correlation between the presence of intact JIP-1 and sustained JNK activity.

In summary, the results presented in sections 5.2.1 and 5.2.2 showed that high levels of JNK activity correlated with the presence of intact JIP-1, while a decrease in JNK activity correlated with JIP-1 cleavage during TRAIL-, TNF-α-, staurosporine- and anisomycin-induced apoptosis. Also, the inhibition of JIP-1 cleavage by DEVD.fmk during TRAIL-, TNF-α- staurosporine-induced apoptosis was associated with enhanced JNK activation. In addition, the presence of intact JIP-1 during Fas- and H_2O_2-induced apoptosis was coincident with persistent JNK activity. Taken together, these results suggested a link between the cleavage status of JIP-1 and JNK activity during receptor- and chemical-induced apoptosis.

5.2.3. JIP-1 may mediate sustained JNK activation during TRAIL-induced apoptosis

A comparison of the *in vivo* and *in vitro* cleavage of JIP-1 shows that JIP-1 is a poor caspase-3 substrate *in vivo* during apoptosis, possibly because JIP-1 may be inaccessible to caspase-3 due to the interaction of JIP-1 with the JNK pathway kinases (see section 4.3.5, Chapter 4). The interaction of JIP-1 with JNK has been shown to be required for JNK activation (Whitmarsh *et. al.*, 1998; Yasuda *et. al.*, 1999; Whitmarsh *et. al.*, 2001), and consistent with this, the interaction of JIP-1 with JNK1 correlates with JNK activation in N1E-115 cells (Chapter 3). A link between the cleavage status of JIP-1 and JNK activity was observed during apoptosis of HeLa cells (sections 5.2.1 and 5.2.2). Taken together, this suggested that JNK activity might be mediated by an interaction of JNK with JIP-1 during apoptosis of HeLa cells. To test this hypothesis, the interaction of endogenous JIP-1 with JNK1 was examined during TRAIL-induced HeLa cell apoptosis.

5.2.3.1. Immunoprecipitation of JIP-1 and JNK1 from HeLa cell extracts

Before studying the interaction of JIP-1 with JNK1 during TRAIL-induced HeLa cell apoptosis, JIP-1 and JNK antisera (#609 and #355 respectively) were tested for their ability to precipitate endogenous proteins from HeLa cell extracts. The choice of the antibodies for immunoprecipitation and western blotting was based on the results obtained with rat brain and N1E-115 lysates (Chapter 3).

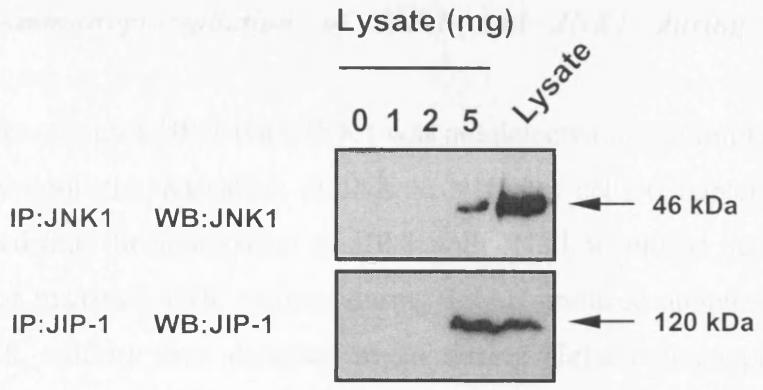

Fig. 5.9. Immunoprecipitation of JNK1 and JIP-1 from HeLa cell extracts.
Extracts from untreated HeLa cells were immunoprecipitated with 5µl JNK1 antiserum #355 or 5µl JIP-1 antiserum #609, and the resulting precipitates were blotted with monoclonal JNK1 antibody (Pharmingen) at 1:1000 dilution, or with monoclonal JIP-1 antibody at 1:5000 dilution. Lysate (200µg) was used as a control. IP = immunoprecipitation; WB = western blot.

Increasing amounts of HeLa cell extracts were immunoprecipitated with JIP-1 and JNK1 antisera, and the presence of the endogenous protein in the immunoprecipitate was detected by western blotting. The results showed that, JIP-1 was detected in #609 precipitates and JNK1 was detected in #355 precipitates only with 5mg of HeLa cell extracts, but not when 1mg or 2mg extract was used (Fig. 5.9). Therefore, 5mg of HeLa cell extracts were used to examine the co-immunoprecipitation of JIP-1 and JNK1 during TRAIL-induced apoptosis.

5.2.3.2. Co-immunoprecipitation of JIP-1 and JNK1 during TRAIL-induced apoptosis

The interaction of JIP-1 with JNK1 was not detected in unstimulated cells but was detected only upon the activation of JNK in N1E-115 cells (Chapter 3). Therefore, it was postulated that the interaction of JIP-1 with JNK1 would be detected only at the time points of maximal JNK activity during TRAIL-induced apoptosis of HeLa cells. Maximal JNK activity was detected at 2h during HeLa cell apoptosis induced by TRAIL, which was coincident with the presence of intact JIP-1 (Figs. 5.1A and 4.4B). A low level of TRAIL-induced JNK activity was detected at 8h, which correlated with the cleavage of JIP-1 (Figs. 5.1A and 4.4BB). The inhibition of JIP-1 cleavage in the presence of DEVD.fmk correlated with TRAIL-induced enhanced JNK activity at 8h (Figs. 5.1A and 4.4B). Therefore, the interaction of JIP-1 with JNK1 was examined in HeLa cells treated with TRAIL for 0h, 2h and 8h, as well as in cells pre-treated with DEVD.fmk followed by TRAIL treatment for 8h.

The results showed that, following TRAIL treatment, JIP-1 was detected in JNK immunoprecipitates and vice versa at 2h, and at 8h with DEVD.fmk pre-treatment (Fig. 5.10A), suggesting an interaction between JIP-1 and JNK1 at these time points. This coincided with the presence of intact JIP-1 and maximal JNK activity (Figs. 5.1A, 4.4B, and 4.8B). At 8h TRAIL treatment in the absence of DEVD.fmk, intact JIP-1 was detected in JNK immunoprecipitates and JNK1 was detected in JIP-1 immunoprecipitates, but the amount of each protein in the immunoprecipitates was much less than that detected at 2h and at 8h with DEVD.fmk pre-treatment (Fig. 5.10A). This correlated with JIP-1 cleavage and a significant decrease in JNK activity (Figs. 5.1A and 4.4B). However, the 100-kDa cleaved JIP-1 fragment was not detected in JNK1 immunoprecipitates at 8h TRAIL treatment (Fig. 5.10A), suggesting an absence of an interaction between the cleaved JIP-1 fragment and JNK1. However, the

possibility that small amounts of the cleaved JIP-1 fragment may interact with JNK1, which may not be detectable by western blotting, cannot be excluded. JIP-1 and JNK1 were not detected in JNK and JIP-1 immunoprecipitates respectively in untreated (control) cells (Fig. 5.10A), suggesting that JIP-1 does not interact with JNK1 in control cells.

The results obtained above were further confirmed by immunoblotting equivalent amounts of lysate and supernatant from the same experiment for JIP-1 and JNK1 to compare the presence/absence of these proteins before and after immunoprecipitation. Equivalent amounts of JIP-1 and JNK1 were present in both the extract and the supernatant from control cells (Fig. 5.10A). Quantification of the amount of JIP-1 and JNK1 proteins left in the supernatant relative to the extract showed that both JIP-1 and JNK1 were completely retained in the supernatant in control samples (Fig. 5.10B). This was consistent with the absence of JIP-1 in JNK1 immunoprecipitates and vice versa at 0h (Fig. 5.10A). A clear difference was observed at 2h, 8h and at 8h plus DEVD.fmk pre-treatment. At 2h and 8h plus DEVD.fmk pre-treatment, JIP-1 and JNK1 were present in the extract but not in the supernatant (Fig. 5.10A). This was consistent with the detection of JIP-1 in the JNK immunoprecipitates and vice versa at these time points (Fig. 5.10A). However, at 8h TRAIL treatment in the absence of DEVD.fmk, the amount of JNK1 retained in the supernatant was 44% of the total amount present in the extract, which was consistent with a small amount of JNK1 present in JIP-1 immunoprecipitates (Fig. 5.10A). The amount of intact JIP-1 retained in the supernatant was 2% of the total amount present in the extract at 8h TRAIL treatment in the absence of DEVD.fmk, whereas 100% of the cleaved JIP-1 fragment was retained in the supernatant at this time point (Fig. 5.10A). This was consistent with the presence of a small amount of intact JIP-1 and the absence of the 100-kDa cleaved JIP-1 fragment in the JNK1 immunoprecipitates (Fig. 5.10A).

Taken together with the results of TRAIL-induced JIP-1 cleavage and JNK activity (section 5.2.1), the above data suggested that in the absence of TRAIL treatment, JIP-1 and JNK1 did not interact. The interaction between JIP-1 and JNK1 was coincident with intact JIP-1 and maximal JNK activity at 2h TRAIL treatment and at 8h TRAIL plus DEVD.fmk pre-treatment. A decrease in JNK activity and JIP-1 cleavage was associated with a reduced ability of JIP-1 to interact with JNK1 at 8h TRAIL treatment, possibly due to the reduction in the amount of intact JIP-1. The results also showed an absence of the interaction of JNK1 with the 100-kDa cleaved

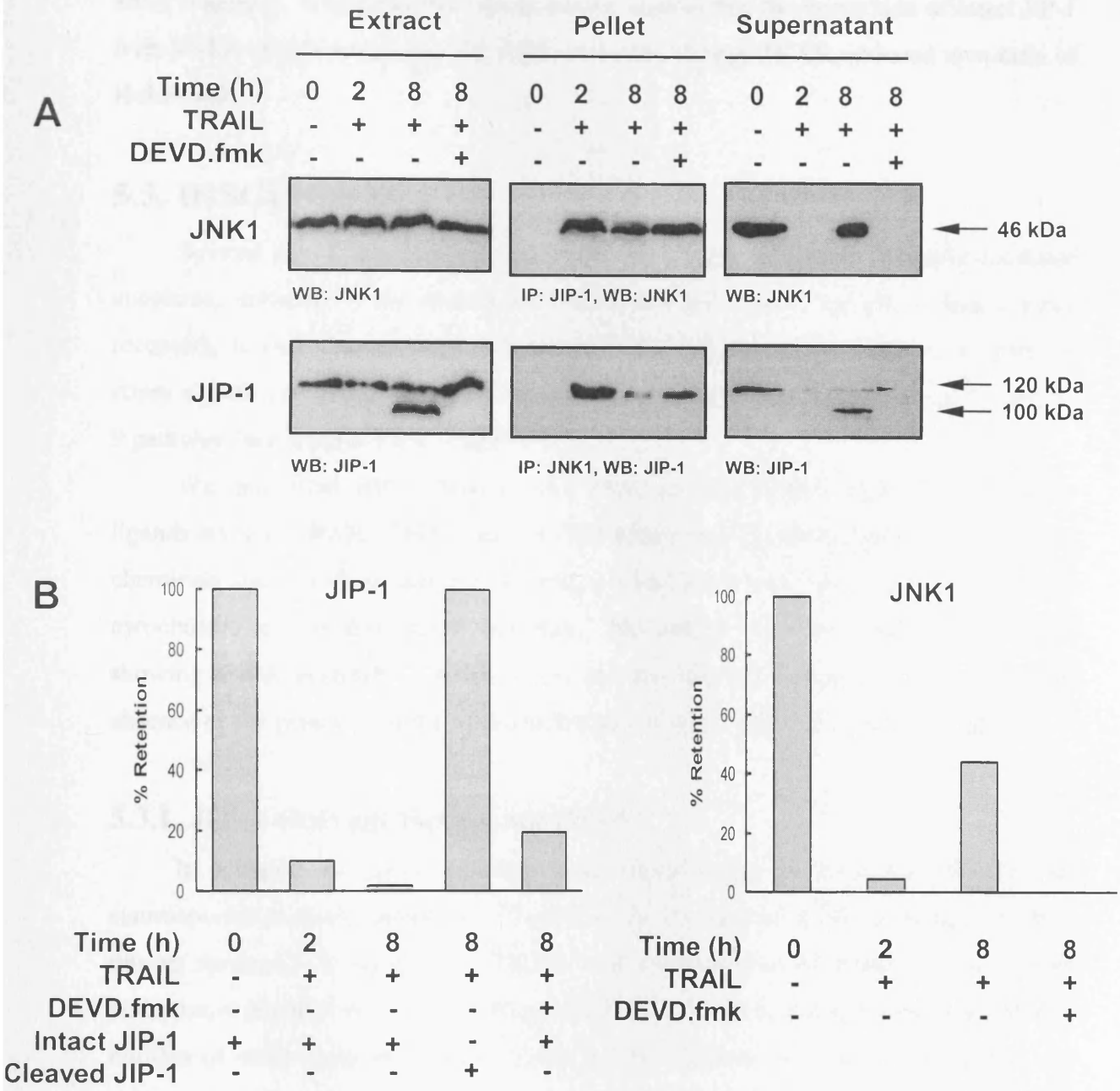

Fig. 5.10. The interaction between JIP-1 and JNK1 during TRAIL-induced apoptosis.

(A) HeLa cells were treated with TRAIL (1μg/ml) ± DEVD.fmk (40μM) for the indicated times, and 5mg of cell extracts were immunoprecipitated with JNK1 and JIP-1 antisera as described in Fig. 5.9. JIP-1 immunoprecipitates were blotted for the presence of JNK1, and JNK1 immunoprecipitates were blotted for the presence of JIP-1 as described in Fig. 5.9. Equivalent volumes of cell extracts and supernatant were blotted for the presence of JNK1 and JIP-1 as described in Fig. 5.9. The data shown are representative of two independent experiments. **(B)** The amount of JIP-1 and JNK1 in the extract and the supernatant was quantified using the ImageQuant™ software, and was expressed graphically as % retention in the supernatant. The data shown are the mean of two independent experiments.

JIP-1 fragment. Taken together, these results suggest that the interaction of intact JIP-1 with JNK1 may be required for JNK activation during TRAIL-induced apoptosis of HeLa cells.

5.3. DISCUSSION

Several signal transduction pathways can trigger apoptosis. Receptor-mediated apoptosis, initiated by the binding of TNF-α, Fas and TRAIL ligands to their cognate receptors, is well characterised (see section 1.6.3, Chapter 1). In addition, a variety of stress signals can trigger apoptosis via the mitochondrial cytochrome c/Apaf-1/caspase-9 pathway (see section 1.6.4, Chapter 1).

We examined JIP-1 cleavage and JNK activity during apoptosis induced by ligands such as TRAIL, TNF-α and Fas that utilise the receptor-mediated pathway, and chemicals such as staurosporine, anisomycin and H_2O_2 that initiate the mitochondrial cytochrome c-mediated death pathway. The results provide correlative evidence showing a link between JNK activation and the cleavage status of JIP-1, and to the absence or the presence of the interaction between JIP-1 and JNK1 during apoptosis.

5.3.1. JIP-1 cleavage during apoptosis

In Chapter 4, JIP-1 cleavage was characterised in response TRAIL- and staurosporine-induced apoptosis. Therefore, to investigate if the cleavage of JIP-1 during apoptosis is peculiar to TRAIL and staurosporine or whether it is a more widespread phenomenon, we investigated JIP-1 cleavage during apoptosis induced by a number of other apoptotic stimuli. These included ligands such as TNF-α and Fas, and chemicals such as MG132, ethanol, glucose, sodium arsenite, anisomycin and H_2O_2. The choice of these stimuli was based on their ability to activate JNK during apoptosis (section 5.1).

5.3.2. JNK activation during apoptosis is independent of caspase-3

DEVD.fmk, a specific caspase-3 inhibitor, inhibited JIP-1 cleavage and enhanced JNK activation during TRAIL-, TNF-α- and staurosporine-induced apoptosis (Figs. 5.1, 5.2, 5.5 and 5.6). This suggests that JNK activation is independent and upstream of caspase-3 and possibly dependent on the presence of intact JIP-1. However, the presence of DEVD.fmk had no effect on JNK activation during anisomycin-induced

apoptosis, even though it did inhibit JIP-1 cleavage (Fig. 5.6B and C), suggesting that JNK activation may be independent of JIP-1. This is in agreement with recent work by Whitmarsh *et. al.* (2001), which suggests that anisomycin-induced JNK activation may be JIP-1 independent since anisomycin stimulated JNK to similar levels in wild type and *Jip-1*$^{-/-}$ neurons. Anisomycin has been reported to activate MKK4 and MKK7 (Tournier *et. al.*, 1999). MKK7 is a part of the JIP-1 scaffold complex, whereas MKK4 is not (Whitmarsh *et. al.*, 1998). Therefore, it is possible that anisomycin-induced JNK activation in the presence of DEVD.fmk in HeLa cells may be mediated by MKK4.

5.3.3. JNK activation may be dependent on JIP-1 during apoptosis

During TRAIL-, TNF-α-, staurosporine- and anisomycin-induced apoptosis, the presence of intact JIP-1 correlated with high levels of JNK activity and the cleavage of JIP-1 was coincident with a decrease in JNK activity (sections 5.2.1 and 5.2.2). Apoptosis induced by Fas and H_2O_2 did not result in JIP-1 cleavage, and this coincided with persistent JNK activity (section 5.2.2). The inhibition of JIP-1 cleavage *in vivo* by DEVD.fmk during TRAIL-, TNF-α- and staurosporine-induced apoptosis was coincident with enhanced JNK activation (Figs. 5.1, 5.2 and 5.9). Taken together, these results suggest a correlation between the status of JIP-1 (intact or cleaved) with high levels of JNK activity during apoptosis, the presence of intact JIP-1 being associated with maximal JNK activation and the cleavage of JIP-1 being associated with a decrease in JNK activity in all cases.

The time points at which JNK activation was detected in the presence and the absence of DEVD.fmk coincided with the co-precipitation of JIP-1 with JNK1 during TRAIL-induced apoptosis (section 5.2.3.2). In addition, the cleavage of JIP-1 correlated with a reduced ability of JIP-1 to interact with JNK1 and a decrease in JNK activity during TRAIL-induced apoptosis (section 5.2.3.2, Fig. 5.10). These results suggested that the interaction of JIP-1 with JNK may be required for JNK activation during TRAIL-induced apoptosis. Since the presence of the intact JIP-1 coincided with maximal JNK activation and the cleavage of JIP-1 coincided with a decrease in JNK activity during TNF-α-, Fas-, staurosporine-, anisomycin- and H_2O_2-induced apoptosis also, it is likely that JNK activation in response to these stimuli may also be mediated by the interaction of JNK with JIP-1. These results suggest that JNK activation may be dependent on an interaction with JIP-1 during HeLa cell apoptosis.

The observation that the presence of intact JIP-1 was coincident with high levels of JNK activity in the presence of DEVD.fmk during TRAIL-, TNF-α-, Fas-, staurosporine- and H_2O_2-induced apoptosis (Figs. 5.1, 5.2, 5.9, 5.11 and 5.12) may not necessarily suggest that JNK activation is dependent on JIP-1. It is possible that DEVD.fmk may inactivate JNK-specific phosphatase(s), which may lead to high levels of JNK activity independently of JIP-1. However, the following observations suggest that JNK activation in the presence of DEVD.fmk may not be a consequence of the inhibition of phosphatase(s). A significant difference in JNK activation in the presence or the absence of DEVD.fmk was not detected at the time points at which JIP-1 was intact during TRAIL-, Fas- staurosporine and H_2O_2-induced apoptosis (sections 5.2.1 and 5.2.2). In addition, JNK activity detected in the presence DEVD.fmk alone was not higher than the basal activity (section 5.2.1), which should have been the case if DEVD.fmk treatment might be resulting in the inactivation of JNK-specific phosphatase(s). Thus most evidence suggests that DEVD.fmk treatment may not result in the inactivation of JNK-specific phosphatase(s). However, this may be ascertained by examining a time course of phosphatase activation in the presence or the absence of DEVD.fmk during TRAIL-, Fas- staurosporine and H_2O_2-induced apoptosis.

5.3.4. A possible role for the JIP-1 scaffold in the activation of JNK during apoptosis

JIP-1 cleavage was found to be a late event compared to PARP cleavage and DNA fragmentation during TRAIL-, TNF-α-, staurosporine- and anisomycin-induced apoptosis of HeLa cells (sections 5.2.1 and 5.2.2), even though all three events are likely to be mediated by caspase-3 (see Chapter 4). The following explanation may account for these observations. JIP-1 knockout studies have shown that the JIP-1 scaffold is required for the activation of JNK *in vivo* (Whitmarsh *et. al.*, 2001), however the interaction of JIP-1 with JNK alone has been shown to be insufficient for the activation of the JNK pathway (Dickens *et. al.*, 1997; Whitmarsh *et. al.*, 1998). Therefore the JIP-1-JNK1 complex detected in HeLa cells (Fig. 5.10A) may contain one or more additional components of the JIP-1 scaffold, namely HPK1, MLK3 or MKK7. Binding of these components to JIP-1 may shield caspase-3 cleavage sites present in JIP-1, thus facilitating maximal JNK activation via the JIP-1 scaffold and preventing JIP-1 cleavage during the early stages of apoptosis. Since the presence of intact JIP-1

correlated with maximal JNK activation during apoptosis induced by all apoptotic stimuli tested, it is possible that the JIP-1 scaffold may mediate JNK activation in all cases. This hypothesis could be tested *in vitro* by pre-forming the JIP-1-JNK-MKK7-MLK3 complex, adding purified caspase-3 and detecting whether JIP-1 is cleaved to 100-kDa, 55-kDa and 45-kDa fragments. If the hypothesis is true, then JIP-1 should remain intact and JIP-1 cleavage products should not be formed.

A decrease in JNK activity was coincident with JIP-1 cleavage during the late stages of TRAIL-, TNF-α-, staurosporine- and anisomycin-induced apoptosis (sections 5.2.1 and 5.2.2). There are two possible explanations for these observations. One explanation is that once the JIP-1 scaffold has served its purpose of activating the JNK pathway, it may disassemble during the late stages of apoptosis. This may expose caspase-3 cleavage sites on JIP-1, thus leading to JIP-1 cleavage and possibly a decrease in JNK activation (see also section 4.3.5, Chapter 4). The mechanism(s) that may cause the disassembly of the JIP-1 scaffold is not known at present. However, a complete loss of intact JIP-1 was not observed during TRAIL-, TNF-α-, staurosporine- and anisomycin-induced apoptosis (Figs. 4.4B, 4.5B, 5.5B and 5.6B). This suggests that all the available JIP-1 is not cleaved, possibly because the uncleaved JIP-1 is complexed with the JNK pathway components. This is in part supported by the co-immunoprecipitation of JIP-1 and JNK1 at 8h following TRAIL treatment (Fig. 5.10A), a time point that is coincident with JIP-1 cleavage (Fig. 4.4B). Persistent JNK activity and the absence of JIP-1 cleavage during Fas- and H_2O_2–induced apoptosis may suggest that a functional JIP-1 scaffold might exist during the late stages of apoptosis, which may prevent the cleavage of JIP-1 by shielding the caspase-3 cleavage sites.

Another possible explanation for the observed decrease in JNK activity coincident with JIP-1 cleavage during the late stages of TRAIL-, TNF-α-, staurosporine- and anisomycin-induced apoptosis (sections 5.2.1 and 5.2.2) is that caspase-3 cleaves JIP-1 that is a part of the JIP-1 scaffold complex. This leads to the disassembly of the scaffold and a consequent decrease in JNK activity. This hypothesis can be tested by examining the cleavage of JIP-1 complexed with JNK, MKK7 and MLK3 by caspase-3 *in vitro* as described in the beginning of this section.

Taken together, the above discussion suggests that the interaction of JIP-1 with the JNK pathway components may account for the relative insensitivity of JIP-1 to caspase-3 cleavage *in vivo* compared to *in vitro* (see also section 4.3.5, Chapter 4), and compared to the caspase-3-mediated PARP cleavage and DNA fragmentation.

However, other reasons for JIP-1 being a poor caspase-3 substrate *in vivo*, discussed in section 4.4.5 (Chapter 4), cannot be excluded. It appears that mechanism(s) to protect JIP-1 from caspase-3-mediated cleavage might have evolved to ensure JNK activation during the early stages of apoptosis.

5.3.6. Role of JNK activity during HeLa cell apoptosis

JNK activation was detected during apoptosis induced by TRAIL in HeLa cells (Fig. 5.1). This is in agreement with similar results obtained in HeLa cells by other groups (Muhlenbeck *et. al.*, 1998; Lin *et. al.*, 2000; Muhlenbeck *et. al.*, 2000). Persistent JNK activity was detected during Fas-induced apoptosis (Figs. 5.7B and 5.11). This is consistent with the results of groups that have reported a correlation between JNK activation and Fas-induced apoptosis in HeLa cells (Yang *et. al.*, 1997; Chang, Yang & Baltimore, 1999). Apoptosis induced by H_2O_2 was accompanied by rapid and sustained JNK activation (Fig. 5.12), a result which is in agreement with the results of Wang *et. al.* (1998).

JNK activity was maintained at high levels during TRAIL-, TNF-α-, Fas-, staurosporine-, anisomycin- and H_2O_2-induced apoptosis (Figs. 5.1A, 5.2A, 5.5C, 5.6C, 5.7C and 5.8C). A possible reason for this could be that active JNK may be required for the release of cytochrome-c from mitochondria, suppression of p53-mediated growth arrest and/or the induction of FasL during apoptosis (see section 1.7.3, Chapter 1). During staurosporine- anisomycin- and H_2O_2-induced apoptosis in HeLa cells, JNK activity would be maximally maintained until the major cytochrome-c-Apaf-1-caspase-9 pathway and the supplementary Fas-FADD-caspase-8 pathway are sufficiently activated to commit cells to die. The mitochondrial pathway can provide an amplification loop for death receptor signalling (Fig. 1.5, Chapter 1). Therefore, during TRAIL-, Fas- and TNF-α-induced apoptosis in HeLa cells, the mitochondrial amplification loop may be activated both by JNK and caspase-8-mediated Bid cleavage (Figs. 1.5 and 1.6, Chapter 1).

The molecular targets of JNK that cause the release of cytochrome c from mitochondria are not known, but are believed to be the pro-apoptotic members of the Bcl-2 family proteins such as Bax and Bid, both of which are present in HeLa cells (Tefani *et. al.*, 2001). HeLa cells also express FasL protein (Mo & Beck, 1999). In HeLa cells, p53 mRNA is translated but leads to an unstable protein product (May,

Jenkins & May, 1991). However, it has been demonstrated that p53 in HeLa cells is stabilised during vitamin C-, leptomycin B- or actinomycin D-induced apoptosis (Hietanen *et. al.*, 2000; Reddy, Khanna & Singh, 2001). It is therefore possible that JNK signalling may stabilise p53, possibly by phosphorylating it (Buschmann *et. al.*, 2001), and channel p53 activity towards apoptosis, possibly through c-Jun-mediated suppression of p53-induced growth arrest.

Thus, in HeLa cells, the targets of JNK signalling are present, and, the activation of JNK, dependent on JIP-1, may play a crucial role in apoptosis progression.

5.3.6. A model for the role of JIP-1 in JNK activation during apoptosis

Based on the above discussions and results presented in Chapter 4, and taking into consideration the evidence for the role of JNK during receptor- and stress-induced apoptosis (section 1.7.3, Chapter 1 and section 5.1, present Chapter), a model for the role of JIP-1 in mediating JNK activation during HeLa cell apoptosis *in vivo* can be postulated.

According to the model presented schematically in Fig. 5.15, JNK is activated upstream of caspase-3 by all the stimuli tested (section 5.3.3), and JNK activation is mediated by its interaction with JIP-1, presumably through the JIP-1 scaffold, during the early stages of apoptosis (sections 5.3.4 and 5.3.5). Activated JNK exerts its pro-apoptotic effects primarily by activating the cytochrome c/Apaf-1/caspase-9 pathway (section 1.7.3, Chapter 1). Both the death receptor and mitochondrial apoptotic pathways converge at the level of caspase-3. The complex of JIP-1 with JNK, and possibly MLK and MKK7, prevents its cleavage by caspase-3 (section 5.3.5). During the late stages of apoptosis, only one pool of JIP-1 molecules is cleaved by caspase-3, possibly because of the scaffold disassembly that exposes the caspase-3 cleavage sites on JIP-1 or caspase-3 cleaves JIP-1 that is a part of the JIP-1 scaffold complex (section 5.3.5). However, the other pool of JIP-1 molecules is still in complex with JNK, and possibly with MLK and MKK7 also, because of which it remains uncleaved and maintains persistent JNK activity in apoptotic cells (section 5.3.5).

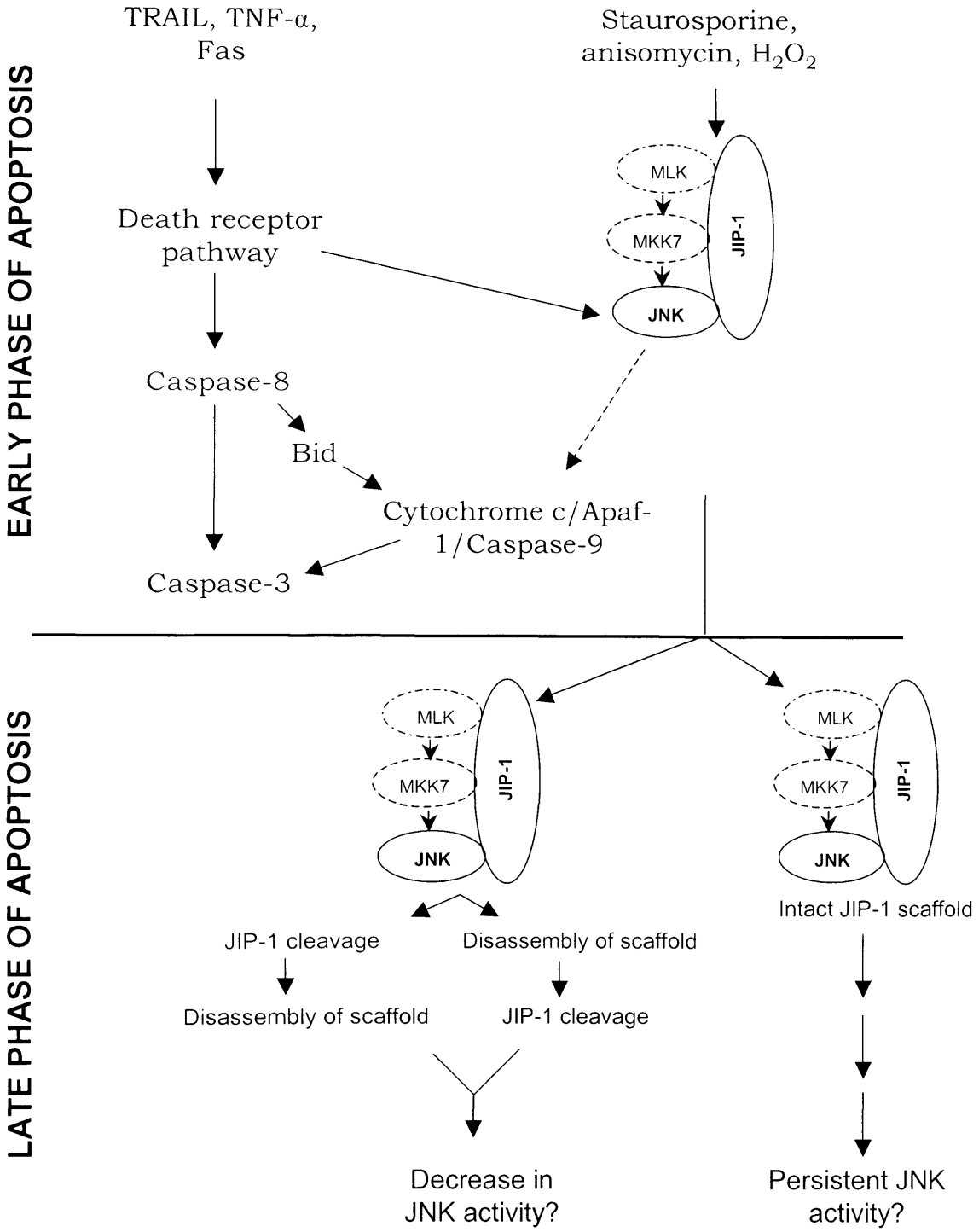

Fig. 5.11. A model for the role of JIP-1 in JNK activation during apoptosis in HeLa cells, based on the results obtained. For explanation see text. JIP-1-JNK interaction is indicated by bold fonts. MLK and MKK7 are represented by dashed lines, since their interaction with endogenous JIP-1 during apoptosis is not known.

FINAL DISCUSSION

The JNKs represent a group of enzymes that are activated by the exposure of cells to cytokines and environmental stresses. The JNK signal transduction pathway responds to cellular stresses and plays a role in embryogenesis, cell survival, proliferation, differentiation and apoptosis. JNK is activated by dual-specificity kinases MKK4 and MKK7, which in turn are activated by a variety of upstream kinases. Genetic and biochemical evidence suggests that the JNK pathway is essential for stress response and apoptosis.

The JIP group of proteins (JIP-1, JIP-2 and JIP-3) function as scaffolds for the JNK pathway. Transient transfection analysis has shown that JIPs interact with JNK, MKK7 and MLK3, form a scaffold and aid the specific activation of the JNK pathway in response to various stress stimuli. However, protein-protein interaction results based on overexpression studies, although very insightful and often correct, do need to be backed up by other approaches. One approach is to study the proposed interactions between endogenous proteins in intact, non-transfected cells. Therefore, this project investigated the endogenous interaction of JIP-1 with the JNK pathway components. The results show the evidence of JIP-1-MLK3 and MLK3-HPK1 interactions in the absence of a stress stimulus, and JIP-1-JNK and MLK3-HPK1 interactions in intact cells upon stress application. These results suggest that the JIP-1 scaffold complex is dynamic in which an exchange of components may take place. Such an exchange of components may result in signal amplification. This contradicts the simple JIP-1 scaffold model in which the kinases bound to JIP-1 sequentially phosphorylate the downstream kinase to activate the JNK pathway with no signal amplification (Whitmarsh *et. al.*, 1998). Clearly, our data need to be supplemented with other approaches such as co-immunolocalisation and the sizing of protein complexes.

The results present the following new findings in the field of JNK signalling research: endogenous interactions between JIP-1, JNK, MLK3 and HPK1 in resting and stressed cells; and a putative role of HPK1 as a bridge between JIP-1 and MLK3, keeping MLK3 in the vicinity of the JIP-1 scaffold following stress. The endogenous JIP-1-MLK3 interaction in resting cells and JIP-1-JNK interaction in stressed cells was recently corroborated by the results of Nihalani *et. al.* (2001).

Genetic evidence supports a pro-apoptotic role of the JNK signalling pathway in both receptor- and stress-mediated apoptosis. The presence of four caspase-3 and one caspase-8 cleavage sites in JIP-1 suggested that JIP-1 might be a target for caspase cleavage during apoptosis. Our results demonstrate JIP-1 to be a caspase-3 substrate

both *in vivo* and *in vitro*. The sites in JIP-1 targeted by caspase-3 are Asp98 and Asp405, as determined by mutational analysis. An examination of JIP-1 cleavage and JNK activity in HeLa cells during apoptosis demonstrated that intact JIP-1 was associated with high levels of JNK activity and the cleavage of JIP-1 was coincident with a decrease in JNK activity. Furthermore, during TRAIL-induced apoptosis, the co-immunoprecipitation of JIP-1 and JNK1 was coincident with JNK activation, whereas a decrease in JNK activity correlated with a reduced ability of JIP-1 to interact with JNK1. These results suggest that the interaction of JIP-1 with JNK may be required for JNK activation, and that the cleavage of JIP-1 may attenuate JNK signalling, *in vivo* during apoptosis. It is possible that JIP-1 cleavage during apoptosis may not totally contribute to JNK inactivation, but it is likely to represent one mechanism used by cells to attenuate JNK signalling.

A recent JIP-1 knockout study shows that the scaffolding function of JIP-1 is essential in mediating JNK signalling during stress and apoptosis (Whitmarsh *et. al.*, 2001). It is interesting to note that the JIP-1 knockout phenotype was not compensated by the presence of JIP-2 or JIP-3 in response to stress and apoptosis, whereas other functions attributed to JIP-1, such as a role in the pathogenesis of type II diabetes, were unaffected (Whitmarsh *et. al.*, 2001). This suggests that the JIP-1 scaffold complex plays an indispensable role in mediating JNK signalling even in the presence of other JIP isoforms and therefore the results of our investigation into the functioning of the JIP-1 scaffold in JNK signalling during stress and apoptosis are highly relevant.

It should also be noted that in *Jip-1*$^{-/-}$ neurons, the activation of the JNK pathway was not detected, whereas in the wild type neurons the JNK pathway was activated (Whitmarsh *et. al.*, 2001). The results presented in Chapter 5 indirectly support the JIP-1 knockout phenotype, because JIP-1 cleavage in response to TRAIL and staurosporine correlated with a complete loss of JNK activity at 8h, suggesting that JIP-1 cleavage has the same effect as the absence of JIP-1 on JNK signalling during apoptosis.

To further investigate the role of JIP-1 in JNK signalling during stress and apoptosis, an antisense approach to decrease the levels of endogenous JIP-1, followed by the application of apoptotic and stressful stimuli, could be carried out.

Scaffolding proteins have been discovered in a wide variety of species, including yeast, *Drosophila* and mammals (Pawson and Nash, 1999). Examples include Ste5 (yeast), inactivation no after-potential D (InaD) (*Drosophila*) and cyclin-dependent kinases (CDKs), A-kinase anchoring proteins (AKAP), kinase suppressor of Ras (KSR),

Rsk1, JIPs and β arrestin-2 (mammals). Although scaffold proteins serve to provide local activation platforms that contribute to signal specificity by insulating different pathways, they are nevertheless involved in mediating a wide variety of responses. For example, Ste5 is required for growth arrest and mating. InaD is essential for phototransduction. AKAP anchor different kinases and phosphatases in an inactive state, close to their substrates and activators. JIP-1 plays a role in the JNK signal transduction in response to stress and apoptosis. Research on scaffold proteins is uncovering fascinating aspects of specificity and regulation of different pathways active in a cell. Our results aid the understanding of the role of JIP-1 in JNK signalling during stress and apoptosis.

BIBLIOGRAPHY

Abderrahmani, A. *et. al.* (2001). The transcriptional repressor rest determines the cell-specific expression of the human mapk8ip1 gene encoding ib1 (jip-1). *Mol. Cell. Biol.* **21**:7256-7267.

Adler, V. *et. al.* (1997). Conformation-dependent phosphorylation of p53. *Proc. Natl. Acad. Sci. USA* **94**:1686-1691.

Adler, V. *et. al.* (1999). Regulation of JNK signalling by GSTp. *EMBO J.* **18**:1321-1334.

Adrain, C. & Martin, S. J. (2001). The mitochondrial apoptosome: a killer unleashed by the cytochrome seas. *Trends Bioch. Sci.* **26**:390-397.

Almeida, E. A. *et. al.* (2000). Matrix survival signalling: from fibronectin via focal adhesion kinase to c-Jun NH(2)-terminal kinase. *J. Cell Biol.* **149**:741-754.

Alnemri, E. S. *et. al.* (1996). Human ICE/CED-3 protease nomenclature. *Cell* **87**:171.

Arends, M. J. & Wyllie, A. H. (1991). Apoptosis: mechanisms and roles in pathology. *Int. Rev. Exp. Pathol.* **32**:223-254.

Arnold, R. *et. al.* (2001). Caspase-mediated cleavage of hematopoietic progenitor kinase 1 (HPK1) converts an activator of NFkappaB into an inhibitor of NFkappaB. *J. Biol. Chem.* **276**:14675-14684.

Ashkenazi, A. & Dixit, V. M. (1998). Death receptors: signalling and modulation. *Science* **281**:1305-1308.

Avdi, N. J. *et. al.* (2001). Tumour necrosis factor-alpha activation of the c-Jun N-terminal kinase pathway in human neutrophils. Integrin involvement in a pathway leading from cytoplasmic tyrosine kinases apoptosis. *J. Biol. Chem.* **276**:2189-2199.

Baker, S.J. & Reddy, E.P. (1998) Modulation of life and death by the TNF receptor superfamily. *Oncogene* **17**:3261-3270.

Becker, A. J. *et. al.* (1999). Differential regulation of apoptosis-related genes in resistant and vulnerable subfields of rat epileptic hippocampus. *Brain Res. Mol. Brain Res.* **67**:172-176.

Beg, A. A. & Baltimore, D. (1996). An essential role for NFκB in preventing TNF-α-induced cell death. *Science* **274**: 782-784.

Behrens, A., Sibilia, M. & Wagner, E. F. (1999). Amino-terminal phosphorylation of c-Jun regulates stress-induced apoptosis and cellular proliferation. *Nat. Gen.* **21**:326-329.

Behrens, A. *et. al.* (2000). Oncogenic transformation by ras and fos is mediated by c-Jun N-terminal phosphorylation. *Oncogene* **19**:2657-2663.

Bennett, M. *et. al.* (1998). Cell surface trafficking of Fas: a rapid mechanism of p53-mediated apoptosis. *Science*, **282**:290-293.

Blank, J. L. *et. al.* (1996). Molecular cloning of mitogen-activated protein/ERK kinase kinases (MEKK) 2 and 3. Regulation of sequential phosphorylation pathways involving mitogen-activated protein kinase and c-Jun kinase. *J. Biol. Chem.* **271**:5361-5368.

Bodmer, J-L. *et. al.* (2000). TRAIL receptor-2 signals through FADD and caspase 8. *Nat. Cell Biol.* **2**:241-243.

Boldin, M. P. *et. al.* (1995). Self-association of the "death domains" of the p55 tumor necrosis factor (TNF) receptor and Fas/APO1 prompts signalling for TNF and Fas/APO1 effects. *J. Biol. Chem.* **270**:387-391.

Boldin, M. P. *et. al.* (1996). Involvement of MACH, a novel MORT1/FADD-interacting protease, in Fas/APO-1- and TNF receptor-induced cell death. *Cell* **85**:803-815.

Bonnotte, B. *et. al.* (1998). Bcl-2-mediated inhibition of apoptosis prevents immunogenicity and restores tumorigenicity of spontaneously regressive tumours. *J. Immunol.* **161**:1433-1438.

Bonny, C., Nicod, P. & Waeber, G. (1998). IB1, a JIP-1-related nuclear protein present in insulin-secreting cells. *J. Biol. Chem.* **273**:1843-1846.

Bonny, C. *et. al.* (2000). IB1 reduces cytokine-induced apoptosis of insulin-secreting cells. *J. Biol. Chem.* **275**:16466-16472.

Bossy-Wetzel, E.,Bakiri, L. & Yaniv, M. (1997). Induction of apoptosis by the transcription factor c-Jun. *EMBO J.* **16**:1695-1709.

Bowman, A. B. *et. al.* (2000). Kinesin-dependent axonal transport is mediated by the sunday driver (SYD) protein. *Cell* **103**:583-594.

Bradford, M. M. (1976). A rapid and sensitive for the quantitation of microgram quantities of protein utilizing the principle of protein-dye binding. *Anal. Biochem.* **72**:248-254.

Budihardjo, I. *et. al.* (1999). Biochemical pathways of caspase activation during apoptosis. *Ann. Rev. Cell Dev. Biol.* **15**:269-290.

Burbelo, P. D. *et. al.* (1995). A conserved binding motif defines numerous candidate target proteins for both Cdc42 and Rac GTPases. *J. Biol. Chem.* **270**:29071-29074.

Buschmann, T. *et. al.* (2001). Jun NH2-terminal kinase phosphorylation of p53 on Thr-81 is important for p53 stabilization and transcriptional activities in response to stress. *Mol. Cell. Biol.* **21**:2743-2754.

Cardone, M. H. *et. al.* (1997). The regulation of anoikis: MEKK-1 activation requires cleavage by caspases. *Cell* **90**:315-323.

Casciola-Rosen, L. *et. al.* (1996). Apopain/CPP32 cleaves proteins that are essential for cellular repair: a fundamental principle of apoptotic death. *J. Exp. Med.* **183**:1957-1964.

Cavigelli, M. *et. al.* (1995). Induction of c-fos expression through JNK-mediated TCF/Elk-1 phosphorylation. *EMBO J.* **14**:5957-5964.

Chae, H. W. *et. al.* (2001). Signal transduction of nitric oxide donor-induced protection in hydrogen peroxide-mediated apoptosis in H9C2 cardiomyoblasts. *Immunopharmacol. Immunotoxicol.* **23**:187-204.

Chainy, G. B. *et. al.* (2000). Anethole blocks both early and late cellular responses transduced by tumor necrosis factor: effect on NF-kappaB, AP-1, JNK, MAPKK and apoptosis. *Oncogene* **19**:2943-50.

Chang, H. Y., Yang, X. & Baltimore, D. (1999). Dissecting Fas signalling with an altered-specificity death-domain mutant: requirement of FADD binding for apoptosis but not Jun N-terminal kinase activation. *Proc. Natl. Acad. Sci. U. S. A.* **96**:1252-1256.

Charette, S. J. *et. al.* (2001). A kinase-independent function of ASK1 in caspase-independent cell death. *J. Biol. Chem.* **276**:36071-36074.

Chaudhary, P. M. *et. al.* (1999). Activation of the c-Jun N-terminal kinase/stress-activated protein kinase pathway by overexpression of caspase-8 and its homologs. *J. Biol. Chem.* **274**:19211-19219.

Chen, C. Y. *et. al.* (1998). Stabilization of interleukin-2 mRNA by the c-Jun NH2-terminal kinase pathway. *Science* **280**:1945-1949.

Chen, C. Y. *et. al.* (2000). Nucleolin and YB-1 are required for JNK-mediated interleukin-2 mRNA stabilization during T-cell activation. *Genes Dev.* **15**:1236-1248.

Chen, J. *et. al.* (2001). Raf-1 promotes cell survival by antagonizing apoptosis signal-regulating kinase 1 through a MEK-ERK independent mechanism. *Proc. Natl. Acad. Sci. U. S. A.* **98**:7783-7788.

Chen, N. *et. al.* (2001). Suppression of skin tumorigenesis in c-Jun NH_2-terminal kinase-2-deficient mice. *Cancer Res.* **61**:3908-39012.

Chen, Y. & Lai, M-Z. (2001). c-Jun NH_2-terminal kinase activation leads to a FADD-dependent but Fas ligand-independent cell death in Jurkat T cells. *J. Biol. Chem.* **276**:8350-8357.

Chen, Y. R., Meyer, C. F. & Tan, T. H. (1996). Persistent activation of c-Jun N-terminal kinase 1 (JNK1) in gamma radiation-induced apoptosis. *J. Biol. Chem.* **271**:631-634.

Chen, Y. R. *et. al.* (1996). The role of c-Jun N-terminal kinase (JNK) in apoptosis induced by ultraviolet C and gamma radiation. *J. Biol. Chem.* **271**:31929-31936.

Chen, Y. R. *et. al.* (1999). Caspase-mediated cleavage and functional changes of hematopoietic progenitor kinase 1 (HPK1). *Oncogene* **18**:7370-7377.

Chen, Y. R. & Tan, T. H. (2000). The c-Jun N-terminal kinase pathway and apoptotic signalling. *Intl. J. Oncol.* **16**:651-662.

Chen, Y. R., Zhou, G. & Tan, T. H. (1999). c-Jun N-terminal kinase mediates apoptotic signalling induced by N-(4-hydroxyphenyl)retinamide. *Mol. Pharmacol.* **56**:1271-1279.

Chen, Z. *et. al.* (1999). ASK1 mediates apoptotic cell death induced by genotoxic stress. *Oncogene* **18**:173-180.

Cheng, J. *et. al.* (2000). Synergistic Interaction of MEK Kinase 2, c-Jun N-Terminal Kinase (JNK) Kinase 2, and JNK1 Results in Efficient and Specific JNK1 Activation. *Mol. Cell. Biol.* **20**:2334-2342.

Chinnaiyan, A. M. *et. al.* (1995). FADD, a novel death domain-containing protein, interacts with the death domain of Fas and initiates apoptosis. *Cell* **81**:505-512.

Chinnaiyan, A. M. *et. al.* (1996). Signal transduction by DR3, a death domain-containing receptor related to TNFR-1 and CD95. *Science* **274**:990-992.

Chow, C. W. *et. al.* (1997). Nuclear accumulation of NFAT4 opposed by the JNK signal transduction pathway. *Science* **278**:1638-1641.

Chow, C. W. *et. al.* (2000). c-Jun NH(2)-terminal kinase inhibits targeting of the protein phosphatase calcineurin to NFATc1. *Mol. Cell. Biol.* **20**:5227-5234.

Coffey, E. T. *et. al.* (2000). Dual roles for c-Jun N-terminal kinase in developmental and stress responses in cerebellar granule neurons. *J. Neurosci.* **20**:7602-7613.

Cohen, G. M. (1997). Caspases: the executioners of apoptosis. *Biochem. J.* **326**:1-16.

Corpet, F. (1988). Multiple sequence alignment with hierarchical clustering. *Nucleic Acids Res.* **16**:10881-10890.

Dan, I., Watanabe, N. M. & Kusumi, A. (2001). The Ste20 group kinases as regulators of MAP kinase cascades. *Trends Cell Biol.* **11**: 220-230.

Darmon, A. J., Nicholson, D. W. & Bleackley, R. C. (1995). Activation of the apoptotic protease CPP32 by cytotoxic T-cell-derived granzyme B. *Nature* **377**:446-448.

Davis, R. J. (2000). Signal transduction by the JNK group of MAP kinases. *Cell* **103**: 239-252.

Davis, Jr. W., Ronai, Z. & Tew, K. D. (2001). Cellular thiols and reactive oxygen species in drug-induced apoptosis. *J. Pharmacol. Exp. Ther.* **296**:1-6.

De Smaele, E. *et. al.* (2001). Induction of *gadd45β* by NF-κB downregulates pro-apoptotic JNK signalling. *Nature* **414**:308-313.

Deacon, K. & Blank, J. L. (1997). Characterization of the mitogen-activated protein kinase kinase 4 (MKK4)/c-Jun NH2-terminal kinase 1 and MKK3/p38 pathways regulated by MEK kinases 2 and 3. *J. Biol. Chem.* **272**:14489-14496.

Deacon, K. & Blank, J. L. (1999). MEK kinase 3 directly activates MKK6 and MKK7, specific activators of the p38 and c-Jun NH2-terminal kinases. *J. Biol. Chem.* **274**:16604-16610.

Derijard, B. *et. al.* (1994). JNK1: a protein kinase stimulated by UV light and Ha-Ras that binds and phosphorylates the c-Jun activation domain. *Cell* **76**:1025-1037.

Derijard, B. *et. al.* (1995). Independent human MAP-kinase signal transduction pathways defined by MEK and MKK isoforms. *Science* **267**:682-685.

Dickens, M. *et. al.* (1997). A cytoplasmic inhibitor of the JNK signal transduction pathway. *Science* **277**:693-696.

Dong, C. *et. al.* (1998). Defective T cell differentiation in the absence of Jnk1. *Science* **282**:2092-2095.

Dorrow, D. S. *et. al.* (1995). Complete nucleotide sequence, expression, and chromosomal localisation of human mixed-lineage kinase 2. *Eur. J. Biochem.* **234**:492-500.

Dumont, J. E., Pecasse, F. & Maenhaut, C. (2001). Crosstalk and specificity in signalling. Are we crosstalking ourselves into general confusion? *Cell. Signal.* **13**:457-463.

Earnshaw, W. C., Martins, L. M., Kaufmann, S. H. (1999). Mammalian caspases: Structure, activation, substrates, and functions during apoptosis. *Ann. Rev. Biochem.* **68**:383-424.

Eferl, R. *et. al.* (1999). Functions of c-Jun in liver and heart development. *J. Cell Biol.* **145**:1049-1061.

Eilers, A. *et. al.* (2001). Direct inhibition of c-Jun N-terminal kinase in sympathetic neurones prevents c-jun promoter activation and NGF withdrawal-induced death. *J. Neurochem.* **76**:1439-1454.

Ellis, R. E., Yuan, J. & Horvitz, H. R. (1991). Mechanisms and functions of cell death. *Ann. Rev. Cell Biol.* **7**:663-698.

Englemann, H. *et. al.* (1990). Antibodies to a soluble form of a tumor necrosis factor (TNF) receptor have TNF-like activity. *J. Biol. Chem.* **265**:14497-14504.

Falcieri, E. *et. al.* (1993). The protein kinase inhibitor staurosporine induces morphological changes typical of apoptosis MOLT-4 cells without concomitant DNA fragmentation. *Biochem. Biophys. Res. Comm.* **193**:19-25.

Fan, G. *et. al.* (1996). Dual leucine zipper-bearing kinase (DLK) activates p46SAPK and p38mapk but not ERK2. *J. Biol. Chem.* **271**:24788-244793.

Fan, M. *et. al.* (2000). Vinblastine-induced phosphorylation of Bcl-2 and Bcl-xL is mediated by JNK and occurs in parallel with inactivation of Raf-1/MEK/ERK cascade. *J. Biol. Chem.* **275**:29980-29985.

Fanger, G. R. *et. al.* (1997). MEKKs, GCKs, MLKs, PAKs, TAKs, and tpls: upstream regulators of the c-Jun amino-terminal kinases? *Curr. Opin. Genet. Dev.* **7**:67-74.

Faris, M. *et. al.* (1998). The c-Jun N-terminal kinase cascade plays a role in stress-induced apoptosis in Jurkat cells by up-regulating Fas ligand expression. *J. Immunol.* **160**:143-144.

Ferrer, I., Segui, J. & Planas, A. M. (1996). Amyloid deposition is associated with c-Jun expression in Alzheimer's disease and amyloid angiopathy. *Neuropathol. App. Neurobiol.* **22**:521-526.

Fleming, Y. *et. al.* (2000). Synergistic activation of stress-activated protein kinase 1/c-Jun N-terminal kinase (SAPK1/JNK) isoforms by mitogen-activated protein kinase kinase 4 (MKK4) and MKK7. *Biochem. J.* **352**:145-154.

Foltz, I. N. *et. al.* (1998). Human mitogen-activated protein kinase kinase 7 (MKK7) is a highly conserved c-Jun N-terminal kinase/stress-activated protein kinase (JNK/SAPK) activated by environmental stresses and physiological stimuli. *J. Biol. Chem.* **273**:9344-51.

Fortin, A. *et. al.* (2001). Apaf1 is a key transcriptional target for p53 in the regulation of neuronal cell death. *J. Cell Biol.* **155**:207-216.

Fraser, A. & Evan, G. (1996). A license to kill. *Cell* **85**:781-784.

Fuchs, S. Y. *et. al.* (1997). c-Jun NH2-terminal kinases target the ubiquitination of their associated transcription factors. *J. Biol. Chem.* **272**:32163-32168.

Fuchs, S. Y. *et. al.* (1998). JNK targets p53 ubiquitination and degradation in nonstressed cells. *Genes Dev.* **12**:2658-2663.

Gabai, V. L. *et. al.* (1997). Hsp70 prevents activation of stress kinases. A novel pathway of cellular thermotolerance. *J. Biol. Chem.* 272:18033-18037.

Gamen, S. *et. al.* (1996). CPP32 inhibition prevents Fas-induced ceramide generation and apoptosis in human cells. *FEBS Lett.* **390**:232-237.

Ganiatsas, S. *et. al.* (1998). SEK1 deficiency reveals mitogen-activated protein kinase cascade crossregulation and leads to abnormal hepatogenesis. *Proc. Natl. Acad. Sci. U.S.A.* **95**:6881-6886.

Garcia-Calvo, A. *et. al.* (1998). Inhibition of human caspases by peptide-based and macromolecular inhibitors. *J. Biol. Chem.* **271**:13273-13282.

Garrington, T. P. & Johnson, G. L. (1999). Organisation and regulation of mitogen-activated protein kinase signalling pathways. *Curr. Opin. Cell Biol.* **11**: 211-218.

Gerwins, P., Blank, J. L. & Johnson, G. L. (1997). Cloning of a novel mitogen-activated protein kinase kinase kinase, MEKK4, that selectively regulates the c-Jun amino terminal kinase pathway. *J. Biol. Chem.* **272**:8288-82895.

Gliniak, B. & Le, T. (1999). Tumor necrosis factor-related apoptosis-inducing ligand's antitumor activity in vivo is enhanced by the chemotherapeutic agent CPT-11. *Cancer Res.* **59**:6153-6158.

Goillot, E. *et. al.* (1997). Mitogen-activated protein kinase-mediated Fas apoptotic signalling pathway. *Proc. Natl. Acad. Sci. U. S. A.* **94**:3302-3307.

Gotoh, Y. & Cooper, J. A. (1998). Reactive oxygen species- and dimerization-induced activation of apoptosis signal-regulating kinase 1 in tumor necrosis factor-alpha signal transduction. *J. Biol. Chem.* **273**:17477-17482.

Graves, J. D. *et. al.* (2001). Both phosphorylation and caspase-mediated cleavage contribute to regulation of the Ste20-like protein kinase Mst1 during CD95/Fas-induced apoptosis. *J. Biol. Chem.* **276**:14909-14915.

Guo, Y. L. *et. al.* (1998). Inhibition of the expression of mitogen-activated protein phosphatase-1 potentiates apoptosis induced by tumor necrosis factor-alpha in rat mesangial cells. *J. Biol. Chem.* **273**:10362-10366.

Gupta, S. *et. al.* (1995). Transcription factor ATF2 regulation by the JNK signal transduction pathway. *Science* **267**:389-393.

Gupta, S. *et. al.* (1996). Selective interaction of JNK protein kinase isoforms with transcription factors. *EMBO J.* **15**:2760-2770.

Gygi, S. P. *et. al.* (1999). Correlation between protein and mRNA abundance in yeast. *Mol. Cell. Biol.* **19**:1720-1730.

Habelhah, H *et. al.* (2001). Identification of new JNK substrate using ATP pocket mutant JNK and a corresponding ATP analogue. *J. Biol. Chem.* **276**:18090-18095.

Hakem, R. *et. al.* (1998). Differential requirement for caspase-9 in apoptotic pathways *in vivo*. *Cell* **94**: 339-352.

Ham, J. *et. al.* (1995). A c-Jun dominant negative mutant protects sympathetic neurons against programmed cell death. *Neuron* **14**:927-939.

Hanafusa, H. *et. al.* (1999). Involvement of the p38 mitogen-activated protein kinase pathway in transforming growth factor-beta-induced gene expression. *J. Biol. Chem.* **274**:27161-27167.

Harding, T. C. *et. al.* (2001). Inhibition of JNK by overexpression of the JNL binding domain of JIP-1 prevents apoptosis in sympathetic neurons. *J. Biol. Chem.* **276**:4531-4534.

Harper, N. *et. al.* (2001). Modulation of tumor necrosis factor apoptosis-inducing ligand- induced NF-kappa B activation by inhibition of apical caspases. *J. Biol. Chem.* **276**:34743-24752.

Harwaood, F. G. *et. al.* (2000). Regulation of FasL by NF-kappaB and AP-1 in Fas-dependent thymineless death of human colon carcinoma cells. *J. Biol. Chem.* **275**:10023-10029.

Hasegawa, J. *et. al.* (1996). Involvement of CPP32/Yama(-like) proteases in Fas-mediated apoptosis. *Cancer Res.* **56**:1713-1718.

Hatai, T. *et. al.* (2000). Execution of ASK-1-induced apoptosis by the mitochondria-dependent caspase activation. *J. Biol. Chem.* **275**: 26576-26581.

Hayashi, T. *et. al.* (2000). c-Jun N-terminal kinase (JNK) and JNK interacting protein response in rat brain after transient middle cerebral artery occlusion. *Neurosci. Lett.* **284**:195-199.

Hehner, S. P. *et. al.* (2000). Mixed-lineage kinase 3 delivers CD3/CD28-derived signals into the IkappaB kinase complex. *Mol. Cell. Biol.* **20**:2556-2568.

Herr, I. *et. al.* (2000). Autoamplification of apoptosis following ligation of CD95-L, TRAIL and TNF-alpha. *Oncogene* **19**:4255-4262.

Herskowitz, I. (1995). MAP kinase pathways in yeast: for mating and more. *Cell* **80**:187-197.

Hibi, M. *et. al.* (1993). Identification of an oncoprotein- and UV-responsive protein kinase that binds and potentiates the c-Jun activation domain. *Genes Dev.* 7:2135-2148.

Hietanen S. *et. al.* (2000). Activation of p53 in cervical carcinoma cells by small molecules. *Proc. Natl. Acad. Sci. U. S. A.* **97**:8501-8506.

Hirai, S.-I. *et. al.* (1998). Differential activation of two JNK activators, MKK7 and SEK1, by MKN28-derived nonreceptor serine/threonine kinase/mixed lineage kinase 2. *J. Biol. Chem.* **273**:7406-7412.

Hirsch, D. D. & Stork, P. J. (1997). Mitogen-activated protein kinase phosphatases inactivate stress-activated protein kinase pathways *in vivo*. *J. Biol. Chem.* **272**:4568-4575.

Ho, F.M. *et. al.* (2000). High glucose-induced apoptosis in human endothelial cells is mediated by sequential activations of c-Jun NH(2)-terminal kinase and caspase-3. *Circulation* **101**:2618-2624.

Ho, S. N. *et. al.* (1989). Site-directed mutagenesis by overlap extension using the polymerase chain reaction. *Gene* **77**:51-59.

Hoeflich, K. P. *et. al.* (1999). Mediation of TNF receptor-associated factor effector functions by apoptosis signal-regulating kinase-1 (ASK1). *Oncogene* **18**:5814-5820.

Holland, P. M. *et. al.* (1997). MKK7 is a stress-activated mitogen-activated protein kinase kinase functionally related to *hemipterous*. *J. Biol. Chem.* **272**:24994-24998.

Holmstrom, T. H. *et. al.* (1998). Suppression of Fas/APO-1-mediated apoptosis by mitogen-activated kinase signalling. *J. Immunol.* **160**:2626-2636.

Holmstrom, T. H. *et. al.* (1999). Inhibition of mitogen-activated kinase signalling sensitises HeLa cells to Fas receptor-mediated apoptosis. *Mol. Cell. Biol.* **19**:5991-6002.

Holmstrom, T. H. *et. al.* (2000). MAPK/ERK signalling in activated T cells inhibits CD95/Fas-mediated apoptosis downstream of DISC assembly. *EMBO J.* **19**:5418-5428.

Holtmann, M. *et. al.* (1999). Induction of interleukin-8 synthesis integrates effects on transcription and mRNA degradation from at least three different cytokine- or stress-activated signal transduction pathways. *Mol. Cell. Biol.* **19**:6742-6753.

Holzman, L. B., Merritt, S. E. & Fan, G. (1994). Identification, molecular cloning, and characterization of dual leucine zipper bearing kinase. *J. Biol. Chem.* **269**:30808-30817.

Hossain, K. *et. al.* (2000). Arsenite induces apoptosis of murine T lymphocytes through membrane raft-linked signalling for activation of c-Jun amino-terminal kinase. *J. Immunol.* **165**:4290-4297.

Hsu, H. *et. al.* (1996). TRADD-TRAF2 and TRADD-FADD interactions define two distinct TNF receptor 1 signal transduction pathways. *Cell* **84**:299-308.

Hu, M. C. *et. al.* (1996). Human HPK1, a novel human hematopoietic progenitor kinase that activates the JNK/SAPK kinase cascade. *Genes Dev.* **10**:2251-2264.

Hu, W. H., Johnson, H. & Shu, H. B. (1999). Tumor necrosis factor-related apoptosis-inducing ligand receptors signal NF-kappaB and JNK activation and apoptosis through distinct pathways. *J. Biol. Chem.* **274**:30603-30610.

Ichijo, H. *et. al.* (1997). Induction of apoptosis by ASK1, a mammalian MAPKKK that activates SAPK/JNK and p38 signalling pathways. *Science* **275**:90-94.

Ikeda, A. *et. al.* (2001). Identification and characterisation of functional domains in a mixed lineage kinase LZK. *FEBS Lett.* **488**:190-195.

Ing, Y. L. *et. al.* (1994). MLK3: Identification of a widely-expressed protein kinase bearing an SH3 domain and a luecine zipper-basic region domain. *Oncogene* **9**:1745-1750.

Inoue, H. *et. al.* (2001). A *Drosophila* MAPKKK, D-MEKK1, mediates stress responses through activation of p38 MAPK. *EMBO J.* **20**:5421-5430.

Ip, Y. T. & Davis, R. J. (1998). Signal transduction by the c-Jun N-terminal kinase (JNK) - from inflammation to development. *Curr. Opin. Cell Biol.* **10**:205-219.

Irmler, M. *et. al.* (1997). Inhibition of death signals by cellular FLIP. *Nature* **388**:190-195.

Ito, M. *et. al.* (1999). JSAP1, a novel jun N-terminal protein kinase (JNK)-binding protein that functions as a scaffold factor in the JNK signalling pathway. *Mol. Cell. Biol.* **19**:7539-7548.

Ito, Y. *et. al.* (2001). Interaction of hematopoietic progenitor kinase 1 and c-Abl tyrosine kinase in response to genotoxic stress. *J. Biol. Chem.* **276**:18130-18138.

Jacobson, M. D., Weil, M. & Raff, M. C. (1996). Role of Ced-3/ICE-family proteases in staurosporine-induced programmed cell death. *J. Cell Biol.* **133**:1041-1051.

Jacobson, M. D. *et. al.* (1997). Programmed cell death in animal development. *Cell* **88**:347-354.

Janicke, R. U. *et. al.* (1996). Specific cleavage of the retinoblastoma protein by an ICE-like protease in apoptosis. *EMBO J.* **15**:6969-6978.

Johnson, R. *et. al.* (1996). Cellular transformation and malignancy induced by Ras require c-Jun. *Mol. Cell. Biol.* **16**:4504-4511.

Kallunki, T. *et. al.* (1996). c-Jun can recruit JNK to phosphorylate dimerisation partners via specific docking interactions. *Cell* **87**:929-939.

Kanamoto, T. *et. al.* (2000). Role of apoptosis signal-regulating kinase in regulation of the c-Jun N-terminal kinase pathway and apoptosis in sympathetic neurons. *Mol. Cell. Biol.* **20**:196-204.

Karin, M. (1995). The regulation of AP-1 activity by mitogen-activated protein kinases. *J. Biol. Chem.* **270**:16483-16486.

Karin, M. & Delhase, M. (1998). JNK or IKK, AP-1 or NF-kappaB, which are the targets for MEK kinase 1 action? *Proc. Natl. Acad. Sci. U. S. A.* **95**:9067-9069.

Kasibhatla, S. *et. al.* (1998). DNA damaging agents induce expression of Fas ligand and subsequent apoptosis in T lymphocytes via the activation of NF-kappa B and AP-1. *Mol. Cell* **1**:543-551.

Katz, S., Heinrich, R. & Aronheim, A. (2001). The AP-1 repressor, JDP2, is a bona fide substrate for the c-Jun N-terminal kinase. *FEBS Lett.* **506**:196-200.

Kawasaki, M. *et. al.* (1999). A *Caenorhabditis elegans* JNK signal transduction pathway regulates coordinated movement via type-D GABAergic motor neurons. *EMBO J.* **18**:3604–3615.

Kelkar, N. *et. al.* (2000). Interaction of a mitogen-activated protein kinase signalling module with the neuronal protein JIP3. *Mol. Cell. Biol.* **20**:1030-1043.

Kemeny, D. M. (1997). Enzyme-linked immunoassays. In *Immunochemistry I: A practical approach* (Edited by A. P. Johnstone & M. W. Turner), Oxford University Press, 1997.

Kiefer, F. *et. al.* (1996). HPK1, a hematopoietic protein kinase activating the SAPK/JNK pathway. *EMBO J.* **15**:7013-7025.

Kidd, V. J. (1998). Proteolytic activities that mediate apoptosis. *Ann. Rev. Physiol.* **60**:533-573.

Kim, A. H. *et. al.* (2001). Akt phosphorylates and negatively regulates apoptosis signal-regulating kinase 1. *Mol. Cell. Biol.* **21**:893-901.

Kim, I. J. *et. al.* (1999). Molecular cloning of multiple splicing variants of JIP-1 preferentially expressed in brain. *J. Neurochem.* **72**:1335-1343.

Ko, Y. G. *et. al.* (2001). Apoptosis Signal-regulating Kinase 1 Controls the Proapoptotic Function of Death-associated Protein (Daxx) in the Cytoplasm. *J. Biol. Chem.* **276**:39103-39106.

Koga, M. *et. al.* (2000) A *Caenorhabditis elegans* MAP kinase kinase, MEK-1, is involved in stress responses. *EMBO J.* **19**:5148–5156.

Kolbus, A. *et. al.* (2000). c-Jun-dependent CD95-L expression is a rate-limiting step in the induction of apoptosis by alkylating agents. *Mol. Cell. Biol.* **20**:575-582.

Kozak, M. (1999). Initiation of translation in prokaryotes and eukaryotes. *Gene* **234**: 187-208.

Kuan, C. Y. *et. al.* (1999). The JNK1 and JNK2 protein kinases are required for regional-specific apoptosis during early brain development. *Neuron* **22**: 667-676.

Kuang, A. A. *et. al.* (2000). FADD is required for DR4- and DR5-mediated apoptosis. *J. Biol. Chem.* **275**:25065-25068.

Krause, A. *et. al.* (1998). Stress-activated protein kinase/Jun N-terminal kinase is required for interleukin (IL)-1-induced IL-6 and IL-8 gene expression in the human epidermal carcinoma cell line KB. *J. Biol. Chem.* **273**:23681-23689.

Kyriakis, J. M. & Avruch, J. (1990). pp54 microtubule-associated protein 2 kinase. A novel serine/threonine protein kinase regulated by phosphorylation and stimulated by poly-L-lysine. *J. Biol. Chem.* **265**:17355-17363.

Kyriakis, J. M. *et. al.* (1994). The stress-activated protein kinase subfamily of c-Jun kinases. *Nature* **369**:156-160.

Kyriakis, J. M. (1999). Signalling by the germinal centre kinase family of protein kinases. *J. Biol. Chem.* **274**: 5259-5262.

Kyriakis, J. M. & Avruch, J. (2001). Mammalian mitogen-activated protein kinase signal transduction pathways activated by stress and inflammation. *Physiol. Rev.* **81**: 808-869.

Laemelli, U. K. (1970). Cleavage of the structural proteins during the assembly of the head of bacteriophage T4. *Nature* **227**:680-685.

Lange-Carter, C. A. *et. al.* (1993). A divergence in the MAP kinase regulatory network defined by MEK kinase and Raf. *Science* **260**:315-319.

Lawler, S. *et. al.* (1998). Synergistic activation of SAPK1/JNK1 by two MAP kinase kinases *in vitro*. *Curr. Biol.* **8**:1387-1390.

Lazebnik, Y. A. *et. al.* (1994). Cleavage of poly(ADP-ribose) polymerase by a proteinase with properties like ICE. *Nature* **371**:346-347.

Lenczowski, J. M. *et. al.* (1997). Lack of a role for Jun kinase and AP-1 in Fas-induced apoptosis. *Mol. Cell. Biol.* **17**:170-181.

Leung, I. W. & Lassam, N. (2001). The kinase activation loop is the key to mixed lineage kinase-3 activation via both autophosphorylation and hematopoietic progenitor kinase 1 phosphorylation. *J. Biol. Chem.* **276**:1961-1967.

Levkau, B. *et. al.* (1998). Caspase-mediated cleavage of focal adhesion kinase pp125FAK and disassembly of focal adhesions in human endothelial cell apoptosis. *J. Exp. Med.* **187**:579-586.

Levresse, V. *et. al.* (2000). Akt negatively regulates the cJun N-terminal kinase pathway in PC12 cells. *J. Neurosci. Res.* **62**:799-808.

Li, K. *et. al.* (2000). Cytochrome c deficiency causes embryonic lethality and attenuates stress-induced apoptosis. *Cell* **101**:389-399.

Li, P. *et. al.* (1997). Cytochrome *c* and dATP-dependent formation of Apaf-1/caspase-9 complex initiates an apoptotic protease cascade. *Cell* **91**:479–489.

Lin, A. *et. al.* (1995). Identification of a dual specificity kinase that activates the Jun kinases and p38-Mpk2. *Science* **268**:286-290.

Lin, Y. *et. al.* (1999). Cleavage of the death domain kinase RIP by Caspase-8 prompts TNF-induced apoptosis. *Genes Dev.* **13**:2514-2526.

Lin, Y. *et. al.* (2000a). The death domain kinase RIP is essential for TRAIL (Apo2L)-induced activation of IkappaB kinase and c-Jun N-terminal kinase. *Mol. Cell. Biol.* **20**:6638-6645.

Ling, P. *et. al.* (1999). Interaction of hematopoietic progenitor kinase 1 with adapter proteins Crk and CrkL leads to synergistic activation of c-Jun N-terminal kinase. *Mol. Cell. Biol.* **19**:1359-1368.

Li-Niculescu, H. *et. al.* (1999). Withdrawal of survival factors results in activation of the JNK pathway in neuronal cells leading to Fas ligand induction and cell death. *Mol. Cell. Biol.* **19**:751-763.

Liu, F. T. *et. al.* (1979). New procedures for preparation and isolation of conjugates of proteins and a synthetic copolymer of D-amino acids and immunochemical characterization of such conjugates. *Biochemistry* **18**:690-693.

Liu, H. *et. al.* (2000). Activation of apoptosis signal-regulating kinase 1 (ASK1) by tumor necrosis factor receptor-associated factor 2 requires prior dissociation of the ASK1 inhibitor thioredoxin. *Mol. Cell. Biol.* **20**:2198-2208.

Liu, X. *et. al.* (1996). Induction of apoptotic program in cell-free extracts: requirement for dATP and cytochrome *c*. *Cell* **86**:147–157.

Liu, X. *et. al.* (1997). DFF, a heterodimeric protein that functions downstream of caspase-3 to trigger DNA fragmentation during apoptosis. *Cell* **89**:175-184.

Liu, Z. G. *et. al.* (1996). Dissection of TNF receptor 1 effector functions: JNK activation is not linked to apoptosis while NF-κB activation prevents cell death. *Cell* **87**:565-576.

Lu, X., Nemato, S. & Lin, A. (1997). Identification of c-Jun NH_2-terminal protein kinase (JNK)-activating kinase 2 as an activator of JNK but not p38. *J. Biol. Chem.* **272**:24751-24754.

Luo, X. *et. al.* (1998). Bid, a Bcl-2 interacting protein, mediates cytochrome *c* release from mitochondria in response to activation of cell surface death receptors. *Cell* **94**:481–490

Ma, W. *et. al.* (2001). Leukocyte-specific adaptor protein Grap2 interacts with hematopoietic progenitor kinase 1 (HPK1) to activate JNK signalling pathway in T lymphocytes. *Oncogene* **20**:1703-1714.

MacDonald, P. H. *et. al.* (2000). Beta-arrestin 2: a receptor-regulated MAPK scaffold for the activation of JNK3. *Science* **290**:1574-1577.

MacFarlane, M. *et. al.* (1997). Identification and molecular cloning of two novel receptors for the cytotoxic ligand TRAIL. *J. Biol. Chem.* **272**:25417-25420.

Marchenko, N. D. *et. al.* (2000). Death signal-induced localization of p53 protein to mitochondria. A potential role in apoptotic signalling. *J. Biol. Chem.* **275**:16202-16212.

Marinissen, M. J. & Gutkind, J. S. (2001). G-protein-coupled receptors and signalling networks: Emerging paradigms. *Trends Pharmacol. Sci.* **22**:368-376.

Marsters, S. A. *et. al.* (1999). Control of apoptosis signalling by Apo2 ligand. *Recent Prog. Horm. Res.* **54**:225-234.

Marti, A. *et. al.* (1997). Actin-binding protein-280 binds the stress-activated protein kinase (SAPK) activator SEK-1 and is required for tumor necrosis factor-alpha activation of SAPK in melanoma cells. *J. Biol. Chem.* **272**:2620-2628.

Matsuda, S. *et. al.* (2001). c-Jun N-terminal kinase (JNK)-interacting protein-1b/islet-brain-1 scaffolds Alzheimer's amyloid precursor protein with JNK. *J. Neurosci.* **21**:6597-6607.

Matsuzawa, A. & Ichijo, H. (2001). Molecular mechanisms of the decision between life and death: Regulation of apoptosis by apoptosis signal-regulating kinase 1. *J. Biochem.* **130**:1-8.

May, E., Jenkins, J. R. & May, P. (1991). Endogenous HeLa p53 proteins are easily detected in HeLa cells transfected with mouse deletion mutant p53 gene. *Oncogene* **6**:1363-1365.

McKinney, M. M. & Parkinson, A. (1987). A simple, non-chromatographic procedure to purify immunoglobulins from serum and ascites fluid. *J. Immunol. Methods* **96**:271-278.

Medema, J. P. *et. al.* (1997). FLICE is activated by association with the CD95 death inducing signalling complex. *EMBO J.* **16**:2794-2804.

Meriin, A. B. *et. al.* (1998). Proteasome inhibitors activate stress kinases and induce Hsp72. *J. Biol. Chem.* **273**:6373-6379.

Merritt, S. E. *et. al.* (1999). The mixed lineage kinase DLK utilizes MKK7 and not MKK4 as substrate. *The Journal of Biological Chemistry* **274**:10195-10202.

Meyer, D., Liu, A. & Margolis, B. (1999). Interaction of c-Jun amino-terminal kinase interacting protein-1 with p190 rhoGEF and its localization in differentiated neurons. *J. Biol. Chem.* **274**:35113-35118.

Miller, W. E. & Lefkowitz, R. J. (2001). Expanding roles for beta-arrestins as scaffolds and adapters in GPCR signalling and trafficking. *Curr. Opin. Cell Biol.* **13**:139-145.

Miura, M., Friedlander, R. M. & Yuan, J. (1995). Tumor necrosis factor-induced apoptosis is mediated by a CrmA-sensitive cell death pathway. *Proc. Natl. Acad. Sci. U. S. A.* **92**:8318-8322.

Miyashita, T. & Reed, J. C. (1995). Tumour suppressor p53 is a direct transcriptional activator of the human bax gene. *Cell* **80**:293-299.

Mo, Y.Y. & Beck, W.T. (1999). DNA damage signals induction of fas ligand in tumor cells. *Mol. Pharmacol.* **55**:216-222.

Moll, U. M. & Zaika, A. (2001). Nuclear and mitochondrial apoptotic pathways of p53. *FEBS Lett.* **493**:65-69.

Moriguchi, T. *et. al.* (1997). A novel SAPK/JNK kinase, MKK7, stimulated by TNFalpha and cellular stresses. *EMBO J.* **16**:7045-7053.

Morishima, Y. *et. al.* (2001). Beta-amyloid induces neuronal apoptosis via a mechanism that involves the c-Jun N-terminal kinase pathway and the induction of Fas ligand. *J. Neurosci.* **21**:7551-7560.

Mosser, D. D. *et. al.* (2000). The chaperone function of Hsp70 is required for protection against stress-induced apoptosis. *Mol. Cell. Biol.* **20**:7146-7159.

Mota, M. *et. al.* (2001). Evidence for a role of mixed lineage kinases in neuronal apoptosis. *J. Neurosci.* **21**:4949-4957.

Muhlenbeck, F. *et. al.* (1998). TRAIL/Apo2L activates c-Jun NH2-terminal kinase (JNK) via caspase-dependent and caspase-independent pathways. *J. Biol. Chem.* **273**:33091-33098.

Muhlenbeck, F. *et. al.* (2000). The tumor necrosis factor-related apoptosis-inducing ligand receptors TRAIL-R1 and TRAIL-R2 have distinct cross-linking requirements for initiation of apoptosis and are non-redundant in JNK activation. *J. Biol. Chem.* **275**:32208-32213.

Muller, M. *et. al.* (1998). p53 activates the CD95 (APO-1/Fas) gene in response to DNA damage by anticancer drugs. *J. Exp. Med.* **188**:2033-2045.

Mundrell, K. *et. al.* (1997). Bcl-2 undergoes phosphorylation by c-Jun N-terminal kinase/stress-activated protein kinases in the presence of the constitutively active GTP-binding protein Rac1. *J. Biol. Chem.* **272**:25238-25242.

Muzio, M. *et. al.* (1996). FLICE, a novel FADD-homologous ICE/CED-3-like protease, is recruited to the CD95 (Fas/APO-1) death--inducing signalling complex. *Cell* **85**:817-827.

Muzio, M. *et. al.* (1998). An induced proximity model for caspase-8 activation. *J. Biol. Chem.* **273**:2926-2930.

Namgung, U. & Xia, Z. (2000). Arsenite-induced apoptosis in cortical neurons is mediated by c-Jun N-terminal protein kinase 3 and p38 mitogen-activated protein kinase. *J. Neurosci.* **20**:6442-6451.

Natoli, G. *et. al.* (1997). Activation of SAPK/JNK by TNF receptor 1 through a noncytotoxic TRAF2-dependent pathway. *Science* **275**:200-203.

Nicholson, D. W. (1999). Caspase structure, proteolytic substrates, and function during apoptotic cell death. *Cell Death Differ.* **6**:1028-1042.

Nihalani, D., Merritt, S. E. & Holzman, L. B. (2000). Identification of structural and functional domains in mixed lineage kinase dual leucine zipper-bearing kinase required for complex formation and stress-activated protein kinase activation. *J. Biol. Chem.* **275**:7273-7279.

Nihalani, D. *et. al.* (2001). Mixed lineage kinase-dependent JNK activation is governed by interactions of scaffold protein JIP with MAPK module components. *EMBO J.* **20**:3447-3458.

Nishina, H. *et. al.* (1997). Impaired CD28-mediated interleukin 2 production and proliferation in stress kinase SAPK/ERK1 kinase (SEK1)/mitogen-activated protein kinase kinase 4 (MKK4)-deficient T lymphocytes. *J. Exp. Med.* **186**:941-953.

Nishina, H. *et. al.* (1999). Defective liver formation and liver cell apoptosis in mice lacking the stress signalling kinase SEK1/MKK4. *Development* **126**:505-516.

Nishitoh, H. *et. al.* (1998). ASK1 is essential for JNK/SAPK activation by TRAF2. *Mol. Cell* **2**:389-395.

Noselli, S. (1998). JNK signalling and morphogenesis in *Drosophila*. *Trends Genet.* **14**:33–38.

Paasinen-Sohns, A. *et. al.* (2000). c-Jun activation-dependent tumorigenic transformation induced paradoxically by overexpression or block of S-adenosylmethionine decarboxylase. *J. Cell Biol.* **151**:801-810.

Palm, K. *et. al.* (1998). Neuronal expression of zinc finger transcription factor REST/NRSF/XBR gene. *J. Neurosci.* **18:**1280-1296

Pan, G. *et. al.* (1997). An antagonist decoy receptor and a death domain-containing receptor for TRAIL. *Science* **277**:815-818.

Park, H. S. *et. al.* (2001). Hsp70 functions as a natural inhibitory protein of c-Jun N-terminal kinase. *EMBO J.* **20**: 446-456.

Pawson, T. & Nash, P. (2000). Protein-protein interactions define specificity in signal transduction. *Genes Dev.* **14**:1027-1047.

Pellet, J. B. *et. al.* (2000). Spatial, temporal and subcellular localization of islet-brain 1 (IB1), a homologue of JIP-1, in mouse brain. *Eur. J. Neurosci.* **12**:621-632.

Perlman, R. *et. al.* (2001). TGF-beta-induced apoptosis is mediated by the adapter protein Daxx that facilitates JNK activation. *Nat. Cell Biol.* **3**:708-714.

Phelan, D. R. *et. al.* (2001). Activated JNK phosphorylates the C-terminal domain of MLK2 that is required for MLK2-induced apoptosis. *J. Biol. Chem.* **276**:10801-10810.

Polyak, K. *et. al.* (1997). A model for p53-induced apoptosis. *Nature* **389**:300-305.

Potapova, O. *et. al.* (2000). Inhibition of c-Jun N-terminal kinase 2 expression suppresses growth and induces apoptosis of human tumour cells in a p53-dependent manner. *Mol. Cell. Biol.* **20**:1713-1722.

Pulverer, B. J. *et. al.* (1991). Phosphorylation of c-jun mediated by MAP kinases. *Nature* **353**:670-674.

Qiao, L. *et. al.* (1996). Staurosporine inhibits the proliferation, alters the cell cycle distribution and induces apoptosis in HT-29 human colon adenocarcinoma cells. *Cancer Lett.* **107**:83-89.

Raitano, A. B. *et. al.* (1995). The Bcr-Abl leukemia oncogene activates Jun kinase and requires Jun for transformation. *Proc. Natl. Acad. Sci. U. S. A.* **92**:11746-11750.

Reddy, V. G., Khanna, N. & Singh, N. (2001). Vitamin C augments chemotherapeutic response of cervical carcinoma HeLa cells by stabilizing P53. *Biochem. Biophys. Res. Commun.* **282**:409-415.

Reinhard, C. *et. al.* (1997). Tumour necrosis factor alpha-induced activation of c-Jun N-terminal kinase is mediated by TRAF2. *EMBO J.* **16**:1080-1092.

Rheaume, E. *et. al.* (1997). The large subunit of replication factor C is a substrate for caspase-3 in vitro and is cleaved by a caspase-3-like protease during Fas-mediated apoptosis. *EMBO J.* **16**:6346-6354.

Riesgo-Escovar, J. R. *et. al.* (1996). The *Drosophila* Jun-N-terminal kinase is required for cell morphogenesis but not for DJun-dependent cell fate specification in the eye. *Genes Dev.* **10**:2759–2768.

Rincon, M. (2001). MAP-kinase signalling pathways in T cells. *Curr. Opin. Immunol.* **13**:339-345.

Rincon, M., Flavell, R. A. & Davis, R. J. (2001). Signal transduction by MAP kinases in T lymphocytes. *Oncogene* **20**:2490-2497.

Robles, A. I. *et. al.* (2001). Apaf-1 is a transcriptional target of p53 in DNA damage-induced apoptosis. *Cancer Res.* **61**:6660-6664.

Rodriguez, G. A., Park, M. & Schlessinger, J. (1997). Activation of the JNK pathway is essential for transformation by the Met oncogene. *EMBO J.* **16**:2634-2645.

Rodriguez, J. & Lazebnik, Y. (1999). Caspase-9 and Apaf-1 form an active holoenzyme. *Genes Dev.* **13**:3179-3184.

Sabapathy, K. *et. al.* (1999). Defective neural tube morphogenesis and altered apoptosis in the absence of both JNK1 and JNK2. *Mech. Dev.* **89**:115-124.

Sakahira, H., Enari, M. & Nagata, S. (1998). Cleavage of CAD inhibitor in CAD activation and DNA degradation during apoptosis. *Nature* **391**:96-99.

Saitoh, M. *et. al.* (1998). Mammalian thioredoxin is a direct inhibitor of apoptosis signal-regulating kinase (ASK) 1. *EMBO J.* 17:2596-2606.

Sanchez, I. *et. al.* (1994). Role of SAPK/ERK kinase-1 in the stress-activated pathway regulating transcription factor c-Jun. *Nature* **372**:794-798.

Sanchez-Perez, I., Murguia, J. R. & Perona, R. (1998). Cisplatin induces a persistent activation of JNK that is related to cell death. *Oncogene* **16**:533-540.

Savill, J. & Fadok, V. (2000). Corpse clearance defines the meaning of cell death. *Nature* **407**:784-788.

Scaffidi, C. *et. al.* (1997). FLICE is predominantly expressed as two functionally active isoforms, caspase-8/a and caspase-8/b. *J. Biol. Chem.* **272**:26953-26958.

Scaffidi, C. *et. al.* (1998). Two CD95(APO-1/Fas) signalling pathways. *EMBO J.* **17**:1675--1687.

Scaffidi, C. *et. al.* (1999). The role of c-FLIP in modulating CD95-induced apoptosis. *J. Biol. Chem.* **274**:1541-1548.

Schaeffer, H. J. & Weber, M. J. (1999). Mitogen-activated protein kinases: Specific messages from ubiquitous messengers. *Mol. Cell. Biol.* **19**: 2435-2444.

Schmitz, I., Kirchhoff, S. & Krammer, P. H. (2000). Regulation of death receptor-mediated apoptosis pathways. *Intl. J. Biochem. Cell Biol.* **32**:1123-1136.

Sharrocks, A. D., Yang, S. H. & Galanis, A. (2000). Docking domains and substrate-specificity determination for MAP kinases. *Trends Biochem. Sci.* **25**:448-453.

Shaulian, E. *et. al.* (2000). The mammalian UV response: c-Jun is required for exit from p53-imposed growth arrest. *Cell* **103**: 897-907.

Shaulian, E. & Karin, M. (2001). AP-1 in cell proliferation and survival. *Oncogene* **20**:2390-2400.

Slee, E. A. *et. al.* (1999). Ordering the cytochrome c-initiated caspase cascade: hierarchical activation of caspases-2, -3, -6, -7, -8, and -10 in a caspase-9-dependent manner. *J. Cell Biol.* **144**:281-292.

Slee, E. A., Adrian, C. & Martin, S. J. (2001). Executioner caspase-3, -6, and -7 perform distinct, non-redundant roles during the demolition phase of apoptosis. *J. Biol. Chem.* **276**:7320-7326.

Sluss, H. K. *et. al.* (1994). Signal transduction by tumor necrosis factor mediated by JNK protein kinases. *Mol. Cell. Biol.* **14**:8376-8384.

Sluss, H.K. *et. al.* (1996) A JNK signal transduction pathway that mediates morphogenesis and an immune response in *Drosophila*. *Genes Dev.* **10**:2745-2758.

Srinivasula, S. M. *et. al.* (1996). Molecular ordering of the Fas-apoptotic pathway: the Fas/APO-1 protease Mch5 is a CrmA-inhibitable protease that activates multiple Ced-3/ICE-like cysteine proteases. *Proc. Natl. Acad. Sci. U. S. A.* **93**:14486-14491.

Stennicke, H. R. *et. al.* (1998). Pro-caspase-3 is a major physiologic target of caspase-8. *J. Biol. Chem.* **273**:27084-27090.

Stennicke, H. R. *et. al.* (1999). Caspase-9 can be activated without proteolytic processing. *J. Biol. Chem.* **274**:8359-8362.

Stennicke, H. R. et. al. (2000). Internally quenched fluorescent peptide substrates disclose the subsite preferences of human caspases 1, 3, 6, 7 and 8. *Biochem. J.* **350**:563-568.

Stockinger, W. *et. al.* (2000). The reelin receptor ApoER2 recruits JNK-interacting proteins-1 and -2. *J. Biol. Chem.* **275**:25625-25632.

Stoneley, M. *et. al.* (2000). c-Myc protein synthesis is initiated from the internal ribosome entry segment during apoptosis. *Mol. Cell. Biol.* **20**:1162-1169.

Strasser, A., O'Connor, L. & Dixit, V. M. (2000). Apoptosis signalling. *Ann. Rev. Biochem.* **69**:217-245.

Stroh, C. & Schulze-Osthoff, K. (1998). Death by a thousand cuts: an ever-increasing list of caspase substrates. *Cell Death Differ.* **5**:997-1000.

Stronach, B. E. & Perrimon, N. (1999). Stress signalling in *Drosophila*. *Oncogene* **18**:6172-6182.

Su, B. *et. al.* (1994). JNK is involved in signal integration during costimulation of T lymphocytes. *Cell* **77**:727-736.

Su, G. H. *et. al.* (1998). Alterations in pancreatic, biliary, and breast carcinomas support MKK4 as a genetically targeted tumor suppressor gene. *Cancer Res.* **58**:2339-2342.

Sun, X. M. *et. al.* (1999). Distinct caspase cascades are initiated in receptor-mediated and chemical-induced apoptosis. *J. Biol. Chem.* **274**:5053-5060.

Takahashi, A. & Earnshaw, W.C. (1996). ICE-related proteases in apoptosis. *Curr. Opin. Genet. Dev.* **6**:50-55.

Talanian, R. V. *et. al.* (1997). Substrate specificities of caspase family proteases. *J. Biol. Chem.* **272**:9677-9682.

Tang, D. & Kidd, V. J. (1998). Cleavage of DFF-45/ICAD by multiple caspases is essential for its function during apoptosis. *J. Biol. Chem.* **273**:28549-28552.

Tang, G. *et. al.* (2001). Inhibition of JNK activation through NF-κB target genes. *Nature* **414**:313-317.

Tanoue, T. *et. al.* (2000). A conserved docking motif in MAP kinases common to substrates, activators and regulators. *Nat. Cell Biol.* **2**:110-116.

Tefani, M. *et. al.* (2001). Induction of the mitochondrial permeability transition mediates the killing of HeLa cells by staurosporine. *Cancer Res.* **61**:2459-2466.

Tew, K. D. *et. al.* (1996). Glutathione-associated enzymes in the human cell lines of the National Cancer Institute Drug Screening Program. *Mol. Pharmacol.* **50**:149-159.

Tewari, M *et. al.* (1995). Yama/CPP32 beta, a mammalian homologue of CED-3, is a CrmA-inhibitable protease that cleaves the death substrate poly(ADP-ribose) polymerase. *Cell* **81**:801-809.

Thompson, N. A. *et. al.* (2001). Islet-brain1/JNK-interacting protein-1 is required for early embryogenesis in mice. *J. Biol. Chem.* **276**:27745-27748.

Thornberry, N. A. *et al.* (1997). A combinatorial approach defines specificities of members of the caspase family and granzyme B. Functional relationships established for key mediators of apoptosis. *J. Biol. Chem.* **272**:17907-17911.

Tibbles, L. A. *et. al.* (1996). MLK-3 activates the SAPK/JNK and p38/RK pathways via SEK1 and MKK3/6. *EMBO J.* **15**:7026-7035.

Tobiume, K. *et. al.* (2001). ASK1 is required for sustained activations of JNK/p38 MAP kinases and apoptosis. *EMBO Rep.* **2**:222-228.

Tomita, Y. *et. al.* (1996). Tetrapeptide DEVD-aldehyde or YVAD chloromethylketone inhibits Fas/Apo-1(CD95)-mediated apoptosis in renal-cell-cancer cells. *Intl. J. Cancer* **68**:132-135.

Tournier, C. *et. al.* (1997). Mitogen-activated protein kinase kinase 7 is an activator of the c-Jun NH2-terminal kinase. *Proc. Natl. Acad. Sci. U. S. A.* **94**:7337-7342.

Tournier, C. *et. al.* (1999). The MKK7 gene encodes a group of c-Jun NH2-terminal kinase kinases. *Mol. Cell. Biol.* **19**:1569-1581.

Tournier, C. *et. al.* (2000). Requirement of JNK for stress-induced activation of the cytochrome c-mediated death pathway. *Science* **288**:870-874.

Tournier, C. *et. al.* (2001). MKK7 is an essential component of the JNK signal transduction pathway activated by proinflammatory cytokines. *Genes Dev.* **15**:1419-1426.

Tohoshima, F., Moriguchi, T. & Nishida, E. (1997). Fas induces cytoplasmic apoptotic responses and activation of the MKK7-JNK/SAPK and MKK6-p38 pathways independent of CPP32-like proteases. *J. Cell Biol.* **139**:1005-1015.

Ura, S. *et. al.* (2001). MST1-JNK promotes apoptosis via caspase-dependent and independent pathways. *Genes to Cells* **6**:519-530.

Utz, P. J. & Anderson, P. (2000). Life and death decisions: regulation of apoptosis by proteolysis of signalling molecules. *Cell Death Differ.* **7**:589-602.

Vacratsis, P. O. & Gallo, K. A. (2000). Zipper-mediated oligomerization of the mixed lineage kinase SPRK/MLK-3 is not required for its activation by the GTPase cdc 42 but Is necessary for its activation of the JNK pathway. *J. Biol. Chem.* **275**:27893-27900.

Verheij, M. *et. al.* (1996). Requirement for ceramide-initiated SAPK/JNK signalling in stress-induced apoptosis. *Nature* **380**:75-79.

Verhey, K. J. *et. al.* (2001). Cargo of kinesin identified as JIP scaffolding proteins and associated signalling molecules. *J. Cell Biol.* **152**:959-970.

Villanueva, A. *et. al.* (2001). *jkk-1* and *mek-1* regulate body movement coordination and response to heavy metals through *jnk-1* in *Caenorhabditis elegans*. *EMBO J.* **20**:5114-5128.

Vogt, P. K. (2001). Jun, the oncoprotein. *Oncogene* **20**:2365-2377.

Wada, T. *et. al.* (2001). Impaired synergistic activation of stress-activated protein kinase SAPK/JNK in mouse embryonic stem cells lacking SEK1/MKK4: different contribution of SEK2/MKK7 isoforms to the synergistic activation. *J. Biol. Chem.* **276**:30892-30897.

Wajant, H. *et. al.* (2000). Inhibition of death receptor-mediated gene induction by a cycloheximide-sensitive factor occurs at the level of or upstream of Fas-associated death domain protein (FADD). *J. Biol. Chem.* **275**:24357-24366.

Wallach, D. *et. al.* (1999). Tumor necrosis factor receptor and Fas signalling mechanisms. *Ann. Rev. Immunol.* **17**:331-367.

Wang, W. *et. al.* (1997). Activation of the hematopoietic progenitor kinase-1 (HPK1)-dependent, stress-activated c-Jun N-terminal kinase (JNK) pathway by transforming growth factor beta (TGF-beta)-activated kinase (TAK1), a kinase mediator of TGF beta signal transduction. *J. Biol. Chem.* **272**:22771-22775.

Wang, X. S. *et. al.* (1996). Molecular cloning and characterization of a novel protein kinase with a catalytic domain homologous to mitogen-activated protein kinase kinase kinase. *J. Biol. Chem.* **271**:31607-31611.

Wang, X. *et. al.* (1998). The cellular response to oxidative stress: influences of mitogen-activated protein kinase signalling pathways on cell survival. *Biochem. J.* **333**:291-300.

Watabe, M. *et. al.* (2000). Activation of MST/Krs and c-Jun N-terminal kinases by different signalling pathways during cytotrienin A-induced apoptosis. *J. Biol. Chem.* **275**:8766-8771.

Watson, A. *et. al.* (1998). Phosphorylation of c-Jun is necessary for apoptosis induced by survival signal withdrawal in cerebellar granule neurons. *J. Neurosci.* **18**:751-762.

Weil, M. *et. al.* (1996). Constitutive expression of the machinery for programmed cell death. *J. Cell Biol.* **133**:1053-1059.

Weiss, L. *et. al.* (2000). Regulation of *c-Jun NH_2-terminal kinase (Jnk)* gene expression during T-cell activation. *J. Exp. Med.* **191**: 139-145.

Whitmarsh, A. J. *et. al.* (1995). Integration of MAP kinase signal transduction pathways at the serum response element. *Science* **269**:403-407.

Whitmarsh, A. J. *et. al.* (1998). A mammalian scaffold complex that selectively mediates MAP kinase activation. *Science* **281**:1671-1674.

Whitmarsh, A. J. & Davis, R. J. (1998). Structural organisation of MAP kinase signalling modules by scaffold proteins in yeast and mammals. *Trends Biochem. Sci.* **23**: 481-485.

Whitmarsh, A. J. *et. al.* (2001). Requirement of the JIP1 scaffold protein for stress-induced JNK activation. *Genes Dev.* **15**:2421-2432.

Widmann, C., Gibson, S. & Johnson, G. L. (1998). Caspase-dependent cleavage of signalling proteins during apoptosis. A turn-off mechanism for anti-apoptotic signals. *J. Biol. Chem.* **273**:7141-7147.

Widmann, C. *et. al.* (1999). Mitogen-activated protein kinase: conservation of a three-kinase module from yeast to human. *Physiological Reviews* **79**:143-180.

Woo, M. *et. al.* (1998). Essential contribution of caspase-3/CPP32 to apoptosis and its associated nuclear changes. *Genes Dev.* **12**: 806-819.

Wu, G. S. *et. al.* (1997). KILLER/DR5 is a DNA damage-inducible p53-regulated death receptor gene. *Nat. Gen.* **17**:141-143.

Wu, Z. *et. al.* (1997). Molecular cloning and characterization of human JNKK2, a novel Jun NH2-terminal kinase-specific kinase. *Mol. Cell. Biol.* **17**:7407-7416.

Xia, Y. *et. al.* (1998). JNKK1 organizes a MAP kinase module through specific and sequential interactions with upstream and downstream components mediated by its amino-terminal extension. *Genes Dev.* **12**:3369-3381.

Xia, Y. *et. al.* (2000). MEK kinase 1 is critically required for c-Jun N-terminal kinase activation by proinflammatory stimuli and growth factor-induced cell migration. *Proc. Natl. Acad. Sci. U. S. A.* **97**:5243-5248.

Xia, Z. *et. al.* (1995). Opposing effects of ERK and JNK-p38 MAP kinases on apoptosis. *Science* **270**:1326-1331.

Xu, X. *et. al.* (1996). Constitutively activated JNK is associated with HTLV-1 mediated tumorigenesis. *Oncogene* **13**:135-142.

Xu, Z. *et. al.* (2001). The MLK family mediates c-Jun N-terminal kinase activation in neuronal apoptosis. *Mol. Cell. Biol.* **21**:4713-4724.

Yan, M. *et. al.* (1994). Activation of stress-activated protein kinase by MEKK1 phosphorylation of its activator SEK1. *Nature* **372**:798-800.

Yang, D. D. *et. al.* (1997a). Differentiation of CD4+ T cells to Th1 cells requires MAP kinase JNK2. *Immunity* **9**:575-585.

Yang, D. D. *et. al.* (1997b). Absence of excitotoxicity-induced apoptosis in the hippocampus of mice lacking the *Jnk3* gene. *Nature* **389**:865-870.

Yang, J. *et. al.* (1997). Prevention of apoptosis by Bcl-2: release of cytochrome *c* from mitochondria blocked. *Science* **275**:1129–1132.

Yang, X. *et. al.* (1997). Daxx, a novel Fas-binding protein that activates JNK and apoptosis. *Cell* **89**:1067-1076.

Yao, Z. *et. al.* (1997). Activation of stress-activated protein kinases/c-Jun N-terminal protein kinases (SAPKs/JNKs) by a novel mitogen-activated protein kinase kinase. *J. Biol. Chem.* **272**:32378-32383.

Yasuda, J. *et. al.* (1999). The JIP group of mitogen-activated protein kinase scaffold proteins. *Mol. Cell. Biol.* **19**:7245-7254.

Yeh, W. C. *et. al.* (1998). FADD: essential for embryo development and signalling from some, but not all, inducers of apoptosis. *Science* **279**:1954-1958.

Yin, D. X. & Schmike, R. T. (1996). Inhibition of apoptosis by overexpressing Bcl-2 enhances gene amplification by a mechanism independent of aphidicolin pretreatment. *Proc. Natl. Acad. Sci. U. S. A.* **93**:3394-3398.

Yoshida, B. A. *et. al.* (1999). Mitogen-activated protein kinase kinase 4/stress-activated protein/Erk kinase 1 (MKK4/SEK1), a prostate cancer metastasis suppressor gene encoded by human chromosome 17. *Cancer Res.* **59**:5483-5487.

Yoshida, H. *et. al.* (1998). Apaf1 is required for mitochondrial pathways of apoptosis and brain development. *Cell* **94**:739-750.

Yuan, J. *et. al.* (1993). The *C. elegans* cell death gene *ced-3* encodes a protein similar to mammalian interleukin-1 beta-converting enzyme. *Cell* **75**:641-652.

Yujiri, T. *et. al.* (1998). Role of MEKK1 in cell survival and activation of JNK and ERK pathways defined by targeted gene disruption. *Science* **282**:1911-1914.

Yujiri, T. *et. al.* (1999). MEK kinase 1 (MEKK1) transduces c-Jun NH2-terminal kinase activation in response to changes in the microtubule cytoskeleton. *J. Biol. Chem.* **274**:12605-12610.

Yujiri, T. *et. al.* (2000). MEK kinase 1 gene disruption alters cell migration and c-Jun NH2-terminal kinase regulation but does not cause a measurable defect in NF-kappa B activation. *Proc. Natl. Acad. Sci. U. S. A.* **97**:7272-7277.

Zanke, B. W. *et. al.* (1996). The stress-activated protein kinase pathway mediates cell death following injury induced by cis-platinum, UV irradiation or heat. *Curr. Biol.* **6**:606-613.

Zhang, Y., Liu, G. & Dong, Z. (2001). MSK1 and JNKs mediate phosphorylation of STAT3 in UVA irradiated mouse epidermal JB6 cells. *J. Biol. Chem.* **276**: 42534-42542.

Zhang, L., Chen, J. & Fu, H. (1999). Suppression of apoptosis signal-regulating kinase 1-induced cell death by 14-3-3 proteins. *Proc. Natl. Acad. Sci. U. S. A.* **96**:8511-8515.

Zhang, Y. *et. al.* (2001). UVA induces Ser381 phosphorylation of p90RSK/MAPKAP-K1 via ERK and JNK pathways. *J. Biol. Chem.* **276**:14572-14580.

Zhou, G. *et. al.* (1999). Hematopoietic progenitor kinase 1 is a component of transforming growth factor beta-induced c-Jun N-terminal kinase signalling cascade. *J. Biol. Chem.* **274**:13133-13138.

Zou, H. *et. al.* (1999). An APAF-1.cytochrome c multimeric complex is a functional apoptosome that activates procaspase-9. *J. Biol. Chem.* **274**:11549-11556.

Zou, X. *et. al.* (2001). The cell cycle-regulatory CDC25A phosphatase inhibits apoptosis signal-regulating kinase 1. *Mol. Cell. Biol.* **21**:4818-4828.